Genetic analysis of marsh spot resistance in cranberry common bean (*Phaseolus vulgaris L.*)

Bosen Jia

Thesis submitted to the University of Ottawa in partial fulfilment of the requirements of the degree

Master of Science in Biology

(Specialization in Bioinformatics)

Supervised by:

Dr. Xuhua Xia

Dr. Frank M. You

Dr. Anfu Hou

Department of Biology

Faculty of Science

University of Ottawa

Abstract

Cranberry common bean (*Phaseolus vulgaris* L.) is planted worldwide and consumed as a critical food source of human protein, fibre, carbohydrates, and minerals. Marsh spot (MS) is a physiogenic disorder which severely impacts seed quality in common beans. Previous studies indicate that MS involves a nutritional disorder caused by Mn deficiency. However, the inheritance and genetic mechanism of MS resistance are still not fully understood.

To investigate the genetics of MS resistance, a population of 138 recombinant inbred lines (RILs) was developed from a bi-parental cross between a susceptible cultivar Messina and a resistant cultivar Cran09. The population and its two parents were evaluated for MS resistance during five consecutive years from 2015 to 2019 in both sandy and heavy clay soils in Morden, Manitoba, Canada. The severities of MS were rated and subsequently converted to MS resistance index (MSRI) and MS incidence (MSI). Statistical analyses indicated that MSI and MSRI were highly correlated (r = 0.96-0.99) and had high broad-sense heritability (H^2) of 86.5% and 83.2%, respectively. Joint segregation analysis (JSA) of 18 phenotypic datasets from five years and two soil types showed that MS resistance was controlled by four major genes with genetic interactions - one of which may suppress the additive effect of the other three genes.

To identify the quantitative trait loci (QTL) and the candidate genes associated with the MS resistance, the 138 RILs and the two parents were sequenced using genotyping by sequencing approach. A total of 52,676 SNPs were detected. After further filtering with a threshold of minor allele frequency > 0.01 and call rate > 20%, 2,061 SNPs were retained and then imputed for genetic map construction and QTL mapping. A genetic map consisting of 2,058 SNP markers on 11 linkage groups or chromosomes was constructed, which covered 1,004 recombination blocks with a total length of 6,449 cM and an average block of 6.42 cM. Three linkage map-based QTL-mapping models ICIM-ADD, ICIM-EPI, and GCIM and one genome-wide association study (GWAS) model RTM-GWAS for 18 phenotypic datasets from different years and soil types were

used for identification of QTL. A total of 36 QTL, including 21 of additive and 15 of epistatic effects, were identified. Functional gene annotation analysis revealed 151 Mn-related candidate genes across the common bean reference genome and 17 of them harbored the six QTL discovered in this study.

In conclusion, MS resistance in common bean is a highly heritable trait and controlled by several major and minor genes. The results of JSA and QTL mapping advance the current understanding of the genetic mechanisms of MS resistance in cranberry common bean, and provide additional resources for application in genomics-assisted breeding and potential isolation and functional characterization of the candidate genes.

Keywords: Marsh spot disease, cranberry common bean, joint segregation analysis (JSA), QTL mapping, genotyping by sequencing (GBS), single nucleotide polymorphism (SNPs), genome-wide association study (GWAS), *Phaseolus vulgaris*

Acknowledgements

It is with the utmost respect and gratitude that I acknowledge the guidance and assistance from one of my supervisors, Dr. Frank M. You, at the Ottawa Research and Development Centre, Agriculture and Agri-food Canada (AAFC). I am thankful for the freedom that he has given me to follow my research passion and for being a supplier of endless research ideas that are tailored to my interests. Over the years, I have grown more and more appreciative to his critical feedback aimed at fostering my scientific maturity. And I would be remiss if I fail to recognize his continued efforts to prepare me for my future pursuit in science, these include providing opportunities in teaching and research mentorships. I am truly grateful to have had the opportunity to pursue my MSc and PhD degree in the Dr. Frank You's laboratory, and I would like to thank him for acknowledging my small successes.

I appreciate my supervisor Dr. Anfu Hou at the Morden Research and Development Centre, AAFC, for his support and assistance in common bean data generation and analysis, and project funding support. I am also deeply indebted to my supervisor Prof./Dr. Xuhua Xia in University of Ottawa. During the two years of study, he has given me the encouragement and advice from his professional insights to improve my research quality and besides that, he also gave me great guidance and a detailed plan in my pursuit of my MSc. I am thankful to Dr. Robert Conner and his Pulse Pathology team for field trials and generously providing the phenotypic data for our research. I am thankful to Prof./Dr. Sylvie Cloutier at University of Ottawa and AAFC, for her great help for re-sequencing common bean population and gave a lot of great comments on my thesis and published articles. I am thankful to my advisory committee members Dr. Marina Cvetkovska, Julian Starr for their critical insights and encouragement in my research and thesis writing.

I thank all past and present lab members of Dr. You lab. Chunfang Zheng, Nadeem Khan, Sampurna Bartaula, Ismael Moumen, Pingchuan Li, Shazadee Hmna and Patrick Fidek. Nadeem and Sampurna are my valuable friends who provided me with much

support and encouragement. I thank Nadeem for his support in my master course learning and research. He gave me a lot of advice when I first went abroad and working on my project right now. I thank Sampurna for his help and assistantance in my graduate studies. Especially I need to thank Chunfang for her support and guidance when I was in trouble with computer problems. She was so professional and skillful in computer science and gave me lots of advice in data analysis.

I would also like to acknowledge my undergraduate professor Dr. Xiangfeng Wang for inspiring my interest in bioinformatics and computational biology. During my graduate studies, He also gave many pertinent advice on biology and computer language even on daily life. Thank you for always encourage me when I felt sad or confusion.

I would not be where I am today without the love and support from my family and friends. I am grateful to my parents for the sacrifices they have made and for their never-ending support that have greatly facilitated my life every day. I'm grateful to my treasured dear sister Xiaoya Wan for her infinite encouragements and support outside of the lab and for being there with me in the bright and dark time. Though countless challenges and lost during the preparation of study and live abroad, I finally overcame with her never-end encouragement and accompany. It's with my special appreciation that I mentioned my best friends Yuxin and my two roommates Zihan and Emma, my three most reliable comrades in my daily life and research life. My decision on studying in Canada were greatly inspired by Yuxin who also made this decision possible. When I first came to Canada, I was unfamiliar with all the lives here. Zihan and Emma always stood on my side to give me advice and support in life especially during this special pandemic time. I appreciated all support and suggestions from you and blessed with enormous fortune of meeting my friends and supervisor Dr. Frank You.

The funding was provided by CAP Pulse Cluster, Manitoba Pulse and Soybean Growers, thanks for their great supporting to our research.

Table of Contents

Acronyms

AIC	Akaike Information Criterion
AFLP	Amplified Fragment Length Polymorphism
BC	Back Cross
BICAT	Bivalent Cation Transporter
BIL	Backcross Inbred Line
CaCA	Ca^{2+}/Cation Antiporter
CATS	Comparative Anchor-Tagged Sequence
CAX	Cation Efflux
CCX	Cation/ Ca^{2+} Exchanger
CDF	Cation Diffusion Facilitator
CIM	Composite Interval Mapping
cM	Centi-Morgans
CV	Coefficient of Variation
DH	Doubled Haploid
EM	Expectation–Maximization
GBS	Genotyping By Sequencing
GCIM	Genome-wide Composite Interval Mapping
GS	Genome Selection
GWAS	Genome-wide Association Studies
ICIM	Inclusive Composite Interval Mapping
ICP	Inductively Coupled Plasma
IM	Interval Mapping
JSA	Joint Segregation Analysis
LD	Linkage Disequilibrium
LOD	Logarithm of The Odds
MAS	Marker-Assisted Selection
MS	Marsh Spot
MSI	Marsh Spot Incidence
MSRI	Marsh Spot Resistance Index
MTP	Metal Transport Protein
NRAMP	Natural Resistance-associated Macrophage Protein
NGS	Next Generation Sequencing
OEC	Oxygen-Evolving Complex
OPT	Oligopeptide Transporter
PS II	Photosystem II
QTL	Quantitative Trait Locus
QTN	Quantitative Trait Nucleotide
RAPD	Randomly Amplified Polymorphic DNA
RE	Restriction Enzyme
RIL	Recombinant Inbred Line
ROS	Reactive Oxygen Species

RTM-GWAS	Restricted Two-Stage, Multi-Locus, Multi-Allele GWAS
SD	Standard Deviation
SEA	Segregation Analysis
SMA	Single Marker Analysis
SNP	Single-Nucleotide Polymorphism
SOD	Superoxide Dismutase
SSR	Simple Sequence Repeat
VIT	Vacuolar Iron Transporter
YSL	Yellow-Stripe Like
ZIP	Zinc Transporter

1. Publications

Jia B, Conner RL, Khan N, Hou A, Xia X, You FM: **Inheritance of marsh spot disease resistance in cranberry common bean (*Phaseolus vulgaris* L.)**. *The Crop Journal* 2021, **9**:456-467

Jia B, Waldo P, Conner RL, Khan N, Hou A, Xia X, You FM: **Marsh spot disease and its causal factor, manganese deficiency in plants: A historical and prospective review**. *Agricultural Sciences* 2021, **12**, 928-948

Jia B, Conner RL, Waldo PC, Khan N, Zheng, C, Cloutier, S, Hou A, Xia X, You FM: **Quantitative trait locus mapping of marsh spot disease resistance in cranberry common bean (*Phaseolus vulgaris* L.)**. *International Journal of Molecular Science* 2022, 23, 7639

2. General introduction (Jia et al., 2021a;Jia et al., 2021b)

2.1 Agriculture of common bean

2.1.1 Common bean production

Common bean (*Phaseolus vulgaris L.*, 2n=2x = 22) is one of the most important grain legumes for human consumption. Common bean is well adapted to the moderate climate environment with an optimal growing temperature of >20 ℃ and <30 ℃, 400mm precipitation and a growing season of 60 - 120 days (Pérez de la Vega et al., 2017). The common bean originates primarily from two gene pools, namely the Mesoamerican and Andean gene pools, which were derived from the same common ancestral population after independent domestication of the plant in both Mesoamerica and South America (Bitocchi et al., 2012).

Common bean as a legume crop contributes to the agricultural sustainability because of its capacity in nitrogen fixation, albeit less efficiency than soybeans. The benefits gained from intercropping and rotation of common bean with cereals were noticeable (Foyer et al., 2016). These tillage methods and improved agronomic practices have also significantly increased bean yield, by raising efficiency of nitrogen-use efficiency and lowering disease incidence. According to Food and Agriculture Organization published dataset, as much as 21 Mt nitrogen was fixed by legumes annually when returning 5-7 Mt of nitrogen to soils from 190 million hector legume fields which would significant ameliorate soil structure and health (Herridge et al., 2008). Legumes have been considered valuable grain crop resource to improve food production and quality. Global climate change tendency has changed the prospect of common bean production. With the increased atmospheric CO_2 levels, using C_3 photosynthesis, legumes would absorb more carbons than cereal crops (Dutta et al., 2022) Warmer growing environment would lead to a shorter growing season; thus, it alleviates common bean from drought which often occurs at the end of the growing season especially in monsoon climate of medium latitudes areas (Foyer et al., 2016). Abiotic stresses, such as high temperature and drought, often affect bean production by increasing defective pollination, pod and flower abortion and therefore reducing seed yield and quality (Mourtzinis et al., 2015). Climate change may make northern hemisphere more suitable for common bean production. There is potential for Canada to expand common bean production in the future (Ramirez-Cabral et al., 2016).

Common beans are classified into various market classes based on seed coat color, patterns, and seed sizes (**Figure 1.1**). Pinto, navy, black, great northern, kidney and cranberry common beans are major market classes in USA and Canada. The seed coat pattern and color traits are controlled by polygenes which scatter across the common bean genome (McClean et al., 2002).

In conventional breeding, the seed coat color and patterns are difficult to be stably inherited to next generation when crosses are made between different market classes due to the quantitative inheritance and complex interactions among the polygenes. For instance, the progeny of a hybrid between cranberry and red beans may appear to be other seed coat color and often difficult to select back to cranberry or red seed coat patterns. To keep the same market class trait and speed up the variety development process, artificial hybrid and crosses are generally made within the same classes. The breeding process might have caused a decrease in genetic diversity which was observed in the two gene pools and in general, the genetic variation in the Andean-derived beans is less than in the Mesoamerican-derived ones (McClean et al., 2004;Schmutz et al., 2014). Based on the evaluation of the degree of relatedness among different market classes using SSR markers, dark red kidney, white kidney, cranberry, most green beans, and yellow beans were grouped into the Andean gene pool (Gioia et al., 2019).

Figure 1.1 Representative seed sizes, shapes and colors in major commercial bean classes (https://michiganbean.com/).

Mineral elements such as Mn, iron and zinc are important for human health. Due to their irreplaceable roles as co-factor in DNA, proteins and other biochemicals, lack

of micronutrition would result in physiological diseases (Welch and Graham, 1999). Biofortification, the process that increases the nutritional value in crop by agricultural approaches, was proposed to solve malnutrition of microminerals in human health especially for those in undeveloped countries (Welch, 2002). Common beans are an important source of protein, vitamins, and minerals. They have been widely planted in both developed and developing countries, especially in Africa and Latin America (Akibode and Maredia, 2012).

In Canada, the common bean is an economically important crop in crop rotation systems. From 2015 to 2019, the area planted with common beans has increased from 105,200 to 160,000 ha, with dry bean production reaching 316,800 Mt by 2019 (Statistics Canada, 2019).

2.1.2 Evolution, domestication and distribution of common bean

About 165,000 years ago, the wild common bean was originated in Mesoamerica diffused southward to the Andean region (Schmutz et al., 2014). After long-term isolation, evolution and independent domestication, at least two distinct gene pools, namely the Mesoamerican (Middle American) and Andean gene pools were formed (Bitocchi et al., 2012;Rendón-Anaya et al., 2017). One significant difference between the Middle American gene pool and the Andean gene pool is their seed size. Usually, the seeds from Middle America are much smaller than those from Andean.

In 1995, Kami et al. proposed a hypothesis that wild common bean is derived from northern Peru and Ecuador. This theory was overturned by Rossi et al. (Rossi et al., 2009) and Bitocchi et al. (Bitocchi et al., 2012) using amplified fragment length polymorphism (AFLP) and comparative anchor-tagged sequence (CATS) markers. Then in 2017, Rendón-Anaya's team discovered a wild bean population in North Peru and Ecuador. They suggested that this population diverged much earlier than divergence between Mesoamerican and Andean gene pools, and should be considered as the sister species and the third gene pool of common bean (Rendón-Anaya et al., 2017).

These gene pools were further domesticated by farmers in Mexico and South America nearly 8000 years ago and spread widely through various landraces. The common beans in Jalisco, Durango, Guatemala, and Mesoamerica regions are developed as the Middle American races, while those in Nueva Granada, Peru, and

Chile were identified as the Andean races (McClean et al., 2002).

Interestingly, the dual gene pools experienced independent domestication history respectively. This case also occurred in rice whose two gene pools *indica* and *japonica* underwent independent domestications as well. But unlike rice, where *indica* and *japonica* shared domestication genes by gene flow (Huang and George, 2011), common beans from Mesoamerican and Andean gene pools underwent parallel selection upon distinct sets of genes and even led to partial reproductive incompatibility. Besides, only few domestication genes were shared among Andean and Middle American gene pool races. These results indicate that domestication traits could be similar within different independent domestication history. Even in the same gene pool, none of domestication related genes were shared by its races. For example, although both Durango and Jalisco races belong to the Middle American gene pool, they only shared few domestication genes such as some disease resistance-responsive genes, yield related genes (**Figure 1.2**) (Singh and Molina, 1996;Schmutz et al., 2014).

Figure 1.2 The distribution of Middle America and Andean races and their origin of common bean (Schmutz et al., 2014;Stephen et al., 2014;Vlasova et al., 2016)

2.2 Common bean genome

Common bean has two reference genomes available for the Andean and Middle American gene pools, respectively. The first reference genome for an inbred landrace (G19833) derived from the Andean pool (Race Peru) was released in 2014 (Schmutz et al., 2014). This assembly contains 11 chromosome-scale pseudomolecules of 473 Mb (of the 587 Mb estimated genome size) (Schmutz et al., 2014). Approximate 45.4% of the assembly are repeat elements, among which 36.7% of whole genome are long terminal repeat (LTR) retrotransposons. A total of 27,197 protein-coding genes including 4,491 alternative transcripts were identified and validated using a *de novo* gene prediction approach and validated with Sanger-derived EST markers and RNA-seq data (Schmutz et al., 2014).

The second reference genome was reported in 2016 for a Mesoamerican type breeding line (BAT93) that represents the Middle American gene pool (Vlasova et al., 2016). The assembled genome size is 549.6 Mb that resembles the previously estimated genome size of G19833 (Pellicer and Leitch, 2020). The BAT93 genome contains 53,904 unique protein encoding genes and includes 97 % of the conserved core eukaryotic genes.

Comparative genome analysis between the BAT93 and G19833 genomes using synteny and phylogeny-based ortholog alignment indicates that 21,604 protein coding genes in G19833 are aligned to 21,600 genes in BAT93. Among these protein coding genes, 1,186 gene pairs out of 21,600 genes have relatively low nucleotide sequence identity (<95 %) (Vlasova et al., 2016), which may show uniqueness of genes in different gene pools. Most of these 1,186 genes pairs are enriched in defense response and terpene synthase activity. A total of 852 disease resistance gene clusters were identified from two reference genomes, but none of them were unique to either of the two gene pools, indicating that resistance genes existed earlier than the divergence of two gene pools (Vlasova et al., 2016).

2.3 Research on common bean abiotic stress resistance

Although the production of common bean reaches 31.4 Mt per year, common bean production still suffers from abiotic stress worldwide, especially in developing

countries where agriculture is limited by low-input chemical fertilizers, and abiotic stress caused by global climate change. Previous studies indicate that marsh spot is an abiotic disease caused by Mn deficiency that results in a seriously reduction in both quality and yield of seeds (Pethybridge, 1936). Drought, deficiency and toxicity of other mineral elements such as Zn, Fe and P have been also reported as influenced constraints to common bean production (Blair et al., 2010;Lauer et al., 2012;Farrow and Andriatsitohaina, 2021). For instance, in tropic and subtropic areas, 40% of bean production were decreased due to phosphorus deficiency (Farrow and Andriatsitohaina, 2021).

Thus, one of common bean breeding goals is to improve resistance to biotic and abiotic stress in cultivars. Genetic improvement of resistance or tolerance to biotic and abiotic stresses using marker-assisted selection (MAS) remarkably improves the common bean production along with the efficiency and precision of breeding (Miklas et al., 2006). In fact, abiotic and biotic resistance genes exist widely in wild common bean resources, and with genomics-assisted breeding, these resistant genes can be transferred into common bean cultivars. How to realize rapid introgression of these valuable genes has become an important challenge for breeders (Foyer et al., 2016).

2.4 Marsh spot disease and its symptoms, and treatments

2.4.1 Marsh spot disease

Marsh spot is a physiogenic disorder affecting seed quality in plants, primarily in peas (Lacey, 1934;Heintze, 1938;Piper, 1941;Reynolds, 1955;Henkens, 1958;Howard et al., 1994;Biddle and Cattlin, 2007) and beans (Hewitt, 1945;Howard et al., 1994;Biddle and Cattlin, 2007). The first description of the marsh spot symptoms on peas was given by De Bruyn in 1933 (De Bruyn, 1933). He noted a brown lesion of varying extent in the flat inner surface of one or both cotyledons while still enclosed in the seed coat. Also, he stated that sometimes this brown lesion was accompanied by partial or entire necrosis of the plumule. Currently, there is renewed interest in marsh spot disease because in susceptible varieties, a brown discoloured spot often occurs at the center of the seeds (**Figure 2.3 C and 2.3 D**).

To date, marsh spot disease is thought to be a physiological disorder caused by an Mn deficiency. This article describes the historical development and major progress on marsh spot disease control and its major causal factor: Mn deficiency-related metabolic

pathways, gene families, and QTL and their predicted candidate genes.

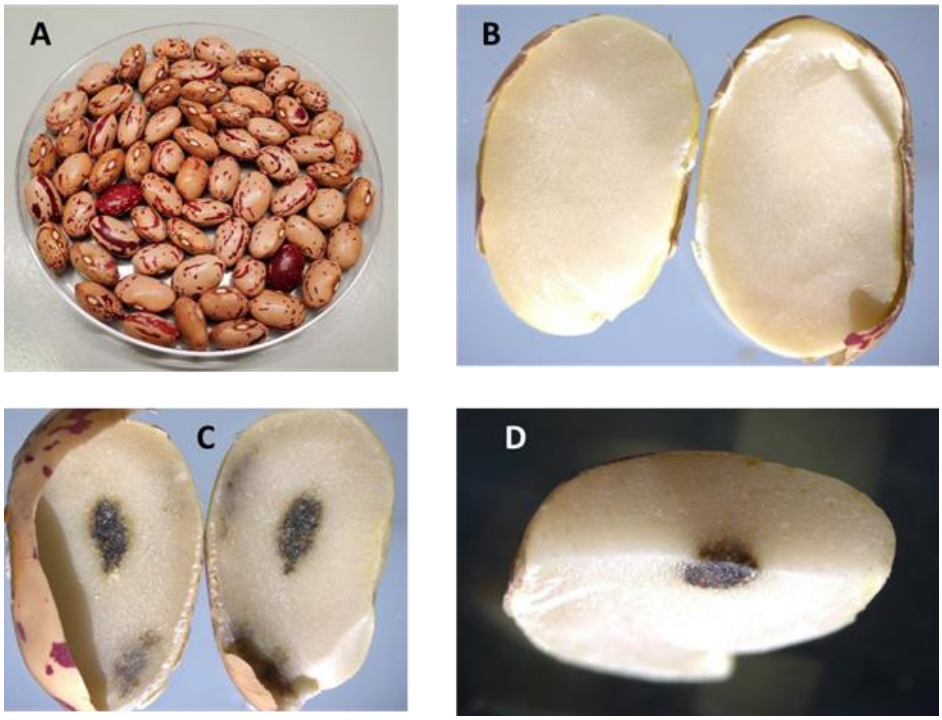

Figure 2.3 Cranberry common bean seeds and the symptoms of marsh spot disease. **A**. The exterior seed color of cranberry market class (cultivar Messina). **B**. Marsh spot-free split seed of the resistant cranberry common bean cultivar Cran09. **C**. Split seed with a high marsh spot rating of the susceptible cranberry common bean cultivar Messina (Jia et al., 2021a). **D**. Cross section of a seed with marsh spot disease showing the depth of the spot.

2.4.2 Symptoms and signs of marsh spot disease

In 1944, several pulse species, including peas (*Pisum sativum*), broad beans (*Vicia faba*), runner beans (*Phaseolus coccineus*), French (dwarf) beans (*P. vulgaris*) and Phaseolus vulgaris (*var. Masterpiece*) were raised at Long Ashton, England, in manganese (Mn)-deficient sand cultures, using a refined pot-culture procedure/way, and the pods were left on the plants until they dried before harvesting (Hewitt, 1945). Severe marsh spots in peas and mild to severe marsh spot symptoms in broad beans and runner beans were observed. The cotyledon center was sunken, brown, and pithy. Also, the embryos in beans often exhibited a browning of the plumule, which also was observed in peas. However, the dwarf beans did not show any symptoms of marsh spot (Hewitt, 1945). At the same time, the symptoms on leaves which were caused by Mn deficiency were extremely severe in dwarf beans, while in pea and broad bean the leaf symptoms were mild. One explanation for this observation was that pea and broad bean (0.5 m ~ 2 m

and 0.3 m ~ 1.2 m in plant height, respectively) were taller than dwarf bean (0.1 m ~ 0.3 m in plant height) and usually had a longer growth period (6-7 months and 8 months, respectively). Taller plants have to cope with a permanently fluctuating availability of soil nutrients, both in space and time (Maillard et al., 2015). As Mn can only be easily transported by xylem, but hardly in the phloem (Graham et al., 1988), Mn is difficult to remobilize in plants. Mn accumulated in the old leaves cannot be remobilized to other tissues in large amounts. Therefore, most Mn deficiency symptoms may present in old tissues in pea and broad bean with longer growth period rather than in the seeds.

The size of the marsh spots in the seeds varied. Some spots were quite small, while others expanded to the complete cotyledons of the seeds. The plumule could be altered when the discoloration was great. However, it was unusual to see any damage to the plumule. Broad cotyledon necrosis predisposed the seeds to attack by secondary bacterial or fungal organisms, making the damage more severe. Sometimes there was no internal visual discoloration, but only a denseness of the central tissue (Furneaux and Glasscock, 1936).

A discoloured spot in seeds was usually observed at the center of the adaxial surface of each endosperm's cotyledon. Under a microscope, the discoloured area seems to be caused by the cell death underneath the cotyledons' skin. The starch stored in those cells was transformed or replaced by a brown substance, which eventually discoloured the cell walls and invaded the intercellular spaces (Reynolds, 1955).

The seed germination rate can be severely reduced by marsh spot. For pea seeds with more than a 20% damaged area, the germination rate was much lower than that of normal seeds (De Bruyn, 1939). For instance, when both cotyledons had large specks with the same conditions on the plumule, the seeds had difficulty to germinate (De Bruyn, 1939).

2.4.3 Causal factor of marsh spot disease: Mn deficiency

Initially, brown spot symptoms were believed to be caused by microorganisms, so scientists attributed marsh spot to a bacterial infection. However, they failed to isolate any pathogens from peas. Lacey (1934) performed an examination to detect bacteria on the cotyledons of seeds with marsh spot symptoms and inoculated healthy plants using the tissues from marsh spot seeds. However, no marsh spot symptoms developed when the inoculated seeds were planted under the same soil conditions. Also, no bacteria were

extracted from marsh spot seeds, indicating that the marsh spot was not incited by a pathogen. Later, Pethybridge (1936) observed that marsh spots occurred in a plot of peas growing alongside oats affected with grey speck. This observation made him consider whether marsh spots in peas were also affected by an Mn deficiency like a grey speck in oats. Furthermore, Furneaux and Glasscock (1936) using a colorimetric method discovered that pea seeds with marsh spot symptoms had a lower Mn content than healthy ones. Then, Heintze (1938) used a hydroponic method for growing peas and investigated several traits (i.e., root length, flowering time, and seed formation) at different concentrations of Mn^{2+}. Consequently, it was confirmed that the marsh spot was caused by an Mn deficiency (Heintze, 1938).

Heintze (1938) grew peas in a sand-bentonite culture medium and showed that if no Mn was added to the culture medium, 12-15% of the seeds exhibited symptoms of marsh spot. However, no seeds had the marsh spot symptoms if Mn was added to the medium. He also designed experiments in which zinc or molybdenum was added into a water culture with a low Mn concentration to investigate their importance. The results showed that additions of sodium molybdate and zinc sulphate to Mn deficient soils generally increased the incidence of marsh spot in peas, but not in the soil with an ample supply of Mn. Those results also indicated that sodium molybdate affects Mn uptake processes within the plants and possibly suppressed Mn uptake (Reynolds, 1955).

Samuel and Piper (1929) stated that no other obvious Mn deficiency symptoms were observed in peas with marsh spot seeds during their vegetative growth. The marsh spot symptoms could only be detected in mature seeds. Therefore, marsh spot may be caused by a partial Mn deficiency as a severe deficiency led to the plants' death before seed development (Samuel and Piper, 1929). To assess this theory, the effects of different quantities of Mn on the growth of peas were examined using a water-culture technique that enabled the strict control of Mn concentrations available to the plants (Piper, 1941). When no Mn was added to water culture, specks occurred on the young leaves, and the growing tips often were dead. Most plants did not reach the flowering stage. When sufficient Mn was supplied in the nutrient solutions, plants could grow normally and produce seeds. While small amounts of Mn that were insufficient for normal growth requirements still enabled the seeds to form, but the seeds showed marsh spot symptoms, and the size of the spots were greatest at the lower Mn concentrations (Piper, 1941).

Moreover, at low concentrations of Mn, marsh spot symptoms more frequently

occurred on the late-maturing seeds. Following the application of sufficient Mn to the nutrient solutions, marsh spot symptoms did not occur on newly developed seeds, even though specks remained on earlier formed seeds. This confirmed that the marsh spot might result from a partial deficiency of Mn. Although this disease did not affect pea reproduction itself, the quality of seeds produced was reduced (Reynolds, 1955).

However, Moraghan and Grafton (2000) noted that cranberry common bean (*P. vulgaris*) cultivars may display differences in susceptibility to marsh spot. Four cranberry common bean cultivars were planted in two soil types (i.e., acid and calcareous) in North Dakota; although whole seed Mn content was relatively high in all cultivars, marsh spot symptoms were still observed. It also was noted that the application of manganese sulfate did not decrease the incidence of seeds with marsh spot. This indicated that marsh spot might also be affected by other micronutrients (Moraghan and Grafton, 2000).

2.4.4 Treatments for controlling marsh spot disease

Mn treatments can be applied to reduce plant Mn deficiency symptoms. In some fenland and marsh areas, where the marsh spot disorder most widely occurs, Mn treatments are considered as a vital routine step (Henkens, 1958). Most growers realize the importance of spraying Mn treatments at flowering time to avoid marsh spot symptoms in the seeds (Koopman, 1937). However, the manganese sulphate's application to prevent Mn deficiency in peas is still limited because unclear symptoms during vegetative and reproductive growth do not allow the farmer to determine whether the supplementary Mn is required (Reynolds, 1955). An additional issue that warrants consideration is the extent of crop damage resulting from the use of spraying machines or chemical fertilizers. Another important factor is the careful application of lime, particularly on black fen and neutral or slightly acid soils. The shell marl forms of black peat have shown to be associated with high incidences of severe marsh spot symptoms.

Manganese sulphate sprays help control marsh spot disease in peas and increase seed weight and yield. The seed yields of the two peas varieties, Jumboka and Zelka, were significantly increased from 345 - 350 g to 417 - 455 g per plot (Koopman, 1937) in response to sprays of $MnSO_4$. Increases up to 81% in extra seed yield in peas were obtained following sprays with manganese salts' solutions (Lewis, 1939). These results

demonstrate that the supplement of Mn can improve the seed production.

However, the application of manganese salts may delay ripening. For instance, manganese sulphate's application to peas at flowering time delayed maturity by ten days compared to the untreated plots (Furneaux and Glasscock, 1936).

2.5 Physiological and genetic points of view for marsh spot disease

2.5.1 Physiological viewpoint of Mn in plants

To date, the physiological mechanism of marsh spot resistance is still unknown. Although the main objective of this research was to detect genetic variation related to marsh spot resistance, the genes underlying Mn-related physiological process may be important candidate genes for the identified QTL. Understanding of the Mn-related physiological process such as transporter and absorption will also be useful for future investigation of physiological and genetic mechanisms of marsh spot resistance.

In one of the photosynthetic pathways, photosystem II (PSII), Mn is a critical element in the oxygen-evolving complex metalloenzyme cluster (Hoecker et al., 2017). The confirmed formula $Mn_4Ca_1O_xCl_{1-2}(HCO_3)_y$, which is known as the tetra-nuclear Mn cluster, is bound by the reaction center protein PsbA (D1) of the oxygen-evolving complex (OEC) (Dasgupta et al., 2008). Most of the Mn elements present in plants are involved in this process. Thus, Mn deficiency will lead to a decreased amount of the Mn-complex in the PSII system. For this reason, low concentrations of Mn will make PSII complex unstable and they may even disintegrate, eventually resulting in a low photosynthetic rate. Since leaves are almost the only source of organic matter for seed production, decreases in the amounts of photosynthate in the leaves would have a large negative impact on seed production and finally lead to the development of marsh spot symptoms. Moreover, because of low mobilization of Mn in the phloem, usually the new leaves first turn yellow while the old ones remain green (Dasgupta et al., 2008).

In addition to PSII in photosynthesis, the detoxification of reactive oxygen species (ROS) also requires Mn. One of the key characteristics of plant mitochondria is that when mitochondria respire, the redox centers will inevitably produce ROS to regulate plant metabolism and growth(Foyer and Noctor, 2003). Also, ROS are involved in the regulation of nuclear transcription.

However, ROS concentration has to be rigorously controlled by the antioxidant

system, since increased ROS levels may threaten the cellular machinery. The fragile cytoplasm and cell membranes can be disrupted by superoxide ROS. In a plants cell, superoxide dismutase (SOD) is a unique enzyme that assists cells in the dismutation of superoxide radicals of H_2O_2 and O_2. A high concentration of Mn^{2+} was observed in the complexes with amino acids, peptides, nucleotides, and carbohydrates in the mitochondria. Mn is a cofactor of MnSOD, an important enzyme that is produced by the mitochondria, which produces H_2O_2 and O_2 (Gutteridge and Halliwell, 2010). When plants are under oxidative stress, Mn^{2+} also can substitute for iron in some proteins to alleviate iron toxicity. Furthermore, one of the oxalate oxidases that are involved in the oxidation of oxalic acid is also an Mn-dependent enzyme.

Reduced MnSOD often alters the mitochondrial redox equilibrium and plant growth. Moreover, the oxidizing reaction is relatively intense during seed formation and germination with lots of O_2^- being produced. Therefore, a lack of Mn may result in malfunction of MnSOD, and the accumulation of ROS would eventually lead to the death of cell. Then necrosis, an oxidative stress symptom, which is first manifested as brown specks between the veins could be caused by the over accumulation of ROS within the chloroplasts (Loneragan, 1988).

Young leaves display the first symptoms of Mn deficiency. Pale mottled leaves in addition to the interveinal chlorosis are considered as the main symptoms of this deficiency (Schmidt et al., 2016). If a severe Mn deficiency occurs, leaves display gray speck symptoms, that appear as brownish, necrotic spots. Brown spots also occur within the plant seeds, i.e., marsh spot symptoms. Brodaley et al reported that if the free oxygen radicals are high in chloroplasts, then they will reduce MnSOD activity, which ultimately results in the formation of necrotic spots (Broadley et al., 2012).

Besides, Mn-dependent enzymes, Mn also plays a major role in the synthesis pathways of isoprenoid, lignin, and cuticular waxes in leaves (Engelsma, 1972;Rohdich et al., 2006;Hebbern et al., 2009). Isoprenoid exists widely in plants, including diversiform primary and secondary metabolites such as carotene and hormones. Those components are closely associated with the cell membrane, electron transfer, and photoprotection. When plants lack Mn, those biochemical processes also will be affected. Mn-deficiency also leads to a low concentration of lignin, especially in the roots. Therefore, maldeveloped roots often predispose plants to pathogens and weed competition, which subsequently results in lower productivity (Sax, 1923).

These Mn-dependent components have special functions in plant growth and

development; the lack of Mn or production of these components may lead to physiological diseases in plants, such as marsh spot.

Mn deficiency often occurs in plants growing in soils with low available Mn and in highly leached tropical soils. It is also common in high pH soils having free carbonates, especially those with a high organic matter content (Broadley et al., 2012). In Mn-deficient plants, dry matter production (Ohki et al., 1979), net photosynthesis, and chlorophyll content can decrease quickly (Shenker et al., 2004). In contrast, rates of respiration and transpiration remain unaltered (Ohki et al., 1979). Mn-deficient oat plants are more sensitive to damage by freezing temperatures and a range of soil-borne, root-rotting fungal diseases . A reduction in the number of kernels and grain yield in Mn-deficient oat plants is probably due to a mixture of low pollen fertility and a reduced carbohydrate supply for grain filling. Leaves of plants with low Mn tend to be yellow, especially the young leaves. When Mn deficiency is relatively severe, leaves will curl up and wilt. Sometimes some brown spots occur on the leaves. Mn deficiency is known to reduce yield and overall plant health in soybean (*Glycine max*) (Reynolds, 1955).

2.5.2 Mn uptake in some model plants and related gene families

As previously mentioned, Mn^{2+} is only available in an ionic form to plants. Most of the proteins responsible for the transport of Mn across membranes are not only responsible for this metal, but also other cations, especially divalent cations such as Fe^{2+}, Zn^{2+}, Cu^{2+}, Cd^{2+}, Ca^{2+}, Co^{2+}, and Ni^{2+}. Thus, sometimes the expression of genes that code for these protein families are regulated by the concentrations of other cations. It may be that the genes have diverse regulatory factor domains for different cations. More investigation, including the modification of specificity, is required to understand the low specificity in physiological relevance. For example, in the Mn/Fe transporter *AtMTP8*, Fe transport activity can be disrupted by inducing mutations in those Fe-binding domains with no impact on its Mn^{2+} transport capability (Chu et al., 2017). These Mn transport related genes may be putative candidate genes for marsh sport resistance because the disease is related to Mn availability (Appendix 1).

The zincs (ZIP) transporters commonly occur in bacteria, fungi, plants, and animals and are expected to be associated with Fe^{2+}, Zn^{2+}, Cd^{2+}, Co^{2+}, Cu^{2+}, and Mn^{2+} transport. They have eight transmembrane domains (TMD) with extracellular N- and C-termini and a cytosolic histidine-rich loop. YSL transporters are linked to the oligopeptide

transporter (OPT) family and occur only in plants, bacteria, fungi, and archaea. Members of the YSL family are predicted to transport metals (Mn^{2+}, Zn^{2+}, Cu^{2+}, Ni^{2+}, Cd^{2+}, Fe^{2+}) complexed to non-proteinogenic amino acids, such as nicotinamide (NA) or Phyto-siderophores (Guerinot, 2000;Giles et al., 2017).

The cation diffusion facilitator (CDF) family, which includes metal transport proteins (MTP) in higher plants (Kolaj-Robin et al., 2015;Renfrew et al., 2018) is common among plant organisms. Most CDFs are $Metal^{2+}/H^{+}(K^{+})$ antiporters and mediate the efflux of Zn^{2+}, Co^{2+}, Fe^{2+}, Cd^{2+}, Ni^{2+}, and/or Mn^{2+}. The majority have six TMDs with histidine-rich regions at their cytosolic N- and/or C-terminus and additionally between the 4th and 5th TMD. Based on their phylogenetic relationships, the CDF family can be classified into the three major metal transporter subgroups that include Zn-CDFs, Zn/Fe-CDFs, and Mn-CDFs (Montanini et al., 2007).

Other gene families such as BICAT (Bivalent Cation Transporter) (Hoecker et al., 2017), CaCA (Ca^{2+}/cation antiporter) (Pittman and Hirschi, 2016), VIT (The vacuolar iron transporter) (Cao, 2019) also are present in most plants. BICAT joins in the transport of Mn and Ca. Cation/Ca^{2+} exchanger (CCX) and the H^{+}/cation exchanger (CAX) are two important subfamilies in CaCA, which have been observed to be related to Mn transport. VIT transports carry both Fe^{2+} and Mn^{2+}, but their actual functions are still unclear. P2A-type Ca^{2+}-ATPases, which belong to plant P-type Ca^{2+}-ATPases, also play a role in Mn^{2+} transport. Some important gene families reported in seed development are listed in **Table 2.1.**

Table 2.1 Mn transport gene families involved in seed development.

Family	Species	Subcellular	Gene expression response	Reference
CaCA				
HvCAX2	Tomato		Up-regulated by c(Ca), c(Na)	Edmond et al. (2009)
OsCAX1a	Rice	Tonoplast		Kamiya et al. (2006)
OsCAX3	Rice			Kamiya et al. (2006)
CDF/MTP				
AtMTP8	*Arabidopsis*	Tonoplast	Up-regulated by Mn –Fe	Eroglu et al. (2016)
AtNRAMP3	*Arabidopsis*	Tonoplast	Up-regulated by Fe	Thomine et al. (2000)
AtNRAMP4	*Arabidopsis*	Tonoplast	Up-regulated by Fe	Lanquar et al. (2010)
YSL				
OsYSL2	Rice	Plasma membrane	Up-regulated by Fe, down-regulated by Mn	Koike et al. (2004)
ZIP				
HvlRT1	Barley	Plasma membrane	Up-regulated by Fe	Pedas et al. (2008)

2.5.3 Gene families of manganese transport among plant tissues

Since Mn was identified as a factor that can lead to marsh spot development, the process of Mn transportation from soil and finally into the plant cell should be examined. The first step in a plant's utilization of Mn is its absorption from the soil by the roots. Mn absorption occurs using an active transport system located in the epidermal root cells. It is then carried as the divalent cation of Mn^{2+} within the plants (Marschner, 1995). They are two main phases in the Mn absorption process. The initial, rapid uptake phase is reversible and does not require any energy consumption, Mn^{2+} and Ca^{2+} or other cations can be freely interchanged in the rhizosphere. Mn^{2+} is absorbed by the negatively charged cell wall constituents in the root-cell apoplastic spaces. In the second phase, which is not rapid, the Mn^{2+} exchange becomes more difficult. Plant metabolism influences the absorption in the symplast (Eugene et al., 1968), although the mechanisms are not precisely known (Humphries, 2007). The speed of ion carriers and channels that are involved in Mn^{2+} transportation vary dramatically. The amount of transported molecules through the plasma membrane can vary from thousands to millions (Humphries, 2007).

The distribution of Mn from the root cells in a plant requires primary movement in the xylem and transfer from the xylem to the phloem. The transpiration stream leads to xylem transfer from roots to the above-ground components of the plants. The phloem

has membrane proteins that control cation movement (Marschner, 1995). Mn moves slowly in the phloem. Mn redistribution often varies among plant species and with the growth stage. For example, insufficient Mn transport from roots to the seeds has been observed in wheat (*Triticum aestivium*) at maturity (Waters and Sankaran, 2011). The importance of the xylem in the Mn transport should be emphasized due to the low Mn mobility in the phloem.

Some proteins involved in Mn uptake by the roots have been studied in model plants such as *Arabidopsis*, rice (*Oryza sativa*) and barley (*Hordeum vulgare*) (Curie et al., 2000;Pedas et al., 2008;Sasaki et al., 2012). Natural resistance-associated macrophage protein (NRAMP) families are members of the major proteins implicated in Mn transportation from the root to the stem. Transporters that participate in Mn uptake, xylem loading, and root-to-shoot translocation have been more thoroughly studied in rice (*Oryza sativa*) compared to other plant species (Shao et al., 2017). *OsNRAMP5*, the first Mn^{2+} transporter gene identified in rice, is involved in the Mn^{2+} uptake and translocation (Sasaki et al., 2012). It was localized in the plasma membrane on the distal side of cells in the root and endodermis and is responsible for the initial absorption of Mn^{2+} from a soil solution. In addition, in *Arabidopsis*, *AtNRAMP1*, which is a homolog of *OsNRAMP5* in rice, also mediated Mn uptake (Cailliatte et al., 2010). The expression of *AtNRAMP1* in *Arabidopsis* is moderately upregulated by the lack of Mn (Cailliatte et al., 2010). Recently in barley, *HvNRAMP5*, a homolog of rice *OsNRAMP5*, was reported to be involved in Mn uptake and was observed in the plasma membrane of the epidermal cells (Wu et al., 2016). The expression of *HvNRAMP5* was up-regulated by a Fe limitation rather than an Mn deficiency. In various root structures, Mn uptake was influenced by the environment (i.e., climate and soil type), which resulted in different responses to variations in Mn availability among species (Rieuwerts et al., 1998). Fe limitation may also explain why in a previous study, marsh spot was not clearly associated with Mn deficiency (Moraghan and Grafton, 2000). Compared to *OsNRAMP5*, *AtNRAMP1* and *HvNRAMP5,* which were localized in the epidermis, *OsNRAMP3* was responsible for the transfer of Mn^{2+} from the xylem to the phloem at the basal node of rice (Yamaji et al., 2013). However, at high Mn availability, it also was distributed to mature tissues. Therefore, in rice nodes, *OsNRAMP3* functions as a switch for Mn distribution, whereby the protein is activated or deactivated in response to fluctuating Mn concentrations. When Mn was limited, there would be more Mn transferred to the upper node/panicle through the phloem under the control of

OsNRAMP3 (Yamaji et al., 2013). A homolog of *OsNRAMP3* also may have an influence on Mn transpiration flow to plant seeds.

The transporter gene *OsMTP9*, located near to *OsNRAMP5* in root epidermis endothelial cells, is responsible for the Mn^{2+} uptake and translocation (Ueno et al., 2015). Subsequently, *OsMTP9* was located in the plasma membrane on the proximal side of those rice cell layers, where it arbitrates the export of Mn^{2+} into the stele (Sasaki et al., 2012). Mn^{2+} uptake and root-to-shoot translocation were highly diminished when either *OsMTP9* or *OsNRAMP5* was knocked out, which indicates that those transporter genes were responsible for moving Mn^{2+} from the soil to the xylem. Radial movement of Mn^{2+} was carried out by polarly localized transporters at both the exodermis and the endodermis, which provided a unidirectional flow of Mn from the soil to the stele. Thus, in soils within the same concentration of Mn, total amounts of absorbed Mn would be significantly different during the expression presence of *OsNRAMP5, OsMTP9* and their homologs (Sasaki et al., 2012).

Moreover, Yellow Stripe-Like (YSL) transporters were also involved in Mn uptake. In the long-distance transport and distribution of Mn in rice, it may be conveyed as Mn^{2+}-Na^{+} as well as an Fe-Na complex (Koike et al., 2004). Since *OsYSL2* also was observed in developing seeds, Mn accumulation in seeds was regulated by *OsYSL2*. In *Arabidopsis*, the YSL family also was reported to contribute to Mn translocation. Decreases in Mn concentration have been observed in leaves during *Arabidopsis* senescence, while in *ysl1ysl3* double mutant plants the Mn concentration remained at the same level (Waters et al., 2006). Hence, both *AtYSL1* and *AtYSL3* are thought to be the Mn^{2+}-Na^{+} transporters. In the absence of *AtYSL1* and *AtYSL3,* Mn could not be transported to new tissues from ageing leaves.

Unlike NRAMP, the expression of the two members of the ZIP (Zrt and Irt-like protein) family, *AtZIP1* and *AtZIP2*, were not affected by Mn deficiency (Milner et al., 2012). Those two proteins were involved in the transport of Mn in root stellar cells. Both of them were expressed in the root stele, but at different subcellular locations. *AtZIP1* was present in the tonoplast and took part in remobilizing Mn from the vacuoles to the cytoplasm. In contrast, *AtZIP2* was positioned in the plasma membrane and may regulate Mn uptake into root stellar cells. In barley, *HvIRT1*, which also belongs to the ZIP family, was involved in Mn uptake, and its expression was moderately induced by Mn deficiency (Pedas et al., 2008).

2.5.4 Protein families involved in manganese transport among subcellular components

After Mn has been transported into plant tissues and enters a plant cell, Mn is further transferred to provide an adequate quantity to the Mn dependent targets or for storage. Mn was reported in all organelles, including ER, Golgi apparatus, mitochondria, plastids, and peroxisomes, where it performs specific cellular functions as previously mentioned. In addition, despite the importance of Mn transportation in plant, the storage and accumulation of Mn, especially in vacuoles and chloroplasts, may also play a role in Mn deficiency that results in marsh spot disease. As previously mentioned, Mn is required in photosynthesis, especially in the formation of Mn_4Ca –clusters in the OEC of PS II. *AtBICAT1* and *ATBICAT2*, two members of BICAT family, which were reported to be the Mn transporters in chloroplast membranes involving Mn distribution and loading on the chloroplast (Demaegd et al., 2013;Brandenburg et al., 2017). *AtBICAT1* was identified on the thylakoid membrane and mediated Ca^{2+} and Mn^{2+} flux into the thylakoid lumen (Schneider et al., 2016;Frank et al., 2019). In *bicat1* mutants, there was a transient elevation of the stromal free Ca^{2+} when mutants were induced by a light-to-dark shift. *AtBICAT1* were supposed to be involved in the process of flux into thylakoids for Mn_4Ca-cluster assembly and regulated numerous processes in chloroplasts by affecting the homeostasis of stromal Ca^{2+}(Sello et al., 2018). *AtBICAT2*, another member of BICAT family, have been reported to be located on the chloroplast envelope and join in the mediating Ca^{2+} and Mn^{2+} homeostasis in organs (Eisenhut et al., 2018;Frank et al., 2019). The expression of both *AtBICAT1* and *ATBICAT2* could alleviate sensitivity Ca^{2+} and Mn^{2+} phenotypes of yeast mutants. The location where *AtBICAT2* was expressed could cause chlorosis and defective thylakoid stacking.The plant growth was severely impaired by the decreasing PS II complexes that lead to diminished photosynthetic activity (Eisenhut et al., 2018;Frank et al., 2019).

Mn-CDF comprises a subgroup of the CDF/MTP families that participate in the sequestering of Mn into the vacuoles. *AtMTP8*, one of the members of Mn-CDF, plays an important role during seed development. *AtMTP8* has been identified as a transporter of Fe and Mn (Chu et al., 2017). An analysis of metal localization in embryos by XRF tomography showed that *AtMTP8* is responsible for the specific accumulation of Mn in

the subepidermal cells on the abaxial side of the cotyledons and cortical cells of the hypocotyl, which were very close to the location of marsh spot symptoms (Chu et al., 2017). A similar distribution of Fe and Mn in all the cell types of *Arabidopsis* embryos was observed in an mtp8vit1 double mutant. These results indicate that Mn and Fe allocation are determined by the two primary transporter genes, *AtMTP8*, and *AtVIT1* (Chu et al., 2017).

The VIT gene *AtVIT1*, also was identified as a vacuolar Fe/Mn transporter. In *Arabidopsis, AtVIT1* was involved in the allocation of Fe to perivascular strands of seed embryos. When either *VIT1* or *MTP8* was silenced, the location where Mn and Fe accumulated dramatically changed. Fe or Mn was not accumulated in specific cell types, but distributed among all cell types in the seeds. Those mutants later showed symptoms of micronutrient deficiencies (Chu et al., 2017).

In rice, when *OsVIT1* and *OsVIT2* were ectopically expressed in yeast, a Fe^{2+} and a Zn2+ sensitive strain showed increased accumulations of Fe^{2+}, Zn^{2+} and Mn^{2+} in the vacuole. Similar to *AtVIT1*, when analyzing the metal composition of the vacuole, significant Mn accumulation was reported in cells in which those two genes were expressed (Zhang et al., 2012). Moreover, two VIT homologs were located in the tonoplasts of wheat. Only one of them, *TaVIT2*, could supply an Mn-sensitive yeast strain with Mn. By overexpressing *TaVIT1* by controlling an endosperm promoter, Mn content in wheat grains was significantly increased (Connorton et al., 2017a). Although proteins in other plants such as pea or beans have not been fully examined, those plants or cultivars with homologous VIT families would probably prevent marsh spot symptoms from forming in their seeds.

The CAX family mainly regulates the influx of cations into the vacuole. Its members are metal transporters that arbitrate the influx of cations into the vacuole (Enrico et al., 2012). CAX2-like transporters of other species, such as tomato (*Solanum lycopersicum*) *LeCAX2* and barley *HvCAX2*, transported Ca^{2+} and Mn^{2+} into yeast vacuoles upon heterologous expression, but with different transport kinetics (Edmond et al., 2009). *HvCAX2* was expressed ubiquitously in the roots, shoots, immature flowering spikes, and seeds, preferentially in the embryo rather than in the endosperm of barley seeds (Edmond et al., 2009).

Two NRAMP transporters, *AtNRAMP3* and *AtNRAMP4*, localized in the tonoplast of *Arabidopsis* (Thomine et al., 2003). Although the number of *AtNRAMP3* and *AtNRAMP4* proteins were not affected by a lack of Mn, the expression of *AtNRAMP4*

was induced under Fe-limited conditions (Lanquar et al., 2005). In *Arabidopsis* leaf mesophyll cells with the *nramp3* and *nramp4* double mutants, Mn concentrations were similar to those in the wild-type plant cells, while an increased accumulation of Mn in the vacuoles was observed. In the case of an Mn deficiency, diminished growth was observed in the double mutant. This was correlated to reduced photosynthetic activity caused by a shortage of Mn for the formation of OEC complexes in PSII (Lanquar et al., 2010). In addition, those two proteins also regulated the exportation of Mn from the leaf vacuoles to the seeds. Thus, the absence of *AtNRAMP3* and *AtNRAMP4* affected nutrient distribution in the leaves and uptake by seeds. Some transporters observed in seed subcellular components are shown in **Figure 2.4**.

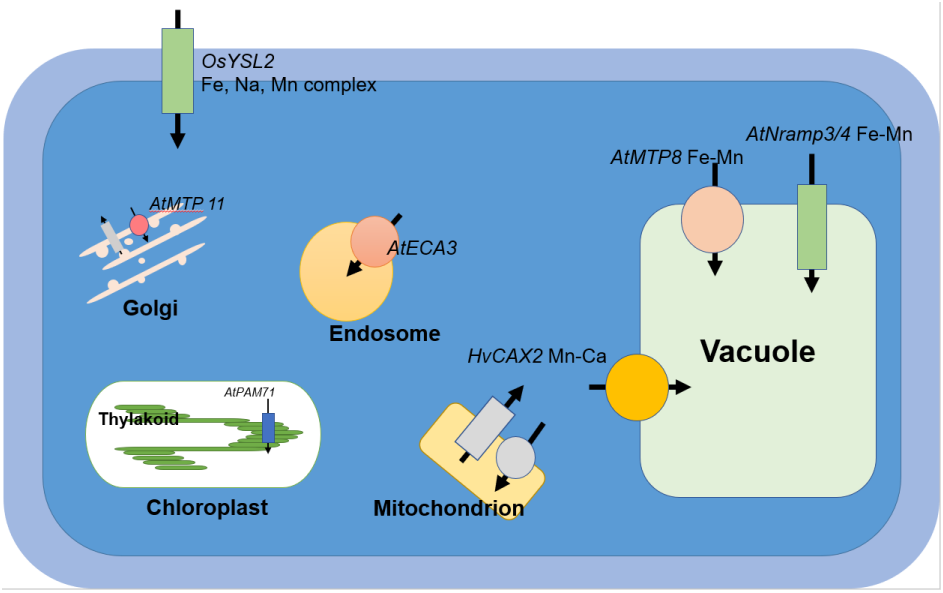

Figure 2.4 Subcellular components of Mn transport genes in plant seed cells. *OsYSL2* participates in the Mn-Na complex from the apoplast to cytoplasm. Then, *AtECA3* partitions Mn in the vesicles (Mills et al., 2008). *AtMTP8* and *AtNRAMP3/4* are two transmembrane proteins, which are responsible for the import and export of Mn from the vacuole. Golgi secretes vesicles with the help of *AtMTP11* (Delhaize et al., 2007). *AtPAM71* is an essential protein in the absorption of Mn by the thylakoid. Although Mn widely exists among subcellular components, some of the proteins (colored in grey) involved in Mn transport are still unknown.

2.5.5 Previous studied on quantitative trait loci (QTL) and candidate genes associated with marsh spot disease resistance and Mn deficiency

Some major and minor QTL associated with Mn efficiency-related traits have been reported. With the help of inductively coupled plasma (ICP) spectrophotometry to measure Mn concentrations in common bean seeds, Blair et al detected three QTL that

were associated with Mn concentration (Blair et al., 2011). Leplat et al performed chlorophyll a fluorescence analysis on 248 barley varieties, which were cultivated in six low Mn concentration fields for quantifying Mn deficiency. Using the genome-wide association study (GWAS) they detected 54 QTL related to the generation of PSII subunit proteins, germin-like proteins, and Mn superoxide dismutase (Leplat et al., 2016).

Most studies have focused on Mn accumulation in plant seeds. A total of six QTL that control Mn concentration in lentil (*Lens culinaris*) seeds were identified using linkage-based mapping of 120 lentil recombinant inbred lines (RILs); these major QTL explained 15-24.1% of Mn concentration variation (Ates et al., 2018). Ten QTL for Mn concentration in canola (*Brassica napus*) seeds were detected, which were distributed across 8 chromosomes, and explained 9.1-16.4% of the total variation (Ding et al., 2010). In a study of *Lotus japonicus*, two QTL associated with Mn concentration explained 35.2% of the phenotypic variation and were identified on chromosomes 1 and 2 (Klein and Grusak, 2009). Using RILs derived from a cross of 93–11 with PA64s (with a high grain Mn concentration), one major QTL controlling Mn accumulation in rice grains was identified (Liu et al., 2017a). Some of the QTL mapping studies related to Mn efficiency are listed in **Table 2.2**.

2.6 Joint segregation analysis

2.6.1 Basic principle

Some quantitative traits are controlled by a few major genes and a series of polygene of which major genes can be detected separately and polygenes are collectively spotted. Genetic models for those quantitative traits are usually composed of mixed major-gene plus polygenes with additive, dominant and epistatic effects.

Joint segregation analysis (JSA) has been developed to jointly use phenotypic data from different generations of a bi-parental population to test whether the frequency distribution of the phenotypic data of a trait is best-fitted to the theoretical distribution of the trait underlying the specified genetic model (Zhang et al., 2003b). JSA hypothesizes that the distribution of the trait phenotypes in a segregation population (such as DH and RIL) is a mixed distribution consisting of several individual normal distributions (called component distributions) that are modified by both polygenes and environments. Each component distribution may be formed due to a major gene (Gai et

al., 2007). Based on the number of major genes (one major gene, two major genes, three major genes, and four major genes), the combinations of major genes and polygenes (one major gene with polygenes, two major genes with polygenes, and three major genes with polygenes), and different gene effects (additive and dominance effects of major genes, additive × additive, additive × dominance, dominance × additive, dominance × dominance epistatic effects of major genes and polygenes), different genetic models have been developed for different types of genetic populations (Zhang et al., 2001;Zhang et al., 2003b). For each proposed model, the joint maximum-likelihood function is constructed from the phenotypic data of the genetic populations, including the segregation population (HD or RIL) and their two parents, to estimate genetic parameters (such as μ and σ^2) of each component distribution through an Iterated Expectation and Conditional Maximization (IECM) algorithm (Wang, 1996;Zhang et al., 2001;Gai et al., 2007). The selection of the best-fit genetic model is based on three criterions: (1) the smallest Akaike Information Criterion (Zhang et al., 2003b;Koike et al., 2004), (2) the highest heritability of the proposed gene model (the proportion of phenotypic variance explained by the model) (Beshir et al.) and no significant statistical difference between the empirical data distribution and the theoretical distribution underlying the genetic model. *AIC* is calculated by the formula $AIC = 2k - 2\ln\hat{L}$, where k is the number of estimated parameters in the model and $\hat{L}$ is the maximized value of the likelihood function for the model. The statistical tests include uniformity tests (U_1^2, U_2^2, and U_3^2) for the mean, second moment and variance, as well as Smirnov (nW^2) and Kolmogorov (D_n) statistical tests to test the significant differences between the empirical data distribution and the theoretical distribution underlying the hypothesized models (Zhang et al., 2003b). Finally, the related genetic parameters, including gene effects and genetic variances of major genes and polygenes and their corresponding heritability values are calculated from the estimates of component distributions (Zhang et al., 2001;Zhang et al., 2003b;Gai et al., 2007).

Table 2.2 QTL loci and candidate genes related to Mn efficiency.

Species	Trait	No. QTL	Chr	Material	Potential functional gene	Marker	Method	Reference
Phaseolus vulgaris	Seed Mn con.	3	Chr 1, 5, 8	RILs		SSR, RFLP	CIM	Blair et al. (2016)
Lotus japonicus	Seed Mn con.	2	Chr 1,2	RILs		SSR, dCAPS	MQM	Klein and Grusak (2009)
Lens culinaris	Seed Mn con.	6	Chr 1, 3, 7	RILs		SNP	CIM	Ates et al. (2018)
Brassica napus	Seed Mn con.	10	A3, A4, A6, A10 C3, C8, A1, A9, A10	RILs	CAX, UGP, IRT1, NRAMP5 and AZF2	SNP	CIM	Ding et al. (2010)
Oryza sativa	Seed Mn., Cd. con.	11 minor, 1 major	Chr 1-10, qGMN7.1 on Chr 7	RILs, CSSL	OsNRAMP5	SNP, InDel, SSR	IM	Liu et al. (2017a)
Oryza sativa	Seed Mn con.	1	Chr 4	RILs	OsZIP3	SSR	GLM, MLM	Nawaz et al. (2015)
Brassica rapa	Leave Mn con.	2	Chr 5,6	DH		AFLP, SRAP, ESTP	MQM, IM	Wu et al. (2008)
Hordeum vulgare	Chl a fluor., leave Mn con.	54 (Chl a fluor.), 4 leave Mn con.)	Chr 2-7	248 Barely varieties	AK368229, MLOC_18354.1, MLOC_38362.2, AK368229, MLOC_18354.1 (Chl a/b binding); MLOC_75098.2, AK367749 (Mn binding); MLOC_3173.4, AK374059, AK357955 (PP2C); MLOC_40094.1 (PSI); AK251925.1, MLOC_82113.1, AK249774.1, MLOC_77860.1, AK369292 (PSII)	SNP	MLM	Leplat et al. (2016)

Mn con.: Mn concentration; Cd con.: Cd concentration; fluor.: fluorescence; P: phosphorus concentration; CSSL: chromosome segment substitution line; SNP: single nucleotide polymorphism; AFLP: Amplified fragment

length polymorphism; SSR: simple sequence repeat; SRAP: sequence-related amplified polymorphism; ESTP: expressed sequence tagged polymorphism; dCAPS: derived cleaved amplified polymorphic sequence; InDel: insertion and deletion sequence; IM: Interval mapping; CIM: Composite interval mapping; MLM: Mixed linear model; GLM: Generalized linear model; MQM: Multiple QTL mapping.

2.6.2 Genetic models

To date, some genetic models have been derived from 14 different populations that have been implemented in the R package SEA (https://cran.r-project.org/web/packages/SEA/index.html) : 1) SEA-F2 (F_2); 2) SEA-F3 ($F_{2:3}$); 3) SEA-DH (DH or RIL); 4) SEA-BIL (B_1); 5) SEA-BC (B_1 & B_2); 6) SEA-BCF ($B_{1:2}$ & $B_{2:2}$); 7) SEA-G4F2 (P_1, P_2, F_1 and F_2); 8) SEA-G4F3 (P_1, P_2, F_1 and $F_{2:3}$); 9) SEA-G3DH (P_1, P_2 and DH); 10) SEA-G5BC (P_1, P_2, F_1, B_1 and B_2); 11) SEA-G5BCF (P_1, P_2, F_1, $B_{1:2}$ and $B_{2:2}$); 12) SEA-G5 (P_1, P_2, F_1, F_2 and $F_{2:3}$); 13) SEA-G6 (P_1, P_2, F_1, F_2, B_1 and B_2); 14) SEA-G6F (P_1, P_2, F_1, $F_{2:3}$, $B_{1:2}$ and $B_{2:2}$) (**Table2.3**).

Table 1.3 Genetic population types included in the R package SEA (https://cran.r-project.org/web/packages/SEA/index.html).

No.	Population	Population abbreviation	No.	Population	Population abbreviation
1	F_2	SEA-F2	8	P_1, F_1, P_2 and $F_{2:3}$	SEA-G4F3
2	$F_{2:3}$	SEA-F3	9	P_1, P_2 and DH and RIL	SEA-G3DH
3	DH and RIL	SEA-DH	10	P_1, F_1, P_2 and B_1 and B_2	SEA-G5BC
4	BIL	SEA-BIL	11	P_1, F_1, P_2 and $B_{1:2}$ and $B_{2:2}$	SEA-G5BCF
5	B_1 and B_2	SEA-BC	12	P_1, F_1, P_2, F_2 and $F_{2:3}$	SEA-G5
6	$B_{1:2}$ and $B_{2:2}$	SEA-BCF	13	P_1, F_1, P_2, F_2 and B_1 and B_2	SEA-G6
7	P_1, F_1, P_2 and F_2	SEA-G4F2	14	P_1, F_1, P_2, $F_{2:3}$, $B_{1:2}$ and $B_{2:2}$	SEA-G6F

DH: doubled haploid; RIL: recombinant inbred line; BIL: backcross inbred line; $B_1 = F_1 \times P_1$; $B_2 = F_1 \times P_2$; $B_{1:2}$ and $B_{2:2}$ families are derived from B_1 and B_2, respectively.

SEA has implemented a total of 35 genetic models that hypothesize zero to four major genes with additive, dominant and epistatic effects and/or polygenes for the DH or RIL population to detect the most likely genetic models underlying traits (**Table 2.4**).

Table 2.4 Thirty-five genetic models for the DH or RIL population in SEA.

No.	Model	No. of major genes	Major gene effect	Polygenes effect
1	PG-AI	0	-	Additive-epistasis
2	PG-A	0	-	Additive
3	1MG-A	1	Additive	
4	MX1-A-AI	1	Additive	Additive-epistasis
5	MX1-A-A	1	Additive	Additive
6	2MG-EA	2	Equally additive	
7	2MG-ED	2	Epistatic dominance	
8	2MG-ER	2	Epistatic recessive	
9	2MG-AE	2	Additive effect	
10	2MG-CE	2	Complementary effect	
11	2MG-DE	2	Duplicate effect	
12	2MG-IE	2	Inhibiting effect	
13	MX2-AI-AI	2	Additive-epistasis	Additive-epistasis
14	MX2-AI-A	2	Additive-epistasis	Additive
15	MX2-A-A	2	Additive	Additive
16	MX2-EA-A	2	Equally additive	Additive
17	MX2-ED-A	2	Epistatic dominance	Additive
18	MX2-ER-A	2	Epistatic recessive	Additive
19	MX2-AE-A	2	Additive effect	Additive
20	MX2-CE-A	2	Complementary effect	Additive
21	MX2-DE-A	2	Duplicate effect	Additive
22	MX2-IE-A	2	Inhibiting effect	Additive
23	3MG-AI	3	Additive-epistasis	
24	3MG-A	3	Additive	
25	3MG-CEA	3	Completely equally additive	
26	3MG-PEA	3	Partially equally additive	
27	MX3-AI-AI	3	Additive-epistasis	Additive-epistasis
28	MX3-AI-A	3	Additive-epistasis	Additive
29	MX3-A-A	3	Additive	Additive
30	MX3-CEA-A	3	Completely equally additive	Additive
31	MX3-PEA-A	3	Partially equally additive	Additive
32	4MG-AI	4	Additive-epistasis	
33	4MG-CEA	4	Completely equally additive	
34	4MG-EEA	4	Two equally additive	
35	4MG-EEEA	4	Three equally additive	

CE, *AABB*: (*AAbb*+*aaBB*+*aabb*); ER, *AABB*:*AAbb*:(*aaBB*+*aabb*); ED, (*AABB*+*AAbb*):*aaBB*:*aabb*; DE, (*AABB*+*AAbb*+*aaBB*):*aabb*; IE, (*AABB*+*aaBB*+*aabb*):*Aabb*.

2.6.3 Software tool

The R package SEA is developed based on the framework of the Microsoft Visual Studio 2010 platform and C++ programming language (https://cran.r-project.org/web/packages/SEA/index.html). Both single- and joint multi-generation analysis can be performed using SEA package. To date, the software supports 14 genetic populations (**Table 2.3**) and 35 genetic models are implemented for DH or RIL population (**Table 2.4**). In particular, this package implements the estimation of posterior probabilities of major-gene genotypes for each line using Monte Carlo algorithm, providing an approach to predict the genotypes of individuals in the

population for the underlying genetic model.

The SEA has a graphics user interface (Rendón-Anaya et al.) and can run on both Windows and Linux systems. In the GUI of SEA, users need to choose a phenotypic dataset file, a population, a genetic model and number of plants measured in each family (**Figure 2.5**). Then press 'RUN' button to start running the program. As soon as the execution is done, the result file in .csv format can be downloaded by pressing 'Download result'. The result file includes maximum likelihood estimation, AIC value, first and second genetic parameters and their statistical test results for each model (**Figure 2.6**). Besides, posterior probability of genotype of each individual in the population can also be calculated (**Figure 2.7**).

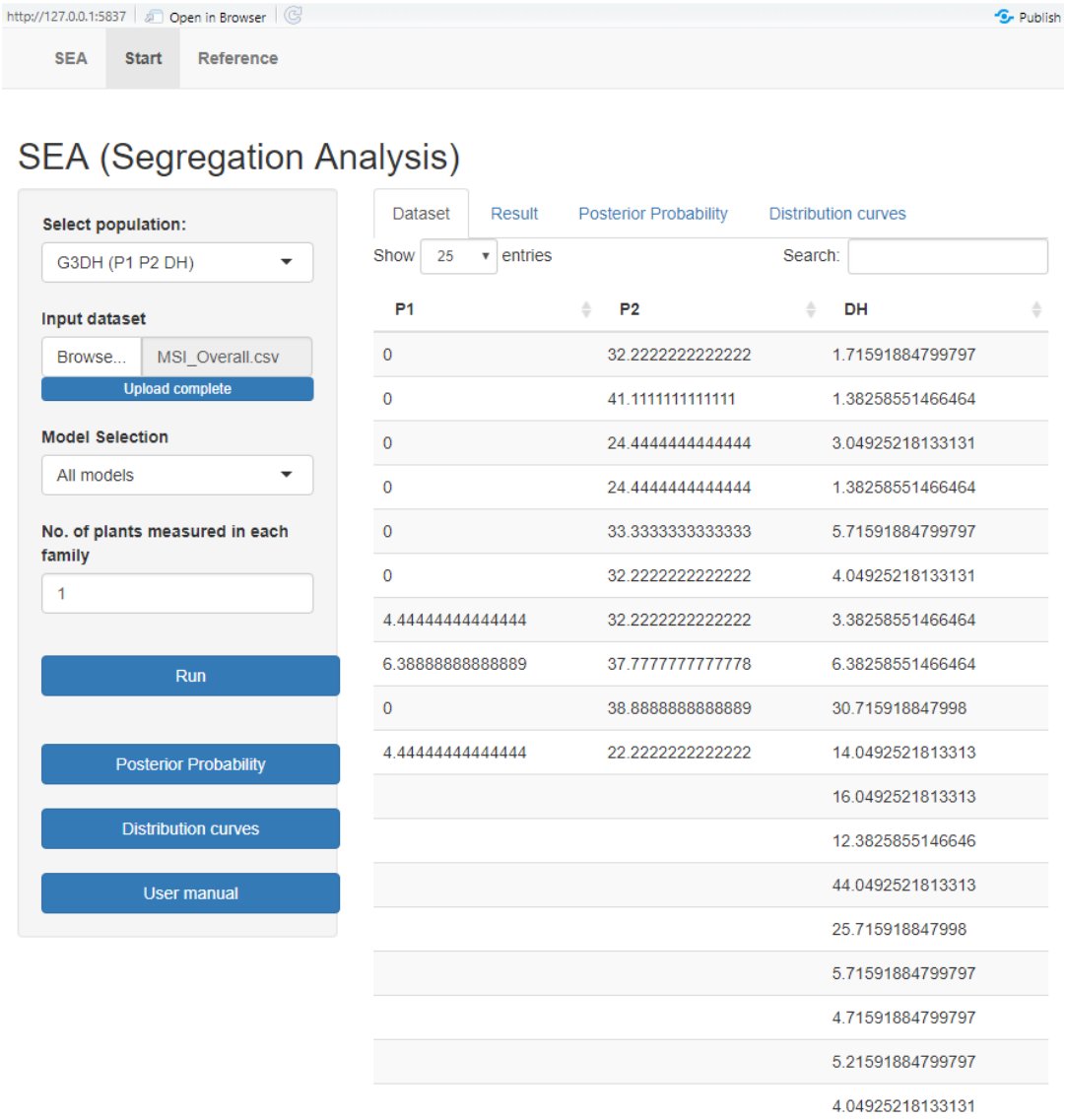

Figure 2.5 Graphics user interface of SEA showing input dataset file and parameter selection (population, genetic model and number of plants in each family).

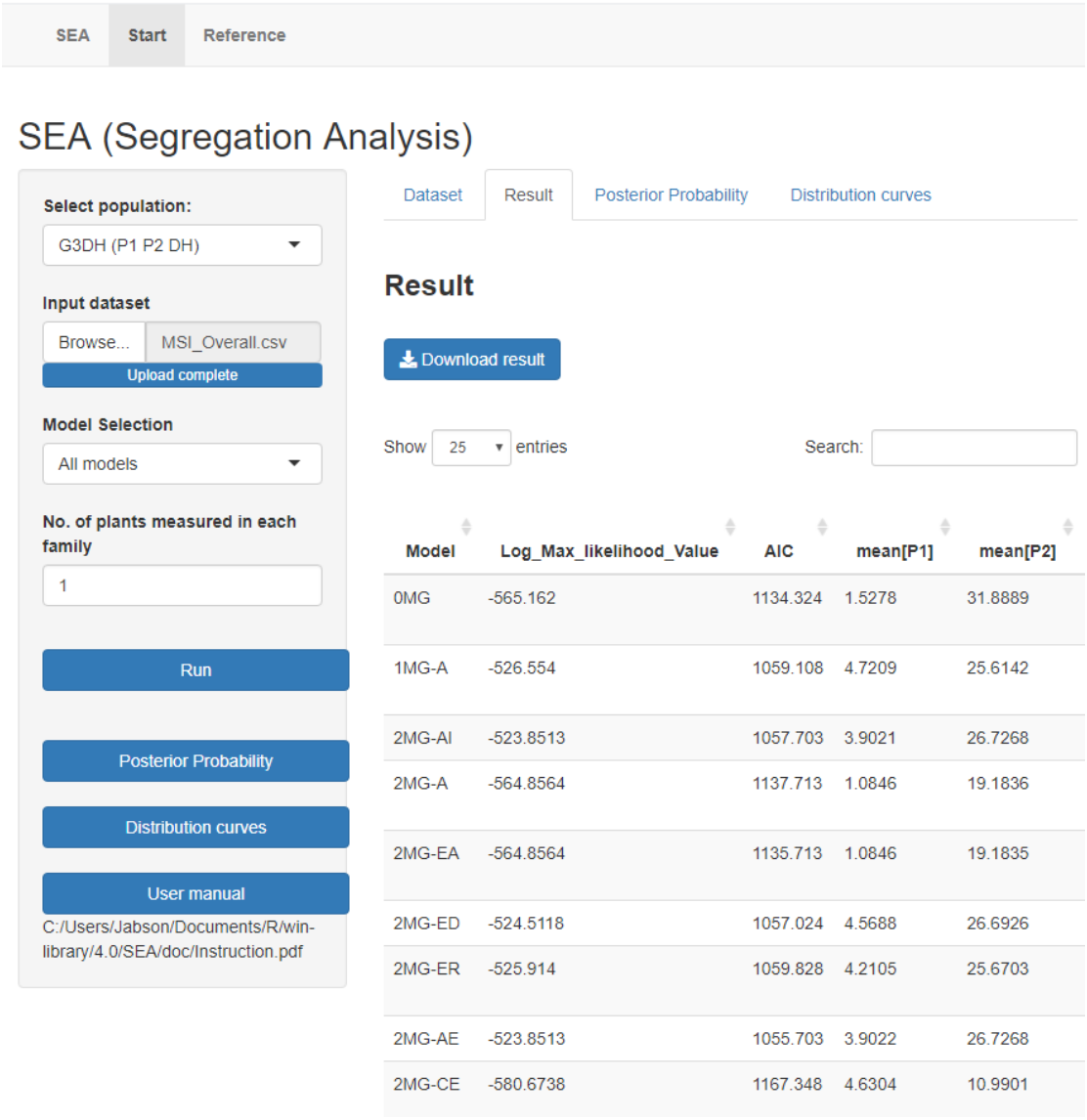

Figure 2.6 The result of SEA program.

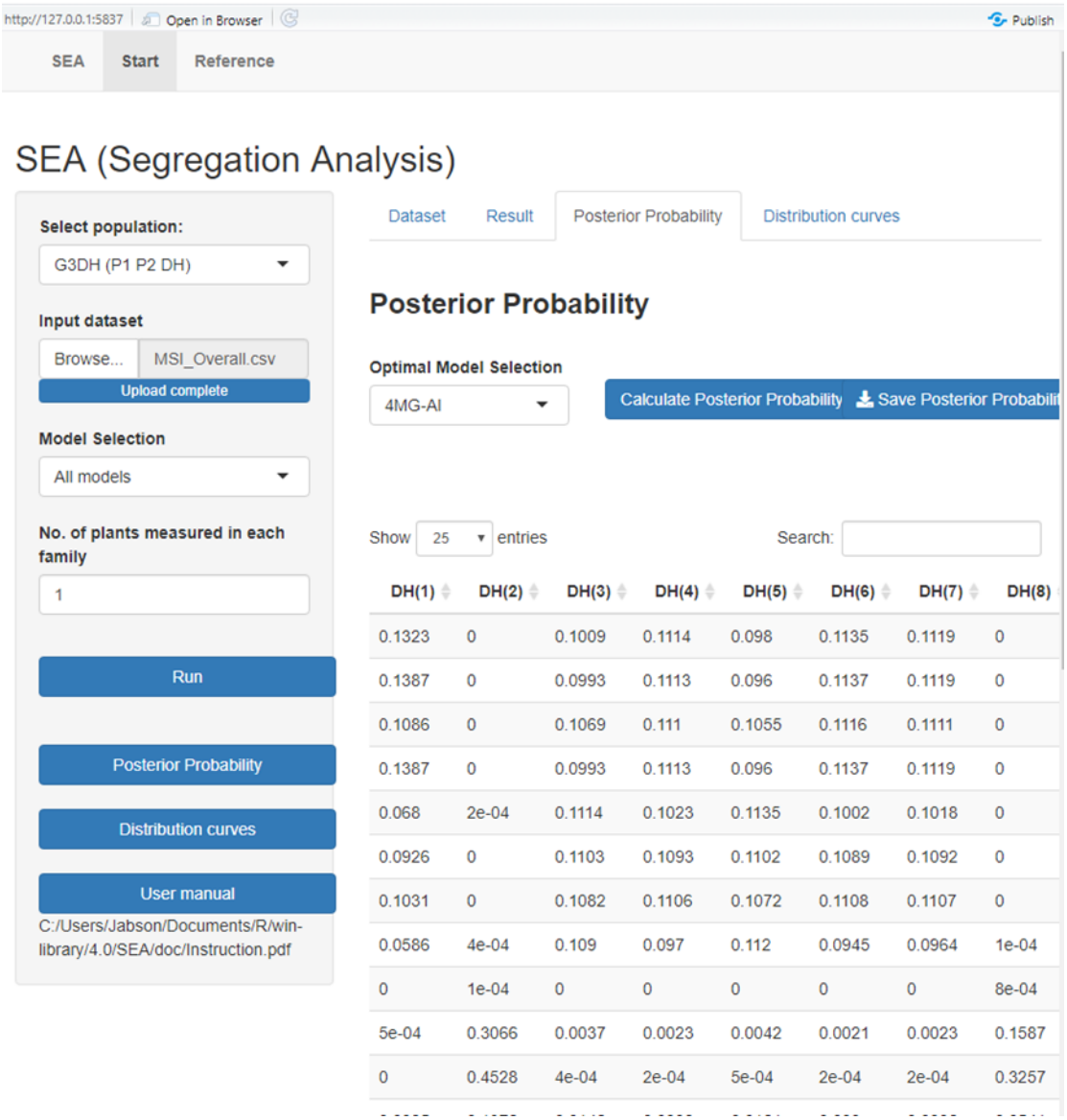

Figure 2.7 Posterior probability of the selected optimal model in SEA.

2.7 Linkage based QTL mapping

2.7.1 Genomics assisted selection

Traditionally, breeders develop new cultivars through field performance evaluation records across diverse environments, and they only select the best plants that meet their target traits for generation advancement. But this trait phenotype-assisted selection takes a long time and may lose some valuable genes during the selection process (Collard and Mackill, 2008). In some extreme cases that phenotypic variation is mostly caused by environment, it is difficult for breeders to select individuals from their phenotypic performance. With the development of genotyping technologies, marker

assisted selection (MAS) has been widely used for breeding of some major genes-controlled traits (Collard and Mackill, 2008) . However, most traits of economic and agronomic importance are quantitative and genetically controlled by both major genes and polygenes. In addition, unlike most Mendelian diseases in humans that result from protein-coding mutations (Lander and Botstein, 1989), complex traits are often caused by rare mutations or those noncoding-mutations that are considered to regulate gene expression (Boyle et al., 2017). MAS refers to a strategy where interested traits can be archived by indirectly using molecular markers. Genomic selection (GS) is one of markers-based selection approaches, involving all genetic markers across genome. Owing to the development of sequencing technology, molecular markers such as genome-wide single nucleotide polymorphisms (SNPs) can be effectively detected at a low cost; then researchers can use SNPs to detect potential QTL or quantitative trait nucleotides (QTNs) in genomes, thus allowing breeders to develop superior cultivars through genomics-based selection for qualitative and quantitative trait improvement (Edwards et al 1987). The resources such as high-resolution genetic maps and solid QTL would greatly facilitate marker assisted selection (Perumalsamy et al., 2010) (**Figure 2.8**).

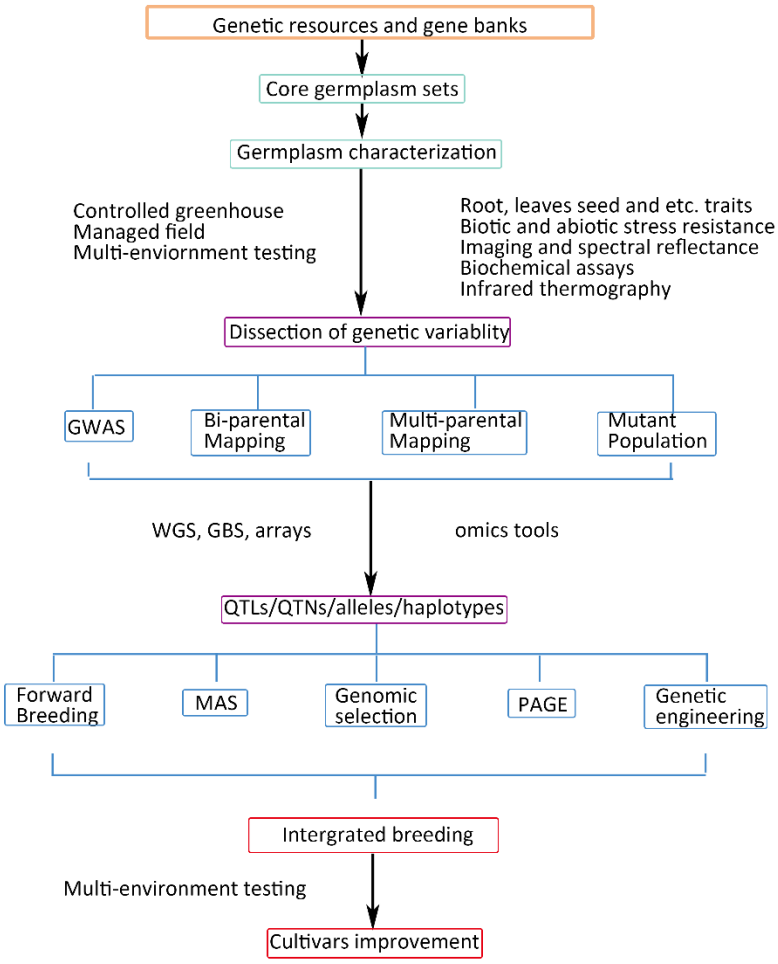

Figure 2.8 Major strategies of molecular marker assisted selection for crop improvement.

2.7.2 SNP discovery

2.7.2.1 Next generation sequencing (NGS)

Next generation sequencing (NGS) (Chung et al., 2017) has become one of indispensable technologies in biological studies. Advancement in sequence technology including sequencing approaches, library construction and data analysis methods reduce sequencing costs and thus leading to great progress in many research fields. NGS contains two major paradigms: short-read and long-read sequencing. Short-read sequencing is mainly used for population-level research and variant discovery, or just sequence the specific clusters of genes or exomes, while long-read sequencing is suitable for whole genome assembly (Sara et al., 2016). In general, NGS mainly includes three most commonly used methods: (1) the Roche/454 FLX (http://www.454.com), (2) the Illumina/Solexa Genome Analyzer

(http://www.illumina.com), and (Beshir et al.) the Applied Biosystems SOLiDTM System (http://marketing.appliedbiosystems.com).

454 FLX sequencing technology was first proposed by Jonathan Rothberg (Green et al., 2006). 454 sequencing first breaks DNA into 300-800bp fragments by nebulization, then each fragment is ligated with different adaptors at both end and construct DNA libraries. DNA is further amplified 1 million times by emulsion PCR and finally sequenced by a large-scale parallel pyrosequencing. 454 FLX had discontinued since 2014.

SOLiDTM (http://marketing.appliedbiosystems.com) fragments DNA and add adaptors to construct single-strand DNA libraries. Then emulsion PCR is used for amplification as well. Unlike 454 and Illumina, SOLiDTM adopts DNA ligase with a two-base encoding scheme for sequencing. Each data point includes two bases and each base is tested two times which significantly improve accuracy and avoid many problems occurred in high-throughput sequencing approaches such as inaccurate recording of homopolymer sequences (Karp and Rabin, 1987;Shendure et al., 2005). So that sequence errors and positive variation could be better distinguished.

The Genome Analyzer was first proposed by Solexa and then improved by Illumina (Kircher and Kelso, 2010). With the DNA polymerase and fluorophore-labeled terminator nucleotides, Illumina technology uses reversible terminator chemistry synthesis for DNA amplification and sequencing. Clonal amplification is based on solid-phase PCR where single-stranded DNA fragments with hundred base pairs length are ligated to adapters and then hybrid with flow cells. Then DNA amplification will occur on flow cell surface with complementary oligonucleotide binding to the free 3' end of adapter, forming a bridge structure so called bridge PCR. Because single DNA fragments are fixed to one channel on flow cell, after amplification, each channel would contain millions DNA and form the cluster. Double strand DNAs will then be filtered to single strand for next sequencing. Later, four fluorophore-labeled terminator nucleotides are added into reaction. Each cycle will gain one image to identify one read for sequence until total read length reach to 100bp length (Kircher and Kelso, 2010).

In the NGS platforms for short reads, 454 FLX platform can generate longest reads with up to 500bp to date (Margulies et al., 2005). Thus, 454 FLX platform is more applicable for *de nova* sequencing on unknown genome, while when it comes to continuous repeat sequences, the accuracy would lower down. Compare with 454 FLX, SOLiDTM and Illumina have shorter reads about 30 bp and 300bp length, respectively.

Although SOLiDTM has higher accuracy on SNP discovery, Illumina outperformed SOLiDTM in high throughput especially in population research. Illumina is suitable for genome resequencing because of its high throughput and low cost. Thus, Illumina befits our research better.

2.7.2.2 Genotyping by sequencing (GBS)

Genotyping-by-sequencing (GBS) is a novel genotyping method to identify genome-wide SNPs using NGS technology (Elshire et al., 2011). , GBS outperforms other approaches such as SNP array in accuracy on detection of rare alleles (Darrier et al., 2019). Two strategies had been reported for GBS with NGS technologies, multiplex enrichment PCR with a set of detected SNPs and restriction enzyme (RE) digestion without prior SNP discovery. The first method aims to amplify specific areas of genome using PCR primes. And in the second approach, GBS simplifies the complexity of genomes by using restriction enzyme digestion to cleave genomes into fractions with the help of DNA barcode adapters. Then fragmented DNA is amplified by PCR and sequenced by NGS technology. Because most restriction sites in genomes are relatively conservative, GBS is a feasible and stable approach to survey a large number of markers for a population. Besides, REs used in GBS such as *Ape*KⅠ, *Msp*Ⅰ and *Pst*Ⅰ are sensitive to methylation, which significantly reduce disturbance from repetitive sequence when appropriate RE is selected for library construction (Elshire et al., 2011). A subset of the genome fractions could be gained within specific REs, providing higher coverage per locus. However, at the same time some crucial genomic region can be ignored by GBS because of the lack of REs binding loci. To deal with this problem, several GBS libraries which employed different REs combination have been proposed such as Double-digested GBS (Poland et al., 2012), Double-digested RAD-seq (Stolle and Moritz, 2013) and Restriction enzyme sequence comparative analysis (Monson-Miller et al., 2012).

In sequenced accessions or lines, genetic variants such as InDels and SNPs can be marked across genome. For example, using *Ape*KⅠGBS library, a total of 75,000 sequence tags detected by GBS procedures were mapped to reference genomes from common bean RILs, which demonstrated the availability of GBS approach (Hart and Griffiths, 2015).

Furthermore, appropriate enzymes can increase the coverage of SNPs across the genome. For large and complex genomes, library construction for GBS can use restriction enzyme digestion to reduce genome size; for small genomes like flax and common bean, whole genome resequencing is also applicable at a low cost (Chung et al., 2017).

GBS provides a fast, low-cost and high-throughput methods for genome-wide genetic variation analysis, combining procedures of marker discovery and genotyping. In addition, complex genome can also be directly genotyped without reference genome or previous information.

Currently, QTL mapping requires high-density genome-wide SNPs to detect potential loci associated with important traits and GBS has been widely used for genotyping in GWAS, linkage-based QTL mapping, MAS and genomic selection in molecular breeding (He et al., 2014).

2.7.3 Bi-parental genetic population

For QTL mapping, a population of sufficiently large size needs to be constructed. Mapping populations basically can be divided into two types, temporary populations such as F_2 populations, and permanent populations, such as backcross (BC), DH and RIL (Sandhu et al., 2018) populations. In this study, we constructed an RIL population for QTL mapping. When constructing an RIL population, progenies from the F_2 generation were self-pollinated for at least eight generations via single seed descent method. Thus, genotypes of all RILs are considered to be highly homozygous so that they can be used to detect QTL effects under multiple environments. The development of an RIL population often takes 4-5 years and cannot be used to evaluate dominance because all loci are homozygous.

The RIL populations have been widely used for QTL mapping in common bean and other crops. For example, an RIL population of 237 individuals with 300 RELF (restriction fragment length polymorphisms) markers with the SAM (single marker analysis) model were used for QTL-mapping in tomato, and six QTL were detected for quality traits (Andrew et al., 1988). An RIL population containing 240 common wheat lines with combined 185 SSR and 73 STS markers detected three major QTL that control starch granule size on chromosome 1DL, 7BL and 4AL, which explained

genetic variation from 3.8% to 5.8% (Feng et al., 2013). Using GBS technology, a black common bean RIL population of 85 individuals with ~80,000 SNP markers was also used and 27 QTL for eight seed hardness related traits were identified (Sandhu et al., 2018).

2.7.4 Genetic map

2.7.4.1 Concept of genetic map

During meiosis phase of sexual reproduction, genes or markers always incline to inherit along with their close neighbors; this tendency is named linkage. A genetic map is established to show the intensity of linkage, representing the relative positions of genes and markers across chromosomes. A higher recombination frequency corresponds to a greater distance on a genetic map. Unlike physical map which shows the actual position of genes or markers estimated by the number of nucleotide pairs, a genetic map provides information of relative orders and distances of markers that are sorted into linkage groups. Centimorgans (cM) is the unit of distance measured in genetic map, as 1 cM refers to 1% probability that two markers would be exchanged during chromosome recombination. A precision genetic map would be the foundation of accurate QTL detection and effective MAS at genomic level. Meanwhile, a genetic map would also be a powerful tool for further fine mapping and gene cloning and vice versa.

2.7.4.2 Genetic map construction

In general, genetic map is based on chromosome segregation through crossing-over. To construct a high-density genetic map, a plenty of markers are required. During last 20 years, various markers have been utilized in genetic map construction. Randomly amplified polymorphic DNA (RAPD) (Levin et al., 1993), amplified fragment length polymorphism (AFLP) (Otsen et al., 1996), and microsatellites or simple sequence repeats (SSRs) (Mba et al., 2001) are commonly used in early stage. Among them, SSR would be an optimal marker type for genetic map construction. SSRs are affluent and widely distributed across the whole genome and can be easily detected by PCR without DNA sequencing which was expensive at early stage. But now, SSRs are basically replaced by SNP markers for high-resolution linkage map due to their much higher

density across genome and automated, cheap, fast genotyping at a low error rate.

Construction of a linkage genetic map usually follows these steps: (1) establish a proper biparental mapping population, (2) develop polymorphic markers from the mapping population and perform statistical tests on the polymorphic markers to remove strongly distorted markers, (3) construct linkage groups of the quality markers, and (4) calculate the relative genetic distances between markers.

After the molecular markers have been developed from a mapping population, whether these markers follow a theoretical Mendelian segregation ratio in the population should be tested as segregation distortion would lower further statistical power on QTL identification (Liu et al., 2010). Statistical methods for testing segregation include binomial test, standard normal test, Pearson chi-squared test, and likelihood ratio chi-squared test (Wu et al., 2007).

Two-point and three-point analyses were used for calculating the marker order and recombinant fraction between only two or three markers. With increasing number of markers, the maximum likelihood function was proposed to estimate the order and recombination fraction of markers and that with the highest likelihood is selected. Then the recombination fraction is transferred to genetic distance by a map function. Morgan, Haldane and Kosambi map functions are most commonly used. The Morgan map function is applicable for a genetic map with markers of short distance (cM). The Haldane map function is suitable for long distance conversion, while the Kosambi map function outperforms previous two for long distance markers.

2.7.5 Linage based QTL mapping methods

2.7.5.1 Principle of Linage based QTL mapping

Quantitative trait locus (QTL) refers to a genome region which is associated with a quantitative trait. Linkage-based QTL mapping lays the foundation for causal gene identification and gene cloning as it pins a QTL onto a marker interval and many candidate genes controlling phenotypes are located around the QTL (Tsai et al. 2020). Besides, QTL mapping can estimate QTL effect, or a contribution percentage of a QTL to phenotype variance. Additive, dominant and epistatic effects of genes can be estimated by multiple statistical models (Gallais et al., 2001) The first linkage between morphological markers (seed color or pattern) and quantitative trait (seed size) was

reported in 1923 (Sax, 1923). Then Thoday (1961) showed that QTL could be located by their linkage relationship with Mendelian marker loci and the number of markers is the major limited factor for QTL detection. Later, various molecular markers such as AFLP, RAPD, SSR and SNP have been developed to surmount the limitations (Thoday, 1961).

Linkage based QTL mapping mainly includes several steps: (1) construct a biparental mapping population, (2) develop high-density molecular markers, (3) construct a linkage map, (4) evaluate trait phenotypes of the population in multiple environments (over years and locations), and (5) QTL mapping and candidate gene prediction using the genotypic and phenotypic data with various statistical models.

2.7.5.2 QTL mapping models

Many linkage-based statistical models have been proposed to detect QTL associated with traits for biparental populations, such as single marker analysis (SMA) (Engelsma) (Engelsma, 1972;Haley and Knott, 1992) , interval mapping (IM) (Jansen, 1994), composite interval mapping (CIM) (Zeng, 1994), inclusive composite interval mapping (ICIM) (Wang et al., 1999), and genome-wide composite interval mapping (GCIM) (Zhang et al., 2020).

SMA does not need a comprehensive genetic map, however, it cannot distinguish single QTL from a QTL cluster. Unlike SMA, IM requires to construct a comprehensive genetic map and then adopt maximum likelihood and a simple regression model for QTL positioning and additive effect estimating. When multiple QTL exist in one region, the detected loci may deviate from its real loci due to interactions among the QTL. To increase accuracy and power of QTL detection, the CIM model that combines multiple linear regression with IM was proposed (Zeng, 1994). CIM is more stable and powerful to detect QTL across the whole genome as the linear model of CIM takes into consideration background markers, but epistatic effects and interactions between environment and genes are not considered. In contrast, ICIM based on a mixed linear model provides functions to estimate QTL and environment interaction and epitasis (Wang et al., 1999). All these statistical models are designed to detect major-effect QTL. Recently, a new statistical model, genome-wide composite interval mapping (GCIM), was proposed to estimate both large and small effect QTL (Zhang et al., 2020). GCIM

is based on CIM and includes two steps. The first step is to scan putative QTL across genome by a single-locus random mixed linear model used in genome-wide association studies (GWAS). In this step, the background markers in CIM are replaced by estimated polygenic variance in GWAS. Then, these selected putative QTL are integrated into a multi-QTL mixed linear model. The QTL effects are calculated by empirical Bayes with the likelihood ratio test employed on true QTL detection (Zhang et al., 2020). In addition, several similar QTL mapping methods, such as penalized maximum likelihood mapping (Zhang and Xu, 2005), multiple-interval mapping (Kao et al., 1999), multi-marker analysis mapping (Broman and Speed, 2002) have been proposed for detection of minor-effect QTL.

In addition, the statistical power of all models depends on several factors: (1) sample sizes, (2) allele frequency and segregation at quantitative trait loci and their effects, the distribution of these alleles and their effects being additive, dominance or epistasis, (3) the number of loci that are in association with the trait; and (4) proper populations constructed for QTL-mapping.

2.7.5.3 Software tools available for QTL mapping

To date, there are many released software tools available for the CIM method, such as QTL PLABQTL (Utz and Melchinger, 1996), QGene (Nelson, 1997), HAPPY (Mott et al., 2000), Map Manager (Manly et al., 2001), and QTL Express (Seaton et al., 2002). QTLnetwork (Yang et al., 2008) and QTL IciMapping (Meng et al., 2015) can perform ICIM analysis. GCIM is implemented in the R package, QTL.gCIMapping.GUI v2.0. In addition, some software tools, such as R/qtl (Broman et al., 2019), mpMap (Huang and George, 2011) and DOQTL (Gatti et al., 2014) also provide functions for QTL detection.

2.7.5.4 Candidate gene prediction

QTL mapping by biparental populations provides the location of a QTL as a confidence interval between two markers. Candidate genes are generally the genes with known biological function directly or indirectly regulating the developmental processes of the investigated traits, which could be confirmed by evaluating the effects of the causative gene variants in an association analysis.

Candidate genes can be predicted using the position-dependent strategy that seeks candidate genes from the genes in the vicinity of QTL (Lou et al., 2006). This strategy successfully combines candidate gene scanning and candidate gene analysis with linkage between molecular markers and genes. This approach has proven its efficiency in many studies (Van Laere et al., 2003;Sutter et al., 2007;Jinge et al., 2019). For example, one insulin-like growth factor gene that related to dog body size was detected in the 15 Mb interval region near QTL (Sutter et al., 2007).

However, the identified QTL only have their statistical meaning without any knowledge of specific functional feature. Sometimes identified QTL are not causal loci or have incomplete linkage with important functional variants (Zhu and Zhao, 2007). In addition, even true variants are included in the QTL region and vicinity, because most genetic architecture remains obscure, the function of variants may not be significant. For example, the most detected QTL are associated with or close to long regulator elements whereas regulated genes are far from the QTL region in vertebrates (Kikuta et al., 2007). Thus, for each gene or variant contained in the QTL region, its biological process, and regulator element domains should be well predicted. Some methods such as BMRF (bagging Markov random field, a network-based prediction approach) has been proven its availability in rice QTL candidate genes prediction (Bargsten et al., 2014). Besides, some advanced candidate gene prediction strategies, such as transcriptome expression, comparative genome are also useful (Shinozuka et al., 2012;Mikhaylova and Thornton, 2019).

2.8 The scope and purpose of this study

In recent years, numerous QTL have been successfully identified using different statistical models with biparental genetic populations. As described in 1.3.1, although marsh spot disease was discovered in beans in 1930s, its genetic mechanism is still unknown. The purpose of this study was to use different genetic analysis methods to explore inheritance of marsh spot disease resistance in cranberry common bean. An RIL population of 138 individuals was derived from a cross between a highly resistant cultivar Cran09 and a susceptible cultivar Messina and the marsh spot resistance was evaluated during five years at two different soil types. This study was to perform genetic analysis at a phenotypic level using the JSA approach, and then perform QTL

mapping at a molecular level to validate and identify QTL and their potential candidate genes associated with mash spot disease resistance, and eventually design molecular markers for marker assisted breeding. The outcomes of the research will provide a basic oversight of genetic basis of marsh spot resistance and molecular markers for common bean breeding improvement.

2.8.2 Hypothesis

Marsh spot resistance in cranberry common bean is controlled by few major genes and polygenes. Major- and small-effect QTL associated with marsh spot resistance exist and can be detected using linkage-based QTL mapping approach.

2.8.3 Specific objectives

(1) Perform statistical analysis on the phenotype data of marsh spot resistance;
(2) Perform genetic analysis of marsh spot resistance at a phenotypic level;
(3) Generate SNP data by GBS and data quality control;
(4) Perform QTL mapping to identify large- and small-effect QTL associated with marsh spot resistance and develop molecular markers to assist breeding selections in common bean;
(5) Predict candidate genes collocated with the identified QTL for marsh spot resistance.

3. Inheritance of marsh spot disease resistance in cranberry common bean (*Phaseolus vulgaris* L.) (Jia et al., 2021a)

Jia B, Conner RL, Khan N, Hou A, Xia X, You FM: **Inheritance of marsh spot disease resistance in cranberry common bean (*Phaseolus vulgaris* L.)**. *The Crop Journal* 2021, **9**:456-467

3.1 Abstract

Common bean (*Phaseolus vulgaris L.*) is an annual legume crop that is grown worldwide for its edible dry seeds and tender pods. Marsh spot (MS) of the seeds is a physio-genic stress disease affecting seed quality in beans. Studies have suggested that this disease involves a nutritional disorder caused by manganese deficiency, but the inheritance of resistance to this disease has not been reported. A biparental genetic population composed of 138 recombinant inbred lines (RILs) was developed from a cross between an MS resistant cultivar 'Cran09' and an MS susceptible cultivar 'Messina'. The 138 RILs and their two parents were evaluated for MS resistance during five consecutive years from 2015 to 2019 in sandy and heavy clay soils in Morden, Manitoba, Canada. The MS incidence (MSI) and the MS resistance index (MSRI) representing disease severity were shown to be both highly correlated heritable traits that had high broad-sense heritability values (H^2) of 86.5% and 83.2%, respectively. No significant differences for MSI and MSRI were observed between the two soil types in all five- (MSI) or four-year (MSRI) data collection, but significant correlations among years were observed despite MS resistance was moderately affected by year. The MSIs and MSRIs displayed a right-skewed distribution, indicating a mixed genetic model involving a few major genes and polygenes. Using the joint segregation analysis method, the same four major genes with additive-epistasis effects showed the best fit for both traits, explaining 84.4% and 85.3% of the phenotypic variance for MSI and MSRI, respectively. For both traits, the *M1, M2, M3* and *m4* acted as the favorable (resistant) alleles for the four genes where *M* and *m* represent two alleles of each gene. However, due to epistatic effects, only the individuals of the *M1M2M3M4* haplotype appeared to be highly resistant, whereas those of the *m1m2m3M4* haplotype were the most susceptible. The m4 allele significantly suppressed the additive effects of *M1M2M3* on resistance, but decreased susceptibility due to the additive effects of *m1m2m3*. Further quantitative trait locus (QTL) mapping is warranted to identify and

validate individual genes and develop molecular markers for marker-assisted selection of resistant cultivars.

Keywords: Cranberry common bean, marsh spot resistance, recombinant inbred line (RIL), joint segregation analysis, major gene, polygene

3.2 Introduction

Common bean (*Phaseolus vulgaris L.*, 2n = 2x = 22) is one of the most important grain legumes for human consumption. The wild common bean originates from two gene pools, namely the Mesoamerican and Andean gene pools, both derived from the same common ancestral population (Bitocchi et al., 2012;Rendón-Anaya et al., 2017). These gene pools were further domesticated by farmers in Mexico and South America nearly 8000 years ago. Nowadays, common beans are an important source of protein, vitamins, and minerals. Common beans have been widely planted in both developed and developing countries, especially in Africa and Latin America (Akibode and Maredia, 2012). In Canada, the common bean is an economically important crop that also plays an important role in crop rotation. From 2015 to 2019, the area planted with common beans has increased from 105,200 to 160,000 ha, with dry bean production reaching 316,800 Mt in Canada by 2019 (Statistics Canada, 2019). However, significant yield losses caused by abiotic and biotic stresses are common (Mittler, 2006;Ramegowda and Senthil-Kumar, 2015). In tropical and subtropical regions, where acidic soil leads to mineral deficiency, low availability of soil minerals can be a major production constraint (Stephen et al., 2014). In addition, since climate change impacts crop production, genetic improvement for abiotic tolerance should be a promising approach to significantly increase common bean yield.

Marsh spot (MS) is a common disease affecting seed quality in market classes such as cranberry common beans and pea. In susceptible varieties, a discolored brown spot often occurs at the center of the seeds, which reduces seed quality and affects consumption values (Pethybridge, 1936). To date, only a few studies on MS disease have been reported. MS was first observed in peas grown in Britain (Samuel and Piper, 1929). The brown spot symptoms were thought to be caused by a pathogen, and scientists initially attributed MS to bacterial infection, but this initial assumption was disregarded as they failed to isolate the putative causal pathogens from peas (Reynolds,

1955). Later similar symptoms caused by Mn deficiency was observed to occur alongside oats (*Avena sativa L.*) affected with grey speck (Pethybridge, 1936). Because grey speck in oats is caused by manganese (Mn) deficiency, scientists speculated that it could also be the cause of MS in legumes. A hydroponics growing method was employed to further investigate the effects of Mn^{2+} concentration on root length, flowering time, and seed formation in pea (Heintze, 1938). A refined pot-culture technique was later performed in Long Ashton, England, United Kingdom, to grow many pulse species, including peas *(Pisum sativum L.*), broad beans (*Vicia faba L.*), runner beans (*P. coccineus L.*), green and French (dwarf) beans (*P. vulgaris L.*), in Mn-deficient sand medium. Examination of the seeds revealed typical severe marsh spots in peas and mild to severe marsh spot symptoms in broad and runner beans (Hewitt, 1945). These results confirmed that MS is caused by Mn deficiencies.

Manganese uptake may be a factor causing an Mn deficiency. Soil types can influence metal uptake by plants (Kandpal et al., 2005;Bornø et al., 2019). Soil characters such as metal concentration, soil pH, cation exchange capacity, organic matter and soil structure vary dramatically among different soil types and have proven to affect metal uptake (Jung, 2008). Sandy and heavy clay soils are two major mineral soil types in Canada. Sandy soil consists of larger particles compared to heavy clay, allowing water and nutrients to leach more easily in this coarse texture soil. Conversely, heavy clay soils have a greater water and nutrient retention capacity. Plant roots grow rapidly and smoothly in friable sandy soils, but water and metal can more easily become limiting. In heavy clay soil, though plenty of water and nutrients exist, clay soil may be too tight for plants to penetrate, so water and nutrients may be tightly absorbed and not available to the crop (Passioura, 1991). Moreover, pH is higher in heavy clay (6.5–7.0) than in sandy soil (5.5–6.5), which also affects metal uptake because metal solubility decreases in alkaline soil and increases in acidic soil (Garcia Miragaya, 1984). Mn^{2+} is the only metal form available to plants (Pittman, 2005), and there is basically a proportional linear relationship between metal uptake and soil pH (Farrah and Pickering, 1979;Garcia Miragaya, 1984). Thus, Mn should be more soluble at equivalent Mn concentration, and therefore more available to plants in sandy than in heavy clay soils (Rieuwerts et al., 1998). Other factors, such as organic matter content, microbiome, quantity and reactivity of hydrous oxides, also influence metal uptake (Cataldo and Wildung, 1978;Rieuwerts et al., 1998).

Genetic studies of MS resistance in beans have not been reported. Whether the MS

is a quantitative or a qualitative trait and is controlled by few major genes, polygenes, or both is still uncertain. Joint segregation analysis (JSA) has been developed to jointly use phenotypic data from different generations of a biparental population to compare the frequency distribution in a real dataset with the theoretical distribution underlying the genetic model (Zhang et al., 2003b). Using JSA, major gene effects can be separated individually, while polygenes can be collectively detected. This method was initially used for a population comprising parents (P_1 and P_2), F_1, F_2 and $F_{2:3}$ generations (Wang, 1996;Gai and Wang, 1998), and was subsequently extended to the analysis of various biparental populations, such as DH/RIL (Zhang et al., 2001), back-cross (BC) (Zhang et al., 2000), back-cross inbred line (Maillard et al.) (Wang et al., 2013) and their combinations. The R package SEA, released in 2018 and recently updated, allows data analysis of 14 different population types and multiple genetic models with up to four major genes (https://cran.r project.org/web/packages/SEA/index.html) (Zhang et al., 2003b). JSA has been widely used since the 1990s in genetic studies of several plant species such as soybean (*Glycine max* L.) (Wang and Gai, 2001;Wang et al., 2010), chickpea (*Cicer arietinum L.*) (Anbessa et al., 2006), wheat *(Triticum aestivum* L.) (Zhang et al., 2005;Khan et al., 2012), maize (*Zea mays* L.) (Gang et al., 2007), rapeseed (*Brassica napus* L.) (Zhang et al., 2010;Cao et al., 2013), melon (*Cucumis melo* L.) (Qi et al., 2015), pepper (*Piper nigrum* L.) (Wei et al., 2020), crape myrtle (*Lagerstroemia indica* L.) (Ye et al., 2017), chrysanthemum (*Chrysanthemum* × *morifolium*) (Song et al., 2018), and iris (*Iris germanica* L.) (Fan et al., 2020).

The objective of this study was to determine the inheritance of MS in cranberry common beans using the developed biparental RIL population with the JSA method. This study constitutes the first report of MS inheritance in beans.

3.3 Materials and methods

3.3.1 Population

A cross between the highly MS resistant cultivar ‘Cran09’ and the MS-susceptible cultivar ‘Messina’ was made to produce F_1 seeds. These F_1 seeds were planted in the greenhouse at the Morden Research and Development Centre, Morden, Manitoba, Canada to produce the F_2 generation. A total of 138 $F_{2:8}$ RILs were developed through single-seed descent from 2013 to 2015. The seeds of each individual plant in the last generation were bulk-harvested to produce 138 RILs.

3.3.2 The construction of RIL population and experimental design

The 138 RILs and their two parents were tested under two field soil types (sandy and heavy clay soil) for five years (2015–2019) using a partially-balanced lattice design with three replications, on the experimental fields of the Morden Research and Development Centre, Morden, Manitoba, Canada (49º11′N, 98º5′W). Five soil samples in each soil type of MS field sites were obtained each year. The soil samples were analyzed for pH values, Mn concentrations and other mineral material contents by the private firm FarmersEdge (https://www.farmersedge.ca/). According to the soil test results, textures of the soils at the experimental field sites were either heavy clay or sandy soil with low concentrations of manganese. Throughout the five-year field study, cereal crops were grown on each of the field sites in the year prior to the MS study. Each year, herbicide and fertilizer applications were made to maximize bean seed yield (Growers, 2020).

In a 5-m row with 75 cm row-spacing, 95 seeds of each RIL were planted. All plants were harvested at maturity. Ten seeds of each RIL were randomly selected after harvest and graded for MS incidence (MSI) (percentage of seeds with symptoms) and for MS severity on a scale of 0–5, where 0 represents no symptom, and 5 represents severe symptoms (**Appendix 2**).

Marsh spot resistance index (MSRI), ranging from 0 to 5, was calculated to represent the disease severity or resistance level of each line:

$$\text{MSRI} = \frac{\sum_{i=0}^{n}(\text{number of seeds at a rating with } 0-5 \text{ scale} \times \text{the rating})}{\text{Total number of seeds}}$$

where, n is the total number of ratings and i = 0, 1, …, 5, respectively.

3.3.3 Weather data collection

To determine whether the MS resistance is related to the weather conditions, the weather data, including temperature and precipitation during growth seasons of five years (2015–2019), were collected from the Morden Research and Development Centre, Agriculture and Agri-Food Canada.

3.3.4 Statistical analysis

A significantly right-skewed distribution for both MSI and MSRI justified the use of

data transformations of the phenotypic datasets such as a square root or logarithm, but these failed to improve the normality of the data distributions significantly. Thus, non-parametric statistical tests were adopted for statistical analyses. To test the statistical differences of MSI and MSRI between years and soil types, the paired samples Wilcoxon test was used with the R function "wilcox.test" (https://www.r-project.org/). The R function "cor" was used to measure the Spearman rank correlation coefficients of MSI and MSRI between different years. All statistical figures were drawn using the R package ggplot2 (https://cran.r-project.org/web/packages/ggplot2/index.html).

To exclude effects due to years or soil types, the mean value of each line across years or soil types was calculated by removing year and/or soil type effects:

$$\overline{Y_i} = \mu + \sum_{j=1}^{n}(Y_{ij} - \overline{Y_j}),$$

where $\overline{Y_i}$ is the mean value of the ith line across years or soil types; μ is the overall mean of all lines across years or soil types; Y_{ij} is the observation value of the ith line at the *j*th year or soil type; $\overline{Y_j}$ is the mean of all lines at the *j*th year or soil type; *n* is the number of years (5) or soil types (2). A similar method was used to calculate the adjusted mean value of each line across all years and soil types. In this case, *n* is 10 (5 years and 2 soil types), $\overline{Y_j}$ is the mean of all lines at the jth year/soil type combination, and μ is the overall mean of all lines across years and soil types.

Furthermore, bidirectional cluster analysis with the Ward method was performed to group the RIL lines and years using the R package 'pheatmap' (https://cran.r-project.org/web/packages/pheatmap).

3.3.5 Broad-sense heritability

The variances were estimated using the R package lme4 (Bates et al., 2015) according to a linear model as follows:

$$Y_{ij} = \mu + \alpha_i + \beta_j + \gamma_c + \lambda_k + \tau_l + \sigma + \rho + \varepsilon,$$

where Y_{ij} is the observed value of the *i*th row and *j*th column, μ is the population mean; α_i and β_j are the random effects of the *i*th row and *j*th column, respectively; γ_c is the fixed effect of the *c*th soil type; λ_k is the random effect of *k*th year, τ_l is the random genetic effect of the lth line, ρ and σ are the interaction effects between lines and years and between lines and soil types, respectively; and ε is the random error.

Broad-sense heritability (H^2) was estimated using

$$H^2 = \sigma^2_g / (\sigma^2_g + \sigma^2_{gy}/yr + \sigma^2_{gs}/sr + \sigma^2_e /ysr),$$

where σ^2_g is the genetic variance; σ^2_e is the error variance; σ^2_{gy} is the interaction variance between lines and years; σ^2_{gs} is the interaction variance between lines and soil types; r is the number of replications; y is the number of years; and s is the number of soil types.

3.3.6 Joint segregation analysis (JSA)

JSA was adopted to dissect the trait distribution of the RIL population to determine whether MS resistance was controlled by a few major genes and/or polygenes and to estimate the number of major genes and their additive dominant and epistatic effects. All the genetic analyses were performed using the R package SEA (https://cran.r-project.org/web/packages/SEA/index.html) (Zhang et al., 2003b). A total of 35 genetic models available in SEA were assessed to detect the most likely genetic models underlying MSI and MSRI (**Table 1.4**). JSA was conducted separately for a total of 18 phenotypic datasets of the 138 RILs and two parents, including ten for combinations of five individual years and two soil types, two mean datasets for two soil types across five years, five mean datasets for five years across two soil types, and one overall mean dataset for five years and two soil types.

Three criteria were used to select the best-fit genetic models: (1) the smallest Akaike Information Criterion (Zhang et al., 2003b;Koike et al., 2004), (2) the highest heritability of the proposed gene model (the proportion of phenotypic variance explained by the model), and no significant difference from uniform, Smirnov and Kolmogorov statistics tests.

3.4 Results

3.4.1 Genetic variation of marsh spot resistance

The 138 RILs and parents (Cran09 and Messina) were rated for MS over five years in both soil types. Cran09 appeared to be highly resistant to MS in all years and soil types, having low average MSI (1.5% ± 2.5%) and MSRI ratings (0.04 ± 0.07). In contrast, Messina was highly susceptible with high average MSI (31.9% ± 6.5%) and MSRI ratings (0.8 ± 0.2) across all years and soil types, showing a substantial difference in MS rating between the two parents (**Table 3.1**).

Table 3.1 Marsh spot incidence (MSI) and marsh spot resistance index (MSRI) of the 138 RILs and their two parents across 5 years and two soil types (sandy and heavy clay).

Dataset	MSI				MSRI			
	Mean ± SD	CV (%)	Range	H^2 (%)	Mean ± SD	CV (%)	Range	H^2 (%)
RIL population								
H-2015	7.4 ± 12.6	170.4	0.0–66.7	92.22	0.2 ± 0.4	200.9	0.0–2.3	92.63
S-2015	7.0 ± 10.9	156.5	0.0–73.3	77.33	0.1 ± 0.3	183.3	0.0–2.0	78.28
T-2015	7.2 ± 10.9	151.6	0.0–68.3	85.56	0.2 ± 0.3	176.2	0.0–1.9	82.18
H-2016	6.1 ± 9.1	149.5	0.0–46.7	79.06	0.1 ± 0.2	165.5	0.0–1.0	88.74
S-2016	7.0 ± 10.5	152.2	0.0–43.3	73.92	0.2 ± 0.3	151.7	0.0–1.0	63.60
T-2016	6.5 ± 9.0	138.3	0.0–36.7	81.82	0.2 ± 0.2	143.7	0.0–0.9	79.21
H-2017	5.6 ± 8.8	156.1	0.0–40.0	95.40	0.1 ± 0.2	184.9	0.0–1.0	95.63
S-2017	6.9 ± 9.9	143.5	0.0–43.3	97.13	0.2 ± 0.2	158.3	0.0–1.1	96.95
T-2017	6.3 ± 8.2	131.0	0.0–38.3	76.04	0.1 ± 0.2	147.8	0.0–0.9	74.82
H-2018	11.0 ± 11.7	106.3	0.0–50.0	65.46	0.3 ± 0.4	112.5	0.0–1.5	60.77
S-2018	9.1 ± 10.6	116.8	0.0–56.7	76.32	0.2 ± 0.3	126.3	0.0–1.5	67.60
T-2018	10.0 ± 9.2	93.0	0.0–48.3	64.29	0.3 ± 0.3	100.5	0.0–1.4	62.09
H-2019	9.5 ± 11.8	124.8	0.0–50.0	88.89	0.3 ± 0.4	140.3	0.0–1.9	79.26
S-2019	7.1 ± 7.8	112.6	0.0–33.3	62.24	0.2 ± 0.2	124.4	0.0–1.1	59.10
T-2019	8.3 ± 8.2	98.8	0.0–33.3	56.23	0.2 ± 0.2	108.2	0.0–1.1	48.63
H-5yrs	7.9 ± 9.1	115.3	0.0–42.9	89.65	0.2 ± 0.3	127.2	0.0–1.2	88.42
S-5yrs	7.4 ± 7.9	107.6	0.0–45.3	85.91	0.2 ± 0.2	114.4	0.0–1.1	85.19
Overall	8.0 ± 8.3	106.3	0.0–43.7	86.51	0.2 ± 0.2	114.1	0.0–1.2	83.29
Cran09 (P_1)								
H-2015	0.0 ± 0.0	-	0.0–0.0	-	0.0 ± 0.0	-	0.0–0.0	-
S-2015	0.0 ± 0.0	-	0.0–0.0	-	0.0 ± 0.0	-	0.0–0.0	-
T-2015	0.0 ± 0.0	-	0.0–0.0	-	0.0 ± 0.0	-	0.0–0.0	-
H-2016	0.0 ± 0.0	-	0.0–0.0	-	0.0 ± 0.0	-	0.0–0.0	-
S-2016	0.0 ± 0.0	-	0.0–0.0	-	0.0 ± 0.0	-	0.0–0.0	-
T-2016	0.0 ± 0.0	-	0.0–0.0	-	0.0 ± 0.0	-	0.0–0.0	-
H-2017	0.0 ± 0.0	-	0.0–0.0	-	0.0 ± 0.0	-	0.0–0.0	-
S-2017	0.0 ± 0.0	-	0.0–0.0	-	0.0 ± 0.0	-	0.0–0.0	-
T-2017	0.0 ± 0.0	-	0.0–0.0	-	0.0 ± 0.0	-	0.0–0.0	-
H-2018	4.4 ± 8.8	198.4	0.0–20.0	-	0.1 ± 0.3	198.4	0.0–0.6	-
S-2018	6.4 ± 7.5	117.9	0.0–20.0	-	0.2 ± 0.2	150.5	0.0–0.7	-
T-2018	5.4 ± 1.4	25.4	4.4–6.4	-	0.2 ± 0.0	13.9	0.1–0.2	-
H-2019	0.0 ± 0.0	-	0.0–0.0	-	0.0 ± 0.0	-	0.0–0.0	-
S-2019	4.4 ± 7.3	163.5	0.0–20.0	-	0.1 ± 0.2	172.5	0.0–0.6	-
T-2019	2.2 ± 3.1	141.4	0.0–4.4	-	0.1 ± 0.1	141.4	0.0–0.1	-
H-5yrs	0.9 ± 2.0	223.6	0.0–4.4	-	0.0 ± 0.1	223.6	0.0–0.1	-
S-5yrs	2.2 ± 3.1	140.6	0.0–6.4	-	0.1 ± 0.1	139.2	0.0–0.2	-
Overall	1.5 ± 2.5	164.7	0.0–6.4	-	0.0 ± 0.1	162.7	0.0–0.2	-
Messina (P_2)								
H-2015	32.2 ± 19.2	59.7	10.0–60.0	-	0.8 ± 0.6	65.5	0.2–1.7	-
S-2015	41.1 ± 15.4	37.4	20.0–60.0	-	0.9 ± 0.5	52.5	0.2–1.7	-
T-2015	36.7 ± 6.3	17.1	32.2–41.1	-	0.9 ± 0.1	8.0	0.8–0.9	-
H-2016	24.4 ± 15.9	65.0	10.0–60.0	-	0.7 ± 0.5	70.5	0.3–2.0	-
S-2016	24.4 ± 15.1	61.7	0.0–50.0	-	0.7 ± 0.5	66.3	0.0–1.3	-
T-2016	24.4 ± 0.0	0.0	24.4–24.4	-	0.7 ± 0.0	2.2	0.7–0.7	-
H-2017	33.3 ± 12.3	36.7	20.0–50.0	-	0.7 ± 0.2	31.6	0.4–0.9	-
S-2017	32.2 ± 16.4	50.9	10.0–60.0	-	0.9 ± 0.5	53.6	0.3–1.5	-
T-2017	32.8 ± 0.9	2.4	32.2–33.3	-	0.8 ± 0.1	18.7	0.7–0.9	-
H-2018	32.2 ± 16.4	50.9	0.0–50.0	-	0.9 ± 0.5	59.9	0.0–1.6	-
S-2018	37.8 ± 16.4	43.5	10.0–60.0	-	0.8 ± 0.4	54.0	0.3–1.7	-
T-2018	35.0 ± 3.9	11.2	32.2–37.8	-	0.8 ± 0.0	2.8	0.8–0.9	-
H-2019	38.9 ± 14.5	37.4	20.0–60.0	-	1.2 ± 0.6	52.3	0.3–2.1	-
S-2019	22.2 ± 16.4	73.9	0.0–50.0	-	0.6 ± 0.6	89.9	0.0–1.8	-
T-2019	30.6 ± 11.8	38.6	22.2–38.9	-	0.9 ± 0.4	40.2	0.6–1.2	-
H-5yrs	32.2 ± 5.2	16.0	24.4–38.9	-	0.8 ± 0.2	23.0	0.6–1.2	-
S-5yrs	31.6 ± 8.2	26.0	22.2–41.1	-	0.8 ± 0.1	15.2	0.6–0.9	-
Overall	31.9± 6.5	20.3	22.2–41.1	-	0.8 ± 0.2	19.0	0.6–1.2	-

H, heavy clay soil; S, sandy soil; T, two soil types combined; 5 yrs, five years combined; CV, coefficient of variation; SD, standard deviation; H^2, broad-sense heritability. '-' represents unavailability of results.

The 138 RILs derived from Cran09 and Messina showed considerable variation in their MS rating, exceeding those of their two parents. The MSIs ranged from 0 to 43.67%, indicating transgressive segregation in the RILs compared to Can09 (1.5) and Messina (31.9) (**Table 3.1**). Similar results were obtained for MSRI, with a range of 0–1.2 in the segregating population, and MSRIs of 0.04 and 0.8 for Cran09 and Messina,

respectively (**Table 3.1**).

Both MSIs and MSRIs of the RIL population were right-skewed in all datasets (**Figure 231**), indicating that the two traits were mostly controlled by a few major genes or a mixed genetic model involving major genes plus polygenes. Cluster analysis grouped the 138 RILs and the two parents into a resistant (R) and a susceptible (S) group for MSI (**Appendix 3a**) and MSRI (**Appendix 3b**). The parents Cran09 and Messina were classified separately into the R and S groups, respectively. Most of the RILs were included in the R group.

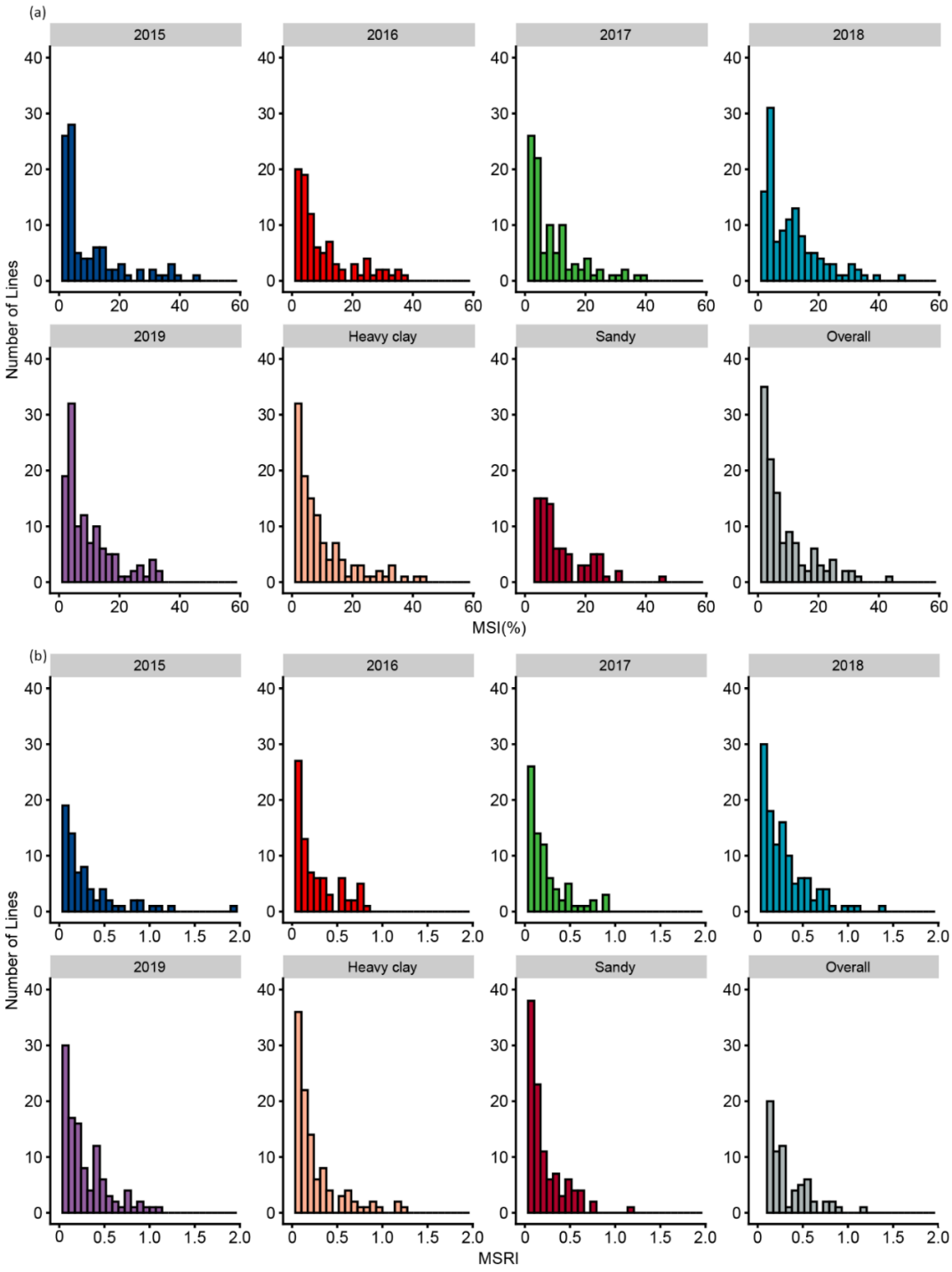

Figure 3.1 Histograms of marsh spot incidence (MSI, %) (a) and marsh spot resistance index (MSRI) (b) in different years, soil types and overall mean values.

MSI and MSRI showed broad-sense heritability (H^2) of 86.51% and 83.29%, respectively, for the overall mean dataset across all five years and two soil types. In the heavy clay and sandy soil types, H^2 was estimated at 89.65% and 85.91% for MSI and 88.41% and 85.24% for MSRI, respectively. In the datasets of individual years and soil types, the highest H^2 estimates were 97.13% for MSI and 96.95% for MSRI in the S-

2017 dataset. Overall, both traits had high H^2 regardless of years or soil types, indicating that MS resistance was highly heritable (**Table 3.1**). Significant high correlations were observed between the two traits in all datasets based on Spearman rank correlation coefficient of 0.96–0.99 (**Table 3.2**).

Table 3.2 Spearman rank correlation coefficients between mash spot incidence (MSI) and mash spot resistance index (MSRI) in 18 phenotypic datasets.

Year	Soil type	*r*
2015	Heavy clay	0.97
2015	Sandy soil	0.97
2016	Heavy clay	0.96
2016	Sandy soil	0.97
2017	Heavy clay	0.97
2017	Sandy	0.98
2018	Heavy clay	0.97
2018	Sandy	0.97
2019	Heavy clay	0.98
2019	Sandy	0.96
2015	Two soils	0.98
2016	Two soils	0.98
2017	Two soils	0.98
2018	Two soils	0.98
2019	Two soils	0.98
Five years	Heavy clay	0.99
Five years	Sandy	0.99
Five years	Two soils	0.99

Note: Sample size is 138.

3.4.2 Marsh spot resistance affected by years and soil types

Due to the skewed distribution of MSI and MSRI in the RIL population, a non-parametric paired-sample Wilcoxon test was used to test the differences in MSRI and MSI between years or soil types. For MSI, no significant differences were detected between 2016 and 2017 or between 2017 and 2018, but the other comparisons were significantly different at 5% or 1% probability levels (**Figure 3.2a**). Mean values across years were used for bi-directional cluster analysis. The latter grouped the 2016, 2017 and 2018 data together (**Appendix 3a**). For MSRI, no significant differences were observed among 2016, 2017 and 2018 or between 2018 and 2019 (**Figure 3.2b**). Cluster analysis generated results similar to MSI in that the first three years (2016–2018) and the last two years (2019 and 2010) were clustered into two separate groups (**Appendix 3**). Taken together, the disease ratings of the Cran09/Messina RIL population and its two parents were similar in 2016–2018 and in 2019–2020 but differed between the two groups (**Appendix 3**).

No significant differences were observed between the two soil types for MSI in all five years or in the overall mean dataset (**Figure 3.2c**). Similar results were obtained for MSRI with the exceptions of 2017 and 2018, where a significant difference was

observed between the two soil types (**Figure 3.2d**). The overall results suggest that the MS ratings are not significantly affected by soil type.

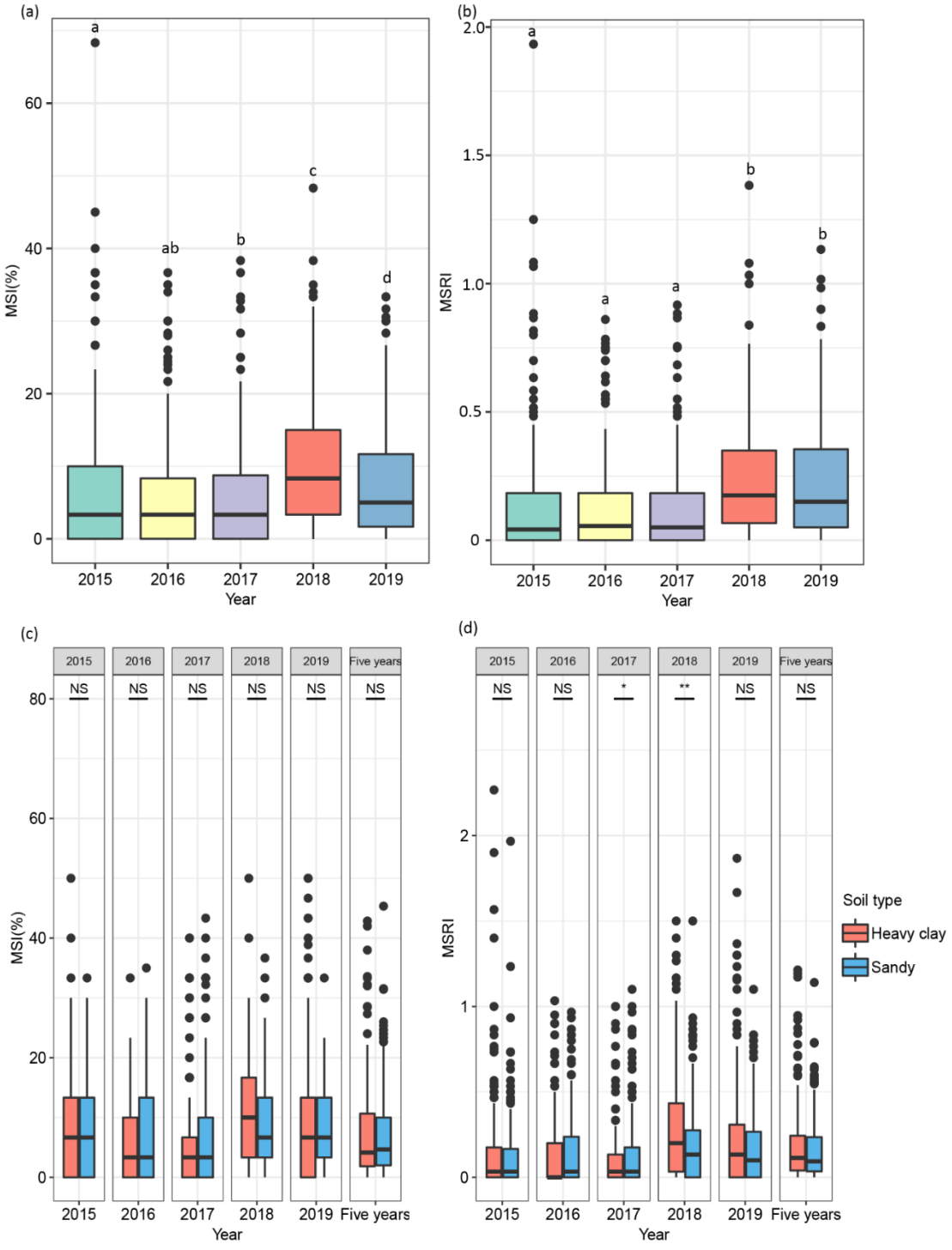

Figure 3.2 Boxplots of marsh spot incidence (MSI, %) (a and c) and marsh spot resistance index (MSRI) (b and d) across five years (a and b) and between the two soil types across five years and five-year means (c and d). The paired samples Wilcoxon test was used to test for significant differences between the two soil types. *, $P < 0.05$; **, $P < 0.01$; NS, not significant.

To determine whether climate and additional soil conditions impact the MS

resistance, the temperature and precipitation data during growth periods were collected, and pH and mineral concentration, including Mn concentration for both sandy soil and heavy clay fields, were tested. The patterns of temperature changes during growth periods were similar among the five years in Morden, Manitoba, Canada (**Appendix 4a**). The precipitation varied dramatically during five years from May to September, but no obvious patterns were observed (**Appendix 4b**).

Soil pH varied from 7.2 to 7.6 and was similar in two soil types for five years (**Appendix 5b**). However, the soil Mn concentration varied largely in different years. During 2015–2017, the soil Mn concentrations were 19.5–48.5 mg L^{-1} and 4.3–10.9 mg L^{-1} for heavy clay and sandy soil fields, respectively. In contrast, in 2018 and 2019, the soil Mn concentrations decreased to 4.2–4.5 mg L−1 and 3.1–3.4 mg L^{-1} for two soil type fields, respectively (**Appendix 5**).

3.4.3 Assessment of genetic models

A total of 35 genetic models (**Table 2.4**), including two with polygenes only (i.e., PG-AI and PG-A), 17 with mixed models including 1–4 major genes in combination with polygenes, and 16 with 1–4 major genes only, were tested for both MSI and MSRI. For the RIL population, the SEA R package provides only major gene models for the proposed four-gene inheritance (i.e., 4MG-X, where X represents different genetic effects); thus, no polygenes were assessed in four-gene models (**Table 2.4**). For each of the proposed models, a total of 18 phenotypic datasets (**Table 3.1**) for MSI and MSRI were analyzed, and the results are listed in Tables S3 and S4. To choose the best-fit model, the average AIC values of 18 phenotypic datasets were calculated for each model. However, AIC values estimated from different phenotypic datasets were not comparable. For each phenotypic dataset, relative AIC values of genetic models were calculated by setting the highest AIC values in all genetic models to 100%, and then calculating a percentage of the AIC over the maximum AIC. The best-fit model was the one with the lowest average relative AIC value of the 18 phenotypic datasets.

Figure 3.3a and **b** depict the average relative AIC values of all 35 genetic models for MSI and MSRI. The model 4MG-AI had the lowest AIC values for both traits with 22.10% and 42.93% for MSI and MSRI, respectively, and also explained the highest proportion of the phenotypic variance (*h2*) with 96% ± 40% and 74% ± 21% for MSI and MSRI, respectively (**Figure 3.3 c** and **d**), indicating that the same model with four

major genes with additive-epistasis was optimal for both traits.

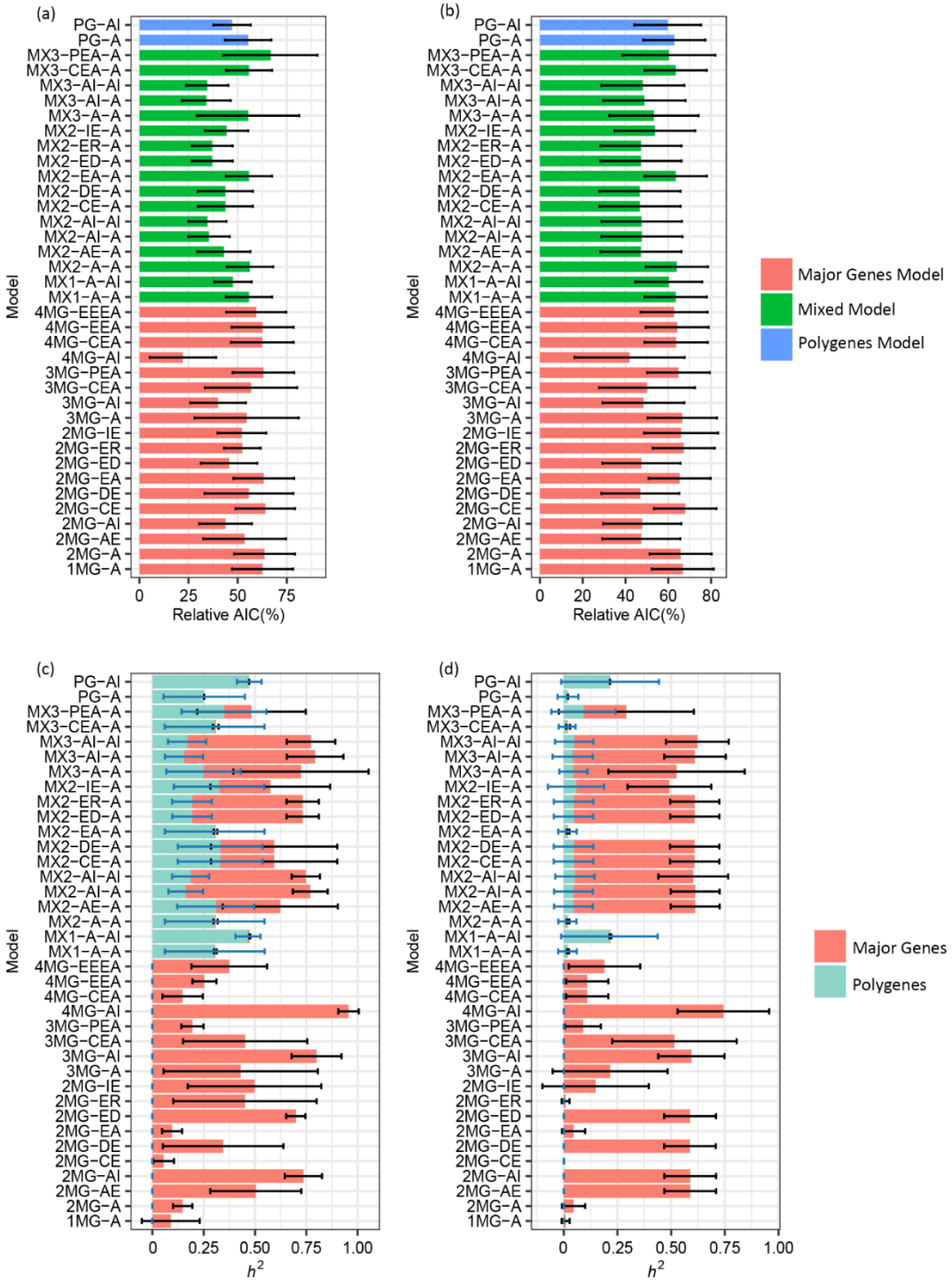

Figure 3.3 Bar charts of the relative AIC values (a and b) and heritability (h^2) estimates (c and d) of the 35 genetic models tested for the18 phenotypic datasets of marsh spot incidence (MSI) (a and c) and marsh spot resistance index (MSRI) (b and d) across five years and two soil types. For each phenotypic dataset, the highest AIC values in all genetic models were set as 100%. The relative AIC of each genetic model was calculated as a percentage of the AIC over the maximum AIC. The best model was the one with the lowest relative AIC.

Out of the 35 genetic models (**Table 2.5**), there were the other four-gene models

(i.e., 4MG-EEEA, 4MG-EEA, and 4MG-CEA) that all included major genes with only additive effects. These models had much higher relative AIC values than 4MG-AI, and also showed fairly low *h2* estimates (15%–37%, for MSI and 11%–19% for MSRI) (**Figure. 3.3c and d**), thereby pointing toward the role of epistasis in MS resistance inheritance.

The 4MG-AI model was further statistically tested for uniformity using uniformity, Smirnov and Kolmogorov statistical tests to determine whether the theoretical distribution underlying the genetic models fits the empirical data distribution. **Table 3.3** lists the statistical test results for the 4MG-AI model in eight mean datasets for MSI and MSRI. No significant differences were observed for most of the tests of goodness-to-fit (U_1^2, U_2^2, U_3^2, nW^2, and D_n) in 4MG-AI (**Table 3.3**) while most of the tests for the other models showed significant differences (**Appendix 7, 8**). Therefore, it was reasonable to deduce that MSI and MSRI were controlled predominately by four major genes with both additive and epistatic effects (4MG-AI).

Table 3.3 AIC values and statistical tests of the 4MG-AI models for marsh spot incidence (MSI) datasets of the 138 RILs and two parents.

Trait	Dataset	Population	AIC	$P(U_1^2)$	$P(U_2^2)$	$P(U_3^2)$	$P(nW^2)$	$P(D_n)$
MSI	Overall	P_1	1030.38	0.36	0.33	0.73	0.09	0.02
		P_2	1030.38	0.96	0.48	0.01**	0.31	0.29
		RIL	1030.38	0.93	0.67	0.17	0.26	0.06
	H-5yrs	P_1	974.08	0.40	0.33	0.54	0.16	0.09
		P_2	974.08	0.21	0.39	0.18	0.19	0.17
		RIL	974.08	0.94	0.81	0.52	0.37	0.09**
	S-5yrs	P_1	971.24	0.88	0.91	0.91	0.54	0.44
		P_2	971.24	0.88	0.51	1.5E-03**	0.29	0.32
		RIL	971.24	0.83	0.61	0.24	0.19	0.05
	T-2015	P_1	900.71	0.30	0.23	0.47	0.18	0.16
		P_2	900.71	0.71	0.90	0.05	0.53	0.50
		RIL	900.71	0.84	0.81	0.86	0.08	0.01*
	T-2016	P_1	866.39	0.63	0.42	0.16	0.30	0.33
		P_2	866.39	0.07	0.15	0.20	0.10	0.12
		RIL	866.39	0.81	0.84	0.93	0.03*	8.1E-05**
	T-2017	P_1	849.14	0.60	0.40	0.17	0.29	0.31
		P_2	849.14	0.14	0.12	0.64	0.18	0.21
		RIL	849.14	0.85	0.90	0.83	0.07	6.3E-04**
	T-2018	P_1	971.42	0.94	0.77	0.39	0.89	0.96
		P_2	971.42	0.54	0.37	0.22	0.60	0.55
		RIL	971.42	0.95	0.96	0.96	0.71	0.54
	T-2019	P_1	954.77	0.86	0.87	0.96	0.89	0.95
		P_2	954.77	0.99	0.43	1.8E-03**	0.35	0.50
		RIL	954.77	0.95	0.85	0.60	0.45	0.15
MSRI	Overall	P_1	−141.05	0.44	0.45	0.99	0.09	0.02*
		P_2	−141.05	0.35	0.70	0.04	0.28	0.15
		RIL	−141.05	0.92	0.62	0.11	0.17	0.03*
	H-5yrs	P_1	−120.00	0.36	0.37	0.96	0.14	0.06
		P_2	−120.00	0.40	0.74	0.05	0.38	0.37
		RIL	−120.00	0.89	0.78	0.56	0.39	0.08
	S-5yrs	P_1	−154.23	0.81	0.96	0.26	0.37	0.28
		P_2	30.84	0.43	0.97	1.2E-03**	0.19	0.25
		RIL	−154.23	0.78	0.66	0.48	0.26	0.07
	T-2015	P_1	−197.48	0.28	0.23	0.50	0.18	0.16
		P_2	−154.23	0.59	0.95	0.07	0.56	0.37

Trait	Dataset	Population	AIC	$P(U_1^2)$	$P(U_2^2)$	$P(U_3^2)$	$P(nW^2)$	$P(D_n)$
		RIL	−197.48	0.77	0.68	0.60	0.04*	5.0E-04**
	T-2016	P_1	−207.16	0.37	0.27	0.35	0.22	0.20
		P_2	−207.16	0.01**	0.00**	1.6E-03**	0.02*	1.0E-06**
		RIL	−207.16	0.92	0.74	0.34	0.03*	1.1E-04**
	T-2017	P_1	−236.90	0.46	0.32	0.25	0.25	0.24
		P_2	−236.90	0.93	0.43	4.3E-03**	0.39	0.50
		RIL	−236.90	0.77	0.75	0.86	0.06	1.9E-03**
	T-2018	P_1	−51.23	0.73	1.00	0.18	0.58	0.57
		P_2	−51.23	0.04*	0.01**	0.07	0.04*	0.03*
		RIL	−51.23	0.87	0.90	0.90	0.89	0.57
	T-2019	P_1	−55.27	0.66	0.64	0.85	0.83	0.93
		P_2	−55.27	0.94	0.43	4.3E-03**	0.39	0.50
		RIL	−55.27	0.81	0.80	0.94	0.41	0.08

*, $P < 0.05$; **, $P < 0.01$. AIC, Akaike information criterion; $P(U_1^2)$, $P(U_2^2)$, and $P(U_3^2)$ represent P-values of χ^2 statistics with one degree of freedom to test the expected distribution of the selected genetic model with the empirical data distribution; $P(nW^2)$, P-value of Smirnov's statistics; $P(D_n)$, P-value of Kolmogorov's statistics (Zhang et al. [22]); 4MG-AI, four major genes with additive-epistasis genetic model that had the lowest AIC; H, heavy clay soil; S, sandy soil; T, two soil types combined; 5yrs, five years combined.

3.4.4 Genetic analysis of the best-fit genetic model

Table 2.4 lists the first- and second-order genetic parameters for the best-fit model 4MG-AI, estimated in the eight mean phenotypic datasets. These parameters included additive effects of the four major genes (d_a, d_b, d_c, and d_d), epistatic effects of paired genes (i_{ab} - i_{cd}), genetic variances of major genes (σ_M^2) and polygenes plus residual (σ_{R+P}^2), and heritability (h^2, a proportion of phenotypic variance explained by major genes). The additive effects of the first three major genes (a, b, and c) appeared to be negative in contrast to the fourth gene (d), which appeared to be positive for both traits in most datasets (**Table 3.4**). The four major genes explained 84.37% to 98.17% of the phenotypic variance for MSIs and 85.30% to 98.54% of phenotypic variance for MSRI in the phenotypic datasets. Although the additive effects of the four genes were all negative in some genetic models estimated from different datasets (**Table 3.4**), the genetic architecture of the four genes in these models performed similarly. Hereafter only the best-fitted models obtained from the overall mean phenotypic dataset are exhibited (**Table 3.4**).

Table 3.4 First and second order genetic parameters of the 4MG-AI model based on eight phenotypic datasets of marsh spot incidence (MSI) and marsh spot resistance index (MSRI).

Dataset	m	d_a	d_b	d_c	d_d	i_{ab}	i_{ac}	i_{ad}	i_{bc}	i_{bd}	i_{cd}	σ^2_{R+P}	σ^2_M	h^2
MSI														
H-5yrs	10.77	−4.11	−3.38	−4.36	1.66	2.22	3.73	−0.87	3.81	0.44	−3.61	7.76	75.30	90.65
S_5yrs	10.46	−3.08	−2.46	−3.92	2.45	1.38	3.29	−1.37	3.64	−0.16	−3.65	9.85	53.15	84.37
T-2015	13.73	−10.36	−7.39	−7.70	−2.56	4.16	6.55	4.01	3.52	4.76	−2.21	3.17	114.88	97.32
T-2016	7.94	−5.38	−4.16	−3.52	−0.52	3.57	3.19	1.70	1.95	1.72	−2.57	1.57	78.80	98.04
T-2017	9.57	−6.31	−3.88	−4.88	0.17	2.60	4.56	0.48	3.23	2.14	−2.89	1.23	65.96	98.17
T-2018	12.02	−6.08	−5.38	−4.99	−1.47	4.10	4.54	1.65	4.62	2.68	−1.54	3.68	81.54	95.68
T-2019	9.95	−3.84	−3.62	−2.86	1.56	2.50	2.77	−0.53	2.76	0.17	−2.30	7.44	59.74	88.93
Overall	10.65	−3.53	−1.99	−3.74	1.94	1.55	3.40	−1.84	3.33	0.20	−3.67	10.08	54.49	84.39
MSRI														
H-5yrs	0.30	−0.18	−0.13	−0.13	−0.03	0.09	0.12	0.05	0.07	0.06	−0.06	0.00	0.06	92.59
S-5yrs	0.26	−0.09	−0.05	−0.09	0.05	0.05	0.09	−0.05	0.10	0.00	−0.10	0.00	0.03	88.50
T-2015	0.36	−0.31	−0.22	−0.16	−0.12	0.16	0.13	0.12	0.04	0.12	0.02	0.00	0.08	98.54
T-2016	0.18	−0.12	−0.08	−0.10	−0.01	0.05	0.09	0.01	0.07	0.04	−0.05	0.00	0.04	98.06
T-2017	0.23	−0.14	−0.11	−0.10	0.00	0.07	0.10	0.04	0.05	0.02	−0.05	0.00	0.04	97.30
T-2018	0.28	−0.14	−0.11	−0.11	−0.04	0.09	0.12	0.05	0.09	0.06	−0.04	0.00	0.06	93.60
T-2019	0.27	−0.13	−0.12	−0.10	−0.02	0.10	0.10	0.03	0.09	0.04	−0.07	0.01	0.05	87.83
Overall	0.27	−0.05	−0.05	−0.10	0.01	0.08	0.08	−0.05	0.08	−0.03	−0.09	0.01	0.04	85.30

m and *d* represent population mean and additive effect, respectively; *i* represents additive × additive-epistatic effect between two major genes; σ^2_{R+P} represents the variance of residual and polygenes; σ^2_M represents the variance of major genes. Subscripts *a*, *b*, *c* and *d* represent the four major genes. 4MG-AI, genetic model of four major genes with additive-epistasis. h^2, proportion of phenotypic variance explained by the major genes modeled; H, heavy clay soil; S, sandy soil; T, two soil types combined; 5yrs, five years combined.

The additive effects of the four major genes were −3.53, −1.99, −3.74 and +1.94 for MSI, and −0.05, −0.05, −0.10 and +0.01 for MSRI, respectively. Large digenic epistatic effects, even greater than additive effects, were also observed, ranging from −3.67 to 3.40 for MSI and from −0.09 to 0.08 for MSRI. Since MSI and MSR are two non-independent traits and they were highly correlated (**Table 3.3**), we hypothesized the two traits shared the same four genes. Thus, for simplicity, gene symbols *M1, M2, M3* and *M4* corresponding to four genes (a–d) were assigned to both traits with alleles *M* and *m*. If *M1, M2*, and *M3* are considered favorable alleles for the first three genes due to their negative effects on symptom development, then *m4* would be a favorable allele for the *M4* gene due to its positive effect on symptom development.

Based on the 4MG-AI model, the posterior probability of all 16 genotypes of four genes for 138 RILs was estimated (**Appendix 9, 10**), which allows us to predict the possible genotype of each RIL. The most likely genotype of an RIL was the one that had the highest posterior probability among all 16 genotypes. If two or more genotypes shared the same highest probability, all of them were assigned to the RIL. In addition, to clarify the possible genotypes graphically, a value of zero was assigned to the remaining genotypes. As such, the heat maps of the highest posterior probabilities with the possible genotypes are depicted in **Figure 3.4a** for MSI and **Figure 3.4b** for MSRI. All RILs were assigned to 14 genotypes for MSI (**Figure 3.4a**) and to all 16 genotypes for MSRI (**Figure 3.4b**).

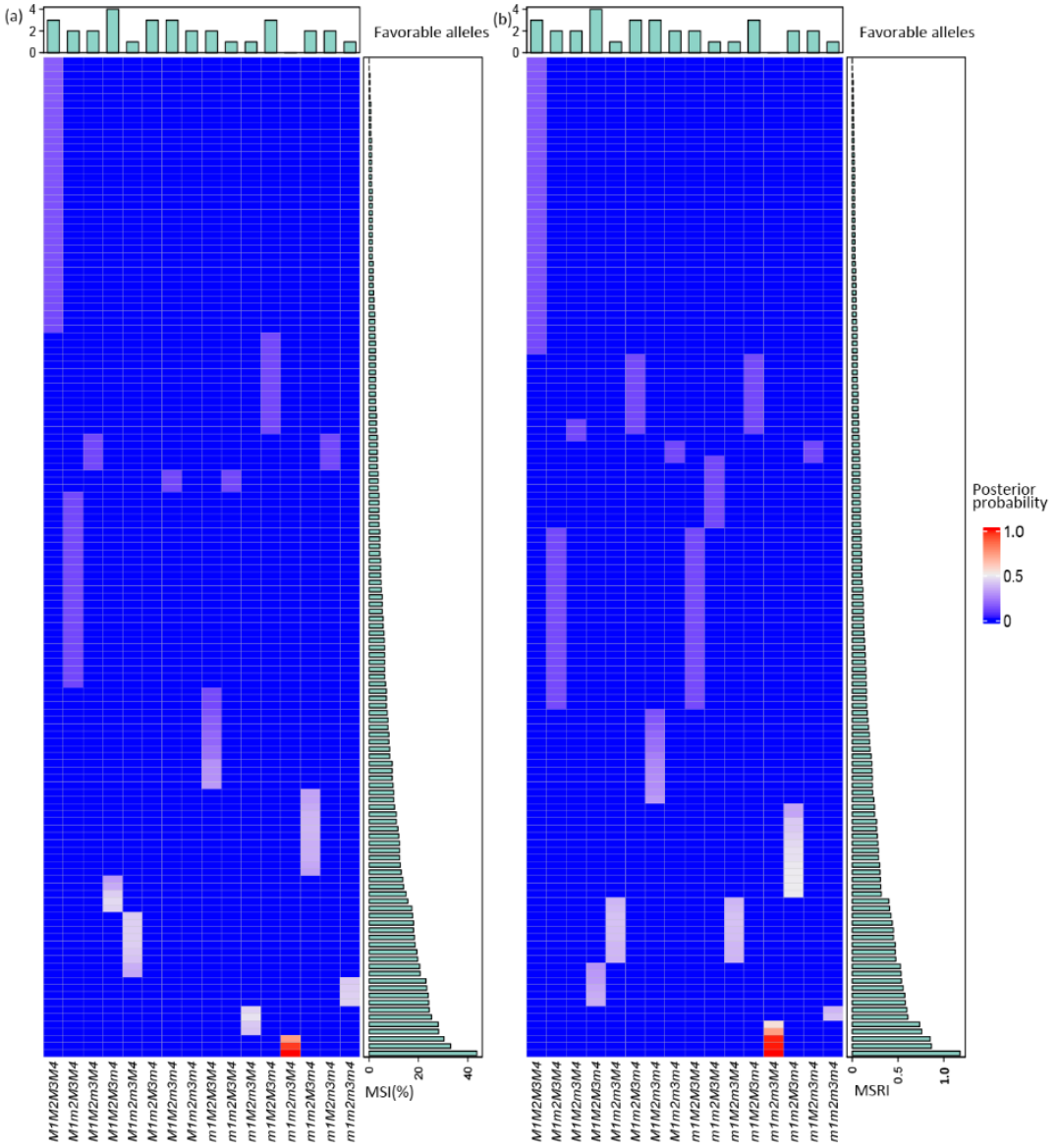

Figure 3.4 Posterior probability of each of 16 genotypes of four major genes in the 4MG-AI model for marsh spot incidence (MSI) (a) and marsh spot resistance index (MSRI) (b) in the RIL population of 138 lines. The mean dataset over five years and two soil types were used.

For MSI (**Figure 3.4a**), the three most susceptible lines (30.3%–43.7% MSI) had the haplotype *m1m2m3M4*, i.e., the four unfavorable alleles. In contrast, the 39 top resistant lines (0–2.3% MSI) had the haplotype *M1M2M3M4* that had three of the four favorable alleles (*M1–M3*). However, if the RILs had all four favorable alleles (*M1M2M3m4*), they turned out to be relatively susceptible (14.0%–17.7% of MSI). Similarly, for MSRI, the four most susceptible lines (0.75–1.2 MSRI) had a haplotype *m1m2m3M4*, all unfavorable alleles. The top 41 resistant lines (0–0.05 MSRI) had the haplotype *M1M2M3M4* containing three of the four favorable alleles (*M1–M3*). The outcome was the same as for MSI in which the lines with all four favorable alleles (*M1M2M3m4*) were susceptible (0.5–0.6).

Further analysis indicated that MS ratings decreased with favorable alleles from zero to three, confirming that three of the four genes were primarily additive, but the fourth may suppress the expression of the other three genes (**Figure 3.5**).

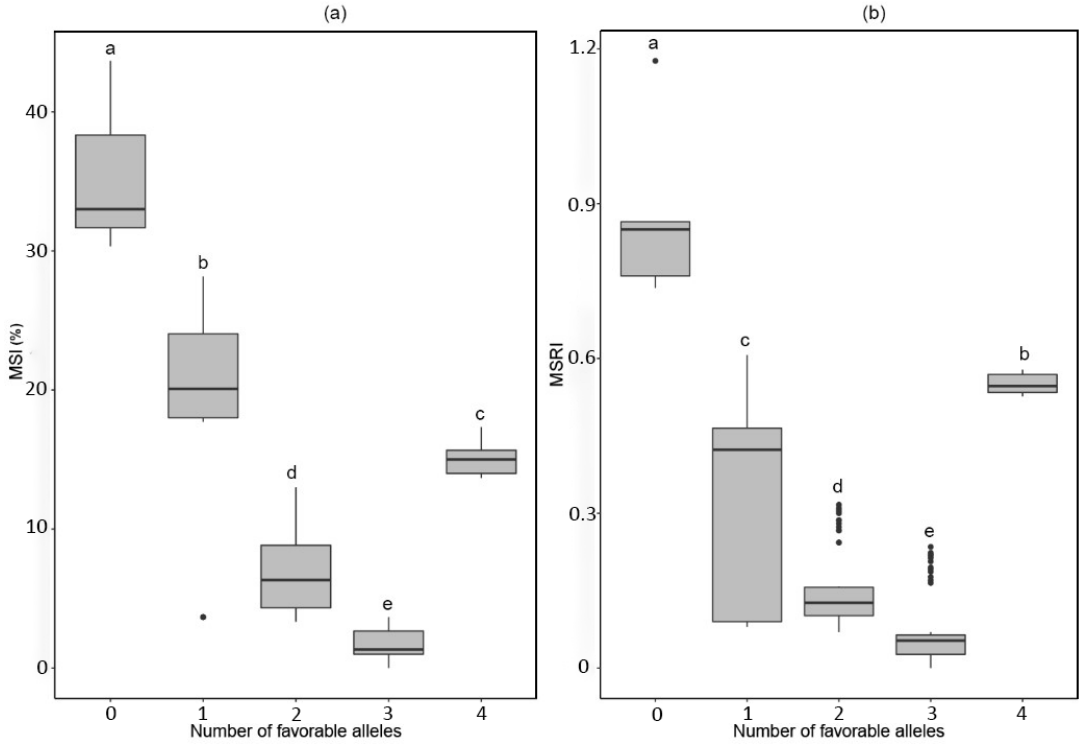

Figure 3.5 Relationship between marsh spot incidence (MSI) (a) and marsh spot resistance index (MSRI) (b) with the number of favorable alleles in the RIL population of 138 lines underlying the 4MG-AI model. The letters on the top of boxes represent statistical significance at the 5% probability level.

Therefore, the epistatic interactions among the four genes were further analyzed (**Appendix 6**). Although complex digenetic interaction effects were observed among

the four genes, the first three genes (*M1, M2*, and *M3*) behaved mostly in an additive manner (**Appendix 6b-d, f-h**), while *M4* significantly promoted or impeded expression of additive resistance conferred by the first three genes (**Appendix 6a, e**).

The *M4* gene had significant epistatic effects on the *M1, M2,* and *M3* genes. The *M4* allele with the *M1M2M3* haplotype resulted in the highest resistance, whereas the *m4* allele suppressed the additive effects of *M1M2M3*. Conversely, the *M4* allele assisted the expression of the additive effects of *m1m2m3*, resulting in the most susceptible plants.

The resistant parent Cran09 had an average MSI and MSRI of 1.5% and 0.04, respectively, while MSI and MSRI values in the susceptible parent Messina were 31.9% and 0.80, respectively. According to the ratings of the parents, it seemed reasonable to infer that Cran09 had the haplotype of *M1M2M3M4*, and that Messina may have the haplotype *m1m2m3M4*, *m1m2m3m4* or *m1M2m3M4*. However, because 14–16 genotypes were inferred in the RILs (**Figure 3.4**), *m1m2m3m4* was the most likely haplotype that could account for the segregation of 16 genotypes.

3.5 Discussion

MS is a common disease leading to seed quality and yield losses in cranberry common beans and other common beans. Although MS disease was reported in beans in the 1930s (Furneaux and Glasscock, 1936;Heintze, 1938), the genetics of its resistance remained unknown. This study is the first report on the inheritance of MS resistance in cranberry or other common beans. The study will facilitate discovering the genetic mechanisms controlling MS resistance, identifying associated genes, and developing molecular markers for resistance breeding.

This study developed a new genetic population consisting of 138 RILs derived from a cross between the resistant cultivar Cran09 and the susceptible cultivar Messina. MS ratings of the 138 RILs were evaluated over five years under two soil types, demonstrating that the genes associated with MS resistance in the two parents segregated and recombined to produce a genetic variation exceeding the performance of the two parents, thereby rendering this population useful for genetic studies and QTL mapping.

To study MS resistance, MSI and MSRI, which represent the incidence and severity

of MS disease, respectively, were evaluated. Spearman rank correlation and genetic analysis of the phenotypes suggested that these two traits were highly correlated ($r > 0.96$) and most likely had similar or the same genetic architecture.

Previous studies have confirmed that MS disease is most likely caused by Mn deficiency caused by low soil Mn or poor Mn uptake (Samuel and Piper, 1929;Furneaux and Glasscock, 1936;Piper, 1941;Reynolds, 1955); hence, the potential link between MS and soil type (Kandpal et al., 2005;Bornø et al., 2019). Thus, in this study, MS resistance was evaluated under the two soil types, sandy and heavy clay soil. The two soil types had similar Mn levels but different soil structures. No significant difference in MSI or MSRI between soil types was found. In addition, similar MS ratings among 2015, 2016 and 2017 and between 2018 and 2019 were observed, but significant differences existed between the first three years and the last two years. We analyzed the changes in temperature and precipitation during growth periods of five years, but no patterns of either temperature or rainfall were found to relate to the differences of MS resistance between years. However, the soil Mn concentrations in 2015–2017 were significantly higher than those in 2018–2019 (**Appendix 6a**), which may result in the differences of MS resistance between the years of 2015–2017 and the years of 2018–2019. This result also indirectly confirms that MS disease is associated with Mn deficiency. However, although the soil Mn concentration is much lower in sandy soil than in heavy clay, the Mn nutrition is more easily absorbed by plants in sandy soil (Rieuwerts et al., 1998), resulting in no significant differences in MS resistance between the two soil types. Overall, the evaluation of the MS resistance of the population across five years and two soil types strongly indicates that MS rating is less affected by environment than by genes. High broad-sense heritability estimates of both traits also support this conclusion. Thus, MS resistance is a relatively stable and heritable character.

The significantly right-skewed distribution of MSI and MSRI observed suggested the reasonable hypothesis of MSI and MSRI being most likely controlled by few major genes plus some minor-effect polygenes. Joint segregation analysis provided an efficient approach to dissect this type of skewed distribution to determine whether the trait is controlled by major genes and/or polygenes in genetic populations such as double haploid and RIL (Wang, 1996;Wang and Gai, 2001;Zhang et al., 2001;Zhang et al., 2003b;Wang et al., 2010). It has been successfully applied to dissect some complex quantitative traits, especially those involving major genes plus polygenes, such as

disease resistance (Wang et al., 2010), male sterility (Wei et al., 2020), and flowering date (Zhang et al., 2001). In the present study, JSA showed that for both MSI and MSRI, 4MG-AI (four major genes with additive and epistatic effects) was the best genetic model among the 35 tested (**Table 2.4**). This is the first empirical dataset of plant quantitative traits that fits a four major gene system using JSA. Theoretically, only the genetic model supporting a maximum of four pairs of major genes without polygenes has been developed and evaluated using simulation data of a RIL population (Wang et al., 2010), and implemented in the R package SEA V1.0 (https://cran.r-project.org/web/packages/SEA/index.html). Though 4MG-AI was considered the best-fit model based on the AIC criterion, various statistical tests, and heritability of the model (proportion of phenotypic variance explained by the model), additional major genes and/or polygene should not be excluded because of the theoretical limit in the development of genetic models with more major genes and polygenes. In addition, we tested the models with one to three major genes plus polygenes, from which polygenes explained 0–47.19% of the phenotypic variance. Therefore, we deduce that polygenes could also be a portion that confers MS resistance.

The SEA package provides a function that estimates the posterior probability of all genotypes underlying genetic models, which can be used to predict the most probable genotype of individuals of a population by selecting the genotype with the highest probability as the candidate genotype. Based on the predicted genotypes of population individuals, we can further analyze additive and epistatic effects of all genes in the best-fit genetic models in detail. Using this method, we found that digenetic epistatic interaction significantly suppressed additive effects of genes in MS resistance.

3.6 Conclusion

The evaluation of MS resistance in a RIL population of 138 lines suggested that MSRI and MSI were stable and heritable traits. The JSA of the RIL population and its parents revealed that both traits were controlled by four pairs of major genes (*M1, M2, M3, and M4*) with additive and epistatic effects. Among them, *M4* performed as a key suppressor that affected additive effects of the other three genes on MS resistance. The individuals with the *M1M2M3M4* haplotype were the most resistant, but those with the *M1M2M3m4* haplotype were susceptible. Further QTL mapping would be useful to identify the individual genes or QTL on chromosomes, explore their genetic

mechanisms, and develop corresponding markers for molecular breeding of resistant cultivars.

4. Quantitative trait locus mapping of marsh spot resistance in cranberry common bean (*Phaseolus vulgaris* L.) (Jia et al., 2022)

Jia B, Conner RL, Waldo PC, Khan N, Zheng, C, Cloutier, S, Hou A, Xia X, You FM: **Quantitative trait locus mapping of marsh spot disease resistance in cranberry common bean (*Phaseolus vulgaris* L.)**. *International Journal of Molecular Science* 2022, 23(14):7639

4.1.1 Abstract

Dry common bean (*Phaseolus vulgaris* L.) is a food crop that is an important source of dietary proteins and carbohydrates. Marsh spot is a physiological disorder that diminishes seed quality in beans. Prior research suggested that this disease is likely caused by manganese (Mn) deficiency during seed development and that marsh spot resistance is controlled by at least four genes. In this study, genetic mapping was performed to identify quantitative trait loci (QTL) and the potential candidate genes associated with marsh spot resistance. All 138 recombinant inbred lines from a bi-parental population were sequenced using a genotyping by sequencing approach. A total of 52,676 single nucleotide polymorphism (SNP) markers were identified and filtered to generate a high-quality set of 2,066 SNPs for QTL mapping. A genetic map based of 2,061 SNP markers distributed on 11 chromosomes and covering 5,980 cM was constructed. A total of 21 QTL were identified using additive effect models, and an additional 13 epistatic QTL interacting with four of the 21 QTL were identified using an epistasis model. Through genome-wide scans of the genes located within 100 kb interval flanking each QTL, 17 Mn-deficiency related candidate genes co-located within six QTL. Among these six QTL, *QTL.5.2* had the highest R^2 and harbored two important Mn transporter genes: the zinc transporter (ZIP) coding gene *Phvul.005G048900* and the cation efflux (CAX) family protein-coding gene *Phvul.005G049300*. These results advance the current understanding of the genetic mechanisms of marsh spot resistance in cranberry common bean, and provide new genomic resources for use in genomics-assisted breeding and for candidate gene isolation and functional characterization.

Keywords: Marsh spot disease, cranberry common bean, QTL mapping, genotyping

by sequencing (GBS), single nucleotide polymorphisms (SNPs), genome-wide association study (GWAS), *Phaseolus vulgaris*

4.2 Introduction

Dry common bean (*Phaseolus vulgaris* L., 2n=2x=22) is a widely grown grain legume crop planted in Canada with area up to 160,000 ha and dry seed production to 316,800 Mt (Statistics Canada, 2019). As reported by FAO (Food and Agriculture Organization), common bean global production reached to 28.9 million tons within 33.1 million ha around world in 2019. Over half of the global production was shared by Asian (Database, 2019). It is not only a crucial crop for food security but it is also highly nutritious, meeting human nutrition requirements for proteins, vitamins, minerals, carbohydrates and other nutrition. Common bean is a high-quality and low-cost source of proteins, especially valuable for developing countries.

One of the most important goals in common bean breeding is yield. High yield cultivars are more likely to be selected during long-time domestication, and recent research also focused on improving bean yield (Rosales-Serna et al., 2004;Blair et al., 2006;Ndakidemi et al., 2006). With the help of new cultivars and technologies, the average common bean yield has achieved a remarkable increase of approximately 420 kg per ha during the past 20 years (FAOSTAT., 2018).

Other traits such as micronutrient contents or resistance to abiotic and biotic stresses are also crucial to sustain common bean yield and quality. Marsh spot disease is a physiological disorder that affect both seed yield and quality of pulse crops, primarily in peas (Lacey, 1934;Heintze, 1938;Piper, 1941;Reynolds, 1955;Henkens, 1958;Howard et al., 1994;Biddle and Cattlin, 2007) and beans (Hewitt, 1945;Howard et al., 1994;Biddle and Cattlin, 2007). Marsh spot, first reported in 1933 on pea, is characterized by a brown lesion in the flat inner surface of one or both cotyledons that is sometimes accompanied by partial or entire necrosis of the plumule (De Bruyn, 1933). In bean seeds affected by marsh spots, discolored lesions usually occur at the center of the adaxial surface of each cotyledons within the seed (Jia et al., 2021b). These spots may be caused by cell death underneath the cotyledon's skin (Reynolds, 1955). A brown substance replaces the starch originally stored in those cells and eventually seed staining becomes visible (Reynolds, 1955). Previous studies indicated that marsh spot is caused by a manganese (Mn) deficiency (Lewis, 1939;Wilson, 1979;Graham et al.,

1988;Humphries, 2007;Schmidt et al., 2016;Jia et al., 2021b).

Although marsh spot disease was discovered in 1933, its inheritance has been scantily studied because nutrient deficiencies do not generally get the same attention as pathogen susceptibilities . While some chemical treatments have been used to reduce the incidence and severity of marsh spots (Koopman, 1937;Lewis, 1939), genetic improvement remains the most efficient and environment-friendly approach. To understand the genetic mechanism of marsh spot disease, an $F_{2:7}$ population consisting of 138 recombinant inbreeding lines (RILs) from a cross between the susceptible cultivar 'Messina' and the resistant cultivar 'Cran09' was evaluated for the presence and extent of marsh spot lesions over a five year period on two soils: sand and heavy clay (Jia et al., 2021a). Marsh spot incidence (MSI) and resistance index (MSRI) were used to estimate the disease severity (Jia et al., 2021a). The highly correlated MSRI and MSI showed high broad-sense heritability values (H^2) of 86.5% and 83.2%, respectively (Jia et al., 2021a). There was no significant difference between the two soil types across five years. We also employed joint segregation analysis on the phenotypic data of marsh spot reactions, which revealed that at least four major genes controlled marsh spot resistance (Jia et al., 2021a). Here we report on the quantitative trait loci (QTL) associated with marsh spot resistance and on the putative candidate genes with a goal to assist in the development of diagnostic markers for marker-assisted breeding and to provide genomics resources towards the cloning of the causal genetic features of marsh spot in beans.

4.3 Materials and methods

4.3.1 Recombinant inbred line (RIL) population

A $F_{2:7}$ RIL population of 138 individuals derived from a cross between the marsh spot susceptible cultivar "Messina" and the highly-resistant cultivar 'Cran09' was generated (Jia et al., 2021a). F_2 plants were selfed and propagated by single seed descent to the F_7 generation to ensure a high percentage (>98%) of homozygosity.

4.3.2 Phenotyping of marsh spot resistance

From 2015-2019, the 138 RILs and their two parents were evaluated for marsh spot

severity in sandy and heavy clay soils as previously described (Jia et al., 2021a). Briefly, the field trials were conducted in a partially-balanced lattice design with three replications at the Morden Research and Development Centre, Morden, Manitoba, Canada (49°11′N, 98°5′W). Each line was planted in a 5m-long row with 75 cm spacing between rows, and herbicides and fertilizers were applied to ensure optimal growth following standard commercial production guidelines. After harvest, ten seeds were randomly selected from each line and rated for marsh spot severity using a 0 to 5 scale, where 0 indicates no symptoms and 5 represents the most severe symptoms. Marsh spot resistance index (MSRI) was used to estimate the severity of the disease for each of the RILs:

$$\text{MSRI} = \frac{\sum_{i=0}^{n}(\text{number of seeds at a rating with } 0-5 \text{ scale} \times \text{the rating})}{\text{Total number of seeds}},$$

where n is the total number of ratings and i = 0, 1, …, 5, respectively.

A total of 18 phenotypic datasets were collated: ten for each combination of the five years and two soil types, five for the means of each year over the soil types, two for the means of soil types over the five years and one for the means overall years and soil types. Statistical illustrations were drawn using the R package 'ggplot2' (https://cran.r-project.org/web/packages/ggplot2/index.html). The detailed ratings for marsh spot and the analyses of the phenotypic data were carried out as previously described (Jia et al., 2021a;Jia et al., 2021b).

4.3.3 Genotyping by sequencing and SNP identification

Seeds of the individual RILs along with the parental lines were grown in a growth chamber. At the 2-leaf stage, 75mg of leaf tissue was sampled and flash-frozen in liquid nitrogen before being lyophilized in a FreeZone benchtop freeze-dryer (Labconco, Kansas City, MO, USA). Genomic DNA was extracted using the DNeasy 96-well kit (Qiagen, Germantown, MD, USA) and quantified with the Quant-iT™ PicoGreen™ dsDNA assay kit (ThermoFisher, Waltham, Massachusetts, USA) following the manufacturer's instructions. The DNA samples were diluted to 20ng/µl, and 10 µl of each sample was used for library construction.

The library preparations and sequencing service were provided by the Centre d'expertise et de services Génome Québec . The GBS (genotyping by sequencing) library was constructed for each of the 138 RILs and ten libraries each for the parents,

for a total of 158 libraries. Library construction was conducted at the Institute of Integrative Biology and System (IBIS, Université Laval, Québec, QC, Canada) using the MspI/PstI restriction enzyme combination as previously described (Colston-Nepali et al., 2019). The 158 indexed libraries were pooled and sequenced on twenty 35M-read NovaSeq 6000 lanes using the paired-end 150bp (PE150) mode at the Centre d'expertise et de services Génome Québec (Montréal, QC, Canada).

As cranberry common bean belongs to the Andean gene pool (Gioia et al., 2019), the common bean reference genome v2.1 of Andean type landrace G19833 (Schmutz et al., 2014) was used as a reference for SNP discovery. The generated raw read data were filtered using the AGSNP pipeline (You et al., 2011) for standard quality and aligned to the reference genome using the Burrows-Wheeler Alignment tool (BWA V0.78-r455). Variant detection was performed using SAMTools (Bonfield et al., 2021). The entire procedure was implemented in the updated custom GBS analysis pipeline (Kumar et al., 2012;You et al., 2012). As a quality check, only SNPs that were polymorphic between parents and that segregated in the RIL population were selected. Then, SNPs with a minor allele frequency > 0.01 and call rate > 20% was retained. Missing SNPs were then imputed using Beagle (Mayoral et al., 2014) to produce the SNP dataset for linkage map construction. SNPs were assigned to LD blocks (D' > 0.8) using the R package gpart (http://bioconductor.org/packages/release/bioc/html/gpart.html) and one representative SNP was chosen to represent each block. Because the construction of genetic linkage map and the detection of QTL may be influenced by segregation distortion, the Chi-square test in IciMapping V4.0 (Wang et al., 1999) was used to evaluate the significance of segregation ratios and SNPs significantly deviating from the expected 1:1 ratio ($P < 0.05$) were excluded.

4.3.4 Genomic heritability

Genomic heritability (h^2), representing the proportion of additive genetic variance component of the total phenotypic variance, was estimated for all SNPs using the R package 'sommer' (https://cran.r-project.org/web/packages/sommer/index.html) with the genomic best linear unbiased prediction (GBLUP) model (Covarrubias-Pazaran, 2016;Lan et al., 2020).

4.3.5 Construction of linkage map

Construction of the linkage map was performed using QTL IciMapping V4.0 software (Wang et al., 1999). The SNPs were divided into linkage groups based on their physical positions on chromosomes and subsequently ordered based on their recombinant frequencies. A maximum recombination frequency of 0.35 centiMorgan (cM) was used from three criterion options . Genetic map distances were estimated using the Kosambi mapping function (Kosambi, 1944). The linkage groups were assigned to their corresponding chromosomes based on the SNPs identified on the reference genome (Schmutz et al., 2014).

4.3.6 QTL identification

IciMapping V4.0 (Wang et al., 1999) with the inclusive composite interval mapping (ICIM) and composite interval mapping (CIM) models was used for QTL mapping of the RIL population. In ICIM, forward and backward stepwise regressions were first computed, and Expectation–maximization (EM) iterations were then applied to consider all markers simultaneously. The additive (ICIM-ADD) and additive + epistatic (ICIM-EPI) models were used to detect QTL with additive and/or epistatic effects, respectively.

Genome-wide composite interval mapping (GCIM) (Su et al., 2020) was also used to detect large and small effect QTL. The GCIM model includes two steps. The first involves the scanning of putative QTL across the genome using a single-locus random mixed linear model used in genome-wide association studies (GWAS), and the second is the integration of the selected putative QTL into a multi-QTL mixed linear model. The QTL effects were calculated by empirical Bayes method with the likelihood ratio test employed on true QTL detection (Su et al., 2020). GCIM was implemented using the R package QTL.gCIMapping.GUI (https://cran.r-project.org/web/packages/QTL.gCIMapping.GUI/index.html).

Permutation tests of 1000 iterations (Churchill and Doerge, 1994) under the type I error $\alpha = 0.05$ was performed to obtain the LOD scores to be used as thresholds of significance for QTL detection.

A haplotype block-based GWAS method, RTM-GWAS (restricted two-stage,

multi-locus, multi-allele GWAS) (He et al., 2017), was also employed to detect QTL regions. RTM-GWAS first groups all SNP markers that shared strong linkage disequilibrium (LD) (D'> 0.8) into LD blocks, and then uses those LD blocks for QTL detection. A significance level of 0.05 was used for the pre-selection of individual candidate markers under the single locus model, and an experiment-wide significance level of 0.05 was used for the stepwise regression to declare the significant QTL under the multi-locus model.

One way-ANOVA was performed for each QTL to further test the statistical significance of MSRI between QTL alleles in all 18 phenotypic datasets. QTL were considered as single fixed factors with two or more alleles. In addition, the R^2 of each QTL was estimated as the proportion of phenotypic variation in the RIL population explained by alleles of the QTL. A higher R^2 value indicates the QTL has a stronger effect on the marsh spot resistance. The average R^2 of a QTL was calculated using R^2 values that were statistically significant in all 18 datasets.

To calculate the relative contribution (RC) of each QTL to total phenotypic variation, the relative R^2 value of each QTL was calculated based on a linear model containing all QTL using the R package 'relaimpo' (https://cran.rstudio.com/web/packages/relaimpo/index.html).

4.3.7 Favorable alleles

To determine the number of favorable alleles of each RIL, the mean MSRI of individuals with the same alleles was calculated for each allele of the identified QTL. If a QTL spans more than two SNPs, the number of alleles present at a QTL may be greater than two. Theoretically, no recombination between SNPs within a QTL region is expected, and thus most QTL had only two alleles. The recombinant alleles had very low frequencies in the population. These recombinant alleles may be due to rare recombination events between SNPs or resulted from the errors of SNP imputation. Therefore, only two alleles with the highest frequencies were considered for each QTL. The allele with a high mean MSRI value was assigned a favorable allele, whereas another allele with a low mean MSRI value was assigned an unfavorable allele. For each of the RILs, the total number of favorable alleles for all QTL were counted.

4.3.8 Candidate gene prediction

To predict the candidate genes associated with marsh spot disease resistance, a list of gene families related to Mn deficiency or Mn content in plants was compiled (**Appendix 11**) (Jia et al., 2021b) based on the common bean reference genome sequence (Schmutz et al., 2014). The protein sequences of Mn-deficiency-related gene families from common bean, *Arabidopsis*, rice (*Oryza sativa*) and barley (*Hordeum vulgare* L) (https://www.ncbi.nlm.nih.gov/guide/proteins/) were extracted and BLAST (basic alignment search tool) (Zhang and Madden, 1997) searches were performed against the common bean reference genome sequence to locate the bean orthologous sequences. A total of 154 candidate genes were thus identified based on their sequence similarity with Mn-deficiency-related gene families from other species , belonging to ten Mn-deficiency-related gene families. A genome-wide scan was performed to identify the ones located within 100 Kb of QTL to constitute the list of candidate genes co-located with the identified QTL.

4.4 Results

4.4.2 SNP Identification

A total of 13,064,398 paired-end genotyping by sequencing (GBS) reads corresponding to 196 Mb were generated from the sequencing of the 138 recombinant inbred lines (RILs). Considering a genome size of 473 Mb (Schmutz et al., 2014), the average genome coverage was 3.65X per line, ranging from 0.12X to 11.97X. To identify the parental origin of the variants identified in the RILs, the two parents were sequenced at a high coverage depth of 32.89X for Cran09 and 29.45X for Messina. An average of 78.56% of the reads of the RILs were aligned to the Andean type common bean genome G19833 reference genome (V2.1) (Schmutz et al., 2014), ranging from 66.54% to 82.70% (**Appendix 12**).

A total of 54,620 SNPs was identified by aligning GBS reads of the 138 RILs to the reference genome (V2.1) (Schmutz et al., 2014). Filtering for minor allele frequency > 0.01and call rate > 20% yielded a total of 2,066 SNPs. In addition, eight SNPs mapped to small scaffolds and were removed (**Appendix 13**). The SNPs were distributed across the whole genome, with an average of 188 SNPs per chromosome. Some regions on

Chr 2, 3, 4, 6 displayed high-density SNP regions (**Appendix 14**). Among the 2,058 SNPs, 1,863 SNPs were polymorphic between parents (Cran09 and Messina), and 195 SNPs had no call in one of the parent. Then, 785 SNPs that had significant segregation distortion at a 0.05 probability level were eliminated. Finally, 1273 SNPs were further imputed and used for linkage map construction (**Table 4.1**). .

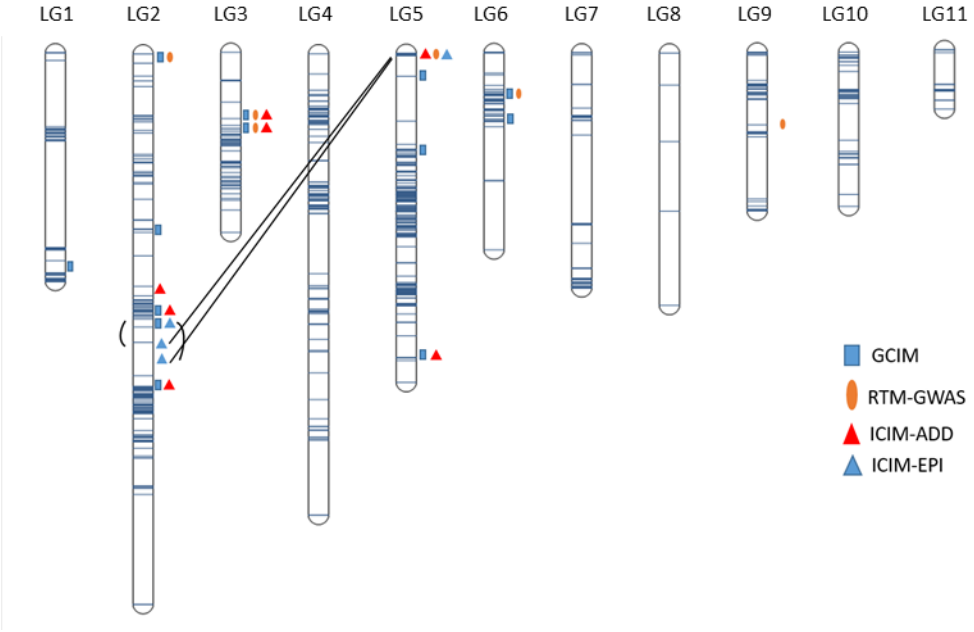

Figure 4.1 QTL associated with for marsh spot resistance index (MSRI) identified using four statistical models represented in the linkage map. Two QTL with significant epistasis effects are linked by a line.

Table 4.1 Number of markers on the linkage groups (chromosomes)

Linage group (chromosome)	No. of markers	Total distance (cM)	No. of recombination blocks	Mean distance between markers ± std deviation (cM)
1	101	131	27	4.86 ± 13.40
2	263	305	96	3.18 ± 7.17
3	115	105	41	2.56 ± 3.75
4	160	257	69	3.73 ± 7.10
5	360	186	76	2.44 ± 4.39
6	71	114	28	4.08 ± 9.60
7	72	135	21	6.41 ± 11.52
8	9	144	4	36.11 ± 14.80
9	59	93	26	3.59 ± 7.73
10	44	91	26	3.50 ± 5.40
11	19	38	9	4.20 ± 6.32
Total	1273	1599	434	3.78 ± 8.13

4.4.2 High-density genetic map

A genetic map of the 11 linkage groups or chromosomes was constructed containing 1273 SNP markers ranging from 9 on chromosome 8 to 360 on chromosome 5. Most

SNPs that were identified on the same chromosomes on the reference sequence were grouped into the same linkage groups (Appendix 15) and showed consistent orders in the physical chromosomes (Appendix 16). The map consisted of 423 recombination intervals with a total length of 1599 cm and an average interval of 3.78 cm (**Table 4.1**). Since only nine markers were retained on chromosome 8 after removing SNPs of significant segregation distortion, a large average interval (36.11 cm) between markers was obtained.

4.4.3 Genomic heritability

The genomic heritability (h^2) of common bean resistance to marsh spot was estimated for MSRI using the genetic additive variance of all SNPs and phenotype by GBLUP. The h^2 estimates ranged from 12.07% to 55.91 % in all 18 datasets with the highest h^2 (55.78%) originating from the overall mean dataset of MSRI (**Table 4.2**).

Table 4.2 Genomic heritability ($h^2 \pm s$) of the marsh spot resistance index (MSRI) of 138 RILs from the Cran09/Messina population

Phenotypic Dataset	Genomic Heritability ($h^2 \pm s$) (%)	Phenotypic Dataset	Genomic Heritability ($h^2 \pm s$) (%)
H2015	24.22 ± 0.09	S2019	12.07 ± 0.07
H2016	18.43 ± 0.08	T2015	32.48 ± 0.10
H2017	32.96 ± 0.10	T2016	28.02 ± 0.01
H2018	33.13 ± 0.10	T2017	45.53 ± 0.11
H2019	32.82 ± 0.10	T2018	45.48 ± 0.10
S2015	27.03 ± 0.10	T2019	41.12 ± 0.11
S2016	24.76 ± 0.10	H-5 yrs	46.46 ± 0.11
S2017	30.37 ± 0.10	S-5 yrs	47.14 ± 0.11
S2018	16.67 ± 0.08	Overall	55.91 ± 0.10

H: heavy clay soil; S: sandy soil; T: means of years over two soil types; H-5 yrs: means of heavy clay soil over five years; S-5 yrs: means of sandy soil over five years; Overall: means over five years and two soil types.

4.4.4 Mapping of additive QTL

Using two genetic map-based statistical models (ICIM-ADD and GCIM) and the haplotype block-based genome-wide association study (GWAS) model RTM-GWAS, a total of 18 QTL were identified from 18 phenotypic datasets. The QTL identified using different models were grouped into single QTL because they co-located on chromosomes or were within the same haplotype block. To validate the QTL identified by the different statistical models and from different phenotypic datasets (environments), we performed single factor (alleles) ANOVA for each identified QTL

using the 18 phenotypic datasets. Two of the 18 QTL had no significant allelic differences in QTL effects in >15 datasets and were removed. The 12 stable QTL presented significant QTL effects in most of the phenotypic datasets (>10) with the mean R^2 ranging from 6.81% (*QTL.6.1*) to 24.52% (*QTL.3.1*), whereas the remaining four QTL (*QTL.1.1*, *QTL.5.1*, *QTL.6.2* and *QTL.9.1*) explained 5.9–7.8% of phenotypic variation in three to five phenotypic datasets, indicative of environment-specific features (**Table 4.3 and Appendix 17, 18, Figure 4.2**).

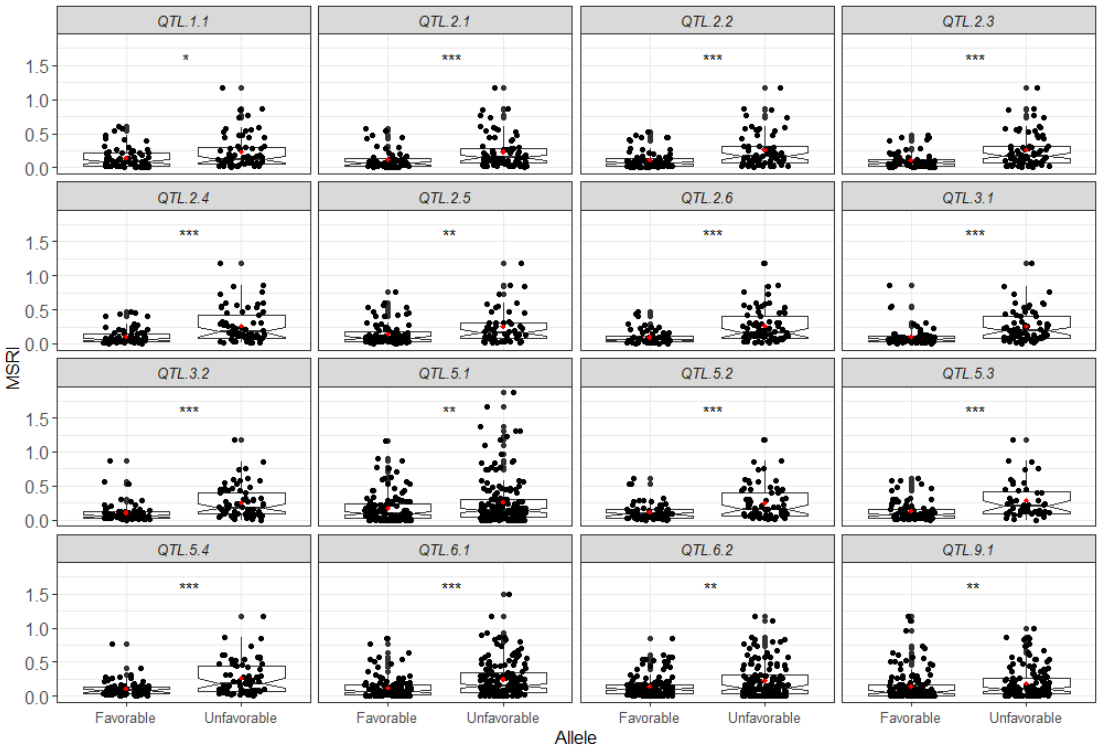

Figure 4. 2 Box plots of 16 QTL associated with marsh spot resistance index (MSRI). *, $P < 0.05$; **, $P < 0.01$; ***, P< 0.0001; ns, not significant. The black dots represent data points and the red dot in each box represent the mean of the data points.

Table 4.3 QTL detected from the RIL population of 138 individuals.

QTL	Flanking Markers and Position	LG pos (cm)	Additive Effect	No. of Datasets [a]	Significant Datasets [b]	Average R^2 (%) [c]	Model
QTL.1.1	Chr1_48339634–Chr1_50146614	119.26–126.33	0.10	1	3	5.92	GCIM
QTL.2.1	Chr2_872663–Chr2_1135128	0.06–5.22	0.05–0.11	6	11	8.30	GCIM, RTM-GWAS
QTL.2.2	Chr2_32113326	97.46	0.07	1	17	9.12	GCIM
QTL.2.3	Chr2_34070996–Chr2_35065692	147.11–151.45	0.15	1	16	11.43	GCIM
QTL.2.4	Chr2_35130486–Chr2_35289581	143.04–142.69	0.07–0.10	5	18	10.42	GCIM, ICIM-ADD
QTL.2.5	Chr2_35344261–Chr2_36750706	128.94–134.16	0.14	1	17	10.02	ICIM-ADD
QTL.2.6	Chr2_37937595–Chr2_38452857	187.14–188.25	0.05–0.51	5	18	12.30	ICIM-ADD, GCIM
QTL.3.1	Chr3_11944447–Chr3_19043093	47.42–51.49	−0.08	5	17	24.52	GCIM, RTM-GWAS, ICIM-ADD
QTL.3.2	Chr3_19701297–Chr3_30221015	48.9–50.4	−0.57–0.17	13	17	21.78	ICIM-ADD, GCIM, RTM-GWAS
QTL.5.1	Chr5_11498360–Chr5_19238819	56.2–57.31	−0.46	1	4	7.39	GCIM
QTL.5.2	Chr5_1647320–Chr5_31681432	12.94–38.3	0.06–0.10	6	18	9.23	GCIM
QTL.5.3	Chr5_38536162–Chr5_38536272	171.77–171.75	0.06–0.13	10	17	10.72	GCIM, ICIM-ADD
QTL.5.4	Chr5_623370–Chr5_673021	0–1.13	−0.10–−0.07	12	17	11.61	ICIM-ADD, RTM-GWAS
QTL.6.1	Chr6_1374720–Chr6_1504675	23.18–23.92	0.04–0.08	4	13	6.81	GCIM, RTM-GWAS
QTL.6.2	Chr6_13598278–Chr6_14124318	39.58–38.48	0.05–0.07	2	5	7.52	GCIM
QTL.9.1	Chr9_17827630–Chr9_20865151	42.84–46.75	0.20	2	3	7.82	GCIM, RTM-GWAS

[a] Number of datasets where QTL detected from; [b] number of datasets which QTL significantly correlated with; [c] the mean of R^2 of QTL in the datasets that showed significant correlation with QTL; Chr: chromosome; LG pos: position on linkage group.

Of the sixteen QTL, one was located on Chr 1, six on Chr 2, two on Chr 3, four on Chr 5, two on Chr 6, and one on Chr 9 (**Table 4.3**). One QTL was identified by a single SNP, or a quantitative trait nucleotide (QTN). In all sixteen QTL, two QTL were detected by three models, seven QTL by two models, and seven QTL by only one model. The LOD value of a QTL represents its significance extent. The LOD values for QTL identified from ICIM-ADD and GCIM varied from 3.14 to 7.58. Thirteen out of sixteen QTL had relatively high absolute values of additive effects (≥0.1) ranging from 0.1 to 0.57 (**Table 4.3**).

4.4.5 Mapping of epistatic QTL

The additive-epistasis model ICIM-EPI was used to detect interactions among QTL. A total of three QTL pairs with significant epistatic effects were identified, involving two additive QTL identified using additive models: *QTL.2.3* and *QTL.5.4* (**Table 4.4, Figure 4.3**). *QTL.5.4* significantly interacted with two additional QTL, *QTL.2.7* and *QTL.2.8* identified by ICIM-EPI, while *QTL.2.3* also interacted with *QTL.2.8* (**Table 4.3**). The LOD values varied from 6.21 to 7.20. The additive effects of the two QTL *QTL.2.3* and *QTL.5.4* were −0.06 and −0.05, respectively, and those of the two interacting QTL *QTL.2.7* and *QTL.2.8* were the same value of 0.04. The epistatic effects of the three pairs of QTL ranged from −0.10 to −0.11. The mean R^2 of QTL ranged from 16.31% to 30.69%, and the highest average R^2 of 30.69% was obtained from the QTL pair *QTL.2.9* and *QTL.5.4*. Despite the significant interactions between pairs of QTL, on average, the number of favorable alleles of individuals tended to be positively correlated with MSRI (**Appendix 19**).

Table 4.4 QTL detected using the additive-epistatic model ICIM-EPI.

QTL 1				QTL 2				No. Datasets with QTL [a]	No. Datasets with Significant [b]	Average of Effect R^2 (%) [c]	Additive Effect of QTL 1	Additive Effect of QTL 2	Epistatic Effect
QTL 1	**Left Marker**	**Right Marker**	**LG pos (cM)**	**QTL 2**	**Left Marker**	**Right Marker**	**LG pos (cM)**						
QTL.5.4	Chr5_673021	Chr5_1647342	1.13–12.92	*QTL.2.7*	Chr2_36996368	Chr2_37937763	160.01–178.45	1	18	30.64	−0.05	0.04	−0.11
QTL.5.4	Chr5_673021	Chr5_1647342	1.13–12.92	*QTL.2.8*	Chr2_37937763	Chr2_37531627	178.45–184.57	2	18	30.69	−0.05	0.04	−0.11
QTL.2.3	Chr2_34070996	Chr2_35065692	147.11–151.45	*QTL.2.8*	Chr2_37937763	Chr2_37531627	178.45–184.57	1	9	16.31	−0.06	0.04	−0.10

[a] Number of datasets where QTL detected from; [b] number of datasets which QTL significant correlated with; [c] the mean of average R^2 of two QTL. C in the Flanking markers and position column represent chromosomes.

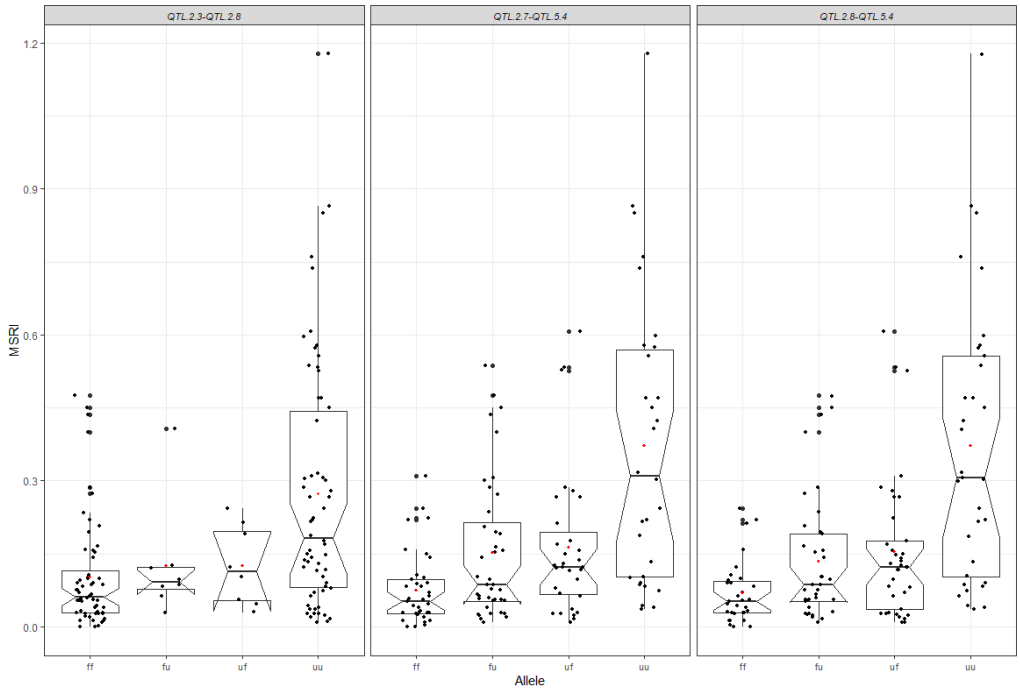

Figure 4.3 Box plots of marsh spot resistance index (MSRI) in terms of the combinations of favorable alleles of 3 QTL pairs identified using the ICIM-EPI model. ff: both QTL1 and QTL2 were favorable alleles. uf: QTL1 was an unfavorable allele while QTL2 was a favorable allele; fu: QTL1 was a favorable allele but QTL2 was an unfavorable allele; uu: both QTL1 and QTL2 were unfavorable alleles.

4.4.6 Contribution of all detected QTL to marsh spot resistance

In examining only additive effects, multiple linear regression models of all 16 QTL for each of 18 phenotypic datasets were constructed to calculate the overall contribution of all QTL to the phenotype variation. The R^2 of the model represents the portion of the phenotypic variation explained by all 16 QTL. The R^2 estimates of the 18 regression models ranged from 46.08% (S2019) to 75.37% (overall dataset), with a mean R^2 of 61.98% (**Figure 4.4**). However, when both additive and epistatic effects of the QTL were considered, i.e., the additional two QTL that were influenced by the significant epistatic effects of three of the 16 QTL, the R^2 estimates of the models increased and ranged from 56.21% to 81.87% with a mean R^2 of 69.64% (**Figure 4.4**).

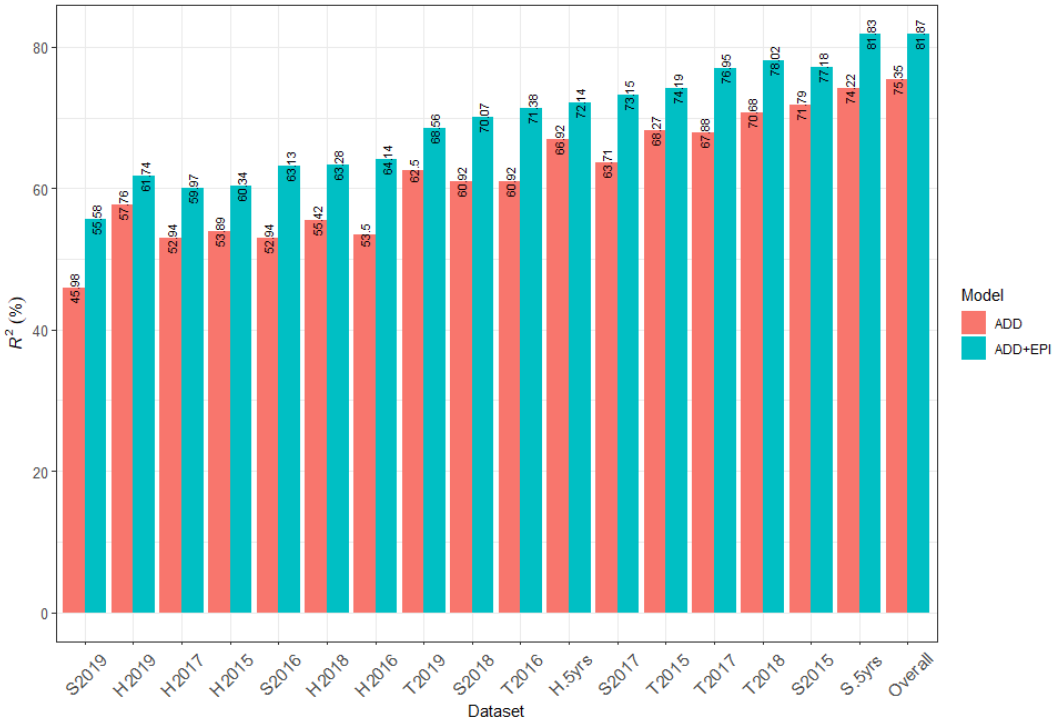

Figure 4.4 Bar chart of R^2 of 16 QTL to the 18 phenotypic datasets of marsh spot resistance index (MSRI). The R^2 value for each phenotypic data set was calculated as the coefficient of determination in the multiple regression of 21 QTL on the phenotypic data set.

The relative contribution (RC) of each QTL to MSRI values estimated in the datasets is listed in **Appendix 19**. *QTL.5.4* which also had a significant epistatic effect with *QTL.2.7* and *QTL.2.8* had the largest RC (13.48%), followed by *QTL.2.1* (10.4%), *QTL.5.3* (9.44%), *QTL.2.6* (8.9%), *QTL.3.2* (8.26%), *QTL.3.1* (8.14%). The remaining QTL had relatively low RCs (ranging from 0.3 to 6.79%). However, due to partial correlation among QTL, the RC and mean R^2 values of QTL were not always consistent (Figure 5). For example, *QTL.3.1* and *QTL.3.2* had the highest mean R^2 values (24.5% and 21.8%, respectively); however, their mean RC values over the 18 datasets were not the highest (7.91% and 7.93%, respectively) (**Figure 4.5, Appendix 20**).

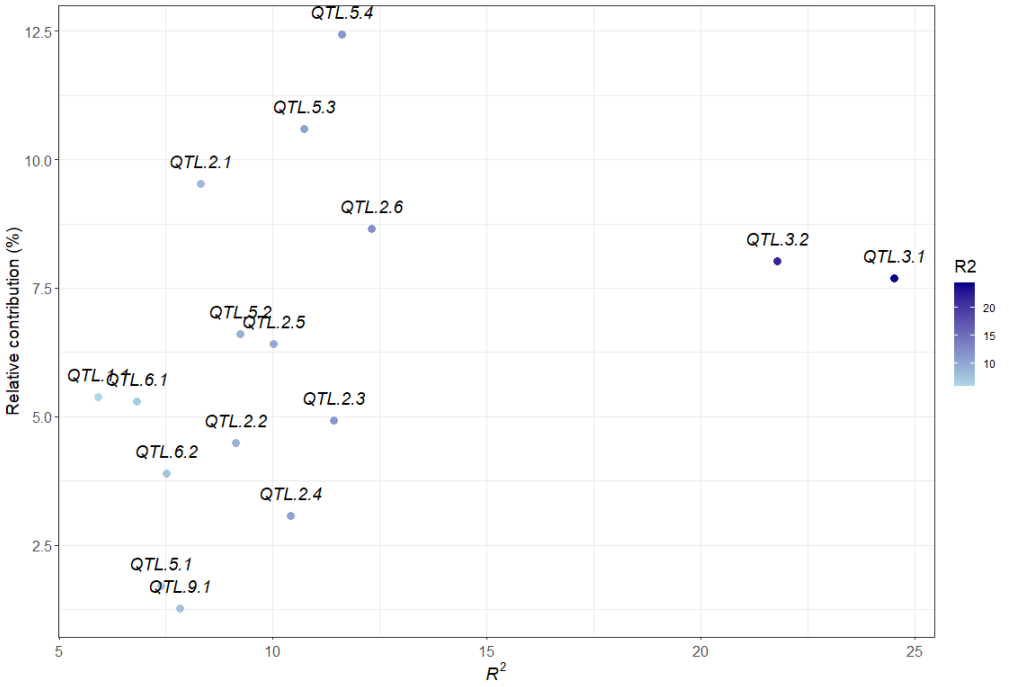

Figure 4.5. Relationship between the relative contributions (%) and mean R^2 of 16 quantitative trait loci (QTL).

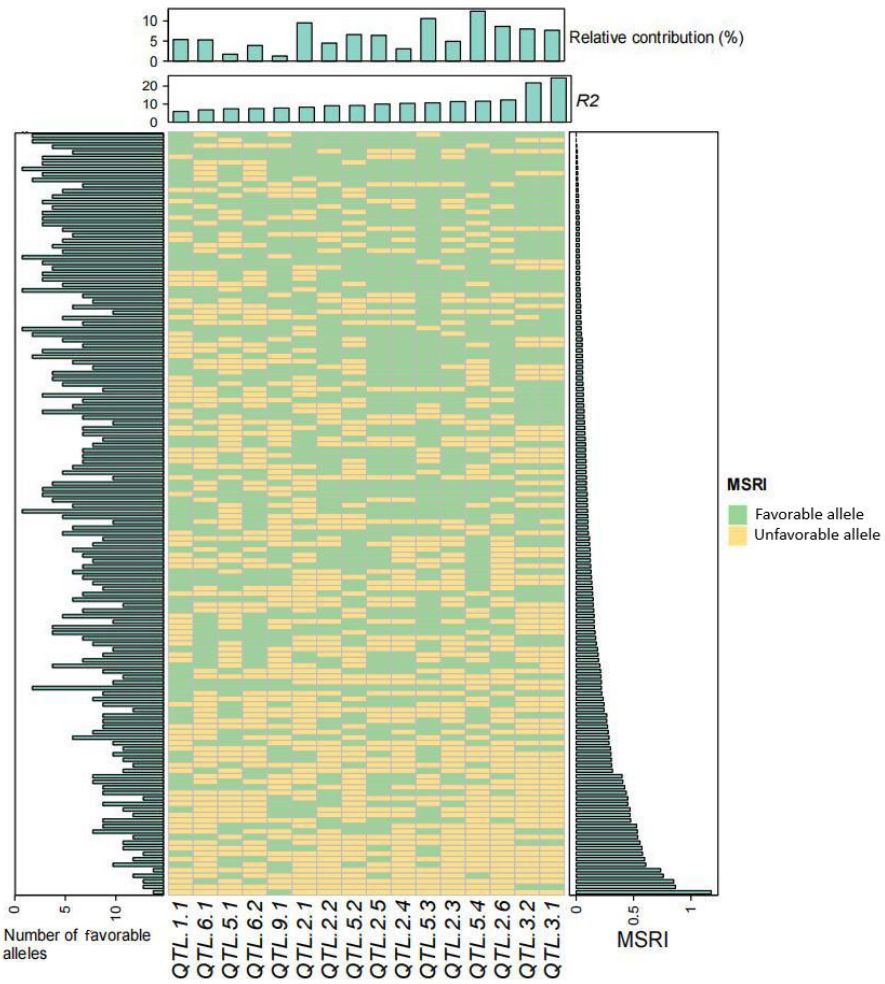

Figure 4.6 Favorable alleles of 16 QTL for marsh spot resistance index (MSRI) in the RIL population of 138 lines. The mean dataset over five years and two soil types was used. R^2 refers to coefficient correlation of QTL to MSRI. NA indicates that the allele is a rare allele that had very low frequency of individuals in the population.

4.4.7 Favorable alleles of QTL in RILs

The number of favorable alleles of the 16 additive QTL (**Table 4.3**) in each RIL is illustrated in **Figure 4.6**. The number of favorable alleles was highly correlated with MSRI values (R^2 = 72.48%) (**Figure 4.7**). To further validate this relationship, the overall dataset of the 15 most resistant lines (0.01 ± 0.01 of MSRI) and the 15 most susceptible lines (0.66 ± 0.19 of MSRI) was extracted. The number of favorable alleles of the 15 most resistant lines (11.5 ± 1.8) was significantly higher than that of the 15 most susceptible lines (3.4 ± 1.6) (**Figure 4.8**). The resistant parent Cran09 and susceptible parent Messina had 12 and 2 favorable alleles for the 16 QTL, respectively.

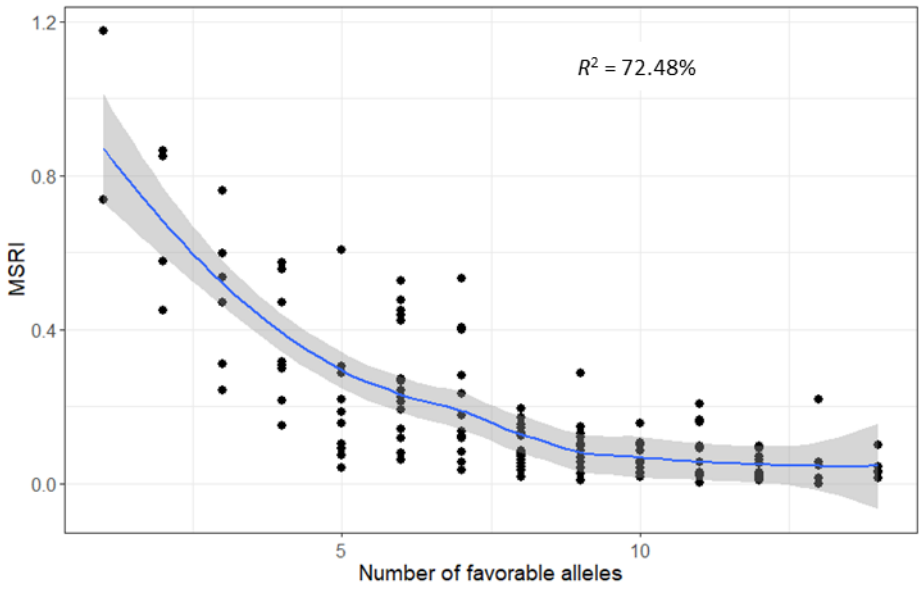

Figure 4.7 Relationship between of marsh spot resistance index (MSRI) and the number of favorable alleles in the 138 RILs. The confidence intervals were drawn with a confidence of 0.99. The data of the overall means over years and soil types was used for calculation.

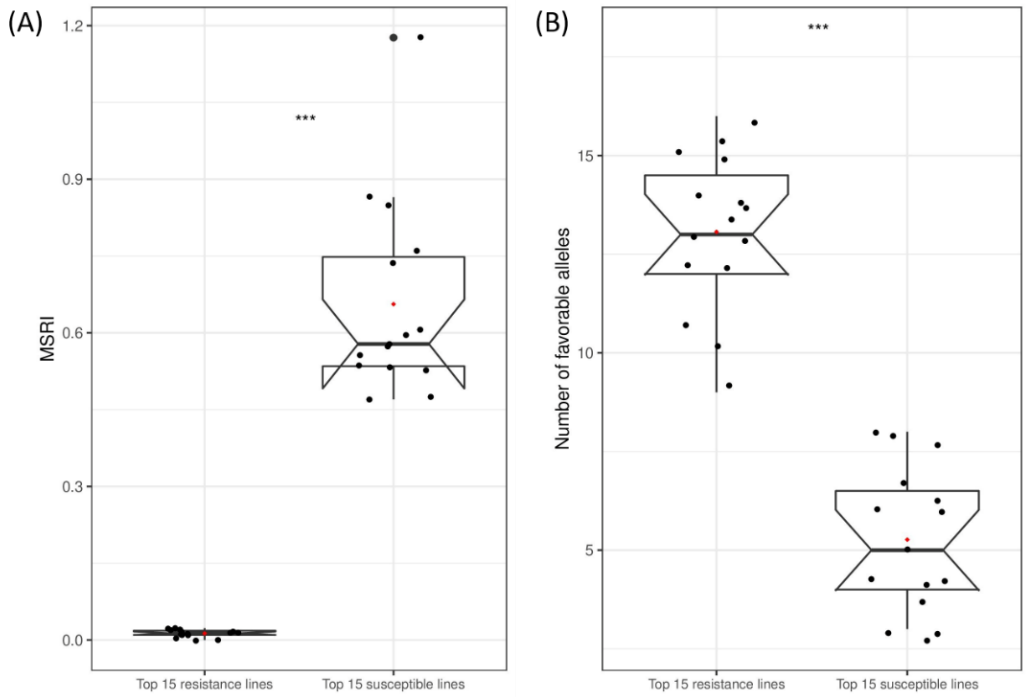

Figure 4.8 Boxplots of the number of favorable alleles (A) and marsh spot resistance index (MSRI) (B) for the 15 most resistant lines and the 15 most susceptible lines. *, $P < 0.05$; **, $P < 0.01$; ***, P< 0.0001; NS, not significant.

4.4.8 Candidate genes of major QTL

Since marsh spot disease is most likely caused by Mn deficiency, all potential candidate genes associated with Mn deficiency and Mn content in plants were screened (Jia et al., 2021b). A list of 151 annotated genes likely related to Mn deficiency or Mn content were identified from other plant species, such as *Arabidopsis*, rice (*Oryza sativa*) and barley (*Hordeum vulgare*) and mapped the common bean reference genome. Then, a window of upstream and downstream 100 Kb flanking each QTL region was scanned to identify QTL harboring such genes. Seven of the QTL co-located with a total of 13 genes (**Table 4.5**). Among them, four QTL (*QTL.1.1*, *QTL.3.1*, *QTL.3.2*, and *QTL.5.2*) harbored eight genes encoding heavy metal transport/detoxification superfamily protein. In particular, two QTL (*QTL.3.1* and *QTL.3.2*) which explained the highest phenotypic variation of 12.2–24.5% harbored five metal transport genes *Phvul.003G086300*, *Phvul.003G092500*, *Phvul.003G104900*, *Phvul.003G099700*, and *Phvul.003G108900* in a large genomic region of 16.8–27.5 Mb on chromosome 3. Other gene families, including one zinc transporter (ZIP), ZIP metal ion transporter, cation efflux family, natural resistance-associated macrophage protein (NRAMP), and manganese tracking

factor for mitochondrial SOD2 were also co-located to *QTL.2.3*, *QTL.5.2*, or *QTL.9.1* (**Table 4.5**). These genes are responsible for Mn transporter, metals homeostasis, and detoxification in plants and very likely to be causal genes controlling marsh spot.

Table 4.5 Candidate genes co-located in the regions of the QTL.

QTL	Gene	Chr	Gene Coordinates [(a)]	Annotation
QTL.1.1	*Phvul.001G250300*	1	50100939–50102262	Heavy metal transport/detoxification superfamily protein
	Phvul.001G247400	1	49894723–49895275	Heavy metal transport/detoxification superfamily protein
QTL.2.3	*Phvul.002G184200*	2	34468080–34481795	ZIP metal ion transporter family
QTL.3.1	*Phvul.003G086300*	3	16877488–16879137	Heavy metal transport/detoxification superfamily protein
QTL.3.2	*Phvul.003G092500*	3	21113140–21115717	Heavy metal transport/detoxification superfamily protein
	Phvul.003G104900	3	23350962–23352673	Heavy metal transport/detoxification superfamily protein
	Phvul.003G099700	3	25708027–25708491	Heavy metal transport/detoxification superfamily protein
	Phvul.003G108900	3	27536901–27538128	Heavy metal transport/detoxification superfamily protein
QTL.5.2	*Phvul.005G095400*	5	29797811–29799135	Heavy metal transport/detoxification superfamily protein
	Phvul.005G049300	5	5742223–5745905	Cation efflux family protein
	Phvul.005G048900	5	5682746–5684903	Zinc transporter 1 precursor
QTL.9.1	*Phvul.009G137100*	9	20653368–20662253	Manganese tracking factor for mitochondrial SOD2
	Phvul.009G127900	9	19429094–19433403	NRAMP metal ion transporter 6

[(a)] 0 represents the candidate gene is included in the QTL region. Min. distance: minimum distance between candidate genes and QTL; Chr: chromosome.

4.5 Discussion

The previous investigation revealed the inheritance of marsh spot resistance in cranberry common beans was likely controlled by at least four genes with additive and epistatic effects (Jia et al., 2021a). Using joint segregation analysis (JSA), the marsh spot phenotypic data of the RIL population best fitted a genetic model with four major genes with additive and interaction effects. The estimated epistatic effects were even larger than additive effects. In this study, using the same population and phenotypic datasets, we identified 16 additive and three pairs of epistatic QTL, validating and confirming that marsh spot resistance is a quantitatively inherited trait controlled by at least four genes. Due to the theoretical limitation of the maximum gene number of the JSA genetic models, a maximum of four major genes can be estimated (Zhang et al., 2003b). In addition, the current version of JSA can only estimate major genes without minor gene effects: so the number of major genes was underestimated and the effects from minor genes were ignored. The current study further validated the previous results, extended the discovery, and proposed candidate genes for the QTL that support the role of Mn in marsh spot disease (Jia et al., 2021a).

4.5.1 Genomic Heritability and Contribution of QTL to Marsh Spot Resistance

To understand the overall contribution of the identified QTL, multiple linear regression models of all QTL on each of the 18 phenotypic datasets were constructed. The average R^2 of the models with both additive and epistatic QTL was greater than that of the models with only additive QTL, indicating that the additional epistatic QTL were also useful for improving marsh spot resistance despite some negative interaction between some epistatic QTL (**Table 4.4**).

The lowest R^2 values were always obtained from the phenotypic data sets of single years with one soil type (2019/Sandy soil and 2016/Sandy soil). The R^2 values of the mean value datasets (such as overall means, means of heavy clay over five years and means of sandy soil over five years) were greater than those from the single environments (single year and single soil type), showing the strong environmental effects on QTL. Of all identified QTL, most were detected from the overall mean dataset or several other mean datasets. Thus, the phenotypic data over multiple years

and/or multiple locations helps to identify stable QTL (Lan et al., 2020).

In the overall mean dataset, genomic heritability (h^2) was estimated to be 55.91%, indicating that the 1,273 SNPs identified in the RIL population explained more than half of the phenotypic variance. The missing proportion of the phenotypic variation could be the result of the non-additive effects of SNP markers or missed SNPs in marker-poor regions (Liu et al., 2017b). The h^2 estimates also varied from different phenotypic datasets. For example, the h^2 was extremely low (12.07%) in the 2019/sandy soil dataset (S2019). MSRI observations in S2019 were significantly lower than those of other datasets possibly due to the higher concentration of Mn in the sandy soil field in 2019. Thus, the estimation of h^2 is possibly affected by interaction between genetic background and environment (Poveda et al., 2017).

The overall R^2 values of all the identified QTL estimated in the regression models (75.37%) were higher than the h^2 estimates (55.91%) (Table **4.2**). The difference between the two estimates may be because different statistical models were used but this result implied that most of the QTL associated with marsh spot resistance existing in this RIL population may have been already identified using a combination of different statistical models.

4.5.2 Statistical Models for QTL Identification and QTL Validation

Each statistical model for QTL mapping has its own advantages and limitations. The simultaneous utilization of multiple models would be a reasonable and practical strategy to make full use of their merits and overcome potential disadvantages. Several statistical models have been developed for QTL mapping in bi-parental populations, involving linkage map-based models and GWAS models (Wen et al., 2018;You et al., 2018;Lan et al., 2020). In this study, four statistical models were used to identify QTL, including three linkage map-based models (i.e., ICIM-ADD, ICIM-EPI and GCIM) and one haplotype block based GWAS model (i.e., RTM-GWAS). Unlike traditional interval mapping (IM) and composite interval mapping (CIM) models, the ICIM model can control polygenetic background through prerequisite selection of markers in QTL mapping. Those polygenes with large and moderate effects were well controlled to reduce the rate of false positives (Li et al., 2007;Bernardo, 2013). GCIM provides a new method to control polygenetic background by estimating polygenetic variance in

GWAS, which can control the background of polygenes with large, moderate and small effects. Compared with ICIM models, GCIM outperformed ICIM in small effect QTL detection. However, in some cases in the GCIM model several peaks around one QTL could be identified at the same time, thus the true QTL was difficult to define. For example, four QTL, *QTL.2.3, QTL2.4, QTL.2.5* and *QTL.2.6* neighbored each other on the genetic map, but they overlapped in terms of their physical chromosomal locations (**Table 4.3**). They might be one on a physical position or more QTL on the genetic map. RTM-GWAS first generates and groups SNPs into LD blocks, and then QTL mapping is performed based on these LD blocks, through a process called SNPLDBs (He et al., 2017). The employment of LD blocks as markers can notably decrease the possibility of false positives during multiple hypothesis in the GWAS model (Mueen Alam et al., 2019). In this study, all 16 QTL were identified using three genetic map-based models (**Table 4.3**), demonstrating their detection power in QTL mapping (Shi et al., 2020;Su et al., 2020;Ren et al., 2021), whereas six of them was validatedby RTM-GWAS. These results indicate that the value of using of multiple models that combine the genetic map-based and GWAS models facilitate detection of QTL with small effects and the validation of QTL.

Further validation of the QTL can also be achieved through the use of linear regression models as performed herein where significant correlations between QTL alleles and phenotypes of RILs was shown. Although significant correlations were confirmed for most of the putative QTL identified by statistical models, two of the 18 original QTL did not pass the significance test and were declared false positive QTL.

While all statistical models may result in some false positive QTL, the use of multiple QTL models and other validation methods such as the linear regression models can be capitalized upon to identify them.

4.5.3 Additive/ Epistatic QTL and Genomics-Assisted Selection

With the development of genotyping technologies, genomics-assisted selection such as marker-assisted selection (MAS) and genomic selection (GS) have been widely used for selection of traits controlled by major genes or polygenes in many crops including common bean (Collard and Mackill, 2008;He et al., 2019;Keller et al., 2020;Delfini et al., 2021). MAS and GS aim at predicting the phenotypes of individuals based on the use of known molecular marker information without expensive or time-consuming phenotyping of the individuals. MAS tends to select superior lines through major genes

or large-effect QTL, while GS utilizes high-density genome-wide markers or QTL to predict the performance of individuals.

In this study, a total of 16 additive and three pairs of epistatic QTL have been identified. These QTL explained most phenotypic variation for marsh spot resistance. The accumulation of favorable alleles in RILs via hybridization of two parents and recombination has greatly improved common bean resistance to marsh spot. The most resistant RILs had significantly greater favorable additive alleles than the most susceptible RILs (**Figure 4.8B**). The number of favorable alleles in an RIL had a significantly positive correlation with marsh spot resistance (i.e., negative correlation with MSRI) (**Figure 4.7**), showing a significant increase in the number of favorable alleles from susceptible to resistance lines (**Figure 4.6**). MAS or GS are both effective to pyramid favorable alleles of QTL to develop future resistant cultivars in plant breeding. The lines containing more favorable alleles especially those of QTL with high R^2 and relatively large contributions will be preferentially selected in breeding. In this study, *QTL.5.3* and *QTL.5.4* had the highest RC while *QTL.3.1* and *QTL.3.2* had the highest R^2 values (Figure **4.3**). These four QTL could be taken into consideration for future breeding. For those epistatic QTL, additive effects still contributed resistance to marsh spot disease. Therefore, in a breeding program, the epistatic effect of QTL markers should also be considered in the selection of molecular markers for optimal QTL combinations.

A total of 1.273 SNP markers were identified from the RIL population in this study. The estimates of genomic heritability (h^2) for marsh spot resistance indicate that more than half of the phenotypic variation can be explained using these SNPs, providing potential to perform GS to improve marsh spot resistance in common bean breeding.

4.5.4 Candidate Gene Prediction

Although QTL mapping or GWAS have been widely used to identify QTL or QTNs associated with traits of importance and to predict potential candidate genes, their applications were limited. First of all, prediction of candidate genes relies on whether the detected QTL/QTNs are not false positives. Then the application of designating a potential candidate gene of a QTL depends on many other factors, such as the number of markers used, marker density on chromosomes, the recombination rate of genomic regions, and so on. To date, the most popular and simple approach for predicting candidate genes is to investigate the annotated genes in the vicinity of the QTL, such

as a window of a specific physical distance flanking the QTL (Kumar et al., 2015;Sertse et al., 2019a;Sertse et al., 2019b;You and Cloutier, 2020). Although functional validation is the ultimate goal, candidate gene prediction of QTL/QTNs based on chromosomal location combined to *a priori* knowledge of gene functions have the potential to significantly narrow down the candidate gene list. This approach requires a list of annotated genes associated with the traits that have been validated to some extent in previous studies.

Marsh spot symptoms are likely caused by Mn deficiency due to the low availability of soil Mn, a limited capacity for Mn uptake and transport, and/or because of interference from other physiological pathways involving Mn, such as deoxidation (Lewis, 1939;Wilson, 1979;Graham et al., 1988;Humphries, 2007;Schmidt et al., 2016;Jia et al., 2021b). Our previous study indirectly showed that Mn concentration in soil may be associated with the development of marsh spot in cranberry common beans (Jia et al., 2021a). Here candidate genes with possible function as Mn transporter and deoxidation were annotated. Two Mn transporter protein-coding genes are located at *QTL 5.2*: one is the zinc transporter (ZIP) coding gene, and the other one is the cation efflux (CAX) family protein-coding gene. ZIP family members are involved in the transport of Mn in stellar root cells and present in the tonoplast and, took part in remobilizing Mn from the vacuoles to the cytoplasm (Pedas et al., 2008). The members of the CAX family are metal transporters and mainly control the influx of cations into the vacuole (Enrico et al., 2012). CAX-like transporters were found in other species, such as *LeCAX2* in tomato (*Solanum lycopersicum* L.), and *HvCAX2* in barley (*H. vulgare*). They are expressed ubiquitously in the roots, shoots, immature spikes and seeds (Edmond et al., 2009).

Mn, naturally plentiful in most soils, should be adequately available to plants. However, deficiencies occur when in soils with high pH, high organic matter or during cold and wet conditions. Some of the identified candidate genes could play a role in Mn regulation in plants. Such as ZIP gene mentioned above, the expression of ZIP gene could allow plants absorb more Mn from soil or remobilizing more Mn to seeds during germination, thus, the development of marsh spot in seed could be prevented or relieved.

4.6 Conclusion

QTL mapping in this study determined that marsh spot resistance in cranberry common bean is a high-heritability trait that is genetically controlled by multiple genes. Although four gene loci with additive and epistatic effects have been detected through joint segregation analysis at a phenotype level as reported previously (Jia et al., 2021a), 21 additive and 13 epistatic QTL were further identified via QTL mapping at the genomic level in this study. These QTL explained up to 68% of phenotypic variation. Despite epistatic effects between some QTL, there existed a significant correlation between the number of favorable alleles of the additive QTL and marsh spot resistance (R^2 = 77%), which confirmed that the favorable alleles of these QTL are additive, and can be pyramided in future common bean cultivars by MAS. These QTL will facilitate the development of molecular markers for resistance breeding. In addition, 17 candidate genes related to Mn deficiency or Mn content in plants were shown to be co-located within six QTL regions. Those genes will be further validated in future functional genomic studies to determine their potential to improve marsh spot resistance in of germplasm or new cultivars by adopting modern genetic improvement techniques such as genome or gene editing.

5. General discussion and conclusion

The wild common bean originated in Mesoamerica diffused southward to the Andean region (Schmutz et al., 2014). After long-term isolated evolution and independent domestication, common beans were divided into two distinct gene pools, Mesoamerican (Middle American) and Andean gene pools. The cranberry common bean as a market class, was derived from Nigeria. Because of its universal attributions in food cooking and processing, the common bean has become one of the most consumed and ponderable crops, which plays a crucial role in staple food sources and the human daily diet. Common beans contain rich nutritive composition and are almost recognized as a 'complete food' (Aguilera and Steinsapir, 1985).

MS resistance in common beans is a physiological disorder related to Mn-deficiency that damages seed quality in beans. Due to limited physiological and genetic research on MS, the breeding for MS resistance had been slackened. The discovery of underlying genetic mechanisms and variation of MS resistance was emphasized to prevent of possible devastation to seed yield and quality.

A genetic population containing 138 lines was constructed and evaluated for MS severity. Two parents, the susceptible cultivar Messina and the resistant cultivar Cran09 had significant phenotypic difference in MS resistance, thus ensuring sufficient phenotypic variation in the inbred lines. In plant breeding, the RIL populations has been widely used to generate pure lines for breeding selection and genetic studies (Rifkin, 2012;Priyadarshan, 2019).

Since the mid-20th century, QTL mapping has been proposed and has become one of the most vital approaches for identification of favorable genes or loci associated with important traits in plant genetics and breeding. QTL mapping aimed at detecting genetic variations which were in charge of the significant differences between individuals.

QTL mapping advances genetic research of agronomical and biological-related traits in common beans. In the 1970s, Coyan with his team first identified genetic markers associated with common bean disease resistance (Coyne et al., 1973). After that, numerous researches using QTL mapping were performed to discover major genes and their effects on common bean disease resistance. Until now, many QTL associated with common bean abiotic stresses such as resistance to by-2 potyvirus (Hart and Griffiths, 2015), seed iron and zinc concentration (Cichy et al., 2009;Blair et al., 2010;Blair et al., 2011), and phosphorus levels (Cichy et al., 2009;Blair et al.,

2010;Blair et al., 2011;Hart and Griffiths, 2015). Abiotic stresses have an important impact on agriculture production, especially in those underdeveloped countries that suffer from global climate change, drought, and other plants diseases. Low-input agricultural systems make them difficult to tackle the increasing frequency and severity of abiotic constraints. Therefore, unrevealing molecular mechanisms in response to abiotic stress is very important in common bean breeding and production.

We analyzed the inheritance and genetic mechanism of MS resistance from both phenotypic and genotypic levels in this study. The genetic analysis of phenotypic data using JSA provides insight into a possible inheritance model for MS resistance in cranberry common beans. Although limited model options and algorithms implemented in the JSA software package (Zhang et al., 2003a) restricted the detection power of the true inheritance models, the results from JSA provide a highly possible underlying genetic model with additive/epistatic effects of major genes and polygenes for MS resistance.

Further QTL mapping identified a total of 16 additive and 3 epistatic QTL with large or small effects. In general, the phenotypic performance of a trait in a pure population is primarily composed of genetic, environmental, their interaction , and error effects. The genetic effect can be split into three parts: (1) QTL additive effect generally contributing the most variation of a trait, (2) interaction or epistatic effect of QTL by QTL, and (3) the interaction effect between QTL and environment (G x E). Not only additive effect, but the interaction between QTL explained a large proportion of total variation for MS resistance. Epistasis is regarded as a critical proportion of the genetic architecture in quantitative traits (Sofi, 2007). Some studies have suggested epistatic effects play an important role in traits controlled by several genes/QTL in the autogamous plant such as the common bean (Holland, 2001).

The results obtained from JSA and QTL mapping in this study are largely consistent. JSA suggested that MS resistance was controlled by some major genes and several polygenes with additive and epistatic effects, whereas the QTL mapping study identified some additive and epistatic QTL, located the QTL on chromosomes, and predicted potential candidate genes related to Mn deficiency or Mn transport that may be associated with MS resistance (Jia et al., 2021a), further validating the JSA results and expanding the discovery. The approach combining JSA and QTL mapping provided high confidence for genetic analysis of MS resistance.

The 16additive and 3 epistatic QTL identified in this study explained most phenotypic variation for MS resistance. The multiple regression models with all 21 additive QTL explained 27.2% to 61.2% of the phenotypic variation with an average of 46.4% over all 18 phenotypic datasets. When all additive and epistatic QTL were considered, the models with 34 QTL explained 42.0% to 68.7% with a mean of 56.1%. These results indicated that the effects of the identified QTL are primarily additive, suggesting the use of these QTL in resistance breeding by means of the pyramiding of favorable alleles in individuals. In fact, the examination of the favorable alleles for the identified QTL in RILs have demonstrated the successful accumulation of favorable alleles in RILs via hybridization of the susceptible cultivar Messina and the resistant cultivar Cran09 and recombination of the loci associated with MS resistance. A significantly positive correlation between the number of favorable alleles in RILs and MS resistance indicated a significant increase in the number of favorable alleles from susceptible to resistance lines, allowing breeders to improve breeding efficiency of MS resistance breeding by genomics-assisted approaches, such as MAS or GS.

MAS and GS have been successfully used in improving plant resistance to diseases (Boopathi, 2013;Paterson, 2013;Rychel-Bielska et al., 2020). MAS and GS aim at predicting the phenotypes of individuals based on the use of known molecular marker information without expensive or time-consuming phenotyping of the individuals. MAS tends to select individual lines through major-effect QTL. Thus, those major QTL with large effects allowed the use of MAS for MS resistance breeding.

GS, which adopted genome-wide genetic markers to predict the performance of individuals, are widely used in plant breeding, primarily for polygenic trait selection. According to the estimates of genomic heritability, more than half of the phenotypic variation in the RILs can be explained by the 2,058 identified SNPs, showing the possibility to improve MS resistance using all SNPs in GS. In addition, because most of the phenotypic variation for MS resistance was explained by the identified QTL, GS using the identified QTL will be another choice.

To date, the popular and simple approach for predicting candidate genes is to investigate the annotated genes in the vicinity of the QTL, such as a window of a specific physical distance flanking the QTL (Rychel-Bielska et al., 2020) . We found 17 candidate genes co-located with the six QTL. These genes may be involved in the process of Mn transportation, re-mobilization, and de-oxidation in plants. Previous studies have shown that MS disease may be caused by Mn-deficiency (Jia et al., 2021b).

However, the reaction on MS disease in common bean may be a complex process and have not been fully studied. Further functional genomic studies for these candidate genes are warranted to validate their functions and determine their capability to improve MS resistance in the development of new germplasm or cultivars by adopting modern genetic improvement techniques such as gene cloning or gene editing.

6. Limitation and suggested future studies

QTL mapping provides a useful statistical genetics method to identify QTL and candidate genes associated with MS resistance. However, the limitation common for all QTL mapping studies is the validation of identified QTL and candidate genes. Various statistical models for QTL mapping identify significant QTL related to traits of interest, but some of these QTL may be false-positives. In order to reduce false-positive QTL, we took several steps in this study. First, we used two linkage-based statistical models and one LD-based GWAS model to identify both large- and small-effect QTL, resulting in a total of 18 unique QTL (16 additive and 3 pairs of epistatic) from the genome-wide SNP dataset. Most of QTL were identified by more than one model. This has proven to be a good strategy to take advantage of the strength of each model and to overcome their shortcomings (He et al., 2018;Lan et al., 2020). Second, we performed post-QTL identification analysis by testing the statistical significance of each identified QTL by removing potentially redundant and false-positive QTL. Overall, the methodology used herein constitutes a powerful strategy, combining different statistical tools and methods to identify the most reliable QTL-trait association and reduce the limitation.

Present QTL mapping methods are limited to predicting candidate genes related to the traits. This mostly depends on the population type and size, the density of genome-wide markers, and so on. The major method for predicting candidate genes from identified QTL remains to scan the annotated genes in their vicinity. To find potential candidate genes, we first narrowed the candidate genes to the gene families related to Mn deficiency or Mn content in plants (Jia et al., 2021b) based on the common bean reference genome sequence (Schmutz et al., 2014). Second, we reduced these candidate genes to the candidates located within a window size of 100 Kb flanking each QTL. In this way, we identified 13 Mn-deficiency related candidate genes co-located within six QTL. Many of them were located within the QTL regions between two flanking markers. These candidate genes need to be further validated through functional genomics studies. Within whole genome sequencing, a new population such as near isogenic lines (NIL) could be constructed to provide more recombinant events for breeders to fine map the genetic variations. Gene function annotation could be validated by using mutation population or Crisper/Case9 technology.

To further validate the identified QTL, molecular markers of these QTL, such as the breeder-friendly kompetitive allele-specific PCR (KASPar) markers, can be designed, and used for a genetic panel that has been phenotyped for MS resistance. The validated large-effect markers can be further used for MAS. Alternatively, all QTL markers can be used to establish genomic selection (GS) models to evaluate the prediction ability of MS resistance, and used for predicting genomic estimated breeding values (GEBVs) of germplasm or breeding lines in breeding programs (Hayes et al., 2009;Boopathi, 2013;Paterson, 2013).

7. Conclusion

Common bean (*Phaseolus vulgaris L.*) is an important worldwide legume crop for its edible dry seeds and tender pods. Marsh spot (MS) disease is a physio-genic abiotic stress primarily in pea and beans affecting seed quality and market value. Previous studies have proved that manganese (Mn) deficiency is the major factor causing MS symptoms. Until this study, no genetic analysis of MS resistance has been reported in either peas or beans. To investigate the inheritance of MS resistance in common bean, a biparental genetic population composed of 138 RILs was developed and the MS resistance of the population was evaluated during five consecutive years in two soil types (sandy and heavy clay). The RILs and two parents were also re-sequenced. Genetic analysis at the phenotypic level indicates that MS resistance is less affected by either different years or different soil types and its broad-sense heritability was greater than 80%.

Joint segregation analysis (JSA) provides a classic genetic analysis method to determine the possible number of genes and their overall effect using phenotypic data. This method is based on proposed theoretical genetic models and find the best one to fit the distribution of phenotypic data. Using JSA, we identified four major genes with additive-epistasis effects, explaining over 80% the phenotypic variation for MS resistance. In addition, we found one of the four gene significantly suppressed the additive effects of other three genes. Thus, further QTL mapping was warranted to identify and locate individual genes on chromosomes. We first obtained 1,273 high-quality SNPs and constructed a high-density genetic map. Based on this genetic map and 18 phenotypic data sets, we identified 16 additive and 3 pairs of epistatic QTL. We also identified 17 Mn-deficiency related candidate genes co-located within six QTL.

In summary, we present the first report on MS resistance inheritance at phenotypic and genomic levels to dissect genetic architecture of MS resistance using both JSA and QTL mapping. JSA and QTL mapping demonstrate that MS resistance is a highly heritable trait and controlled by a few large- and small-effect genes or QTL loci. The results obtained in this study advance the current understanding of the genetic mechanisms of marsh spot resistance in cranberry common bean, and provide genomic resources for use in genomics-assisted breeding and for candidate gene isolation and functional characterization.

8. Reference

Uncategorized References

Aguilera, J.M., and Steinsapir, A. (1985). Dry processes to retard quality losses of beans (*Phaseolus vulgaris*) during storage. *Canadian Institute of Food Science and Technology Journal* 18, 72-78.

Akibode, C.S., and Maredia, M.K. (2012). "Global and regional trends in production, trade and consumption of food legume crops", in: *Department of Agricultural, Food, and Resource Economics.*).

Alejandro, S., Cailliatte, R., Alcon, C., Dirick, L., Domergue, F., Correia, D., Castaings, L., Briat, J.-F., Mari, S., and Curie, C. (2017). Intracellular distribution of manganese by the trans-golgi network transporter NRAMP2 is critical for photosynthesis and cellular redox homeostasis. *The Plant Cell* 29, 3068-3084.

Anbessa, Y., Warkentin, T., Vandenberg, A., and Ball, R. (2006). Inheritance of time to flowering in chickpea in a short-season temperate environment. *Jouranal of Heredity* 97, 55–61.

Andrew, H.P., Eric, S.L., John, D.H., Susan, P., Stephen, E.L., and Steven, D.T. (1988). Resolution of quantitative traits into Mendelian factors by using a complete linkage map of restriction fragment length polymorphisms. *Nature* 335, 721.

Araki, R., Murata, J., and Murata, Y. (2011). A novel barley Yellow Stripe 1-like Transporter (HvYSL2) localized to the root endodermis transports metal–phytosiderophore complexes. *Plant and Cell Physiology* 52, 1931-1940.

Ates, D., Aldemir, S., Yagmur, B., Kahraman, A., Ozkan, H., Vandenberg, A., and Tanyolac, M.B. (2018). QTL mapping of genome regions controlling manganese uptake in lentil seed. *G3 Genes|Genomes|Genetics* 8, 1409-1416.

Bargsten, J.W., Nap, J.-P., Sanchez-Perez, G.F., and Van Dijk, A.D.J. (2014). Prioritization of candidate genes in QTL regions based on associations between traits and biological processes. *BMC Plant Biology* 14, 330.

Bates, D., Mächler, M., Bolker, B., and Walker, S. (2015). Fitting linear mixed-effects models using lme4. *Joural of Statistical Software* 67, 48.

Bernardo, R. (2013). Genomewide markers as cofactors for precision mapping of quantitative trait loci. *Theoretical and Applied Genetics* 126, 999-1009.

Beshir, H.M., Walley, F.L., Bueckert, R., Tar, #039, and An, B. (2015). Response of snap bean cultivars to *Rhizobium* inoculation under dryland agriculture in Ethiopia. *Agronomy* 5, 291-308.

Biddle, A.J., and Cattlin, N.D. (2007). *Pests, Diseases, and Disorders of Peas and Beans: A Colour Handbook.* London: CRC Press.

Bitocchi, E., Nanni, L., Bellucci, E., Rossi, M., Giardini, A., Zeuli, P.S., Logozzo, G., Stougaard, J., Mcclean, P., Attene, G., and Papa, R. (2012). Mesoamerican origin of the common bean (*Phaseolus vulgaris* L.) is revealed by sequence data. *Proceedings of the National Academy of Sciences of the United States of America* 109, E788-E796.

Blair, M.W., Astudillo, C., Rengifo, J., Beebe, S.E., and Graham, R. (2011). QTL analyses for seed iron and zinc concentrations in an intra-genepool population of Andean common beans (*Phaseolus vulgaris* L.). *Theoretical and Applied Genetics* 122, 511-521.

Blair, M.W., Iriarte, G., and Beebe, S. (2006). QTL analysis of yield traits in an advanced backcross population derived from a cultivated Andean × wild common bean (*Phaseolus vulgaris* L.) cross. *Theoretical and Applied Genetics* 112, 1149-1163.

Blair, M.W., Medina, J.I., Astudillo, C., Rengifo, J., Beebe, S.E., Machado, G., and Graham, R. (2010). QTL for seed iron and zinc concentration and content in a Mesoamerican common bean (*Phaseolus vulgaris L.*) population. *Theoretical and Appllied Genetics* 121, 1059-1070.

Blair, M.W., Wu, X., Bhandari, D., and Astudillo, C. (2016). Genetic dissection of ICP-detected nutrient accumulation in the whole seed of common bean *(Phaseolus vulgaris* L.). *Frontiers in Plant Science* 7, 219.

Bonfield, J.K., Marshall, J., Danecek, P., Li, H., Ohan, V., Whitwham, A., Keane, T., and Davies, R.M. (2021). HTSlib: C library for reading/writing high-throughput sequencing data. *GigaScience* 10.

Boopathi, N.M. (2013). *Genetic mapping and marker assisted selection basics, practice and benefits.* New Delhi: Springer India.

Bornø, M.L., Müller-Stöver, D.S., and Liu, F. (2019). Biochar properties and soil type drive the uptake of macro- and micronutrients in maize (*Zea mays* L.). *Journal of Soil Science and Plant Nutrition* 182, 149-158.

Boyle, E.A., Li, Y.I., and Pritchard, J.K. (2017). An expanded view of complex traits: From polygenic to omnigenic. *Cell* 169, 1177-1186.

Brandenburg, F., Schoffman, H., Keren, N., and Eisenhut, M. (2017). Determination of Mn concentrations in *Synechocystis* sp. PCC6803 using ICP-MS. *Bio-protocol* 7, e2623-e2623.

Broadley, M., Brown, P., Cakmak, I., Rengel, Z., and Zhao, F.-J. (2012). "Function of nutrients," in *Marschner's Mineral Nutrition of Higher Plants,* ed. H. Marschner. (Oxford: Academic Press), 191-248.

Broman, K.W., Gatti, D.M., Simecek, P., Furlotte, N.A., Prins, P., Sen, Ś., Yandell, B.S., and Churchill, G.A. (2019). R/qtl2: Software for mapping quantitative trait loci with high-dimensional data and multiparent populations. *Genetics* 211, 495-502.

Broman, K.W., and Speed, T.P. (2002). A model selection approach for the identification of quantitative trait loci in experimental crosses. *Journal of the Royal Statistical Society: Series B (Statistical Methodology)* 64, 641-656.

Cailliatte, R., Schikora, A., Briat, J.-F., Mari, S., and Curie, C. (2010). High-affinity manganese uptake by the metal transporter *nramp1* is essential for *Arabidopsis* growth in low manganese conditions. *The Plant Cell* 22, 904-917.

Cao, J. (2019). Molecular evolution of the *vacuolar iron transporter* (*vit*) family genes in 14 plant species. *Genes (Basel)* 10, 144.

Cao, X.W., Liu, B., and Zhang, Y.M. (2013). SEA: A software package of segregation analysis of quantitative traits in plants. *Journal of Nanjing Agricultural University* 36, 1－6.

Castaings, L., Caquot, A., Loubet, S., and Curie, C. (2016). The high-affinity metal transporters NRAMP1 and IRT1 team up to take up iron under sufficient metal provision. *Scientific Reports* 6, 37222.

Cataldo, D.A., and Wildung, R.E. (1978). Soil and plant factors influencing the accumulation of heavy metals by plants. *Environmental Health Perspectives* 27, 149-159.

Chen, Z., Fujii, Y., Yamaji, N., Masuda, S., Takemoto, Y., Kamiya, T., Yusuyin, Y., Iwasaki, K., Kato, S., Maeshima, M., Ma, J.F., and Ueno, D. (2013). Mn tolerance in rice is mediated by MTP8.1, a member of the cation diffusion facilitator family. *Journal of Experimental Botany* 64, 4375-4387.

Cheng, N.-H., Pittman, J.K., Shigaki, T., and Hirschi, K.D. (2002). Characterization of CAX4, an Arabidopsis H^+/cation antiporter. *Plant Physiology* 128, 1245-1254.

Chu, H.-H., Car, S., Socha, A.L., Hindt, M.N., Punshon, T., and Guerinot, M.L. (2017). The Arabidopsis MTP8 transporter determines the localization of manganese and

iron in seeds. *Scientific Reports* 7, 11024-11010.
Chung, Y., Choi, S., Jun, T.-H., and Kim, C. (2017). Genotyping-by-sequencing: a promising tool for plant genetics research and breeding. *Horticulture, Environment, and Biotechnology* 58, 425-431.
Churchill, G.A., and Doerge, R.W. (1994). Empirical threshold values for quantitative trait mapping. *Genetics* 138, 963-971.
Cichy, K.A., Caldas, G.V., Snapp, S.S., and Blair, M.W. (2009). QTL analysis of seed iron, zinc, and phosphorus levels in an andean bean population. *Crop Science* 49, 1742-1750.
Collard, B.C.Y., and Mackill, D.J. (2008). Marker-assisted selection: an approach for precision plant breeding in the twenty-first century. *Philosophical Transactions of the Royal Society of London. Series B, Biological Sciences* 363, 557-572.
Colston-Nepali, L., Tigano, A., Boyle, B., and Friesen, V. (2019). Hybridization does not currently pose conservation concerns to murres in the Atlantic. *Conservation Genetics* 20, 1465-1470.
Connorton, J.M., Jones, E.R., Rodríguez-Ramiro, I., Fairweather-Tait, S., Uauy, C., and Balk, J. (2017a). Wheat vacuolar iron transporter *TaVIT2* transports Fe and Mn and is effective for biofortification. *Plant Physiology (Bethesda)* 174, 2434-2444.
Connorton, J.M., Jones, E.R., Rodríguez-Ramiro, I., Fairweather-Tait, S., Uauy, C., and Balk, J. (2017b). Wheat Vacuolar Iron Transporter TaVIT2 transports Fe and Mn and is effective for biofortification *Plant Physiology* 174, 2434-2444.
Covarrubias-Pazaran, G. (2016). Genome-Assisted Prediction of Quantitative Traits Using the R Package sommer. *PLoS One* 11, e0156744.
Coyne, D., Shuster, M., and Hill, K. (1973). Genetic control of reaction to common blight bacterium in bean (*Phaseolus vulgaris*) as influenced by plant age and bacterial multiplication. *The Journal of the American Society for Horticultural Science*, 98:94-99.
Curie, C., Alonso, J.M., Le Jean, M., Ecker, J.R., and Briat, J.F. (2000). Involvement of NRAMP1 from *Arabidopsis thaliana* in iron transport. *Biochemical Journal* 347 Pt 3, 749-755.
Darrier, B., Russell, J., Milner, S.G., Hedley, P.E., Shaw, P.D., Macaulay, M., Ramsay, L.D., Halpin, C., Mascher, M., Fleury, D.L., Langridge, P., Stein, N., and Waugh, R. (2019). A comparison of mainstream genotyping platforms for the evaluation and use of barley genetic resources. *Frontiers in Plant Science* 10, 544.
Dasgupta, J., Ananyev, G.M., and Dismukes, G.C. (2008). Photoassembly of the water-oxidizing complex in photosystem II. *Coordination Chemistry Reviews* 252, 347-360.
Database, F.S. (2019). Food and Agriculture Organization of the United Nations.
De Bruyn, H.L.G. (1933). Kwade harten van de erwten. *Tijdschrift Over Plantenziekten* 39, 281-318.
De Bruyn, H.L.G. (1939). Mn-deficiency as the cause of marsh spot of pea seeds. *Tijdschrift Over Plantenziekten* 45, 106–120.
Delfini, J., Moda-Cirino, V., Dos Santos Neto, J., Ruas, P.M., Sant'ana, G.C., Gepts, P., and Goncalves, L.S.A. (2021). Population structure, genetic diversity and genomic selection signatures among a Brazilian common bean germplasm. *Science Report* 11, 2964.
Delhaize, E., Gruber, B.D., Pittman, J.K., White, R.G., Leung, H., Miao, Y., Jiang, L., Ryan, P.R., and Richardson, A.E. (2007). A role for the *AtMTP11* gene of *Arabidopsis* in manganese transport and tolerance. *The Plant Journal* 51, 198-

210.
Demaegd, D., Foulquier, F., Colinet, A.-S., Gremillon, L., Legrand, D., Mariot, P., Peiter, E., Van Schaftingen, E., Matthijs, G., and Morsomme, P. (2013). Newly characterized Golgi-localized family of proteins is involved in calcium and pH homeostasis in yeast and human cells. *Proceedings of the National Academy of Sciences* 110, 6859-6864.
Ding, G., Yang, M., Hu, Y., Liao, Y., Shi, L., Xu, F., and Meng, J. (2010). Quantitative trait loci affecting seed mineral concentrations in *Brassica napus* grown with contrasting phosphorus supplies. *Annals of Botany* 105, 1221-1234.
Dutta, A., Trivedi, A., Nath, C.P., Gupta, D.S., and Hazra, K.K. (2022). A comprehensive review on grain legumes as climate‐smart crops: Challenges and prospects. *Environmental Challenges* 7, 100479.
Edmond, C., Shigaki, T., Ewert, S., Nelson, M.D., Connorton, J.M., Chalova, V., Noordally, Z., and Pittman, J.K. (2009). Comparative analysis of CAX2-like cation transporters indicates functional and regulatory diversity. *Biochemical Journal* 418, 145-154.
Eisenhut, M., Hoecker, N., Schmidt, S.B., Basgaran, R.M., Flachbart, S., Jahns, P., Eser, T., Geimer, S., Husted, S., Weber, A.P.M., Leister, D., and Schneider, A. (2018). The plastid envelope chloroplast manganese transporter1 is essential for manganese homeostasis in Arabidopsis. *Molecular Plant* 11, 955-969.
Elshire, R.J., Glaubitz, J.C., Sun, Q., Poland, J.A., Kawamoto, K., Buckler, E.S., and Mitchell, S.E. (2011). A robust, simple genotyping-by-sequencing (GBS) approach for high diversity species (genotyping approach for high diversity species). *PLoS ONE* 6, e19379.
Engelsma, G. (1972). A possible role of divalent manganese ions in the photoinduction of phenylalanine ammonia-lyase. *Plant Physiology (Bethesda)* 50, 599-602.
Enrico, M., Stefan, M., Alexis, D.A., and Réka, N. (2012). Vacuolar transporters in their physiological context. *Annual Review of Plant Biology* 63, 183-213.
Eroglu, S., Meier, B., Von Wirén, N., and Peiter, E. (2016). The vacuolar manganese transporter MTP8 determines tolerance to iron deficiency-induced chlorosis in Arabidopsis. *Plant Physiology (Bethesda)* 170, 1030-1045.
Eugene, V.M., David, P.M., and Benjamin, J.M. (1968). Manganese absorption by excised barley roots. *Plant Physiology (Bethesda)* 43, 527-530.
Fan, Z., Gao, Y., Liu, R., Wang, X., Guo, Y., and Zhang, Q. (2020). The major gene and polygene effects of ornamental traits in bearded iris (*Iris germanica*) using joint segregation analysis. *Scientia Horticulturae* 260, 108882.
Faostat. (2018). FAOSTAT Crop Statistics. *Forest Resources Development Service*.
Farrah, H., and Pickering, W.F. (1979). PH effects in the adsorption of heavy metal ions by clays. *Chemical Geology* 25, 317-326.
Farrow, A., and Andriatsitohaina, R. (2021). *Atlas of common bean production in Africa.*
Feng, N., He, Z., Zhang, Y., Xia, X., and Zhang, Y. (2013). QTL mapping of starch granule size in common wheat using recombinant inbred lines derived from a PH82-2/Neixiang 188 cross. *The Crop Journal* 1, 166-171.
Foyer, C., Lam, H.-M., Nguyen, H., Siddique, K., Varshney, R., Colmer, T., Cowling, W., Bramley, H., Mori, T., Hodgson, J., Cooper, J., Miller, A., Kunert, K., Vorster, B., Cullis, C., Ozga, J., Wahlqvist, M., Liang, Y., Shou, H., and Considine, M. (2016). Neglecting legumes has compromised human health and sustainable food production. *Nature Plants* 2, 1-10.
Foyer, C.H., and Noctor, G. (2003). Redox sensing and signalling associated with reactive oxygen in chloroplasts, peroxisomes and mitochondria. *Physiologia*

Plantarum 119, 355-364.

Frank, J., Happeck, R., Meier, B., Hoang, M.T.T., Stribny, J., Hause, G., Ding, H., Morsomme, P., Baginsky, S., and Peiter, E. (2019). Chloroplast-localized BICAT proteins shape stromal calcium signals and are required for efficient photosynthesis. *New Phytologist* 221, 866-880.

Fu, X.Z., Zhou, X., Xing, F., Ling, L.L., Chun, C.P., Cao, L., Aarts, M.G.M., and Peng, L.Z. (2017). Genome-wide identification, cloning and functional analysis of the Zinc/Iron-regulated Transporter-Like Protein (ZIP) gene family in Trifoliate Orange (*Poncirus trifoliata* L. Raf.). *Frontiers in Plant Science* 8, 588.

Furneaux, B.S., and Glasscock, H.H. (1936). Soils in relation to marsh spot of pea seed. *The Journal of Agricultural Science* 26, 59-84.

Gai, J., Wang, Y., Wu, X., and Chen, S. (2007). A comparative study on segregation analysis and QTL mapping of quantitative traits in plants—with a case in soybean. *Frontiers of Agriculture in China* 1, 1-7.

Gai, J.Y., and Wang, J.K. (1998). Identification and estimation of a QTL model and its effects. *Theoretical and Applied Genetics* 97, 1162–1168.

Gallais, A., ., Dillmann, C., and Goldringer (2001). *Quantitative genetics and breeding methods : The way ahead : 11th Meeting : Aug 2000, Paris, France.*

Gang, Z., Zikai, W., and Bingwei, W. (2007). Major gene plus polygene inheritance of plant height and ear height in micro-edosperm super-high oil corn. *Journal of Anhui Agricultural Science* 35, 5096-5098.

Gao, H., Xie, W., Yang, C., Xu, J., Li, J., Wang, H., Chen, X., and Huang, C.-F. (2018). NRAMP2, a trans-Golgi network-localized manganese transporter, is required for Arabidopsis root growth under manganese deficiency. *New Phytologist* 217, 179-193.

Garcia Miragaya, J. (1984). Levels, chemical fractionation, and solubility of lead in roadside soils of caracas, venezuela. *Soil Science* 138, 147-152.

Gatti, D.M., Svenson, K.L., Shabalin, A., Wu, L.-Y., Valdar, W., Simecek, P., Goodwin, N., Cheng, R., Pomp, D., Palmer, A., Chesler, E.J., Broman, K.W., and Churchill, G.A. (2014). Quantitative trait locus mapping methods for diversity outbred mice. *G3 Genes|Genomes|Genetics* 4, 1623-1633.

Giles, C.D., Brown, L.K., Adu, M.O., Mezeli, M.M., Sandral, G.A., Simpson, R.J., Wendler, R., Shand, C.A., Menezes-Blackburn, D., Darch, T., Stutter, M.I., Lumsdon, D.G., Zhang, H., Blackwell, M.S., Wearing, C., Cooper, P., Haygarth, P.M., and George, T.S. (2017). Response-based selection of barley cultivars and legume species for complementarity: Root morphology and exudation in relation to nutrient source. *Plant Science* 255, 12-28.

Gioia, T., Logozzo, G., Marzario, S., Spagnoletti Zeuli, P., and Gepts, P. (2019). Evolution of SSR diversity from wild types to U.S. advanced cultivars in the Andean and Mesoamerican domestications of common bean (*Phaseolus vulgaris*). *PloS ONE* 14, e0211342.

Graham, R.D., Hannam, R.J., and Uren, N.C. (1988). *Manganese in soils and plants.* Netherlands, Dordrecht: Springer.

Green, R.E., Krause, J., Ptak, S.E., Briggs, A.W., Ronan, M.T., Simons, J.F., Du, L., Egholm, M., Rothberg, J.M., Paunovic, M., and Pääbo, S. (2006). Analysis of one million base pairs of Neanderthal DNA. *Nature* 444, 330-336.

Growers, S.P. (2020). Pulse production manual 2000. *Saskatchewan Pulse Growers,Saskatoon, SK.*

Guerinot, M.L. (2000). The ZIP family of metal transporters. *Biochimica et Biophysica Acta (BBA)* 1465, 190-198.

Gutteridge, J.M.C., and Halliwell, B. (2010). Antioxidants: Molecules, medicines, and myths. *Biochemical and Biophysical Research Communications* 393, 561-564.

Haley, C.S., and Knott, S.A. (1992). A simple regression method for mapping quantitative trait loci in line crosses using flanking markers. *Heredity* 69, 315.

Hart, J.P., and Griffiths, P.D. (2015). Genotyping-by-Sequencing enabled mapping and marker development for the by-2 potyvirus resistance allele in common bean. *The Plant Genome* 8, plantgenome2014.2009.0058.

Hayes, B.J., Bowman, P.J., Chamberlain, A.C., Verbyla, K., and Goddard, M.E. (2009). Accuracy of genomic breeding values in multi-breed dairy cattle populations. *Genetics Selection Evolution* 41, 51.

He, J., Meng, S., Zhao, T., Xing, G., Yang, S., Li, Y., Guan, R., Lu, J., Wang, Y., Xia, Q., Yang, B., and Gai, J. (2017). An innovative procedure of genome-wide association analysis fits studies on germplasm population and plant breeding. *Theoretical and Applied Genetics* 130, 2327-2343.

He, J., Zhao, X., Laroche, A., Lu, Z.-X., Liu, H., and Li, Z. (2014). Genotyping-by-sequencing (GBS), an ultimate marker-assisted selection (MAS) tool to accelerate plant breeding. *Frontiers in Plant Science* 5, 484-484.

He, L., Xiao, J., Rashid, K.Y., Jia, G., Li, P., Yao, Z., Wang, X., Cloutier, S., and You, F.M. (2019). Evaluation of genomic prediction for pasmo resistance in flax. *International Journal of Molecular Sciences* 20, 359.

He, L., Xiao, J., Rashid, K.Y., Yao, Z., Li, P., Jia, G., Wang, X., Cloutier, S., and You, F.M. (2018). Genome-wide association studies for pasmo resistance in flax (*Linum usitatissimum* L.). *Frontiers in Plant Science*, doi: 10.3389/fpls.2018.01982

Hebbern, C.A., Laursen, K.H., Ladegaard, A.H., Schmidt, S.B., Pedas, P., Bruhn, D., Schjoerring, J.K., Wulfsohn, D., and Husted, S. (2009). Latent manganese deficiency increases transpiration in barley (*Hordeum vulgare*). *Plant Physiology* 135, 307-316.

Heintze, S.G. (1938). Readily soluble manganese of soils and marsh spot of peas. *The Journal of Agricultural Science* 28, 175-186.

Henkens, C.H. (1958). The prevention of marsh spot in peas by spraying with manganese sulphate. *Landbouwvoorlichting* 15, 262-265.

Herridge, D.F., Peoples, M.B., and Boddey, R.M. (2008). Global inputs of biological nitrogen fixation in agricultural systems. *Plant and Soil* 311, 1-18.

Hewitt, E.J. (1945). 'Marsh spot' in beans. *Nature* 155, 22-23.

Hirschi, K.D., Korenkov, V.D., Wilganowski, N.L., and Wagner, G.J. (2000). Expression of arabidopsis CAX2 in tobacco. Altered metal accumulation and increased manganese tolerance1. *Plant Physiology* 124, 125-134.

Hoecker, N., Leister, D., and Schneider, A. (2017). Plants contain small families of UPF0016 proteins including the PHOTOSYNTHESIS AFFECTED MUTANT71 transporter. *Plant Signaling & Behavior* 12, e1278101.

Holland, J. (2001). Epistasis and plant breeding. *Plant Breed Review* 21, 27-92.

Howard, R.J., Garland, J.A., and Seaman, W.L. (1994). *Diseases and pests of vegetable crops in Canada.* Ottawa : Canadian Phytopathological Society, c1994.

Huang, B.E., and George, A.W. (2011). R/mpMap: a computational platform for the genetic analysis of multiparent recombinant inbred lines. *Bioinformatics* 27, 727-729.

Humphries, J., Stangoulis, J., Graham, R. (2007). "Manganese," in *Handbook of Plant Nutrition,* eds. A.V. Barker & D.J. Pilbeam. Taylor and Francis, USA.), 351-366.

Jansen, R.C. (1994). High resolution of quantitative traits into multiple loci via interval mapping. *Genetics*, 1447-1455.

Jia, B., Conner, R.L., Khan, N., Hou, A., Xia, X., and You, F.M. (2021a). Inheritance of marsh spot disease resistance in cranberry common bean (*Phaseolus vulgaris*

L.). *The Crop Journal* 9, 456-467.

Jia, B., Conner, R.L., Waldo, P.C., Khan, N., Zheng, C., Cloutier, S., Hou, A., Xia, X., and You, F.M. (2022). Quantitative trait locus mapping of marsh spot disease resistance in cranberry common bean (*Phaseolus vulgaris* L.). *International Journal of Molecular Science* (Under review).

Jia, B., Waldo, P., Conner, R.L., Khan, N., Hou, A., Xia, X., and You, F.M. (2021b). Marsh spot disease and its causal factor, manganese deficiency in plants: A historical and prospective review. *Agricultural Sciences* 12, 928-948.

Jinge, T., Chenglong, W., Jinliang, X., Lishuan, W., Guanghui, X., Weihao, W., Dan, L., Wenchao, Q., Xu, H., Qiuyue, C., Weiwei, J., and Feng, T. (2019). Teosinte ligule allele narrows plant architecture and enhances high-density maize yields. *Science* 365, 658-664.

Jung, M.C. (2008). Heavy metal concentrations in soils and factors affecting metal uptake by plants in the vicinity of a korean Cu-W mine. *Sensors (Basel)* 8, 2413-2423.

Kamiya, T., Akahori, T., Ashikari, M., and Maeshima, M. (2006). Expression of the vacuolar Ca^{2+}/H^{+} exchanger, OSCAX1a, in rice: Cell and age specificity of expression, and enhancement by Ca^{2+}. *Plant and Cell Physiology* 47, 96-106.

Kandpal, G., Srivastava, P.C., and Ram, B. (2005). Kinetics of desorption of heavy metals from polluted soils: Influence of soil type and metal source. *Water, Air & Soil Pollution* 161, 353-363.

Kao, C.-H., Zeng, Z.-B., and Teasdale, R.D. (1999). Multiple interval mapping for quantitative trait loci. *Genetics* 152, 1203-1216.

Karp, R.M., and Rabin, M.O. (1987). Efficient randomized pattern-matching algorithms. *IBM Journal of Research and Development* 31, 249-260.

Keller, B., Ariza-Suarez, D., De La Hoz, J., Aparicio, J.S., Portilla-Benavides, A.E., Buendia, H.F., Mayor, V.M., Studer, B., and Raatz, B. (2020). Genomic prediction of agronomic traits in common bean (*Phaseolus vulgaris* L.) under environmental stress. *Frontiers in Plant Science* 11, 1001.

Khan, M.I., Khattak, G.S.S., Khan, A.J., Khan, A.J., Subhan, F., Mohammad, T., and Ali, A. (2012). Genetic control of flag leaf area in wheat (*Triticum aestivum*) crosses. *African Journal of Agricultural Research* 7, 3978 – 3990.

Kikuta, H., Laplante, M., Navratilova, P., Komisarczuk, A.Z., Engström, P.G., Fredman, D., Akalin, A., Caccamo, M., Sealy, I., Howe, K., Ghislain, J., Pezeron, G., Mourrain, P., Ellingsen, S., Oates, A.C., Thisse, C., Thisse, B., Foucher, I., Adolf, B., Geling, A., Lenhard, B., and Becker, T.S. (2007). Genomic regulatory blocks encompass multiple neighboring genes and maintain conserved synteny in vertebrates. *Genome Research* 17, 545-555.

Kim, S.A., Punshon, T., Lanzirotti, A., Li, L., Alonso, J.M., Ecker, J.R., Kaplan, J., and Guerinot, M.L. (2006). Localization of Iron in *Arabidopsis* seed requires the vacuolar membrane transporter VIT1. *Science* 314, 1295-1298.

Kircher, M., and Kelso, J. (2010). High-throughput DNA sequencing--concepts and limitations. *Bioessays* 32, 524-536.

Klein, M.A., and Grusak, M.A. (2009). Identification of nutrient and physical seed trait QTL in the model legume *Lotus japonicus*. *Genome* 52, 677-691.

Koike, S., Inoue, H., Mizuno, D., Takahashi, M., Nakanishi, H., Mori, S., and Nishizawa, N.K. (2004). OsYSL2 is a rice metal-nicotianamine transporter that is regulated by iron and expressed in the phloem. *The Plant Journal* 39, 415-424.

Kolaj-Robin, O., Russell, D., Hayes, K.A., Pembroke, J.T., and Soulimane, T. (2015). Cation diffusion facilitator family: Structure and function. *FEBS Letters* 589, 1283-1295.

Koopman, C. (1937). Invloed van mangaansulfaatbespuiting tegen kwaadhartigheid bij

schokkererwten. *Tijdschr Over Plantenziekten* 43, 64-66.
Kosambi, D.D. (1944). The estimation of map distance from recombination values. *Annals of Eugenics* 12, 172-175.
Kumar, S., You, F.M., and Cloutier, S. (2012). Genome wide SNP discovery in flax through next generation sequencing of reduced representation libraries. *BMC Genomics* 13, 684.
Kumar, S., You, F.M., Duguid, S., Booker, H., Rowland, G., and Cloutier, S. (2015). QTL for fatty acid composition and yield in linseed (Linum usitatissimum L.). *Theoretical and Applied Genetics* 128, 965-984.
Lacey, M.S. (1934). Studies in bacteriosis: Xxi. An investigation of marsh spot of peas: With a note on the morphological structure. *Annals of Applied Biology* 21, 621-640.
Lan, S., Zheng, C., Hauck, K., Mccausland, M., Duguid, S.D., Booker, H.M., Cloutier, S., and You, F.M. (2020). Genomic prediction accuracy of seven breeding selection traits improved by QTL identification in flax. *International Journal of Molecular Sciences* 21, 1577.
Lander, E.S., and Botstein, D. (1989). Mapping mendelian factors underlying quantitative traits using RFLP linkage maps. *Genetics* 121, 185-199.
Lanquar, V., Lelièvre, F., Bolte, S., Hamès, C., Alcon, C., Neumann, D., Vansuyt, G., Curie, C., Schröder, A., Krämer, U., Barbier-Brygoo, H., and Thomine, S. (2005). Mobilization of vacuolar iron by *AtNRAMP3* and *AtNRAMP4* is essential for seed germination on low iron. *The EMBO Journal* 24, 4041-4051.
Lanquar, V., Ramos, M.S., Lelièvre, F., Barbier-Brygoo, H., Krieger-Liszkay, A., Krämer, U., and Thomine, S. (2010). Export of vacuolar manganese by *AtNRAMP3* and *AtNRAMP4* is required for optimal photosynthesis and growth under manganese deficiency. *Plant Physiology (Bethesda)* 152, 1986-1999.
Lauer, J., Bijlb, C., Grusakc, M., Baenzigerd, P., Bootee, K., Linglef, S., Carterg, T., Kaepplerh, S., Boermai, R., Eizengaj, G., Carterk, P., Goodman, M., Nafzigerm, E., Kidwelln, K., Mitchello, R., Edgertonp, M., Quesenberry, K., and Willcox, M. (2012). The scientific grand challenges of the 21st century for the Crop Science Society of America. *Crop Science* 52, 1003-1010.
Leplat, F., Pedas, P.R., Rasmussen, S.K., and Husted, S. (2016). Identification of manganese efficiency candidate genes in winter barley *(Hordeum vulgare)* using genome wide association mapping. *BMC Genomics* 17, 775.
Levin, I., Crittenden, L.B., and Dodgson, J.B. (1993). Genetic map of the chicken Z chromosome using random amplified polymorphic DNA (RAPD) markers. *Genomics* 16, 224-230.
Lewis, A.H. (1939). Manganese deficiencies in crops. I. Spraying pea crops with solutions of manganese salts to eliminate marsh-spot. *Empire Journal of Experimental Agnculture* 7, 150–154.
Li, H., Ye, G., and Wang, J. (2007). A modified algorithm for the improvement of composite interval mapping. *Genetics* 175, 361-374.
Liu, C., Chen, G., Li, Y., Peng, Y., Zhang, A., Hong, K., Jiang, H., Ruan, B., Zhang, B., Yang, S., Gao, Z., and Qian, Q. (2017a). Characterization of a major QTL for manganese accumulation in rice grain. *Scientific Reports* 7, 17704-17712.
Liu, N., Li, M., Hu, X., Ma, Q., Mu, Y., Tan, Z., Xia, Q., Zhang, G., and Nian, H. (2017b). Construction of high-density genetic map and QTL mapping of yield-related and two quality traits in soybean RILs population by RAD-sequencing. *BMC Genomics* 18, 466.
Liu, X., Guo, L., You, J., Liu, X., He, Y., Yuan, J.E., Liu, G., and Feng, Z. (2010). Progress of segregation distortion in genetic mapping of plants. *Research Journal of Agronomy* 4, 78-83.
Loneragan, J.F. (1988). "Distribution and movement of manganese in plants," in

Manganese in Soils and Plants, eds. R.D. Graham, R.J. Hannam & N.C. Uren. (Dordrecht: Springer), 113-124.

Lou, X.Y., Ma, J.Z., Yang, M.C., Zhu, J., Liu, P.Y., Deng, H.W., Elston, R.C., and Li, M.D. (2006). Improvement of mapping accuracy by unifying linkage and association analysis. *Genetics* 172, 647-661.

Ma, G., Li, J., Li, J., Li, Y., Gu, D., Chen, C., Cui, J., Chen, X., and Zhang, W. (2018). OsMTP11, a trans-Golgi network localized transporter, is involved in manganese tolerance in rice. *Plant Science* 274, 59-69.

Maillard, A., Diquelou, S., Billard, V., Laine, P., Garnica, M., Prudent, M., Garcia-Mina, J.M., Yvin, J.C., and Ourry, A. (2015). Leaf mineral nutrient remobilization during leaf senescence and modulation by nutrient deficiency. *Frontiers in Plant Science* 6, 317.

Manly, K.F., Cudmore, J.R.H., and Meer, J.M. (2001). Map Manager QTX, cross-platform software for genetic mapping. *Mammalian Genome* 12, 930-932.

Margulies, M., Egholm, M., Altman, W.E., Attiya, S., Bader, J.S., Bemben, L.A., Berka, J., Braverman, M.S., Chen, Y.J., Chen, Z., Dewell, S.B., Du, L., Fierro, J.M., Gomes, X.V., Godwin, B.C., He, W., Helgesen, S., Ho, C.H., Irzyk, G.P., Jando, S.C., Alenquer, M.L., Jarvie, T.P., Jirage, K.B., Kim, J.B., Knight, J.R., Lanza, J.R., Leamon, J.H., Lefkowitz, S.M., Lei, M., Li, J., Lohman, K.L., Lu, H., Makhijani, V.B., Mcdade, K.E., Mckenna, M.P., Myers, E.W., Nickerson, E., Nobile, J.R., Plant, R., Puc, B.P., Ronan, M.T., Roth, G.T., Sarkis, G.J., Simons, J.F., Simpson, J.W., Srinivasan, M., Tartaro, K.R., Tomasz, A., Vogt, K.A., Volkmer, G.A., Wang, S.H., Wang, Y., Weiner, M.P., Yu, P., Begley, R.F., and Rothberg, J.M. (2005). Genome sequencing in microfabricated high-density picolitre reactors. *Nature* 437, 376-380.

Marschner, H. (1995). *Mineral Nutrition of Higher Plants.* London: Academic Press.

Mayoral, V., Bharat, S., Rowse, P., Hernández, A., and Mazzolai, B. (2014). Towards an open sourcelinux autopilot for drones *LibreCon*.

Mba, R.E.C., Stephenson, P., Edwards, K., Melzer, S., Nkumbira, J., Gullberg, U., Apel, K., Gale, M., Tohme, J., and Fregene, M. (2001). Simple sequence repeat (SSR) markers survey of the cassava (*Manihot esculenta* Crantz) genome: towards an SSR-based molecular genetic map of cassava. *Theoretical and Applied Genetics* 102, 21-31.

Mcclean, P.E., Lee, R.K., and Miklas, P.N. (2004). Sequence diversity analysis of dihydroflavonol 4-reductase intron 1 in common bean. *Genome* 47, 266-280.

Mcclean, P.E., Lee, R.K., Otto, C., Gepts, P., and Bassett, M.J. (2002). Molecular and phenotypic mapping of genes controlling seed coat pattern and color in common bean (*Phaseolus vulgaris L.*). *Journal of Heredity* 93, 148-152.

Mei, H., Cheng, N.H., Zhao, J., Park, S., Escareno, R.A., Pittman, J.K., and Hirschi, K.D. (2009). Root development under metal stress in *Arabidopsis thaliana* requires the H^+/cation antiporter CAX4. *New Phytologist* 183, 95-105.

Meng, L., Li, H., Zhang, L., and Wang, J. (2015). QTL IciMapping: Integrated software for genetic linkage map construction and quantitative trait locus mapping in biparental populations. *The Crop Journal* 3, 269-283.

Mikhaylova, A.V., and Thornton, T.A. (2019). Accuracy of gene expression prediction from genotype data with predixcan varies across and within continental populations. *Frontiers in Genetics* 10.

Miklas, P.N., Kelly, J.D., Beebe, S.E., and Blair, M.W. (2006). Common bean breeding for resistance against biotic and abiotic stresses: From classical to MAS breeding. *Euphytica* 147, 105-131.

Mills, R.F., Doherty, M.L., López-Marqués, R.L., Weimar, T., Dupree, P., Palmgren, M.G., Pittman, J.K., and Williams, L.E. (2008). *ECA3*, a golgi-localized P_{2A}-Type ATPase, plays a crucial role in manganese nutrition in *Arabidopsis*.

Plant Physiology 146, 116-128.
Milner, M.J., Seamon, J., Craft, E., and Kochian, L.V. (2012). Transport properties of members of the ZIP family in plants and their role in Zn and Mn homeostasis. *Journal of Experimental Botany* 64, 369-381.
Mittler, R. (2006). Abiotic stress, the field environment and stress combination. *Trends in Plant Science* 11, 15-19.
Monson-Miller, J., Sanchez-Mendez, D.C., Fass, J., Henry, I.M., Tai, T.H., and Comai, L. (2012). Reference genome-independent assessment of mutation density using restriction enzyme-phased sequencing. *BMC Genomics* 13, 72.
Montanini, B., Blaudez, D., Jeandroz, S., Sanders, D., and Chalot, M. (2007). Phylogenetic and functional analysis of the Cation Diffusion Facilitator (CDF) family: improved signature and prediction of substrate specificity. *BMC Genomics* 8, 107.
Moraghan, J., and Grafton, G. (2000). 'Marsh Spot' in cranberry bean seed. *Annual Report of the Bean Improvement Cooperative* 43, 9-10.
Morris, J., Tian, H., Park, S., Sreevidya, C.S., Ward, J.M., and Hirschi, K.D. (2008). AtCCX3 is an Arabidopsis endomembrane H^+ -dependent K^+ transporter. *Plant Physiology* 148, 1474-1486.
Mott, R., Talbot, C.J., Turri, M.G., Collins, A.C., and Flint, J. (2000). A method for fine mapping quantitative trait loci in outbred animal stocks. *Proceedings of the National Academy of Sciences* 97, 12649-12654.
Mourtzinis, S., Specht, J.E., Lindsey, L.E., Wiebold, W.J., Ross, J., Nafziger, E.D., Kandel, H.J., Mueller, N., Devillez, P.L., Arriaga, F.J., and Conley, S.P. (2015). Climate-induced reduction in US-wide soybean yields underpinned by region- and in-season-specific responses. *Nature Plants* 1, 14026.
Mueen Alam, K., Fei, T., Wubin, W., Jianbo, H., Tuanjie, Z., Junyi, G., and Christian, W. (2019). Using the RTM-GWAS procedure to detect the drought tolerance QTL-allele system at the seedling stage under sand culture in a half-sib population of soybean [*Glycine max* (L.) Merr.]. *Canadian Journal of Plant Science* 99, 801-814.
Nawaz, Z., Kakar, K.U., Li, X.-B., Li, S., Zhang, B., Shou, H.-X., and Shu, Q.-Y. (2015). Genome-wide association mapping of quantitative trait loci (QTLs) for contents of eight elements in brown rice (*Oryza sativa* L.). *Journal of Agricultural and Food Chemistry* 63, 8008-8016.
Ndakidemi, P.A., Dakora, F.D., Nkonya, E.M., Ringo, D., and Mansoor, H. (2006). Yield and economic benefits of common bean (*Phaseolus vulgaris*) and soybean (*Glycine max*) inoculation in northern Tanzania. *Australian Journal of Experimental Agriculture* 46, 571-577.
Nelson, J.C. (1997). QGENE: software for marker-based genomic analysis and breeding. *Molecular Breeding* 3, 239-245.
Ohki, K., Boswell, F.C., Parker, M.B., Shuman, L.M., and Wilson, D.O. (1979). Critical manganese deficiency level of soybean related to leaf position. *Agronomy Journal* 71, 233-234.
Otsen, M., Den Bieman, M., Kuiper, M.T., Pravenec, M., Kren, V., Kurtz, T.W., Jacob, H.J., Lankhorst, A., and Van Zutphen, B.F. (1996). Use of AFLP markers for gene mapping and QTL detection in the rat. *Genomics* 37, 289-294.
Passioura, J. (1991). Soil structure and plant growth. *Soil Research* 29, 717-728.
Paterson, A.H. (2013). "Marker assisted selection in agriculture". (London: Henry Stewart Talks).
Pedas, P., Ytting, C.K., Fuglsang, A.T., Jahn, T.P., Schjoerring, J.K., and Husted, S. (2008). Manganese efficiency in barley: Identification and characterization of the metal ion transporter HvIRT1. *Plant Physiology (Bethesda)* 148, 455-466.

Pellicer, J., and Leitch, I.J. (2020). The Plant DNA C-values database (release 7.1): an updated online repository of plant genome size data for comparative studies. *New Phytologist* 226, 301-305.

PéRez De La Vega, M., Santalla, M., and Marsolais, F.D.R. (2017). *The common bean genome.* Cham: Springer International Publishing.

Peris-Peris, C., Serra-Cardona, A., Sánchez-Sanuy, F., Campo, S., Ariño, J., and San Segundo, B. (2017). Two NRAMP6 isoforms function as iron and manganese transporters and contribute to disease resistance in rice. *Molecular Plant-Microbe Interactions* 30, 385-398.

Perumalsamy, S., Bharani, M., Sudha, M., Nagarajan, P., Arul, L., Saraswathi, R., Balasubramanian, P., and Ramalingam, J. (2010). Functional marker-assisted selection for bacterial leaf blight resistance genes in rice (*Oryza sativa* L.). *Plant Breeding* 129, 400-406.

Pethybridge, G.H. (1936). Marsh spot in pea seeds: Is it a deficiency disease. *Journal of the Ministry of Agriculture* 43, 55-58.

Piper, C.S. (1941). Marsh spot of peas: A manganese deficiency disease. *The Journal of Agricultural Science* 31, 448-453.

Pittman, J.K. (2005). Managing the manganese: Molecular mechanisms of manganese transport and homeostasis. *New Phytologist* 167, 733-742.

Pittman, J.K., and Hirschi, K.D. (2016). Phylogenetic analysis and protein structure modelling identifies distinct Ca^{2+}/Cation antiporters and conservation of gene family structure within *Arabidopsis* and rice species. *Rice* 9, 3.

Poland, J.A., Brown, P.J., Sorrells, M.E., and Jannink, J.-L. (2012). Development of high-density genetic maps for barley and wheat using a novel two-enzyme genotyping-by-sequencing approach. *PLoS ONE* 7, e32253.

Poveda, A., Chen, Y., Brändström, A., Engberg, E., Hallmans, G., Johansson, I., Renström, F., Kurbasic, A., and Franks, P.W. (2017). The heritable basis of gene-environment interactions in cardiometabolic traits. *Diabetologia* 60, 442-452.

Priyadarshan, P.M. (2019). "Recombinant inbred lines." (Singapore: Springer Singapore), 257-268.

Qi, Z.Y., Li, J.X., Raza, M.A., Zou, X.X., Cao, L.W., Rao, L.L., and Chen, L.P. (2015). Inheritance of fruit cracking resistance of melon (*Cucumis melo* L.) fitting E-0 genetic model using major gene plus polygene inheritance analysis. *Scientia Horticulturae* 189, 168–174.

Ramegowda, V., and Senthil-Kumar, M. (2015). The interactive effects of simultaneous biotic and abiotic stresses on plants: Mechanistic understanding from drought and pathogen combination. *Journal of Plant Physiology* 176, 47-54.

Ramirez-Cabral, N.Y.Z., Kumar, L., and Taylor, S. (2016). Crop niche modeling projects major shifts in common bean growing areas. *Agricultural and Forest Meteorology* 218-219, 102-113.

Ren, T., Fan, T., Chen, S., Ou, X., Chen, Y., Jiang, Q., Diao, Y., Sun, Z., Peng, W., Ren, Z., Tan, F., and Li, Z. (2021). QTL mapping and validation for kernel area and circumference in common wheat via high-density SNP-based genotyping. *Frontiers in Plant Science* 12, 1702.

Rendón-Anaya, M., Montero-Vargas, J.M., Saburido-Álvarez, S., Vlasova, A., Capella-Gutierrez, S., Ordaz-Ortiz, J.J., Aguilar, O.M., Vianello-Brondani, R.P., Santalla, M., Delaye, L., Gabaldón, T., Gepts, P., Winkler, R., Guigó, R., Delgado-Salinas, A., and Herrera-Estrella, A. (2017). Genomic history of the origin and domestication of common bean unveils its closest sister species. *Genome Biology* 18, 60.

Renfrew, A.K., O'neill, E.S., Hambley, T.W., and New, E.J. (2018). Harnessing the properties of cobalt coordination complexes for biological application.

Coordination Chemistry Reviews 375, 221-233.
Reynolds, J.D. (1955). Marsh spot of peas: A review of present knowledge. *Journal of the Science of Food and Agriculture* 6, 725-734.
Rieuwerts, J.S., Thornton, I., Farago, M.E., and Ashmore, M.R. (1998). Factors influencing metal bioavailability in soils: Preliminary investigations for the development of a critical loads approach for metals. *Chemical Speciation & Bioavailability* 10, 61-75.
Rifkin, S.A. (2012). *Quantitative trait loci (QTL) methods and protocols.* New York: Humana Press.
Rohdich, F., Lauw, S., Kaiser, J., Feicht, R., Köhler, P., Bacher, A., and Eisenreich, W. (2006). Isoprenoid biosynthesis in plants 2C-methyl-d-erythritol-4-phosphate synthase (IspC protein) of *Arabidopsis thalian*. *The FEBS Journal* 273, 4446-4458.
Rosales-Serna, R., Kohashi-Shibata, J., Acosta-Gallegos, J.A., Trejo-López, C., Ortiz-Cereceres, J.N., and Kelly, J.D. (2004). Biomass distribution, maturity acceleration and yield in drought-stressed common bean cultivars. *Field Crops Research* 85, 203-211.
Rossi, M., Bitocchi, E., Bellucci, E., Nanni, L., Rau, D., Attene, G., and Papa, R. (2009). Linkage disequilibrium and population structure in wild and domesticated populations of *Phaseolus vulgaris* L. *Evolutionary Applications* 2, 504-522.
Rychel-Bielska, S., Nazzicari, N., Plewiński, P., Bielski, W., Annicchiarico, P., and Książkiewicz, M. (2020). Development of PCR-based markers and whole-genome selection model for anthracnose resistance in white lupin (*Lupinus albus* L.). *Journal of Applied Genetics* 61, 531-545.
Samuel, G., and Piper, C.S. (1929). Manganese as an essential element for plant growth. *Annals of Applied Biology* 16, 493-524.
Sandhu, K., You, F., Conner, R., Balasubramanian, P., and Hou, A. (2018). Genetic analysis and QTL mapping of the seed hardness trait in a black common bean (*Phaseolus vulgaris*) recombinant inbred line (RIL) population. *Molecular Breeding* 38, 1-13.
Sara, G., John, D.M., and Mccombie, W.R. (2016). Coming of age: ten years of next-generation sequencing technologies. *Nature Reviews Genetics* 17, 333.
Sasaki, A., Yamaji, N., Yokosho, K., and Ma, J.F. (2012). Nramp5 is a major transporter responsible for manganese and cadmium uptake in rice. *The Plant Cell* 24, 2155-2167.
Sax, K. (1923). The association of size differences with seed-coat pattern and pigmentation in *Phaseolus vulgaris*. *Genetics* 8, 552-560.
Schmidt, S.B., Jensen, P.E., and Husted, S. (2016). Manganese deficiency in plants: The impact on photosystem II. *Trends in Plant Science* 21, 622-632.
Schmutz, J., Mcclean, P.E., Mamidi, S., Wu, G.A., Cannon, S.B., Grimwood, J., Jenkins, J., Shu, S., Song, Q., Chavarro, C., Torres-Torres, M., Geffroy, V., Moghaddam, S.M., Gao, D., Abernathy, B., Barry, K., Blair, M., Brick, M.A., Chovatia, M., Gepts, P., Goodstein, D.M., Gonzales, M., Hellsten, U., Hyten, D.L., Jia, G., Kelly, J.D., Kudrna, D., Lee, R., Richard, M.M.S., Miklas, P.N., Osorno, J.M., Rodrigues, J., Thareau, V., Urrea, C.A., Wang, M., Yu, Y., Zhang, M., Wing, R.A., Cregan, P.B., Rokhsar, D.S., and Jackson, S.A. (2014). A reference genome for common bean and genome-wide analysis of dual domestications. *Nature Genetics* 46, 707-713.
Schneider, A., Steinberger, I., Herdean, A., Gandini, C., Eisenhut, M., Kurz, S., Morper, A., Hoecker, N., Rühle, T., Labs, M., Flügge, U.I., Geimer, S., Schmidt, S.B., Husted, S., Weber, A.P., Spetea, C., and Leister, D. (2016). The evolutionarily conserved protein photosynthesis affected *mutant71* is

required for efficient manganese uptake at the thylakoid membrane in Arabidopsis. *The Plant Cell* 28, 892-910.

Seaton, G., Haley, C.S., Knott, S.A., Kearsey, M., and Visscher, P.M. (2002). QTL express: mapping quantitative trait loci in simple and complex pedigrees. *Bioinformatics* 18, 339-340.

Sello, S., Moscatiello, R., Mehlmer, N., Leonardelli, M., Carraretto, L., Cortese, E., Zanella, F.G., Baldan, B., Szabò, I., Vothknecht, U.C., and Navazio, L. (2018). Chloroplast Ca^{2+} fluxes into and across thylakoids revealed by thylakoid-targeted Aequorin probes. *Plant Physiology* 177, 38-51.

Sertse, D., You, F.M., Ravichandran, S., and Cloutier, S. (2019a). The complex genetic architecture of early root and shoot traits in flax revealed by genome-wide association analyses. *Frontiers in Plant Science* 10.

Sertse, D., You, F.M., Ravichandran, S., and Cloutier, S. (2019b). The Complex Genetic Architecture of Early Root and Shoot Traits in Flax Revealed by Genome-Wide Association Analyses. *Front Plant Sci* 10, 1483.

Shao, J.F., Yamaji, N., Shen, R.F., and Ma, J.F. (2017). The key to Mn homeostasis in plants: regulation of Mn transporters. *Trends in Plant Science* 22, 215-224.

Shendure, J., Porreca, G.J., Reppas, N.B., Lin, X., Mccutcheon, J.P., Rosenbaum, A.M., Wang, M.D., Zhang, K., Mitra, R.D., and Church, G.M. (2005). Accurate multiplex polony sequencing of an evolved bacterial genome. *Science* 309, 1728-1732.

Shenker, M., Plessner, O.E., and Tel-Or, E. (2004). Manganese nutrition effects on tomato growth, chlorophyll concentration, and superoxide dismutase activity. *Journal of Plant Physiology* 161, 197-202.

Shi, H., Guan, W., Shi, Y., Wang, S., Fan, H., Yang, J., Chen, W., Zhang, W., Sun, D., and Jing, R. (2020). QTL mapping and candidate gene analysis of seed vigor-related traits during artificial aging in wheat (*Triticum aestivum*). *Scientific Reports* 10, 22060.

Shinozuka, H., Cogan, N.O.I., Spangenberg, G.C., and Forster, J.W. (2012). Quantitative trait locus (QTL) meta-analysis and comparative genomics for candidate gene prediction in perennial ryegrass (*Lolium perenne* L.). *BMC Genetics* 13, 101.

Singh, S.P., and Molina, A. (1996). Inheritance of crippled rrifoliolate leaves occurring in interracial crosses of common bean and its relationship with hybrid dwarfism. *Journal of Heredity* 87, 464-469.

Sofi, P. (2007). Implications of epistasis in maize breeding. *International Journal of Plant Breeding and Genetics* 1, 1-11.

Song, X.B., Zhao, X.G., Fan, G.X., Gao, K., Dai, S.L., Zhang, M.M., Ma, C.F., and Wu, X.Y. (2018). Genetic analysis of the corolla tube merged degree and the relative number of ray ﬡorets in chrysanthemum (*Chrysanthemum* × *morifoliumRamat.*). *Scientia Horticulturae* 242, 214–224.

Statistics Canada (2019). *Table 32-10-0007-01 stocks of grain and oilseeds at March 31, July 31 and December 31 (x 1,000)* [Online]. [Accessed].

Stephen, E.B., Idupulapati, M.R., Mura Jyostna, D., and José, P. (2014). Common beans, biodiversity, and multiple stresses: Challenges of drought resistance in tropical soils. *Crop Pasture Science* 65, 667-675.

Stolle, E., and Moritz, R.F.A. (2013). RESTseq - efficient benchtop population genomics with restriction fragment sequencing. *PLoS ONE* 8, e63960.

Su, J., Wang, C., Ma, Q., Zhang, A., Shi, C., Liu, J., Zhang, X., Yang, D., and Ma, X. (2020). An RTM-GWAS procedure reveals the QTL alleles and candidate genes for three yield-related traits in upland cotton. *BMC Plant Biology* 20, 416.

Sutter, N.B., Bustamante, C.D., Chase, K., Gray, M.M., Zhao, K., Zhu, L.,

Padhukasahasram, B., Karlins, E., Davis, S., Jones, P.G., Quignon, P., Johnson, G.S., Parker, H.G., Fretwell, N., Mosher, D.S., Lawler, D.F., Satyaraj, E., Nordborg, M., Lark, K.G., Wayne, R.K., and Ostrander, E.A. (2007). A single *IGF1* allele is a major determinant of small size in dogs. *Science* 316, 112-115.

Takemoto, Y., Tsunemitsu, Y., Fujii-Kashino, M., Mitani-Ueno, N., Yamaji, N., Ma, J.F., Kato, S.-I., Iwasaki, K., and Ueno, D. (2017). The tonoplast-localized transporter MTP8.2 contributes to manganese detoxification in the shoots and roots of *Oryza sativa* L. *Plant and Cell Physiology* 58, 1573-1582.

Thoday, J.M. (1961). Location of polygenes. *Nature* 191, 368-370.

Thomine, S., Lelièvre, F., Debarbieux, E., Schroeder, J.I., and Barbier-Brygoo, H. (2000). Cadmium and iron transport by members of a plant metal transporter family in *Arabidopsis* with homology to *Nramp* genes. *Proceedings of the National Academy of Sciences* 97, 4991-4996.

Thomine, S., Lelièvre, F., Debarbieux, E., Schroeder, J.I., and Barbier-Brygoo, H. (2003). AtNRAMP3, a multispecific vacuolar metal transporter involved in plant responses to iron deficiency. *The Plant Journal* 34, 685-695.

Ueno, D., Sasaki, A., Yamaji, N., Miyaji, T., Fujii, Y., Takemoto, Y., Moriyama, S., Che, J., Moriyama, Y., Iwasaki, K., and Ma, J.F. (2015). A polarly localized transporter for efficient manganese uptake in rice. *Nature Plants* 1, 15170.

Utz, H., and Melchinger, A. (Year). "PLABQTL: a program for composite interval mapping of QTL").

Van Laere, A.S., Nguyen, M., Braunschweig, M., Nezer, C., Collette, C., Moreau, L., Archibald, A.L., Haley, C.S., Buys, N., Tally, M., Andersson, G., Georges, M., and Andersson, L. (2003). A regulatory mutation in IGF2 causes a major QTL effect on muscle growth in the pig. *Nature* 425, 832-836.

Vert, G.G., Grotz, N., DéDaldéChamp, F., Gaymard, F.D.R., Guerinot, M.L., Briat, J.-F.O., and Curie, C. (2002). IRT1, an *Arabidopsis* transporter essential for iron uptake from the soil and for plant growth. *The Plant Cell* 14, 1223-1233.

Vlasova, A., Capella-Gutiérrez, S., Rendón-Anaya, M., Hernández-Oñate, M., Minoche, A., Erb, I., Câmara, F., Prieto-Barja, P., Corvelo, A., Sanseverino, W., Westergaard, G., Dohm, J., Pappas, G., Saburido-Alvarez, S., Kedra, D., and Gonzalez, I. (2016). Genome and transcriptome analysis of the Mesoamerican common bean and the role of gene duplications in establishing tissue and temporal specialization of genes. *Genome Biology* 17, 17-32.

Wang, D.L., Zhu, J., Li, Z.K.L., and Paterson, A.H. (1999). Mapping QTLs with epistatic effects and QTL×environment interactions by mixed linear model approaches. *Theoretical and Applied Genetics* 99, 1255-1264.

Wang, J., and Gai, J. (2001). Mixed inheritance model for resistance to agromyzid beanfly (*Melanagromyza sojae Zehntner*) in soybean. *Euphytica* 122, 9-18.

Wang, J., Li, H., Zhao, T., and Junyi, G. (2010). Establishment of segregation analysis of mixed inheritance model with four major genes plus polygenes in recombinant inbred lines population. *Acta Agronomica Sinica (China)* 36, 191-201.

Wang, J.K. (1996). *Identification of major polygene mixed inheritance of quantitative traits and estimation of genetic parameters of a quantitative trait from F_2 progeny.* PhD, Nanjing Agricultural University, China.

Wang, J.S., Zhao, T., and Gai, J.Y. (2013). Establishment of segregation analysis of mixed inheritance model with four major genes plus polygenes in backcross inbred lines (BIL) populations. *Acta Agronomica Sinica (China)* 39, 198-206

Wang, X., Zhong, F., Woo, C.H., Miao, Y., Grusak, M.A., Zhang, X., Tu, J., Wong, Y.S., and Jiang, L. (2017). A rapid and efficient method to study the function of crop plant transporters in *Arabidopsis*. *Protoplasma* 254, 737-747.

Waters, B.M., Chu, H.-H., Didonato, R.J., Roberts, L.A., Eisley, R.B., Lahner, B., Salt, D.E., and Walker, E.L. (2006). Mutations in *Arabidopsis* yellow stripe-like1 and yellow stripe-like3 reveal their roles in metal ion homeostasis and loading of metal ions in seeds. *Plant Physiology (Bethesda)* 141, 1446-1458.

Waters, B.M., and Sankaran, R.P. (2011). Moving micronutrients from the soil to the seeds: Genes and physiological processes from a biofortification perspective. *Plant Science (Limerick)* 180, 562-574.

Wei, B., Wang , L., Bosland, P.W., Zhang, G., and Zhang, R. (2020). A joint segregation analysis of the inheritance of fertility restoration for cytoplasmic male sterility in pepper. *Journal of the American Society for Horticultural Science* 145, 3-11.

Welch, R.M. (2002). Breeding strategies for biofortified staple plant foods to reduce micronutrient malnutrition globally. *The Journal of Nutrition* 132, 495S-499S.

Welch, R.M., and Graham, R.D. (1999). A new paradigm for world agriculture: meeting human needs: Productive, sustainable, nutritious. *Field Crops Research* 60, 1-10.

Wen, Y., Zhang, Y., Zhang, J., Feng, J.-Y., Dunwell, J.M., and Zhang, Y.-M. (2018). An efficient multi-locus mixed model framework for the detection of small and linked QTLs in F2. *Briefings in Bioinformatics* 20, 1913-1924.

Wilson, K.O.F.C.B.M.B.P.L.M.S.D.O. (1979). Critical manganese deficiency level of soybean related to leaf position. *Agronomy Journal* 71, 233-234.

Wu, D., Yamaji, N., Yamane, M., Kashino-Fujii, M., Sato, K., and Feng Ma, J. (2016). The *HvNramp5* transporter mediates uptake of cadmium and manganese, but not iron. *Plant Physiology (Bethesda)* 172, 1899-1910.

Wu, J., Yuan, Y.-X., Zhang, X.-W., Zhao, J., Song, X., Li, Y., Li, X., Sun, R., Koornneef, M., Aarts, M.G.M., and Wang, X.-W. (2008). Mapping QTLs for mineral accumulation and shoot dry biomass under different Zn nutritional conditions in Chinese cabbage (*Brassica rapa* L. ssp. pekinensis). *Plant and Soil* 310, 25-40.

Wu, R., Casella, G., and Ma, C. (2007). *Statistical Genetics of Quantitative Traits: Linkage, Maps, and QTL (Statistics for Biology and Health).* New York, NY: Springer-Verlag.

Yamada, K., Nagano, A.J., Nishina, M., Hara-Nishimura, I., and Nishimura, M. (2012). Identification of two novel endoplasmic reticulum body-specific integral membrane proteins *Plant Physiology* 161, 108-120.

Yamada, N., Theerawitaya, C., Cha-Um, S., Kirdmanee, C., and Takabe, T. (2014). Expression and functional analysis of putative vacuolar Ca^{2+} transporters (CAXs and ACAs) in roots of salt tolerant and sensitive rice cultivars. *Protoplasma* 251, 1067-1075.

Yamaji, N., Sasaki, A., Xia, J.X., Yokosho, K., and Ma, J.F. (2013). A node-based switch for preferential distribution of manganese in rice. *Nature Communications* 4, 2442.

Yang, J., Hu, C., Hu, H., Yu, R., Xia, Z., Ye, X., and Zhu, J. (2008). QTLNetwork: mapping and visualizing genetic architecture of complex traits in experimental populations. *Bioinformatics* 24, 721-723.

Yang, M., Zhang, W., Dong, H., Zhang, Y., Lv, K., Wang, D., and Lian, X. (2013). OsNRAMP3 is a vascular bundles-specific manganese transporter that is responsible for manganese distribution in rice. *PLoS ONE* 8, e83990.

Yang, M., Zhang, Y., Zhang, L., Hu, J., Zhang, X., Lu, K., Dong, H., Wang, D., Zhao, F.-J., Huang, C.-F., and Lian, X. (2014). OsNRAMP5 contributes to manganese translocation and distribution in rice shoots. *Journal of Experimental Botany* 65, 4849-4861.

Ye, Y.J., Wu, J.Y., Feng, L., Ju, Y.Q., Cai, M., Cheng, T.R., Pan, H.T., and Zhang,

Q.X. (2017). Heritability and gene effects for plant architecture traits of crapemyrtle using major gene plus polygene inheritance analysis. *Scientia Horticulturae* 225, 335–342.

You, F.M., and Cloutier, S. (2020). Mapping quantitative trait loci onto chromosome-scale pseudomolecules in flax. *Methods Protocols* 3, 28.

You, F.M., Deal, K.R., Wang, J., Britton, M.T., Fass, J.N., Lin, D., Dandekar, A.M., Leslie, C.A., Aradhya, M., Luo, M.C., and Dvorak, J. (2012). Genome-wide SNP discovery in walnut with an AGSNP pipeline updated for SNP discovery in allogamous organisms. *BMC Genomics* 13, 354.

You, F.M., Huo, N., Deal, K.R., Gu, Y.Q., Luo, M.C., Mcguire, P.E., Dvorak, J., and Anderson, O.D. (2011). Annotation-based genome-wide SNP discovery in the large and complex *Aegilops tauschii* genome using next-generation sequencing without a reference genome sequence. *BMC Genomics* 12, 59.

You, F.M., Xiao, J., Li, P., Yao, Z., Jia, G., He, L., Kumar, S., Soto-Cerda, B., Duguid, S.D., Booker, H.M., Rashid, K.Y., and Cloutier, S. (2018). Genome-wide association study and selection signatures detect genomic regions associated with seed yield and oil quality in flax. *International Journal of Molecular Sciences* 19, 2303.

Zeng, Z.B. (1994). Precision mapping of quantitative trait loci. *Genetics* 136, 1457-1468.

Zhang, J., and Madden, T.L. (1997). PowerBLAST: a new network BLAST application for interactive or automated sequence analysis and annotation. *Genome Research* 7, 649-656.

Zhang, L.W., Liu, P.W., Hong, D.F., Huang, A.Q., Li, S.P., He, Q.B., and Yang, G.S. (2010). Inheritance of seeds per silique in *Brassica napus* L. using joint segregation analysis. *Field Crops Research* 116, 58–67.

Zhang, Y., Gai, J., and Wang, Y. (2001). An expansion of joint segregation analysis of quantitative trait for using P1, P2 and DH or RIL populations. *Hereditas (Beijing)* 23, 467-470.

Zhang, Y., Gai, J., and Yang, Y. (2003a). The EIM algorithm in the joint segregation analysis of quantitative traits. *Genetical Research* 81, 157-163.

Zhang, Y., Gai, J.Y., and Wang, J.K. (2000). Identification of two major genes plus polygenes mixed inheritance model of quantitative traits in B1 and B2, and F2. *Journal of Mathematical Biology* 15, 358-366.

Zhang, Y., Junyi, G., and Yang, Y. (2003b). The EIM algorithm in the joint segregation analysis of quantitative traits. *Genetic Research (Cambridge)* 81, 157-163.

Zhang, Y., Xu, Y., Yi, H., and Gong, J. (2012). Vacuolar membrane transporters *OsVIT1* and *OsVIT2* modulate iron translocation between flag leaves and seeds in rice. *The Plant Journal* 72, 400-410.

Zhang, Y., Zhang, B.-Q., Gao, D.-R., and Cheng, S.-H. (2005). Analysis on genetic model of wheat scab resistant germplasm H35. *Journal of Triticeae Crops* 25, 39-43.

Zhang, Y.M., and Xu, S. (2005). A penalized maximum likelihood method for estimating epistatic effects of QTL. *Heredity* 95, 96-104.

Zhang, Y.W., Wen, Y.J., Dunwell, J.M., and Zhang, Y.M. (2020). QTL.gCIMapping.GUI v2.0: An R software for detecting small-effect and linked QTLs for quantitative traits in bi-parental segregation populations. *Computational and Structural Biotechnology Journal* 18, 59-65.

Zhu, M., and Zhao, S. (2007). Candidate gene identification approach: progress and challenges. *International Journal of Biological Sciences* 3, 420-427.

9. Appendix

Appendix 1 Mn transport proteins in plants

Family/name	Organ/tissue	Subcellular localization	Gene expression response	Other substrates	Reference
CaCA					
AtCAX2	Root, stem, leaf, flower and fruit	Tonoplast	Unaffect by +Mn	Ca, Cd	Hirschi et al. (2000);Pittman (2005);Edmond et al. (2009)
AtCAX4	Root, stem, leaf, flower and fruit	Tonoplast	Up-regulated by +Mn,+ Ni, and -Ca	Cd, Ca, Zn	Cheng et al. (2002);Mei et al. (2009)
AtCAX5	Root, stem, leaf, flower and fruit	Tonoplast	Up-regulated by +Mn; down-regulated by +Zn	Ca	Edmond et al. (2009)
HvCAX2	Root, leaf and seed		Up-regulated by +Ca and +Na	Ca	Edmond et al. (2009)
OsCAX1	Root, stem, leaf, flower and fruit	Tonoplast		Ca	Kamiya et al. (2006)
OsCAX3	Root, stem, leaf, flower and fruit		Up-regulated by +Ca	Ca	Kamiya et al. (2006)
OsCAX4	Root			Ca, Cu	Yamada et al. (2014)
AtCCX3	Root, stem, leaf and flower	Tonoplast and endomembrane	Up-regulated by +Na and +K	K, Na	Morris et al. (2008)
BICAT					

Family/name	Organ/tissue	Subcellular localization	Gene expression response	Other substrates	Reference
AtBICAT1/PAM71/CCHA1	Leaf	Chloroplast	Unaffect by +Mn	Ca	Schneider et al. (2016);Eisenhut et al. (2018);Frank et al. (2019)
AtBICAT2/CMT1	Root, stem, leaf, flower and fruit	Chloroplast	Down-regulated by +Mn	Ca, Mg	Eisenhut et al. (2018);Frank et al. (2019)
CDF/MTP					
AtMTP8	Root and seed		Up-regulated by +Mn and -Fe	Fe	Eroglu et al. (2016)
AtMTP9			Unaffect by +Mn		Delhaize et al. (2007);Chu et al. (2017)
AtMTP10			Unaffect by +Mn		Delhaize et al. (2007);Chu et al. (2017)
AtMTP11	Root (tips) and leaf(guard cells)		Unaffect by +Mn		Delhaize et al. (2007);Chu et al. (2017)
OsMTP8.1	Root and shoot				Chen et al. (2013);Takemoto et al. (2017)
OsMTP8.2	Root and shoot				Chen et al. (2013);Takemoto et al. (2017)
OsMTP9	Root	Plasma membrane	Unaffected by +Mn		Ueno et al. (2015)
OsMtP11	Root and shoot	Golgi	Up-regulated by +Mn, +Zn, +Cd and +Ni	Co, Ni	Ma et al. (2018)
HvMTP8.1	Root and leaf	Golgi	Down-regulated by -Mn (root); down-regulated by -Mn (shoot)		Pedas et al. (2008)
HvMTP8.2	Root and leaf	Golgi	Down-regulated by +Mn		Pedas et al. (2008)
NRAMP					
AtNRAMP1	Root (Cortex, endodermis) , shoot	Plasma membrane	Up-regulated by -Fe and -Mn	Cd, Fe	Curie et al. (2000);Thomine et al. (2003);Cailliatte et al.

Family/name	Organ/tissue	Subcellular localization	Gene expression response	Other substrates	Reference
					(2010);Castaings et al. (2016)
AtNRAMP2	Root (pericyclic, root tip), leaf vasculature, flower and trichrome	TGN	Up-regulated by –Mn; down-regulated by -Fe	–	Curie et al. (2000);Alejandro et al. (2017);Gao et al. (2018)
AtNRAMP3	Root (stele), leaf vasculature and developing seed	Tonoplast	Up-regulated by –Fe; unaffected by -Mn		Thomine et al. (2000);Lanquar et al. (2005);Lanquar et al. (2010)
AtNRAMP4	Root (stele), leaf vasculature and developing seed	Tonoplast	Up-regulated by –Fe; unaffected by -Mn		Thomine et al. (2000);Lanquar et al. (2005);Lanquar et al. (2010)
OsNRAMP3	Node and leaf vasculature	Plasma membrane	Unaffected by +Mn and -Mn		Yamaji et al. (2013);Yang et al. (2013)
OsNRAMP5	Root (exodermises and stele) and panicle	Plasma membrane	Up-regulated by -Fe (shoot); up-regulated by –Fe and -Zn (root); unaffected by -Mn	Cd, Fe	Sasaki et al. (2012);Yang et al. (2014);Peris-Peris et al. (2017)
OsNRAMP6	Leaves	Plasma membrane	–	Fe	Peris-Peris et al. (2017)
HvNRAMP5	Root (epidermis, stele)	Plasma membrane	Up-regulated by –Fe; unaffected by +Mn	Cd	Wu et al. (2016)
VIT					
AtVIT1	Root, cotyledon and developing seed	Tonoplast	–	Fe	Kim et al. (2006)
OsVIT1	Leaf , root, stem, panicle and embryo	Tonoplast	Down-regulated by -Fe	Fe, Zn	Zhang et al. (2012)
OsVIT2	Leaf, stem, panicle and embryo	Tonoplast	Up-regulated by +Fe; down-regulated by -Fe	Fe, Zn	Zhang et al. (2012);Wang et al. (2017)

Family/name	Organ/tissue	Subcellular localization	Gene expression response	Other substrates	Reference
TaVIT2	Root, shoot and seed	Tonoplast	–	Fe	Connorton et al. (2017b)
AtMEB1	–	ER bodies	–	Fe	Yamada et al. (2012)
AtMEB2	–	ER bodies	–	Fe	Yamada et al. (2012)
YSL					
OsYSL2	Root (phloem), leaf, vascular bundle and developing seed	Plasma membrane	Up-regulated by –Fe; down-regulated by -Mn	Fe	Koike et al. (2004)
OsYSL6	Root and shoot	Plasma membrane	Unaffected by +Mn and -Mn	–	Yang et al. (2014)
HvYSL2	Root (endodermis) and shoot	–	Up-regulated by -Fe	Fe, Zn, Co, Ni, Cu	Araki et al. (2011)
ZIP					
AtIRT1	Root (Cortex, endodermis) and shoot	Plasma membrane	Up-regulated by -Fe		Curie et al. (2000);Thomine et al. (2000);Vert et al. (2002)
AtZIP1	Root (stele) and leaf vasculature	Tonoplast	Up-regulated by -Fe -Zn (root); up-regulated by -Mn(shoot); down-regulated by -Zn (shoot)		Milner et al. (2012)
AtZIP2	Root (stele)	Plasma membrane	Up-regulated by -Fe	Fe, Zn	Milner et al. (2012)
AtZIP5	Root and shoot				Milner et al. (2012)
AtZIP6	Root and shoot			Cd, Fe, Zn	Milner et al. (2012)
AtZIP7	Root and shoot			Cd, Fe, Zn	Milner et al. (2012);Fu et al. (2017)
AtZIP9	Root and shoot				Milner et al. (2012)
HvIRT1	Root and seed	Plasma membrane	Up-regulated by –Fe and -Mn	Fe, Zn	Pedas et al. (2008)

+: excess; -: deficiency .

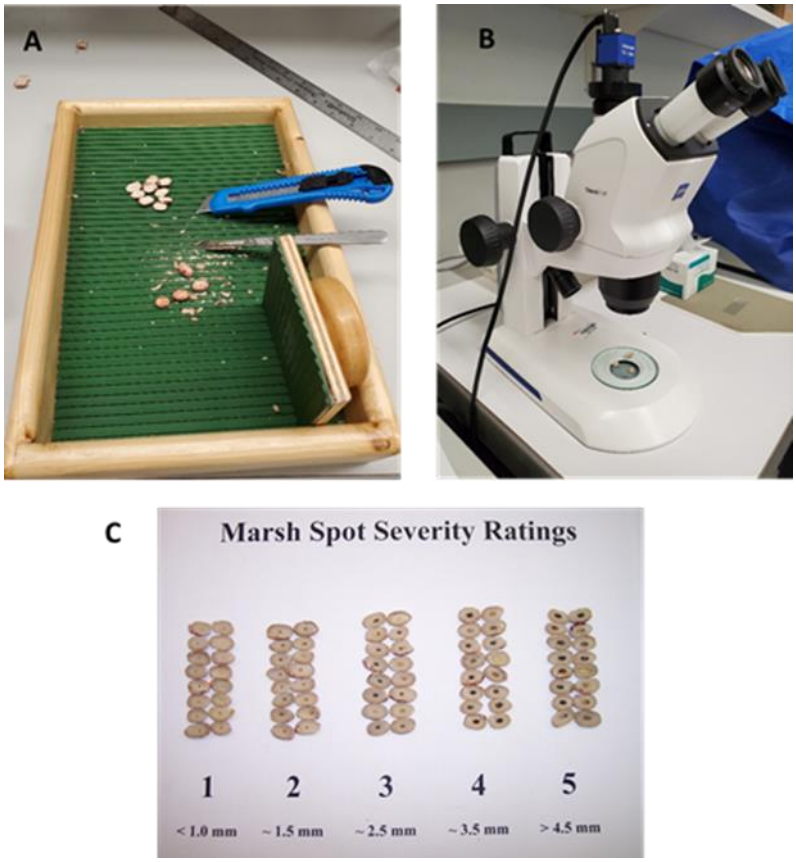

Appendix 2 A marsh sport severity scoring system for cranberry common bean. A. Seed splitting tools to shear the cotyledon halves. Knives can have also been used. B. Steroscope for the close-up photos. C. Marsh spot severity ratings of seeds of cranberry common bean. The numbers from 1 to 5, which indicate the marsh spot severity of the seeds, are related to the size of the discoloured brown spot at the center.

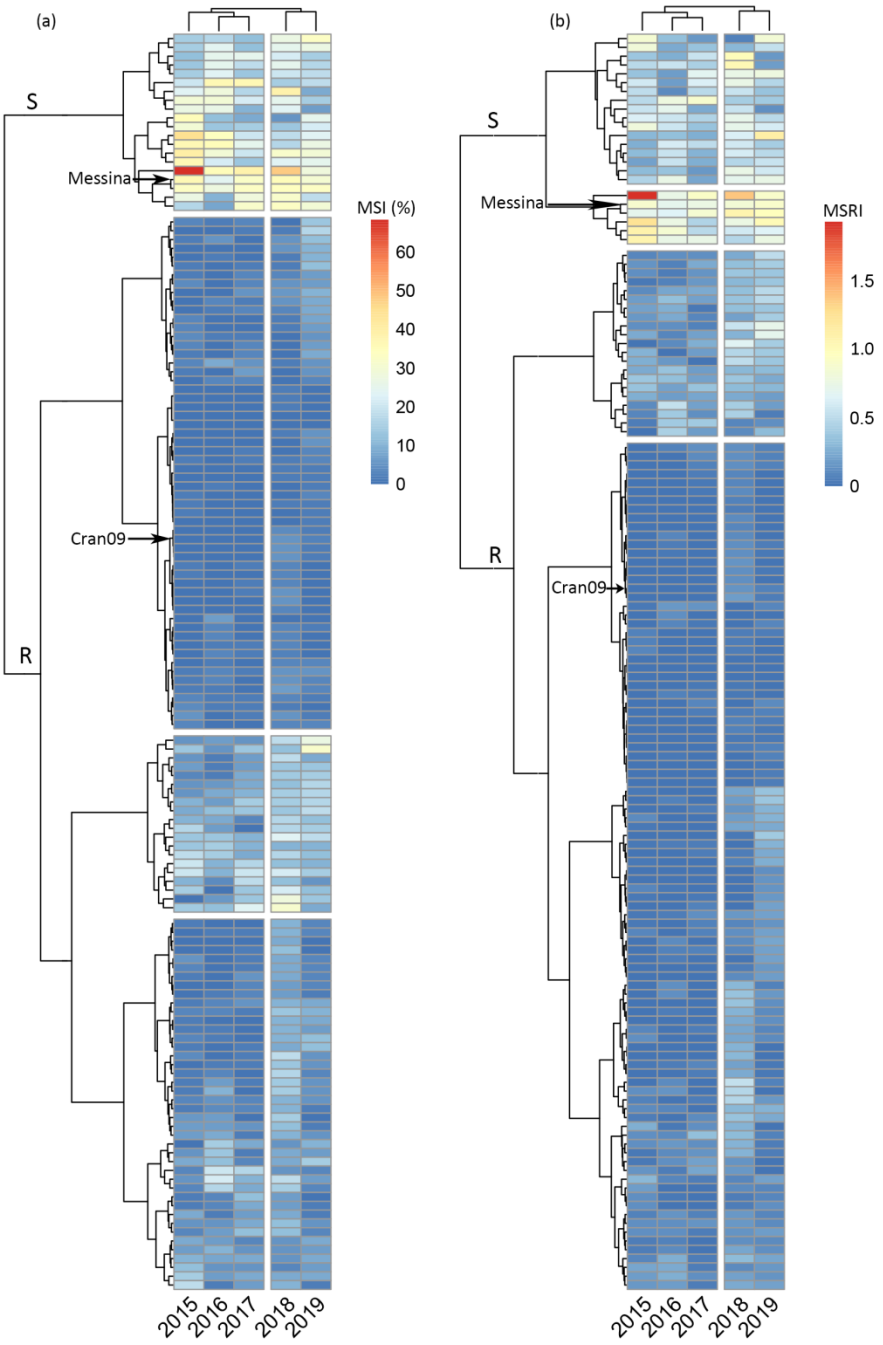

Appendix 3 Bidirectional cluster analysis of 138 RILs for marsh sport incidence (MSI) (a) and marsh spot resistance index (MSRI) (b). The mean values of two soil types were used in the cluster analysis. R refers to the resistance group, while S refers to the susceptible group. Each row in the heat map represents an RIL line.

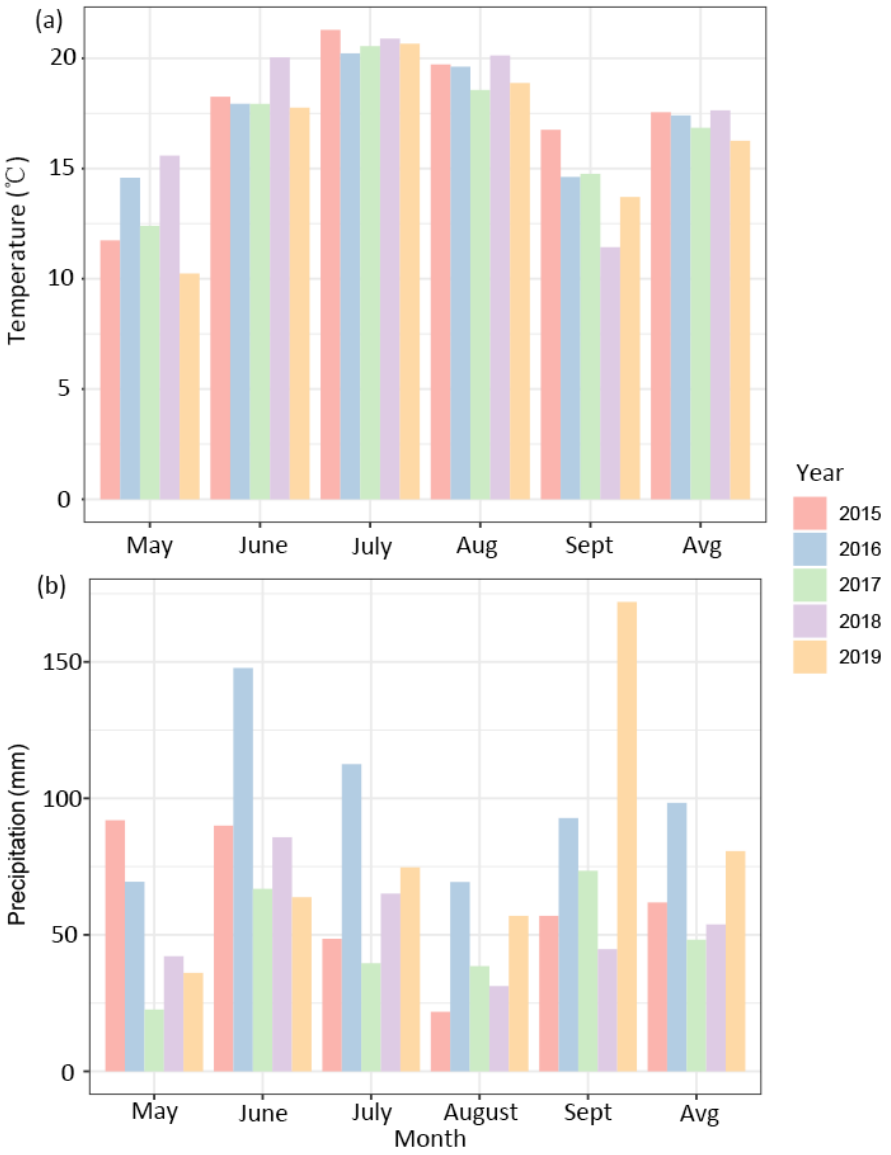

Appendix 4 Bar charts of temperature (a) and precipitation (b) in Morden, Manitoba, Canada, from May to September for five consecutive years from 2015 to 2019.

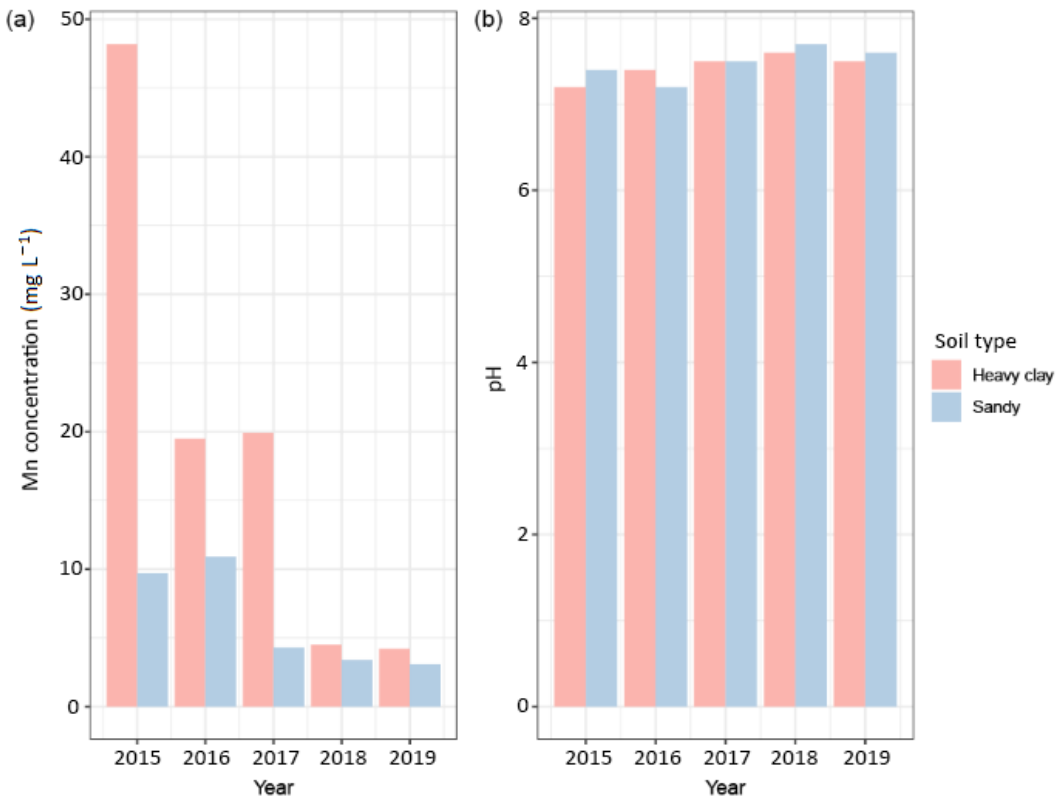

Appendix 5 Bar chart of Mn concentration (a) and pH values (b) of two soil types in Morden, Manitoba, Canada for five consecutive years from 2015 to 2019.

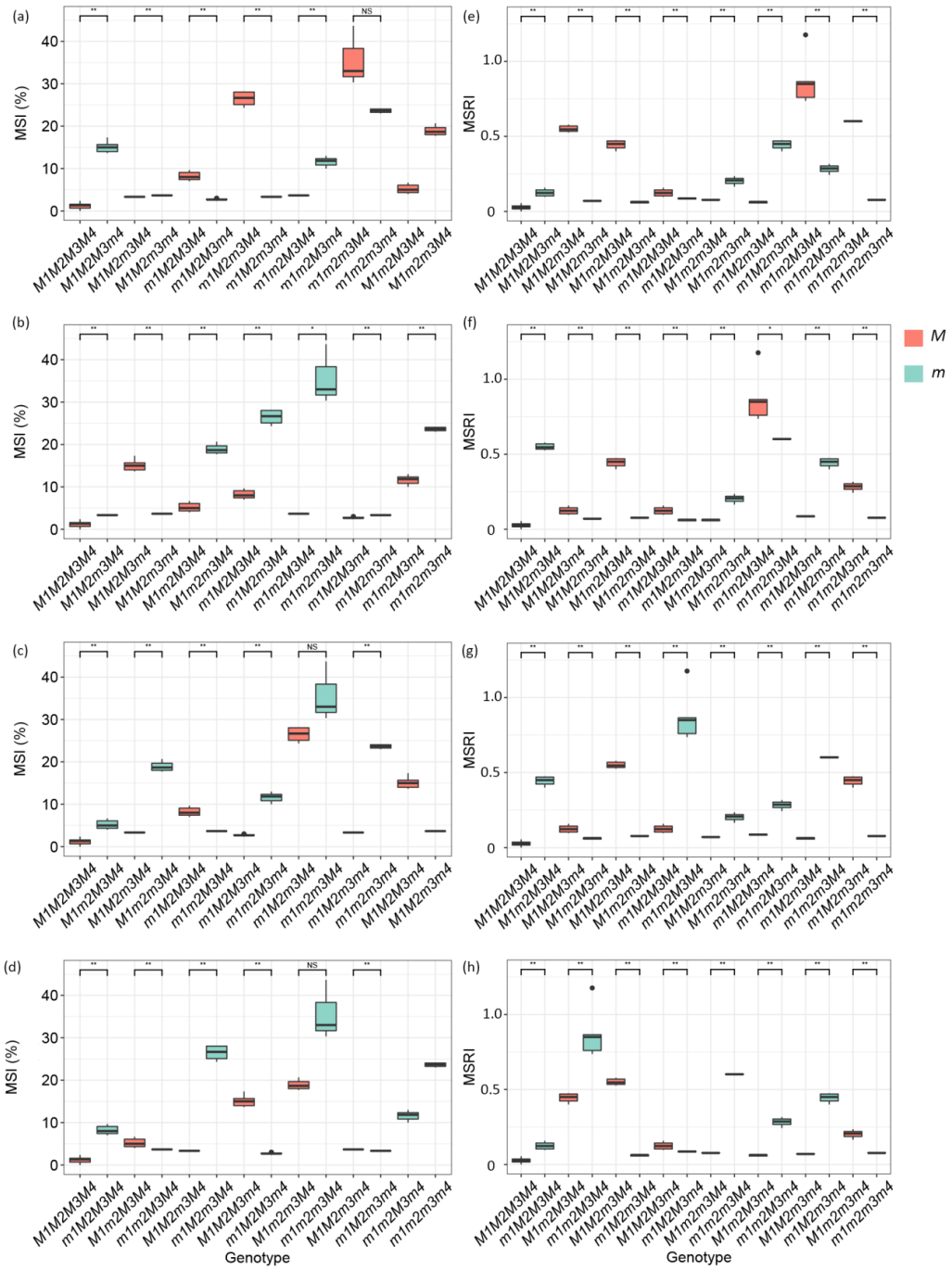

Appendix 6 Comparisons of allele effects of *M* and *m* for each of the four genes underlying the 4MG-AI model in the RIL population, i.e., *M1*(a), *M2* (b), *M3* (c) and *M4* (d) for marsh spot incidence (MSI, %) (left panels) and marsh spot resistance index (MSRI) (right panels). Each RIL was assigned a most likely genotype from the 16 possible combinations of four major genes based on the posterior probability estimated from the underlying genetic model. * and ** represent statistical significance at 5% and 1% probability levels, respectively. NS: not significant.

Appendix 7 Joint segregation analysis (JSA) results of marsh spot incidence (MSI) using 35 genetic models in 18 phenotypic. The data is accessible in Zenodo at https://zenodo.org/record/6574214 .

Appendix 8 Joint segregation analysis (JSA) results of marsh spot resistance index (MSRI) using 35 genetic models in 18 phenotypic datasets. The data is accessible in Zenodo at https://zenodo.org/record/6574214 .

Appendix 9 Posterior probability of 16 genotypes in the recombinant inbred line (RIL) population underlying the 4MG-AI model for marsh spot incidence (MSI).

Lines	*M1M2M3 M4*	*M1M2M3 m4*	*M1M2m3 m4*	*M1M2m3 M4*	*M1m2M3 M4*	*M1m2M3 m4*	*M1m2m3 m4*	*M1m2m3 M4*	*m1M2M3 M4*	*m1M2M3 m4*	*m1M2m3 m4*	*m1M2m3 M4*	*m1m2M3 M4*	*m1m2M3 m4*	*m1m2m3 m4*	*m1m2m3 M4*
X1307-2-1-1	0.13	0.00	0.10	0.11	0.10	0.11	0.11	0.00	0.00	0.12	0.11	0.00	0.10	0.00	0.00	0.00
X1307-2-1-2	0.14	0.00	0.10	0.11	0.10	0.11	0.11	0.00	0.00	0.12	0.11	0.00	0.10	0.00	0.00	0.00
X1307-2-1-3	0.11	0.00	0.11	0.11	0.11	0.11	0.11	0.00	0.01	0.11	0.11	0.00	0.11	0.01	0.00	0.00
X1307-2-1-4	0.14	0.00	0.10	0.11	0.10	0.11	0.11	0.00	0.00	0.12	0.11	0.00	0.10	0.00	0.00	0.00
X1307-2-1-5	0.07	0.00	0.11	0.10	0.11	0.10	0.10	0.00	0.05	0.10	0.11	0.00	0.11	0.04	0.00	0.00
X1307-2-2-1	0.09	0.00	0.11	0.11	0.11	0.11	0.11	0.00	0.02	0.11	0.11	0.00	0.11	0.01	0.00	0.00
X1307-2-2-2	0.10	0.00	0.11	0.11	0.11	0.11	0.11	0.00	0.01	0.11	0.11	0.00	0.11	0.01	0.00	0.00
X1307-2-2-3	0.06	0.00	0.11	0.10	0.11	0.09	0.10	0.00	0.07	0.09	0.10	0.00	0.11	0.06	0.00	0.00
X1307-2-2-4	0.00	0.00	0.00	0.00	0.00	0.00	0.00	0.00	0.00	0.00	0.00	0.18	0.00	0.00	0.09	0.73
X1307-2-2-5	0.00	0.31	0.00	0.00	0.00	0.00	0.00	0.16	0.24	0.00	0.00	0.00	0.00	0.26	0.00	0.00
X1307-3-1-1	0.00	0.45	0.00	0.00	0.00	0.00	0.00	0.33	0.09	0.00	0.00	0.01	0.00	0.10	0.02	0.00
X1307-3-1-2	0.00	0.14	0.01	0.01	0.02	0.01	0.01	0.05	0.35	0.01	0.01	0.00	0.01	0.36	0.00	0.00
X1307-3-1-3	0.00	0.00	0.00	0.00	0.00	0.00	0.00	0.00	0.00	0.00	0.00	0.00	0.00	0.00	0.00	1.00
X1307-3-1-4	0.00	0.01	0.00	0.00	0.00	0.00	0.00	0.05	0.00	0.00	0.00	0.47	0.00	0.00	0.41	0.06
X1307-3-1-5	0.07	0.00	0.11	0.10	0.11	0.10	0.10	0.00	0.05	0.10	0.11	0.00	0.11	0.04	0.00	0.00
X1307-3-2-1	0.08	0.00	0.11	0.11	0.11	0.11	0.11	0.00	0.03	0.10	0.11	0.00	0.11	0.02	0.00	0.00
X1307-3-2-2	0.08	0.00	0.11	0.11	0.11	0.10	0.10	0.00	0.03	0.10	0.11	0.00	0.11	0.03	0.00	0.00
X1307-3-2-3	0.09	0.00	0.11	0.11	0.11	0.11	0.11	0.00	0.02	0.11	0.11	0.00	0.11	0.01	0.00	0.00
X1307-3-2-4	0.01	0.02	0.05	0.04	0.06	0.04	0.04	0.01	0.30	0.03	0.04	0.00	0.05	0.30	0.00	0.00
X1307-3-2-5	0.00	0.20	0.01	0.01	0.01	0.01	0.01	0.09	0.32	0.00	0.01	0.00	0.01	0.34	0.00	0.00
X1307-4-1-1	0.13	0.00	0.10	0.11	0.10	0.11	0.11	0.00	0.00	0.12	0.11	0.00	0.10	0.00	0.00	0.00
X1307-4-1-2	0.07	0.00	0.11	0.10	0.11	0.10	0.10	0.00	0.04	0.10	0.11	0.00	0.11	0.03	0.00	0.00
X1307-4-1-3	0.14	0.00	0.10	0.11	0.10	0.11	0.11	0.00	0.00	0.12	0.11	0.00	0.10	0.00	0.00	0.00
X1307-4-1-4	0.00	0.17	0.01	0.01	0.01	0.01	0.01	0.07	0.34	0.01	0.01	0.00	0.01	0.35	0.00	0.00

Lines	*M1M2M3 M4*	*M1M2M3 m4*	*M1M2m3 m4*	*M1M2m3 M4*	*M1m2M3 M4*	*M1m2M3 m4*	*M1m2m3 m4*	*M1m2m3 M4*	*m1M2M3 M4*	*m1M2M3 m4*	*m1M2m3 m4*	*m1M2m3 M4*	*m1m2M3 M4*	*m1m2M3 m4*	*m1m2m3 m4*	*m1m2m3 M4*
X1307-4-1-5	0.08	0.00	0.11	0.11	0.11	0.11	0.11	0.00	0.03	0.10	0.11	0.00	0.11	0.02	0.00	0.00
X1307-4-2-1	0.13	0.00	0.10	0.11	0.10	0.11	0.11	0.00	0.00	0.12	0.11	0.00	0.10	0.00	0.00	0.00
X1307-4-2-2	0.10	0.00	0.11	0.11	0.11	0.11	0.11	0.00	0.01	0.11	0.11	0.00	0.11	0.01	0.00	0.00
X1307-4-2-3	0.00	0.40	0.00	0.00	0.00	0.00	0.00	0.43	0.02	0.00	0.00	0.04	0.00	0.02	0.09	0.00
X1307-4-2-4	0.15	0.00	0.10	0.11	0.09	0.11	0.11	0.00	0.00	0.12	0.11	0.00	0.10	0.00	0.00	0.00
X1307-4-2-5	0.15	0.00	0.10	0.11	0.09	0.11	0.11	0.00	0.00	0.12	0.11	0.00	0.10	0.00	0.00	0.00
X1307-5-1-1	0.05	0.00	0.11	0.09	0.11	0.09	0.09	0.00	0.08	0.09	0.10	0.00	0.11	0.08	0.00	0.00
X1307-5-1-2	0.15	0.00	0.10	0.11	0.09	0.11	0.11	0.00	0.00	0.12	0.11	0.00	0.10	0.00	0.00	0.00
X1307-5-1-5	0.05	0.00	0.11	0.09	0.11	0.09	0.09	0.00	0.08	0.09	0.10	0.00	0.11	0.08	0.00	0.00
X1307-5-2-1	0.11	0.00	0.11	0.11	0.11	0.11	0.11	0.00	0.01	0.11	0.11	0.00	0.11	0.01	0.00	0.00
X1307-5-2-2	0.13	0.00	0.10	0.11	0.10	0.11	0.11	0.00	0.00	0.12	0.11	0.00	0.10	0.00	0.00	0.00
X1307-5-2-3	0.15	0.00	0.10	0.11	0.09	0.11	0.11	0.00	0.00	0.12	0.11	0.00	0.10	0.00	0.00	0.00
X1307-5-2-4	0.09	0.00	0.11	0.11	0.11	0.11	0.11	0.00	0.02	0.11	0.11	0.00	0.11	0.02	0.00	0.00
X1307-5-2-5	0.14	0.00	0.10	0.11	0.10	0.11	0.11	0.00	0.00	0.12	0.11	0.00	0.10	0.00	0.00	0.00
X1307-6-1-1	0.03	0.01	0.08	0.06	0.08	0.06	0.06	0.00	0.21	0.06	0.07	0.00	0.08	0.20	0.00	0.00
X1307-6-1-2	0.00	0.20	0.00	0.00	0.00	0.00	0.00	0.34	0.00	0.00	0.00	0.18	0.00	0.00	0.28	0.00
X1307-6-1-3	0.04	0.00	0.09	0.08	0.10	0.07	0.07	0.00	0.16	0.07	0.08	0.00	0.09	0.15	0.00	0.00
X1307-6-1-5	0.09	0.00	0.11	0.11	0.11	0.11	0.11	0.00	0.02	0.11	0.11	0.00	0.11	0.02	0.00	0.00
X1307-6-2-1	0.01	0.03	0.05	0.03	0.05	0.03	0.03	0.01	0.32	0.03	0.04	0.00	0.05	0.32	0.00	0.00
X1307-6-2-3	0.08	0.00	0.11	0.11	0.11	0.10	0.11	0.00	0.03	0.10	0.11	0.00	0.11	0.03	0.00	0.00
X1307-6-2-4	0.00	0.17	0.01	0.01	0.01	0.01	0.01	0.07	0.34	0.01	0.01	0.00	0.01	0.35	0.00	0.00
X1307-6-2-5	0.13	0.00	0.10	0.11	0.10	0.11	0.11	0.00	0.00	0.12	0.11	0.00	0.10	0.00	0.00	0.00
X1307-7-1-1	0.14	0.00	0.10	0.11	0.10	0.11	0.11	0.00	0.00	0.12	0.11	0.00	0.10	0.00	0.00	0.00
X1307-7-1-2	0.12	0.00	0.10	0.11	0.10	0.11	0.11	0.00	0.01	0.11	0.11	0.00	0.10	0.00	0.00	0.00
X1307-7-1-3	0.05	0.00	0.11	0.09	0.11	0.09	0.09	0.00	0.08	0.09	0.10	0.00	0.11	0.08	0.00	0.00
X1307-7-1-4	0.11	0.00	0.11	0.11	0.11	0.11	0.11	0.00	0.01	0.11	0.11	0.00	0.11	0.01	0.00	0.00

Lines	*M1M2M3 M4*	*M1M2M3 m4*	*M1M2m3 m4*	*M1M2m3 M4*	*M1m2M3 M4*	*M1m2M3 m4*	*M1m2m3 m4*	*M1m2m3 M4*	*m1M2M3 M4*	*m1M2M3 m4*	*m1M2m3 m4*	*m1M2m3 M4*	*m1m2M3 M4*	*m1m2M3 m4*	*m1m2m3 m4*	*m1m2m3 M4*
X1307-7-2-1	0.01	0.04	0.04	0.03	0.04	0.03	0.03	0.01	0.34	0.02	0.03	0.00	0.04	0.34	0.00	0.00
X1307-7-2-2	0.09	0.00	0.11	0.11	0.11	0.11	0.11	0.00	0.02	0.11	0.11	0.00	0.11	0.02	0.00	0.00
X1307-7-2-3	0.01	0.07	0.03	0.02	0.03	0.02	0.02	0.02	0.36	0.02	0.02	0.00	0.03	0.36	0.00	0.00
X1307-7-2-4	0.11	0.00	0.11	0.11	0.11	0.11	0.11	0.00	0.01	0.11	0.11	0.00	0.11	0.01	0.00	0.00
X1307-7-2-5	0.15	0.00	0.10	0.11	0.09	0.11	0.11	0.00	0.00	0.12	0.11	0.00	0.10	0.00	0.00	0.00
X1307-8-1-1	0.09	0.00	0.11	0.11	0.11	0.11	0.11	0.00	0.02	0.11	0.11	0.00	0.11	0.02	0.00	0.00
X1307-8-1-2	0.07	0.00	0.11	0.10	0.11	0.10	0.10	0.00	0.05	0.10	0.11	0.00	0.11	0.04	0.00	0.00
X1307-8-1-3	0.11	0.00	0.11	0.11	0.10	0.11	0.11	0.00	0.01	0.11	0.11	0.00	0.11	0.01	0.00	0.00
X1307-8-1-4	0.00	0.29	0.00	0.00	0.00	0.00	0.00	0.40	0.00	0.00	0.00	0.11	0.00	0.00	0.20	0.00
X1307-8-1-5	0.00	0.00	0.00	0.00	0.00	0.00	0.00	0.01	0.00	0.00	0.00	0.40	0.00	0.00	0.25	0.35
X1307-8-2-1	0.00	0.17	0.01	0.01	0.01	0.01	0.01	0.07	0.34	0.01	0.01	0.00	0.01	0.35	0.00	0.00
X1307-8-2-2	0.04	0.00	0.10	0.09	0.10	0.08	0.09	0.00	0.12	0.08	0.09	0.00	0.10	0.11	0.00	0.00
X1307-8-2-3	0.11	0.00	0.11	0.11	0.11	0.11	0.11	0.00	0.01	0.11	0.11	0.00	0.11	0.01	0.00	0.00
X1307-8-2-4	0.00	0.42	0.00	0.00	0.00	0.00	0.00	0.27	0.13	0.00	0.00	0.00	0.00	0.15	0.01	0.00
X1307-8-2-5	0.02	0.02	0.06	0.05	0.06	0.04	0.04	0.00	0.28	0.04	0.05	0.00	0.06	0.28	0.00	0.00
X1307-8-3-1	0.00	0.40	0.00	0.00	0.00	0.00	0.00	0.43	0.02	0.00	0.00	0.04	0.00	0.02	0.09	0.00
X1307-8-3-2	0.02	0.02	0.06	0.05	0.06	0.04	0.04	0.00	0.28	0.04	0.05	0.00	0.06	0.28	0.00	0.00
X1307-8-3-3	0.10	0.00	0.11	0.11	0.11	0.11	0.11	0.00	0.01	0.11	0.11	0.00	0.11	0.01	0.00	0.00
X1307-8-3-5	0.06	0.00	0.11	0.10	0.11	0.10	0.10	0.00	0.06	0.09	0.10	0.00	0.11	0.05	0.00	0.00
X1308-2-1-1	0.08	0.00	0.11	0.11	0.11	0.10	0.11	0.00	0.03	0.10	0.11	0.00	0.11	0.03	0.00	0.00
X1308-2-1-2	0.00	0.05	0.00	0.00	0.00	0.00	0.00	0.13	0.00	0.00	0.00	0.38	0.00	0.00	0.42	0.01
X1308-2-1-3	0.11	0.00	0.11	0.11	0.11	0.11	0.11	0.00	0.01	0.11	0.11	0.00	0.11	0.01	0.00	0.00
X1308-2-1-4	0.00	0.03	0.00	0.00	0.00	0.00	0.00	0.08	0.00	0.00	0.00	0.44	0.00	0.00	0.43	0.03
X1308-2-1-5	0.00	0.31	0.00	0.00	0.00	0.00	0.00	0.41	0.00	0.00	0.00	0.10	0.00	0.01	0.17	0.00
X1308-2-1-6	0.12	0.00	0.10	0.11	0.10	0.11	0.11	0.00	0.01	0.12	0.11	0.00	0.10	0.00	0.00	0.00
X1308-2-1-7	0.11	0.00	0.11	0.11	0.10	0.11	0.11	0.00	0.01	0.11	0.11	0.00	0.11	0.01	0.00	0.00

Lines	*M1M2M3 M4*	*M1M2M3 m4*	*M1M2m3 m4*	*M1M2m3 M4*	*M1m2M3 M4*	*M1m2M3 m4*	*M1m2m3 m4*	*M1m2m3 M4*	*m1M2M3 M4*	*m1M2M3 m4*	*m1M2m3 m4*	*m1M2m3 M4*	*m1m2M3 M4*	*m1m2M3 m4*	*m1m2m3 m4*	*m1m2m3 M4*
X1308-4-1-2	0.10	0.00	0.11	0.11	0.11	0.11	0.11	0.00	0.01	0.11	0.11	0.00	0.11	0.01	0.00	0.00
X1308-4-1-3	0.13	0.00	0.10	0.11	0.10	0.11	0.11	0.00	0.00	0.12	0.11	0.00	0.10	0.00	0.00	0.00
X1308-4-1-4	0.10	0.00	0.11	0.11	0.11	0.11	0.11	0.00	0.01	0.11	0.11	0.00	0.11	0.01	0.00	0.00
X1308-4-1-5	0.15	0.00	0.10	0.11	0.09	0.11	0.11	0.00	0.00	0.12	0.11	0.00	0.10	0.00	0.00	0.00
X1308-4-1-6	0.04	0.00	0.10	0.09	0.10	0.08	0.09	0.00	0.12	0.08	0.09	0.00	0.10	0.11	0.00	0.00
X1308-4-1-7	0.10	0.00	0.11	0.11	0.11	0.11	0.11	0.00	0.01	0.11	0.11	0.00	0.11	0.01	0.00	0.00
X1308-5-1-1	0.13	0.00	0.10	0.11	0.10	0.11	0.11	0.00	0.00	0.12	0.11	0.00	0.10	0.00	0.00	0.00
X1308-5-1-2	0.08	0.00	0.11	0.11	0.11	0.11	0.11	0.00	0.03	0.10	0.11	0.00	0.11	0.02	0.00	0.00
X1308-5-1-3	0.00	0.03	0.00	0.00	0.00	0.00	0.00	0.10	0.00	0.00	0.00	0.42	0.00	0.00	0.43	0.02
X1308-5-1-4	0.10	0.00	0.11	0.11	0.11	0.11	0.11	0.00	0.01	0.11	0.11	0.00	0.11	0.01	0.00	0.00
X1308-5-1-5	0.05	0.00	0.10	0.09	0.11	0.09	0.09	0.00	0.10	0.08	0.09	0.00	0.11	0.09	0.00	0.00
X1308-5-1-6	0.11	0.00	0.11	0.11	0.11	0.11	0.11	0.00	0.01	0.11	0.11	0.00	0.11	0.01	0.00	0.00
X1308-5-1-7	0.00	0.03	0.00	0.00	0.00	0.00	0.00	0.09	0.00	0.00	0.00	0.43	0.00	0.00	0.43	0.02
X1308-5-2-3	0.04	0.00	0.10	0.08	0.10	0.08	0.08	0.00	0.14	0.07	0.09	0.00	0.10	0.13	0.00	0.00
X1308-5-2-4	0.13	0.00	0.10	0.11	0.10	0.11	0.11	0.00	0.00	0.12	0.11	0.00	0.10	0.00	0.00	0.00
X1308-5-2-5	0.08	0.00	0.11	0.11	0.11	0.10	0.11	0.00	0.03	0.10	0.11	0.00	0.11	0.03	0.00	0.00
X1308-5-2-6	0.16	0.00	0.09	0.11	0.09	0.11	0.11	0.00	0.00	0.12	0.11	0.00	0.09	0.00	0.00	0.00
X1308-5-2-7	0.00	0.00	0.00	0.00	0.00	0.00	0.00	0.00	0.00	0.00	0.00	0.04	0.00	0.00	0.01	0.95
X1308-6-1-1	0.01	0.03	0.05	0.03	0.05	0.03	0.03	0.01	0.32	0.03	0.04	0.00	0.05	0.32	0.00	0.00
X1308-6-1-2	0.00	0.00	0.00	0.00	0.00	0.00	0.00	0.01	0.00	0.00	0.00	0.41	0.00	0.00	0.26	0.32
X1308-6-1-3	0.00	0.11	0.02	0.01	0.02	0.01	0.01	0.04	0.36	0.01	0.01	0.00	0.02	0.37	0.00	0.00
X1308-6-1-4	0.09	0.00	0.11	0.11	0.11	0.11	0.11	0.00	0.02	0.11	0.11	0.00	0.11	0.02	0.00	0.00
X1308-6-1-5	0.02	0.02	0.06	0.05	0.06	0.04	0.04	0.00	0.28	0.04	0.05	0.00	0.06	0.28	0.00	0.00
X1308-6-1-6	0.09	0.00	0.11	0.11	0.11	0.11	0.11	0.00	0.02	0.11	0.11	0.00	0.11	0.01	0.00	0.00
X1308-6-1-7	0.11	0.00	0.11	0.11	0.11	0.11	0.11	0.00	0.01	0.11	0.11	0.00	0.11	0.01	0.00	0.00
X1308-7-1-1	0.15	0.00	0.10	0.11	0.09	0.11	0.11	0.00	0.00	0.12	0.11	0.00	0.10	0.00	0.00	0.00

Lines	*M1M2M3 M4*	*M1M2M3 m4*	*M1M2m3 m4*	*M1M2m3 M4*	*M1m2M3 M4*	*M1m2M3 m4*	*M1m2m3 m4*	*M1m2m3 M4*	*m1M2M3 M4*	*m1M2M3 m4*	*m1M2m3 m4*	*m1M2m3 M4*	*m1m2M3 M4*	*m1m2M3 m4*	*m1m2m3 m4*	*m1m2m3 M4*
X1308-7-1-2	0.13	0.00	0.10	0.11	0.10	0.11	0.11	0.00	0.00	0.12	0.11	0.00	0.10	0.00	0.00	0.00
X1308-7-1-3	0.00	0.36	0.00	0.00	0.00	0.00	0.00	0.43	0.01	0.00	0.00	0.07	0.00	0.01	0.13	0.00
X1308-7-1-4	0.05	0.00	0.11	0.09	0.11	0.09	0.09	0.00	0.08	0.09	0.10	0.00	0.11	0.08	0.00	0.00
X1308-7-1-5	0.13	0.00	0.10	0.11	0.10	0.11	0.11	0.00	0.00	0.12	0.11	0.00	0.10	0.00	0.00	0.00
X1308-7-1-6	0.04	0.00	0.10	0.09	0.10	0.08	0.09	0.00	0.12	0.08	0.09	0.00	0.10	0.11	0.00	0.00
X1308-7-1-7	0.00	0.42	0.00	0.00	0.00	0.00	0.00	0.42	0.02	0.00	0.00	0.04	0.00	0.02	0.08	0.00
X1308-7-2-1	0.00	0.38	0.00	0.00	0.00	0.00	0.00	0.43	0.01	0.00	0.00	0.05	0.00	0.01	0.11	0.00
X1308-7-2-2	0.04	0.00	0.09	0.08	0.10	0.07	0.07	0.00	0.16	0.07	0.08	0.00	0.09	0.15	0.00	0.00
X1308-7-2-3	0.00	0.23	0.01	0.00	0.01	0.00	0.00	0.11	0.30	0.00	0.01	0.00	0.01	0.31	0.00	0.00
X1308-7-2-4	0.13	0.00	0.10	0.11	0.10	0.11	0.11	0.00	0.00	0.12	0.11	0.00	0.10	0.00	0.00	0.00
X1308-7-2-5	0.00	0.06	0.00	0.00	0.00	0.00	0.00	0.15	0.00	0.00	0.00	0.36	0.00	0.00	0.41	0.01
X1308-7-2-6	0.00	0.44	0.00	0.00	0.00	0.00	0.00	0.41	0.03	0.00	0.00	0.03	0.00	0.03	0.06	0.00
X1308-7-2-7	0.01	0.07	0.03	0.02	0.03	0.02	0.02	0.02	0.36	0.02	0.02	0.00	0.03	0.36	0.00	0.00
X1308-8-1-1	0.03	0.01	0.08	0.06	0.08	0.06	0.06	0.00	0.21	0.06	0.07	0.00	0.08	0.20	0.00	0.00
X1308-8-1-3	0.13	0.00	0.10	0.11	0.10	0.11	0.11	0.00	0.00	0.12	0.11	0.00	0.10	0.00	0.00	0.00
X1308-8-1-4	0.14	0.00	0.10	0.11	0.10	0.11	0.11	0.00	0.00	0.12	0.11	0.00	0.10	0.00	0.00	0.00
X1308-8-1-6	0.15	0.00	0.10	0.11	0.09	0.11	0.11	0.00	0.00	0.12	0.11	0.00	0.10	0.00	0.00	0.00
X1308-8-1-7	0.13	0.00	0.10	0.11	0.10	0.11	0.11	0.00	0.00	0.12	0.11	0.00	0.10	0.00	0.00	0.00
X1308-8-2-1	0.11	0.00	0.11	0.11	0.11	0.11	0.11	0.00	0.01	0.11	0.11	0.00	0.11	0.01	0.00	0.00
X1308-8-2-2	0.03	0.00	0.09	0.07	0.09	0.07	0.07	0.00	0.18	0.06	0.07	0.00	0.09	0.17	0.00	0.00
X1308-8-2-3	0.14	0.00	0.10	0.11	0.10	0.11	0.11	0.00	0.00	0.12	0.11	0.00	0.10	0.00	0.00	0.00
X1308-8-2-4	0.00	0.34	0.00	0.00	0.00	0.00	0.00	0.19	0.22	0.00	0.00	0.00	0.00	0.23	0.01	0.00
X1308-8-2-6	0.11	0.00	0.11	0.11	0.10	0.11	0.11	0.00	0.01	0.11	0.11	0.00	0.11	0.01	0.00	0.00
X1308-8-3-1	0.05	0.00	0.11	0.09	0.11	0.09	0.09	0.00	0.08	0.09	0.10	0.00	0.11	0.08	0.00	0.00
X1308-8-3-2	0.06	0.00	0.11	0.10	0.11	0.10	0.10	0.00	0.06	0.09	0.10	0.00	0.11	0.05	0.00	0.00
X1308-8-3-4	0.08	0.00	0.11	0.11	0.11	0.11	0.11	0.00	0.03	0.10	0.11	0.00	0.11	0.02	0.00	0.00

Lines	*M1M2M3 M4*	*M1M2M3 m4*	*M1M2m3 m4*	*M1M2m3 M4*	*M1m2M3 M4*	*M1m2M3 m4*	*M1m2m3 m4*	*M1m2m3 M4*	*m1M2M3 M4*	*m1M2M3 m4*	*m1M2m3 m4*	*m1M2m3 M4*	*m1m2M3 M4*	*m1m2M3 m4*	*m1m2m3 m4*	*m1m2m3 M4*
X1308-8-3-5	0.13	0.00	0.10	0.11	0.10	0.11	0.11	0.00	0.00	0.12	0.11	0.00	0.10	0.00	0.00	0.00
X1308-8-3-6	0.11	0.00	0.11	0.11	0.11	0.11	0.11	0.00	0.01	0.11	0.11	0.00	0.11	0.01	0.00	0.00
X1308-8-3-7	0.03	0.00	0.09	0.07	0.09	0.07	0.07	0.00	0.18	0.06	0.07	0.00	0.09	0.17	0.00	0.00
X1308-8-4-1	0.12	0.00	0.10	0.11	0.10	0.11	0.11	0.00	0.01	0.11	0.11	0.00	0.10	0.00	0.00	0.00
X1308-8-4-2	0.06	0.00	0.11	0.10	0.11	0.09	0.09	0.00	0.07	0.09	0.10	0.00	0.11	0.07	0.00	0.00
X1308-8-4-3	0.15	0.00	0.10	0.11	0.09	0.11	0.11	0.00	0.00	0.12	0.11	0.00	0.10	0.00	0.00	0.00
X1308-8-4-4	0.00	0.22	0.00	0.00	0.00	0.00	0.00	0.35	0.00	0.00	0.00	0.17	0.00	0.00	0.26	0.00
X1308-8-4-5	0.11	0.00	0.11	0.11	0.10	0.11	0.11	0.00	0.01	0.11	0.11	0.00	0.11	0.01	0.00	0.00
X1308-8-4-6	0.16	0.00	0.09	0.11	0.09	0.11	0.11	0.00	0.00	0.12	0.11	0.00	0.09	0.00	0.00	0.00
X1308-8-4-7	0.10	0.00	0.11	0.11	0.11	0.11	0.11	0.00	0.01	0.11	0.11	0.00	0.11	0.01	0.00	0.00

Appendix 10 Posterior probability of 16 genotypes in the recombinant inbred line (RIL) population underlying the 4MG-AI model for marsh spot resistance index (MSRI).

Lines	*M1M2M3 M4*	*M1M2M3 m4*	*M1M2m3 m4*	*M1M2m3 M4*	*M1m2M3 M4*	*M1m2M3 m4*	*M1m2m3 m4*	*M1m2m3 M4*	*m1M2M3 M4*	*m1M2M3 m4*	*m1M2m3 m4*	*m1M2m3 M4*	*m1m2M3 M4*	*m1m2M3 m4*	*m1m2m3 m4*	*m1m2m3 M4*
X1307-2-1-1	0.14	0.00	0.01	0.11	0.09	0.12	0.11	0.00	0.09	0.12	0.11	0.00	0.10	0.00	0.00	0.00
X1307-2-1-2	0.13	0.00	0.01	0.11	0.09	0.12	0.11	0.00	0.09	0.12	0.11	0.00	0.10	0.00	0.00	0.00
X1307-2-1-3	0.10	0.00	0.02	0.11	0.11	0.11	0.11	0.00	0.11	0.11	0.11	0.00	0.11	0.01	0.00	0.00
X1307-2-1-4	0.13	0.00	0.01	0.11	0.09	0.12	0.11	0.00	0.09	0.12	0.11	0.00	0.10	0.00	0.00	0.00
X1307-2-1-5	0.08	0.00	0.04	0.10	0.11	0.10	0.11	0.00	0.11	0.10	0.11	0.00	0.11	0.02	0.00	0.00
X1307-2-2-1	0.10	0.00	0.03	0.11	0.11	0.11	0.11	0.00	0.11	0.11	0.11	0.00	0.11	0.01	0.00	0.00
X1307-2-2-2	0.11	0.00	0.02	0.11	0.10	0.11	0.11	0.00	0.10	0.11	0.11	0.00	0.11	0.01	0.00	0.00
X1307-2-2-3	0.08	0.00	0.06	0.10	0.12	0.10	0.10	0.00	0.12	0.10	0.10	0.00	0.11	0.03	0.00	0.00
X1307-2-2-4	0.00	0.00	0.00	0.00	0.00	0.00	0.00	0.00	0.00	0.00	0.00	0.00	0.00	0.00	0.02	0.98
X1307-2-2-5	0.00	0.00	0.32	0.01	0.02	0.01	0.01	0.04	0.02	0.01	0.01	0.04	0.01	0.49	0.00	0.00
X1307-3-1-1	0.00	0.13	0.01	0.00	0.00	0.00	0.00	0.40	0.00	0.00	0.00	0.40	0.00	0.04	0.03	0.00
X1307-3-1-2	0.00	0.00	0.34	0.01	0.03	0.01	0.01	0.02	0.03	0.01	0.01	0.02	0.02	0.47	0.00	0.00
X1307-3-1-3	0.00	0.00	0.00	0.00	0.00	0.00	0.00	0.00	0.00	0.00	0.00	0.00	0.00	0.00	0.00	1.00
X1307-3-1-4	0.00	0.35	0.00	0.00	0.00	0.00	0.00	0.14	0.00	0.00	0.00	0.14	0.00	0.00	0.36	0.01
X1307-3-1-5	0.08	0.00	0.05	0.10	0.12	0.10	0.10	0.00	0.12	0.10	0.10	0.00	0.11	0.02	0.00	0.00
X1307-3-2-1	0.10	0.00	0.03	0.11	0.11	0.11	0.11	0.00	0.11	0.11	0.11	0.00	0.11	0.01	0.00	0.00
X1307-3-2-2	0.09	0.00	0.04	0.11	0.11	0.10	0.11	0.00	0.11	0.10	0.11	0.00	0.11	0.02	0.00	0.00
X1307-3-2-3	0.11	0.00	0.02	0.11	0.10	0.11	0.11	0.00	0.10	0.11	0.11	0.00	0.11	0.01	0.00	0.00
X1307-3-2-4	0.03	0.00	0.25	0.05	0.09	0.05	0.06	0.00	0.09	0.05	0.06	0.00	0.07	0.22	0.00	0.00
X1307-3-2-5	0.01	0.00	0.32	0.03	0.06	0.03	0.04	0.00	0.06	0.03	0.04	0.00	0.05	0.33	0.00	0.00
X1307-4-1-1	0.12	0.00	0.01	0.11	0.09	0.12	0.11	0.00	0.09	0.12	0.11	0.00	0.11	0.00	0.00	0.00
X1307-4-1-2	0.06	0.00	0.09	0.09	0.12	0.09	0.10	0.00	0.12	0.09	0.10	0.00	0.11	0.05	0.00	0.00
X1307-4-1-3	0.13	0.00	0.01	0.11	0.09	0.12	0.11	0.00	0.09	0.12	0.11	0.00	0.10	0.00	0.00	0.00
X1307-4-1-4	0.00	0.01	0.30	0.01	0.02	0.00	0.01	0.07	0.02	0.00	0.01	0.07	0.01	0.49	0.00	0.00

Lines	*M1M2M3 M4*	*M1M2M3 m4*	*M1M2m3 m4*	*M1M2m3 M4*	*M1m2M3 M4*	*M1m2M3 m4*	*M1m2m3 m4*	*M1m2m3 M4*	*m1M2M3 M4*	*m1M2M3 m4*	*m1M2m3 m4*	*m1M2m3 M4*	*m1m2M3 M4*	*m1m2M3 m4*	*m1m2m3 m4*	*m1m2m3 M4*
X1307-4-1-5	0.10	0.00	0.03	0.11	0.11	0.11	0.11	0.00	0.11	0.11	0.11	0.00	0.11	0.01	0.00	0.00
X1307-4-2-1	0.13	0.00	0.01	0.11	0.09	0.12	0.11	0.00	0.09	0.12	0.11	0.00	0.10	0.00	0.00	0.00
X1307-4-2-2	0.09	0.00	0.04	0.11	0.11	0.10	0.11	0.00	0.11	0.10	0.11	0.00	0.11	0.02	0.00	0.00
X1307-4-2-3	0.00	0.19	0.00	0.00	0.00	0.00	0.00	0.37	0.00	0.00	0.00	0.37	0.00	0.01	0.06	0.00
X1307-4-2-4	0.14	0.00	0.01	0.11	0.08	0.12	0.11	0.00	0.08	0.12	0.11	0.00	0.10	0.00	0.00	0.00
X1307-4-2-5	0.14	0.00	0.01	0.11	0.08	0.12	0.11	0.00	0.08	0.12	0.11	0.00	0.10	0.00	0.00	0.00
X1307-5-1-1	0.06	0.00	0.11	0.09	0.12	0.08	0.09	0.00	0.12	0.08	0.09	0.00	0.10	0.07	0.00	0.00
X1307-5-1-2	0.14	0.00	0.01	0.11	0.08	0.12	0.11	0.00	0.08	0.12	0.11	0.00	0.10	0.00	0.00	0.00
X1307-5-1-5	0.06	0.00	0.10	0.09	0.12	0.08	0.09	0.00	0.12	0.08	0.09	0.00	0.10	0.06	0.00	0.00
X1307-5-2-1	0.12	0.00	0.01	0.11	0.10	0.11	0.11	0.00	0.10	0.11	0.11	0.00	0.11	0.00	0.00	0.00
X1307-5-2-2	0.13	0.00	0.01	0.11	0.09	0.12	0.11	0.00	0.09	0.12	0.11	0.00	0.10	0.00	0.00	0.00
X1307-5-2-3	0.15	0.00	0.00	0.11	0.08	0.12	0.11	0.00	0.08	0.12	0.11	0.00	0.10	0.00	0.00	0.00
X1307-5-2-4	0.09	0.00	0.03	0.11	0.11	0.10	0.11	0.00	0.11	0.10	0.11	0.00	0.11	0.01	0.00	0.00
X1307-5-2-5	0.13	0.00	0.01	0.11	0.09	0.12	0.11	0.00	0.09	0.12	0.11	0.00	0.10	0.00	0.00	0.00
X1307-6-1-1	0.03	0.00	0.21	0.07	0.10	0.06	0.07	0.00	0.10	0.06	0.07	0.00	0.08	0.16	0.00	0.00
X1307-6-1-2	0.00	0.30	0.00	0.00	0.00	0.00	0.00	0.26	0.00	0.00	0.00	0.26	0.00	0.00	0.17	0.00
X1307-6-1-3	0.03	0.00	0.24	0.06	0.09	0.05	0.06	0.00	0.09	0.05	0.06	0.00	0.07	0.19	0.00	0.00
X1307-6-1-5	0.10	0.00	0.03	0.11	0.11	0.11	0.11	0.00	0.11	0.11	0.11	0.00	0.11	0.01	0.00	0.00
X1307-6-2-1	0.04	0.00	0.20	0.07	0.10	0.06	0.07	0.00	0.10	0.06	0.07	0.00	0.08	0.15	0.00	0.00
X1307-6-2-3	0.07	0.00	0.06	0.10	0.12	0.09	0.10	0.00	0.12	0.09	0.10	0.00	0.11	0.03	0.00	0.00
X1307-6-2-4	0.01	0.00	0.34	0.02	0.04	0.02	0.02	0.01	0.04	0.02	0.02	0.01	0.03	0.41	0.00	0.00
X1307-6-2-5	0.11	0.00	0.01	0.11	0.10	0.11	0.11	0.00	0.10	0.11	0.11	0.00	0.11	0.00	0.00	0.00
X1307-7-1-1	0.13	0.00	0.01	0.11	0.09	0.12	0.11	0.00	0.09	0.12	0.11	0.00	0.10	0.00	0.00	0.00
X1307-7-1-2	0.13	0.00	0.01	0.11	0.09	0.12	0.11	0.00	0.09	0.12	0.11	0.00	0.10	0.00	0.00	0.00
X1307-7-1-3	0.07	0.00	0.06	0.10	0.12	0.09	0.10	0.00	0.12	0.09	0.10	0.00	0.11	0.03	0.00	0.00
X1307-7-1-4	0.12	0.00	0.01	0.11	0.10	0.12	0.11	0.00	0.10	0.12	0.11	0.00	0.11	0.00	0.00	0.00

Lines	*M1M2M3 M4*	*M1M2M3 m4*	*M1M2m3 m4*	*M1M2m3 M4*	*M1m2M3 M4*	*M1m2M3 m4*	*M1m2m3 m4*	*M1m2m3 M4*	*m1M2M3 M4*	*m1M2M3 m4*	*m1M2m3 m4*	*m1M2m3 M4*	*m1m2M3 M4*	*m1m2M3 m4*	*m1m2m3 m4*	*m1m2m3 M4*
X1307-7-2-1	0.02	0.00	0.30	0.04	0.07	0.03	0.04	0.00	0.07	0.03	0.04	0.00	0.05	0.30	0.00	0.00
X1307-7-2-2	0.09	0.00	0.03	0.11	0.11	0.11	0.11	0.00	0.11	0.11	0.11	0.00	0.11	0.01	0.00	0.00
X1307-7-2-3	0.01	0.00	0.34	0.02	0.04	0.01	0.02	0.01	0.04	0.01	0.02	0.01	0.03	0.43	0.00	0.00
X1307-7-2-4	0.12	0.00	0.01	0.11	0.10	0.11	0.11	0.00	0.10	0.11	0.11	0.00	0.11	0.00	0.00	0.00
X1307-7-2-5	0.14	0.00	0.01	0.11	0.09	0.12	0.11	0.00	0.09	0.12	0.11	0.00	0.10	0.00	0.00	0.00
X1307-8-1-1	0.10	0.00	0.02	0.11	0.11	0.11	0.11	0.00	0.11	0.11	0.11	0.00	0.11	0.01	0.00	0.00
X1307-8-1-2	0.08	0.00	0.05	0.10	0.12	0.10	0.10	0.00	0.12	0.10	0.10	0.00	0.11	0.02	0.00	0.00
X1307-8-1-3	0.11	0.00	0.02	0.11	0.10	0.11	0.11	0.00	0.10	0.11	0.11	0.00	0.11	0.01	0.00	0.00
X1307-8-1-4	0.00	0.15	0.01	0.00	0.00	0.00	0.00	0.39	0.00	0.00	0.00	0.39	0.00	0.02	0.04	0.00
X1307-8-1-5	0.00	0.09	0.00	0.00	0.00	0.00	0.00	0.01	0.00	0.00	0.00	0.01	0.00	0.00	0.35	0.54
X1307-8-2-1	0.00	0.00	0.34	0.01	0.03	0.01	0.01	0.02	0.03	0.01	0.01	0.02	0.02	0.47	0.00	0.00
X1307-8-2-2	0.07	0.00	0.08	0.10	0.12	0.09	0.10	0.00	0.12	0.09	0.10	0.00	0.11	0.04	0.00	0.00
X1307-8-2-3	0.12	0.00	0.01	0.11	0.09	0.12	0.11	0.00	0.09	0.12	0.11	0.00	0.11	0.00	0.00	0.00
X1307-8-2-4	0.00	0.00	0.33	0.01	0.02	0.01	0.01	0.04	0.02	0.01	0.01	0.04	0.01	0.49	0.00	0.00
X1307-8-2-5	0.02	0.00	0.27	0.05	0.08	0.04	0.05	0.00	0.08	0.04	0.05	0.00	0.06	0.24	0.00	0.00
X1307-8-3-1	0.00	0.08	0.04	0.00	0.00	0.00	0.00	0.38	0.00	0.00	0.00	0.38	0.00	0.11	0.02	0.00
X1307-8-3-2	0.02	0.00	0.27	0.05	0.08	0.04	0.05	0.00	0.08	0.04	0.05	0.00	0.06	0.24	0.00	0.00
X1307-8-3-3	0.12	0.00	0.01	0.11	0.10	0.11	0.11	0.00	0.10	0.11	0.11	0.00	0.11	0.00	0.00	0.00
X1307-8-3-5	0.09	0.00	0.04	0.11	0.11	0.10	0.11	0.00	0.11	0.10	0.11	0.00	0.11	0.02	0.00	0.00
X1308-2-1-1	0.09	0.00	0.03	0.11	0.11	0.11	0.11	0.00	0.11	0.11	0.11	0.00	0.11	0.01	0.00	0.00
X1308-2-1-2	0.00	0.29	0.00	0.00	0.00	0.00	0.00	0.28	0.00	0.00	0.00	0.28	0.00	0.00	0.16	0.00
X1308-2-1-3	0.10	0.00	0.02	0.11	0.10	0.11	0.11	0.00	0.10	0.11	0.11	0.00	0.11	0.01	0.00	0.00
X1308-2-1-4	0.00	0.34	0.00	0.00	0.00	0.00	0.00	0.18	0.00	0.00	0.00	0.18	0.00	0.00	0.29	0.00
X1308-2-1-5	0.00	0.19	0.00	0.00	0.00	0.00	0.00	0.37	0.00	0.00	0.00	0.37	0.00	0.01	0.06	0.00
X1308-2-1-6	0.13	0.00	0.01	0.11	0.09	0.12	0.11	0.00	0.09	0.12	0.11	0.00	0.10	0.00	0.00	0.00
X1308-2-1-7	0.11	0.00	0.01	0.11	0.10	0.11	0.11	0.00	0.10	0.11	0.11	0.00	0.11	0.00	0.00	0.00

Lines	*M1M2M3 M4*	*M1M2M3 m4*	*M1M2m3 m4*	*M1M2m3 M4*	*M1m2M3 M4*	*M1m2M3 m4*	*M1m2m3 m4*	*M1m2m3 M4*	*m1M2M3 M4*	*m1M2M3 m4*	*m1M2m3 m4*	*m1M2m3 M4*	*m1m2M3 M4*	*m1m2M3 m4*	*m1m2m3 m4*	*m1m2m3 M4*
X1308-4-1-2	0.10	0.00	0.02	0.11	0.10	0.11	0.11	0.00	0.10	0.11	0.11	0.00	0.11	0.01	0.00	0.00
X1308-4-1-3	0.13	0.00	0.01	0.11	0.09	0.12	0.11	0.00	0.09	0.12	0.11	0.00	0.10	0.00	0.00	0.00
X1308-4-1-4	0.09	0.00	0.04	0.11	0.11	0.10	0.11	0.00	0.11	0.10	0.11	0.00	0.11	0.02	0.00	0.00
X1308-4-1-5	0.14	0.00	0.01	0.11	0.08	0.12	0.11	0.00	0.08	0.12	0.11	0.00	0.10	0.00	0.00	0.00
X1308-4-1-6	0.04	0.00	0.18	0.07	0.11	0.06	0.07	0.00	0.11	0.06	0.07	0.00	0.09	0.13	0.00	0.00
X1308-4-1-7	0.11	0.00	0.01	0.11	0.10	0.11	0.11	0.00	0.10	0.11	0.11	0.00	0.11	0.00	0.00	0.00
X1308-5-1-1	0.13	0.00	0.01	0.11	0.09	0.12	0.11	0.00	0.09	0.12	0.11	0.00	0.10	0.00	0.00	0.00
X1308-5-1-2	0.09	0.00	0.04	0.11	0.11	0.10	0.11	0.00	0.11	0.10	0.11	0.00	0.11	0.01	0.00	0.00
X1308-5-1-3	0.00	0.35	0.00	0.00	0.00	0.00	0.00	0.12	0.00	0.00	0.00	0.12	0.00	0.00	0.40	0.01
X1308-5-1-4	0.10	0.00	0.03	0.11	0.11	0.11	0.11	0.00	0.11	0.11	0.11	0.00	0.11	0.01	0.00	0.00
X1308-5-1-5	0.06	0.00	0.11	0.09	0.12	0.08	0.09	0.00	0.12	0.08	0.09	0.00	0.10	0.06	0.00	0.00
X1308-5-1-6	0.10	0.00	0.02	0.11	0.10	0.11	0.11	0.00	0.10	0.11	0.11	0.00	0.11	0.01	0.00	0.00
X1308-5-1-7	0.00	0.33	0.00	0.00	0.00	0.00	0.00	0.22	0.00	0.00	0.00	0.22	0.00	0.00	0.24	0.00
X1308-5-2-3	0.07	0.00	0.06	0.10	0.12	0.09	0.10	0.00	0.12	0.09	0.10	0.00	0.11	0.03	0.00	0.00
X1308-5-2-4	0.12	0.00	0.01	0.11	0.09	0.12	0.11	0.00	0.09	0.12	0.11	0.00	0.11	0.00	0.00	0.00
X1308-5-2-5	0.07	0.00	0.07	0.10	0.12	0.09	0.10	0.00	0.12	0.09	0.10	0.00	0.11	0.03	0.00	0.00
X1308-5-2-6	0.15	0.00	0.00	0.11	0.08	0.12	0.11	0.00	0.08	0.12	0.11	0.00	0.10	0.00	0.00	0.00
X1308-5-2-7	0.00	0.00	0.00	0.00	0.00	0.00	0.00	0.00	0.00	0.00	0.00	0.00	0.00	0.00	0.01	0.99
X1308-6-1-1	0.01	0.00	0.32	0.03	0.06	0.03	0.04	0.00	0.06	0.03	0.04	0.00	0.05	0.33	0.00	0.00
X1308-6-1-2	0.00	0.05	0.00	0.00	0.00	0.00	0.00	0.00	0.00	0.00	0.00	0.00	0.00	0.00	0.22	0.73
X1308-6-1-3	0.01	0.00	0.34	0.02	0.03	0.01	0.02	0.02	0.03	0.01	0.02	0.02	0.02	0.45	0.00	0.00
X1308-6-1-4	0.09	0.00	0.03	0.11	0.11	0.10	0.11	0.00	0.11	0.10	0.11	0.00	0.11	0.01	0.00	0.00
X1308-6-1-5	0.02	0.00	0.28	0.05	0.08	0.04	0.05	0.00	0.08	0.04	0.05	0.00	0.06	0.25	0.00	0.00
X1308-6-1-6	0.10	0.00	0.03	0.11	0.11	0.11	0.11	0.00	0.11	0.11	0.11	0.00	0.11	0.01	0.00	0.00
X1308-6-1-7	0.11	0.00	0.01	0.11	0.10	0.11	0.11	0.00	0.10	0.11	0.11	0.00	0.11	0.00	0.00	0.00
X1308-7-1-1	0.14	0.00	0.01	0.11	0.09	0.12	0.11	0.00	0.09	0.12	0.11	0.00	0.10	0.00	0.00	0.00

Lines	*M1M2M3 M4*	*M1M2M3 m4*	*M1M2m3 m4*	*M1M2m3 M4*	*M1m2M3 M4*	*M1m2M3 m4*	*M1m2m3 m4*	*M1m2m3 M4*	*m1M2M3 M4*	*m1M2M3 m4*	*m1M2m3 m4*	*m1M2m3 M4*	*m1m2M3 M4*	*m1m2M3 m4*	*m1m2m3 m4*	*m1m2m3 M4*
X1308-7-1-2	0.13	0.00	0.01	0.11	0.09	0.12	0.11	0.00	0.09	0.12	0.11	0.00	0.10	0.00	0.00	0.00
X1308-7-1-3	0.00	0.15	0.01	0.00	0.00	0.00	0.00	0.39	0.00	0.00	0.00	0.39	0.00	0.02	0.04	0.00
X1308-7-1-4	0.05	0.00	0.14	0.08	0.11	0.07	0.08	0.00	0.11	0.07	0.08	0.00	0.10	0.09	0.00	0.00
X1308-7-1-5	0.13	0.00	0.01	0.11	0.09	0.12	0.11	0.00	0.09	0.12	0.11	0.00	0.10	0.00	0.00	0.00
X1308-7-1-6	0.05	0.00	0.12	0.09	0.12	0.08	0.09	0.00	0.12	0.08	0.09	0.00	0.10	0.07	0.00	0.00
X1308-7-1-7	0.00	0.19	0.00	0.00	0.00	0.00	0.00	0.36	0.00	0.00	0.00	0.36	0.00	0.01	0.07	0.00
X1308-7-2-1	0.00	0.11	0.02	0.00	0.00	0.00	0.00	0.39	0.00	0.00	0.00	0.39	0.00	0.06	0.02	0.00
X1308-7-2-2	0.06	0.00	0.09	0.09	0.12	0.09	0.10	0.00	0.12	0.09	0.10	0.00	0.11	0.05	0.00	0.00
X1308-7-2-3	0.00	0.00	0.31	0.01	0.02	0.01	0.01	0.06	0.02	0.01	0.01	0.06	0.01	0.49	0.00	0.00
X1308-7-2-4	0.13	0.00	0.01	0.11	0.09	0.12	0.11	0.00	0.09	0.12	0.11	0.00	0.10	0.00	0.00	0.00
X1308-7-2-5	0.00	0.30	0.00	0.00	0.00	0.00	0.00	0.26	0.00	0.00	0.00	0.26	0.00	0.00	0.18	0.00
X1308-7-2-6	0.00	0.08	0.05	0.00	0.00	0.00	0.00	0.37	0.00	0.00	0.00	0.37	0.00	0.13	0.01	0.00
X1308-7-2-7	0.01	0.00	0.34	0.02	0.04	0.02	0.02	0.01	0.04	0.02	0.02	0.01	0.03	0.41	0.00	0.00
X1308-8-1-1	0.02	0.00	0.26	0.05	0.09	0.04	0.05	0.00	0.09	0.04	0.05	0.00	0.07	0.23	0.00	0.00
X1308-8-1-3	0.13	0.00	0.01	0.11	0.09	0.12	0.11	0.00	0.09	0.12	0.11	0.00	0.10	0.00	0.00	0.00
X1308-8-1-4	0.14	0.00	0.01	0.11	0.08	0.12	0.11	0.00	0.08	0.12	0.11	0.00	0.10	0.00	0.00	0.00
X1308-8-1-6	0.14	0.00	0.01	0.11	0.08	0.12	0.11	0.00	0.08	0.12	0.11	0.00	0.10	0.00	0.00	0.00
X1308-8-1-7	0.13	0.00	0.01	0.11	0.09	0.12	0.11	0.00	0.09	0.12	0.11	0.00	0.10	0.00	0.00	0.00
X1308-8-2-1	0.11	0.00	0.02	0.11	0.10	0.11	0.11	0.00	0.10	0.11	0.11	0.00	0.11	0.01	0.00	0.00
X1308-8-2-2	0.06	0.00	0.11	0.09	0.12	0.08	0.09	0.00	0.12	0.08	0.09	0.00	0.10	0.07	0.00	0.00
X1308-8-2-3	0.13	0.00	0.01	0.11	0.09	0.12	0.11	0.00	0.09	0.12	0.11	0.00	0.10	0.00	0.00	0.00
X1308-8-2-4	0.00	0.00	0.32	0.01	0.02	0.01	0.01	0.05	0.02	0.01	0.01	0.05	0.01	0.49	0.00	0.00
X1308-8-2-6	0.11	0.00	0.02	0.11	0.10	0.11	0.11	0.00	0.10	0.11	0.11	0.00	0.11	0.01	0.00	0.00
X1308-8-3-1	0.07	0.00	0.07	0.10	0.12	0.09	0.10	0.00	0.12	0.09	0.10	0.00	0.11	0.04	0.00	0.00
X1308-8-3-2	0.06	0.00	0.10	0.09	0.12	0.08	0.09	0.00	0.12	0.08	0.09	0.00	0.10	0.05	0.00	0.00
X1308-8-3-4	0.10	0.00	0.02	0.11	0.11	0.11	0.11	0.00	0.11	0.11	0.11	0.00	0.11	0.01	0.00	0.00

Lines	*M1M2M3 M4*	*M1M2M3 m4*	*M1M2m3 m4*	*M1M2m3 M4*	*M1m2M3 M4*	*M1m2M3 m4*	*M1m2m3 m4*	*M1m2m3 M4*	*m1M2M3 M4*	*m1M2M3 m4*	*m1M2m3 m4*	*m1M2m3 M4*	*m1m2M3 M4*	*m1m2M3 m4*	*m1m2m3 m4*	*m1m2m3 M4*
X1308-8-3-5	0.13	0.00	0.01	0.11	0.09	0.12	0.11	0.00	0.09	0.12	0.11	0.00	0.10	0.00	0.00	0.00
X1308-8-3-6	0.12	0.00	0.01	0.11	0.09	0.12	0.11	0.00	0.09	0.12	0.11	0.00	0.11	0.00	0.00	0.00
X1308-8-3-7	0.04	0.00	0.16	0.08	0.11	0.07	0.08	0.00	0.11	0.07	0.08	0.00	0.09	0.11	0.00	0.00
X1308-8-4-1	0.12	0.00	0.01	0.11	0.09	0.12	0.11	0.00	0.09	0.12	0.11	0.00	0.11	0.00	0.00	0.00
X1308-8-4-2	0.05	0.00	0.13	0.08	0.12	0.08	0.09	0.00	0.12	0.08	0.09	0.00	0.10	0.08	0.00	0.00
X1308-8-4-3	0.14	0.00	0.01	0.11	0.09	0.12	0.11	0.00	0.09	0.12	0.11	0.00	0.10	0.00	0.00	0.00
X1308-8-4-4	0.00	0.35	0.00	0.00	0.00	0.00	0.00	0.17	0.00	0.00	0.00	0.17	0.00	0.00	0.30	0.00
X1308-8-4-5	0.11	0.00	0.01	0.11	0.10	0.11	0.11	0.00	0.10	0.11	0.11	0.00	0.11	0.00	0.00	0.00
X1308-8-4-6	0.15	0.00	0.00	0.11	0.08	0.12	0.11	0.00	0.08	0.12	0.11	0.00	0.10	0.00	0.00	0.00
X1308-8-4-7	0.09	0.00	0.03	0.11	0.11	0.11	0.11	0.00	0.11	0.11	0.11	0.00	0.11	0.01	0.00	0.00

Appendix 11 Candidate genes across whole reference genome

Gene	Chromosome	Position	Gene families
Phvul.001G088900	1	14088551	YELLOW STRIPE like 6
Phvul.001G105400	1	26290093	calcium exchanger 7
Phvul.001G105400	1	26290093	calcium exchanger 7
Phvul.001G142750	1	38584393	Cation efflux family protein
Phvul.001G177500	1	43453927	NRAMP metal ion transporter family protein
Phvul.001G179100	1	43666739	Heavy metal transport/detoxification superfamily protein
Phvul.001G179100	1	43666739	Heavy metal transport/detoxification superfamily protein
Phvul.001G205300	1	46324641	Heavy metal transport/detoxification superfamily protein
Phvul.001G247400	1	49894723	Heavy metal transport/detoxification superfamily protein
Phvul.001G250300	1	50100939	Heavy metal transport/detoxification superfamily protein
Phvul.001G250300	1	50100939	Heavy metal transport/detoxification superfamily protein
Phvul.001G250300	1	50100939	Heavy metal transport/detoxification superfamily protein
Phvul.002G033800	2	3382174	Heavy metal transport/detoxification superfamily protein
Phvul.002G033800	2	3382174	Heavy metal transport/detoxification superfamily protein
Phvul.002G099700	2	19275657	zinc transporter 10 precursor
Phvul.002G100001	2	19321798	zinc transporter 10 precursor
Phvul.002G113500	2	24370429	Vacuolar iron transporter (VIT) family protein
Phvul.002G176300	2	33458683	Cation efflux family protein
Phvul.002G184200	2	34468080	ZIP metal ion transporter family
Phvul.002G205000	2	37162538	Vacuolar iron transporter (VIT) family protein
Phvul.002G205100	2	37176246	Vacuolar iron transporter (VIT) family protein
Phvul.002G205200	2	37188537	Vacuolar iron transporter (VIT) family protein
Phvul.002G205300	2	37195863	Vacuolar iron transporter (VIT) family protein
Phvul.002G208500	2	37516072	Heavy metal transport/detoxification superfamily protein
Phvul.002G262500	2	43427768	Heavy metal transport/detoxification superfamily protein

Gene	Chromosome	Position	Gene families
Phvul.002G285600	2	45486348	Heavy metal transport/detoxification superfamily protein
Phvul.002G292900	2	46189860	Heavy metal transport/detoxification superfamily protein
Phvul.002G314600	2	48136994	Heavy metal transport/detoxification superfamily protein
Phvul.002G322800	2	48774556	vacuolar iron transporter 1
Phvul.002G322900	2	48779470	vacuolar iron transporter 1
Phvul.002G323700	2	48857307	vacuolar iron transporter 1
Phvul.003G006400	3	760614	YELLOW STRIPE like 7
Phvul.003G006500	3	765645	YELLOW STRIPE like 7
Phvul.003G006500	3	765645	YELLOW STRIPE like 7
Phvul.003G021300	3	2036314	Cation efflux family protein
Phvul.003G022400	3	2135327	Heavy metal transport/detoxification superfamily protein
Phvul.003G086300	3	16877488	Heavy metal transport/detoxification superfamily protein
Phvul.003G092500	3	21113140	Heavy metal transport/detoxification superfamily protein
Phvul.003G099700	3	25708027	Heavy metal transport/detoxification superfamily protein
Phvul.003G104900	3	23350962	Heavy metal transport/detoxification superfamily protein
Phvul.003G108900	3	27536901	Heavy metal transport/detoxification superfamily protein
Phvul.003G108900	3	27536901	Heavy metal transport/detoxification superfamily protein
Phvul.003G108900	3	27536901	Heavy metal transport/detoxification superfamily protein
Phvul.003G219900	3	44817176	Heavy metal transport/detoxification superfamily protein
Phvul.003G262400	3	50155639	zinc transporter 10 precursor
Phvul.003G262500	3	50167952	zinc transporter 10 precursor
Phvul.004G001200	4	36383	Heavy metal transport/detoxification superfamily protein
Phvul.004G019800	4	2331722	Heavy metal transport/detoxification superfamily protein
Phvul.004G049800	4	6070640	calcium exchanger 7
Phvul.004G052700	4	7006062	Heavy metal transport/detoxification superfamily protein
Phvul.004G077300	4	13645167	Heavy metal transport/detoxification superfamily protein

Gene	Chromosome	Position	Gene families
Phvul.004G096500	4	15848521	Vacuolar iron transporter (VIT) family protein
Phvul.004G106900	4	35338479	Heavy metal transport/detoxification superfamily protein
Phvul.004G116300	4	40009283	Heavy metal transport/detoxification superfamily protein
Phvul.004G138900	4	43873548	YELLOW STRIPE like 7
Phvul.004G161300	4	46564258	Heavy metal transport/detoxification superfamily protein
Phvul.005G048900	5	5682746	zinc transporter 1 precursor
Phvul.005G049300	5	5742223	Cation efflux family protein
Phvul.005G095400	5	29797811	Heavy metal transport/detoxification superfamily protein
Phvul.005G131500	5	37041480	Heavy metal transport/detoxification superfamily protein
Phvul.005G182000	5	40667944	NRAMP metal ion transporter 6
Phvul.005G182000	5	40667944	NRAMP metal ion transporter 6
Phvul.005G184600	5	40802614	cation exchanger 2
Phvul.006G001000	6	321846	zinc transporter 1 precursor
Phvul.006G015061	6	2386258	YELLOW STRIPE like 1
Phvul.006G060800	6	16929318	cation exchanger 5
Phvul.006G060800	6	16929318	cation exchanger 5
Phvul.006G067900	6	17933066	cation exchanger 1
Phvul.006G070200	6	18248775	ZIP metal ion transporter family
Phvul.006G080700	6	19279972	Cation efflux family protein
Phvul.006G080700	6	19279972	Cation efflux family protein
Phvul.006G083800	6	19564418	YELLOW STRIPE like 7
Phvul.006G093300	6	20450587	cation exchanger 11
Phvul.006G139900	6	24687127	Heavy metal transport/detoxification superfamily protein
Phvul.006G139900	6	24687127	Heavy metal transport/detoxification superfamily protein
Phvul.006G139900	6	24687127	Heavy metal transport/detoxification superfamily protein
Phvul.006G153400	6	25863506	Heavy metal transport/detoxification superfamily protein

Gene	Chromosome	Position	Gene families
Phvul.007G079100	7	7671485	Vacuolar iron transporter (VIT) family protein
Phvul.008G015500	8	1278190	Cation efflux family protein
Phvul.008G015500	8	1278190	Cation efflux family protein
Phvul.008G015500	8	1278190	Cation efflux family protein
Phvul.008G015500	8	1278190	Cation efflux family protein
Phvul.008G015500	8	1278190	Cation efflux family protein
Phvul.008G058500	8	5220363	Heavy metal transport/detoxification superfamily protein
Phvul.008G070000	8	6339674	vacuolar iron transporter 1
Phvul.008G079500	8	7719539	ZIP metal ion transporter family
Phvul.008G104500	8	11470299	cation exchanger 1
Phvul.008G157800	8	28064702	YELLOW STRIPE like 3
Phvul.008G157800	8	28064702	YELLOW STRIPE like 3
Phvul.008G157800	8	28064702	YELLOW STRIPE like 3
Phvul.008G187600	8	52505573	Vacuolar iron transporter (VIT) family protein
Phvul.008G187600	8	52505573	Vacuolar iron transporter (VIT) family protein
Phvul.008G187600	8	52505573	Vacuolar iron transporter (VIT) family protein
Phvul.008G187600	8	52505573	Vacuolar iron transporter (VIT) family protein
Phvul.008G187600	8	52505573	Vacuolar iron transporter (VIT) family protein
Phvul.008G187600	8	52505573	Vacuolar iron transporter (VIT) family protein
Phvul.008G187600	8	52505573	Vacuolar iron transporter (VIT) family protein
Phvul.008G189300	8	52746631	Heavy metal transport/detoxification superfamily protein
Phvul.008G189400	8	52754968	Heavy metal transport/detoxification superfamily protein
Phvul.008G216200	8	56526044	Heavy metal transport/detoxification superfamily protein
Phvul.008G219600	8	56886320	Heavy metal transport/detoxification superfamily protein
Phvul.008G244200	8	59266794	Cation efflux family protein
Phvul.008G254900	8	60275655	Cation efflux family protein

Gene	Chromosome	Position	Gene families
Phvul.008G259200	8	60615253	ZIP metal ion transporter family
Phvul.008G261500	8	60843461	cation exchanger 1
Phvul.009G027600	9	6422756	Heavy metal transport/detoxification superfamily protein
Phvul.009G038800	9	8217549	Heavy metal transport/detoxification superfamily protein
Phvul.009G038800	9	8217549	Heavy metal transport/detoxification superfamily protein
Phvul.009G038800	9	8217549	Heavy metal transport/detoxification superfamily protein
Phvul.009G038800	9	8217549	Heavy metal transport/detoxification superfamily protein
Phvul.009G040800	9	8411105	vacuolar iron transporter (VIT) family protein
Phvul.009G040800	9	8411105	vacuolar iron transporter (VIT) family protein
Phvul.009G040800	9	8411105	vacuolar iron transporter (VIT) family protein
Phvul.009G048800	9	9593088	YELLOW STRIPE like 3
Phvul.009G048800	9	9593088	YELLOW STRIPE like 3
Phvul.009G069700	9	12141306	NRAMP metal ion transporter 2
Phvul.009G127900	9	19429094	NRAMP metal ion transporter 6
Phvul.009G127900	9	19429094	NRAMP metal ion transporter 6
Phvul.009G137100	9	20653368	manganese tracking factor for mitochondrial SOD2
Phvul.009G164900	9	24527982	Heavy metal transport/detoxification superfamily protein
Phvul.009G247600	9	36846305	Heavy metal transport/detoxification superfamily protein
Phvul.010G001500	10	412065	cation exchanger 3
Phvul.010G001500	10	412065	cation exchanger 3
Phvul.010G021600	10	3076479	Vacuolar iron transporter (VIT) family protein
Phvul.010G021700	10	3083937	vacuolar iron transporter (VIT) family protein
Phvul.010G034132	10	4957830	Heavy metal transport/detoxification superfamily protein
Phvul.010G059200	10	9326694	ZIP metal ion transporter family
Phvul.010G103800	10	37309047	Heavy metal transport/detoxification superfamily protein
Phvul.010G103800	10	37309047	Heavy metal transport/detoxification superfamily protein

Gene	Chromosome	Position	Gene families
Phvul.010G110500	10	38414889	NRAMP metal ion transporter 2
Phvul.010G119900	10	40027163	metal tolerance protein A2
Phvul.010G119900	10	40027163	metal tolerance protein A2
Phvul.010G119900	10	40027163	metal tolerance protein A2
Phvul.010G119900	10	40027163	metal tolerance protein A2
Phvul.010G128500	10	40925634	cation calcium exchanger 4
Phvul.010G160800	10	43922651	NRAMP metal ion transporter 6
Phvul.010G160800	10	43922651	NRAMP metal ion transporter 6
Phvul.010G160800	10	43922651	NRAMP metal ion transporter 6
Phvul.011G058500	11	5228604	ZIP metal ion transporter family
Phvul.011G061200	11	5460629	metal tolerance protein B1
Phvul.011G061200	11	5460629	metal tolerance protein B1
Phvul.011G068500	11	6085721	Heavy metal transport/detoxification superfamily protein
Phvul.011G084200	11	7945552	Heavy metal transport/detoxification superfamily protein
Phvul.011G088100	11	8454876	vacuolar protein sorting 41
Phvul.011G178800	11	48990728	Cation efflux family protein
Phvul.011G178800	11	48990728	Cation efflux family protein
Phvul.L001741	scaffold_142	17190	Heavy metal transport/detoxification superfamily protein
Phvul.L002137	scaffold_13	221624	Heavy metal transport/detoxification superfamily protein
Phvul.L005301	scaffold_14	415497	YELLOW STRIPE like 1
Phvul.L005301	scaffold_14	415497	YELLOW STRIPE like 1
Phvul.L007443	scaffold_15	499839	zinc transporter 11 precursor
Phvul.L007543	scaffold_15	504259	zinc transporter 11 precursor
Phvul.L011443	scaffold_15	796287	ZIP metal ion transporter family

Appendix 12 Statistics of genotyping by sequencing (GBS) reads generated from the 138 RILs and two parents of the cranberry common bean

Item	RILs (138)				Cran09	Messina
	Mean	Min	Max	Std		
Total reads	13,064,398	420,790	42,884,536	7,433,013	117,779,218	105,462,778
Total length (Mb)	1,959.66	63.12	6,432.68	1,114.95	17,666.88	15,819.42
Genome coverage depth	3.65	0.12	11.97	2.08	32.89	29.45
Mapped reads	10,308,751	336,808	32,483,693	5,836,050	92,079,813	84,434,975
Mapped reads %	78.56	66.54	82.7	2.15	77.87	79.75
Mapped length (Mb)	1,546.31	50.52	4,872.55	875.42	13,811.97	12,665.25
Mapped genome coverage depth	2.88	0.09	9.07	1.63	25.71	23.58

Appendix 13 Statistics of single-nucleotide polymorphisms (SNPs) identification from the 138 RILs and two parents

Chromosome	Total SNPs	SNPs with MAF > 0.01, call rate > 20% and polymorphic between two parents
1	3892	174
2	6261	377
3	4390	162
4	5251	203
5	5061	318
6	2857	100
7	3880	95
8	6542	105
9	3042	111
10	3811	93
11	7689	150

MAF: minimum allele frequency

Appendix 14. Relationship between genetic distance (cM) and physical distance(Mb) in 11 chromosomes. Some markers from scaffolds that have not been assigned to chromosomes and from different chromosomes were excluded.

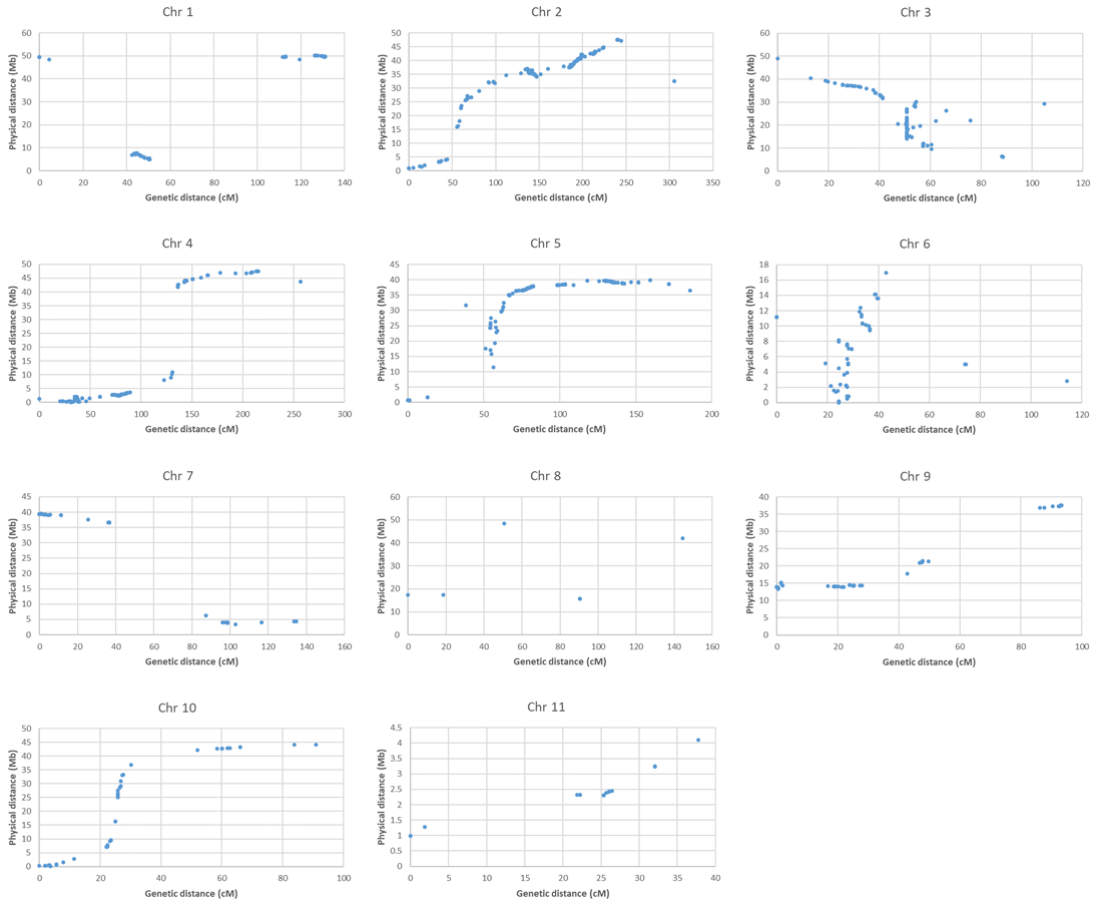

Appendix 15 Linkage map of the cranberry common bean population. The data is accessible in Zenodo at https://zenodo.org/record/6574214 .

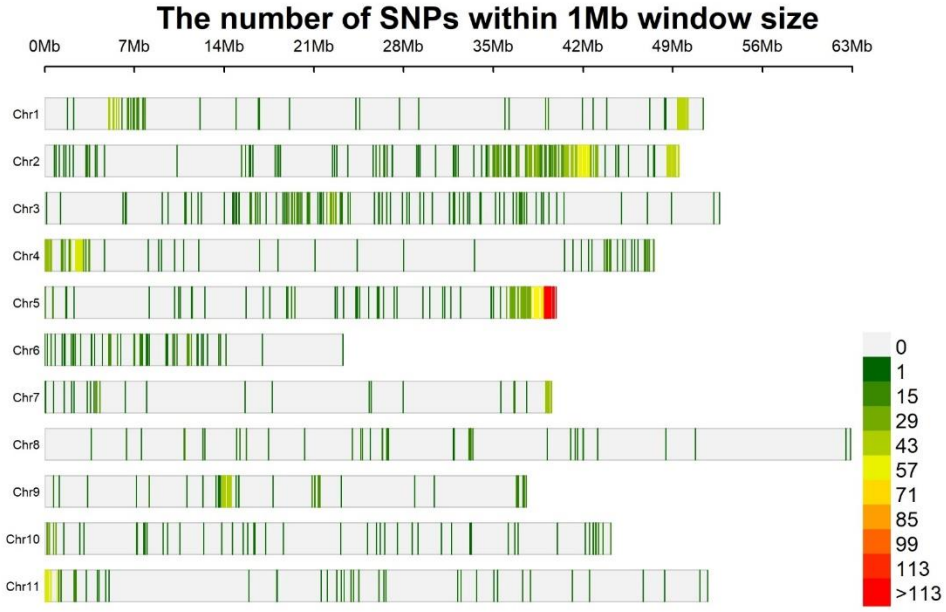

Appendix 16 Distribution of single-nucleotide polymorphisms (SNPs) on 11 common bean chromosomes.

Appendix 17 R^2 of 21 quantitative trait locus (QTL) across 5 years and two soil types (sandy and heavy clay).

Dataset/ QTL	QTL. 2.1	QTL. 2.2	QTL. 2.3	QTL. 2.4	QTL. 2.5	QTL. 2.6	QTL. 2.7	QTL. 3.1	QTL. 3.2	QTL. 3.3	QTL. 3.4	QTL. 3.5	QTL. 3.6	QTL. 5.1	QTL. 5.2	QTL. 5.3	QTL. 6.1	QTL. 6.2	QTL. 9.1	QTL.1 1.1	QTL.1 1.2
H2015	6.518*	7.46**	10.106 ***	10.551 ***	8.958* *	8.707* **	6.639* *	9.524* *	9.069* *	8.268* *	6.534* *	2.783	4.358*	6.548* *	6.414*	7.348* *	1.755	1.467	1.567	9.885** *	1.166
H2016	7.299*	8.46** *	9.028* *	9.808* **	7.545*	10.099 ***	10.809 ***	15.485 ***	16.106 ***	15.161 ***	14.96* **	3.501	11.291 ***	6.785* *	6.994*	13.508 ***	3.045	1.176	4.131	4.612*	1.813
H2017	4.127	11.476 ***	11.021 ***	11.636 ***	9.231* *	9.218* **	8.838* **	8.001*	7.517*	6.062*	6.003* *	3.151	3.224	10.802 ***	10.566 **	6.48*	8.188* *	7.656* *	0.705	5.937**	3.878
H2018	8.827* *	7.659* *	9.676* *	10.162 ***	9.48**	7.581* *	8.799* **	8.931* *	8.15**	7.186* *	6.69**	4.212	4.226	12.97* **	15.594 ***	4.204	2.15	1.474	1.404	7.578**	1.61
H2019	2.964	7.669* *	11.884 ***	12.426 ***	10.754 **	12.186 ***	11.351 ***	8.737* *	7.897*	8.231* *	7.916* **	9.249* *	5.469*	11.971 ***	12.08* **	9.432* *	5.931*	3.861*	0.282	2.097	3.712
S2015	1.49	6.07**	7.513* *	8.164* **	6.243*	6.866* *	6.566* *	12.651 ***	12.365 ***	9.756* **	9.721* **	1.385	4.111	12.083 ***	11.555 ***	2	6.765*	6.361* *	1.494	5.124**	9.946**
S2016	7.273*	10.53* **	10.967 ***	11.114 ***	8.904* *	9.887* **	8.1***	17.829 ***	17.551 ***	16.242 ***	15.572 ***	8.509* *	12.889 ***	7.165* *	6.559*	19.248 ***	2.135	1.16	3.318	12.412* **	2.145
S2017	10.812 **	4.562*	4.314	4.474*	2.961	3.605*	4.82**	8.235* *	8.644* *	8.137* *	7.709* **	3.71	4.876*	9.915* **	14.416 ***	6.731*	6.868*	4.396*	5.753*	5.653**	4.306
S2018	4.567	1.271	3.628	4.521*	3.937	4.561*	1.949	5.601	5.023	5.081*	4.683*	0.692	2.169	10.189 ***	11.025 **	5.125	7.718*	5.608* *	0.054	10.819* **	7.57*
S2019	3.833	4.173*	4.505*	3.834*	2.418	6.298* *	2.812*	2.396	2.537	1.485	0.917	0.541	2.198	4.972*	12.324 ***	1.118	4.218	3.698*	1.143	3.946*	4.389
T2015	4.515	8.41** *	10.873 ***	11.563 ***	9.406* *	9.635* **	8.071* **	12.906 ***	12.414 ***	10.691 ***	9.658* **	2.084	5.098*	10.74* **	10.398 **	5.384	4.271	3.894*	1.854	9.023** *	4.318
T2016	8.567* *	11.69* **	12.397 ***	12.969 ***	10.143 **	12.364 ***	11.516 ***	20.093 ***	20.283 ***	18.947 ***	18.408 ***	6.38*	14.419 ***	8.258* *	7.908*	19.902 ***	2.606	1.43	3.573	10.425* **	2.152
T2017	9.387* *	9.735* **	9.165* *	9.735* **	7.071*	7.766* **	8.616* **	10.596 **	10.683 **	9.4**	9.078* **	3.899	5.357*	13.6** *	15.602 ***	8.525* *	8.835* *	7.643* *	2.452	7.622**	5.275
T2018	9.374* *	6.294* *	9.581* *	10.625 ***	9.341* *	8.755* **	7.46**	9.846* *	8.95**	8.286* *	7.655* *	2.412	4.222	16.024 ***	16.985 ***	6.154*	5.203	3.913*	0.768	12.635* **	4.665
T2019	4.862	9.346* **	12.539 ***	12.901 ***	10.021 **	14.847 ***	11.324 ***	7.995*	7.372*	7.245* *	6.63**	5.923*	4.195	13.651 ***	13.752 ***	7.791*	7.865*	5.83**	0.712	4.135*	5.618
H-5 yrs	7.402*	11.991 ***	15.021 ***	15.859 ***	13.353 ***	13.799 ***	13.271 ***	13.364 ***	12.698 ***	11.871 ***	11.131 ***	5.98*	7.222* *	13.822 ***	13.665 ***	10.545 **	5.012	3.888*	1.155	8.024** *	2.306
G-5 yrs	7.363*	7.821* **	9.504* *	9.998* **	7.214*	9.809* **	7.378* *	13.829 ***	13.612 ***	11.951 ***	11.28* **	2.767	6.311*	14.329 ***	15.723 ***	8.245* *	7.623*	6.565* *	1.432	11.818* **	8.218**
Overall	8.438* *	11.379 ***	14.027 ***	14.927 ***	11.818 ***	13.592 ***	11.903 ***	15.568 ***	14.959 ***	13.706 ***	12.797 ***	4.397	7.859* *	15.962 ***	16.319 ***	10.795 **	6.648*	5.499* *	1.445	11.07** *	5.122
Mean R2	8.30	8.51	10.49	10.29	9.30	9.42	8.72	12.10	11.77	10.37	9.79	7.21	7.74	11.10	12.10	9.58	7.38	5.29	5.75	8.28	8.58

Note: *, p<0.05; **, p<0.01; ***,p<0.001, mean R^2 values were calculated from those datasets which were significant correlation with QTL.

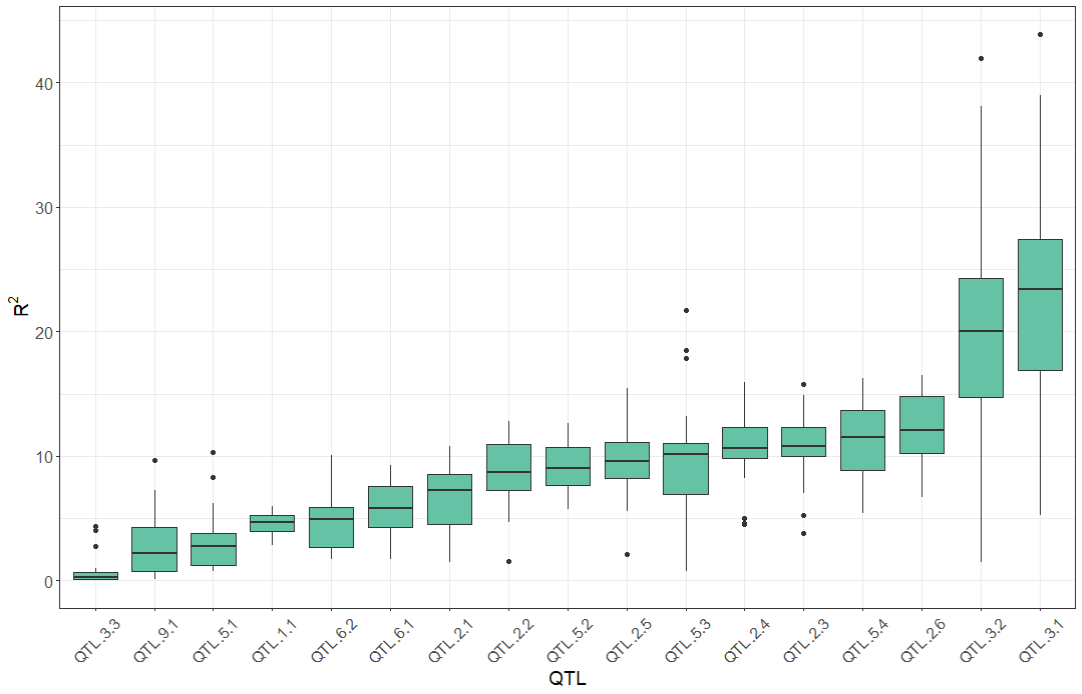

Appendix 18 Boxplots of R^2 of QTL in 18 phenotypic data sets. Only R^2 values from the datasets that had significant correlation with quantitative trait locus (QTL) were used

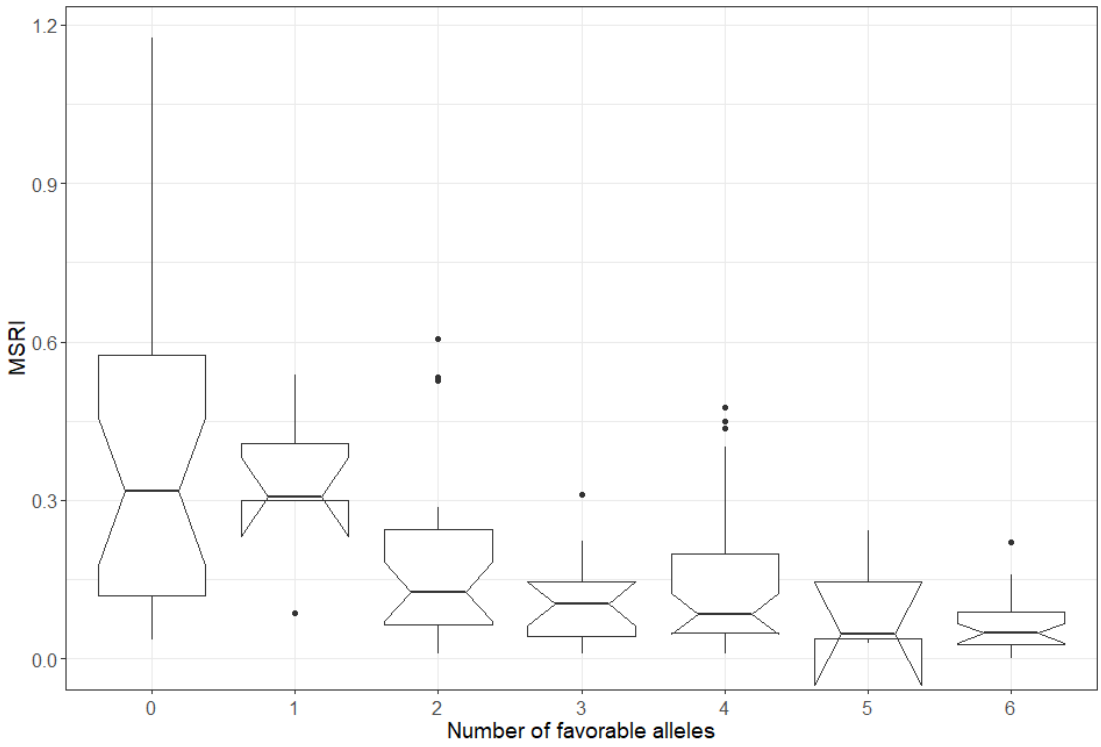

Appendix 19 Relationship between the number of favorable alleles for 3 epistatic quantitative trait locus (QTL) and marsh spot resistance index (MSRI) of the 138 RILs.

Appendix 20 Relative contribution (%) of each quantitative trait locus (QTL) to the marsh spot resistance index (MSRI) of the 138 RILs across 5 years and two soil types (sandy and heavy clay).

Dataset/ QTL	***QTL. 2.1***	***QTL. 2.2***	***QTL. 2.3***	***QTL. 2.4***	***QTL. 2.5***	***QTL. 2.6***	***QTL. 2.7***	***QTL. 3.1***	***QTL. 3.2***	***QTL. 3.3***	***QTL. 3.4***	***QTL. 3.5***	***QTL. 3.6***	***QTL. 5.1***	***QTL. 5.2***	***QTL. 5.3***	***QTL. 6.1***	***QTL. 6.2***	***QTL. 9.1***	***QTL.1 1.1***	***QTL.1 1.2***
H2015	6.57	4.60	6.82	5.50	2.08	3.95	2.96	8.93	1.22	7.97	5.91	1.30	3.81	9.63	1.87	3.25	1.66	3.47	3.26	14.24	1.01
H2016	8.01	4.18	4.28	4.13	1.69	3.83	5.81	8.73	1.41	7.13	7.16	2.09	4.30	8.42	1.21	10.00	2.18	1.72	9.11	3.51	1.09
H2017	4.76	9.45	6.43	5.80	0.69	3.79	3.97	6.18	1.10	3.10	2.96	1.40	1.80	13.15	2.94	2.43	6.69	11.06	0.89	6.43	4.98
H2018	17.61	3.64	5.54	4.37	1.62	3.15	5.78	7.16	1.17	3.13	3.01	3.07	1.98	17.41	3.23	1.02	1.53	1.59	0.67	10.16	3.18
H2019	6.94	3.34	7.00	5.53	2.01	6.13	5.98	4.12	0.77	3.81	3.20	11.45	2.26	12.65	7.40	2.99	4.99	4.13	1.64	0.84	2.80
S2015	3.39	3.20	3.83	3.47	1.22	2.79	2.45	10.86	0.78	6.74	6.34	0.58	3.75	12.82	3.83	0.93	4.81	8.22	1.86	5.47	12.64
S2016	4.74	6.89	5.18	4.43	0.89	3.04	2.89	8.02	1.93	5.48	5.55	4.04	4.66	5.66	1.41	14.43	1.67	1.69	2.90	12.11	2.39
S2017	4.64	3.17	2.09	2.22	0.72	1.49	3.15	5.35	0.86	4.60	4.39	0.57	2.51	17.12	2.86	4.21	6.63	14.09	5.67	7.95	5.71
S2018	7.50	0.93	3.20	3.44	0.25	3.78	1.32	4.56	1.18	3.11	3.24	0.53	1.72	15.07	3.01	2.49	6.28	7.43	0.25	18.72	11.98
S2019	11.15	4.58	2.86	3.48	0.23	8.61	2.71	5.22	0.45	2.58	2.15	0.31	2.53	15.84	5.02	0.89	5.39	5.32	1.51	8.62	10.53
T2015	5.26	4.31	5.79	4.89	1.76	3.68	2.93	10.04	1.03	7.05	5.78	0.77	3.57	12.16	2.86	1.17	3.14	5.84	2.79	10.10	5.08
T2016	6.02	5.77	4.97	4.45	1.14	3.47	4.20	8.49	1.66	6.28	6.36	2.93	4.49	6.94	1.15	12.84	1.88	1.76	5.27	8.21	1.74
T2017	5.00	6.02	4.01	3.86	0.69	2.48	3.63	6.03	1.02	4.03	3.85	0.54	2.24	16.07	2.25	3.51	5.53	12.77	3.06	7.68	5.70
T2018	14.71	2.37	4.68	4.03	0.71	3.19	3.20	6.26	1.21	3.13	3.11	0.90	1.85	17.22	3.39	1.71	3.21	3.56	0.46	14.77	6.31
T2019	9.47	4.02	5.59	4.99	1.12	7.65	5.01	4.90	0.74	3.48	2.85	5.93	1.84	15.46	3.36	2.25	5.96	5.24	1.78	2.80	5.57
H-5 yrs	9.46	5.06	6.74	5.54	1.70	4.49	5.30	6.99	1.16	4.61	4.01	4.02	2.58	13.56	3.34	3.23	3.20	3.98	2.20	6.41	2.43
S-5 yrs	6.83	3.60	3.50	3.43	0.57	3.31	2.31	7.86	1.16	4.93	4.70	0.54	2.66	14.75	2.14	3.04	4.11	7.20	2.39	11.63	9.34
Overall	8.54	4.40	5.26	4.60	1.17	3.98	3.85	7.62	1.21	4.91	4.38	1.80	2.67	14.41	2.65	3.24	3.53	5.21	2.48	8.90	5.20

H: heavy clay soil; S: sandy soil; T: means of years over two soil types; H-5 yrs: means of heavy clay soil over five years; S-5 yrs: means of sandy soil over five years; Overall: means over five years and two soil types.